013534

REPORT ON THE
RECONNAISSANCE SPECTRAL IP SURVEY
TEN'AS PROJECT
WHITEHORSE MINING DISTRICT, Y.T.
FOR
CYPRUS ANVIL MINING CORPORATION

TABLE OF CONTENTS

Part A:	Report	13 pages	Page
1.	Introduction		1
2.	Presentation of Results		2
3.	Discussion of Results		4
4.	Conclusions and Recommendations		8
5.	Certificate - P.G. Hallof		13
6.	Appendix		
Part B:	Illustrations	63 pieces	
	Plan Map (in pocket)	Dwg. S.I.P.P. 3109	
	SIP Data Plots	Dwgs. SIP 1104-1 to -3	
		Dwgs. SIP 1105-1 to -4	
		Dwgs. SIP 1106-1 to -6	
		Dwgs. SIP 1107-1 to -11	
		Dwgs. SIP 1108-1 to -8	
		Dwgs. SIP 1109-1 to -11	
		Dwgs. SIP 1110-1 to -9	
		Dwgs. SIP 1111-1 to -10	

PHOENIX GEOPHYSICS LIMITED

REPORT ON THE
RECONNAISSANCE SPECTRAL IP SURVEY
TENAS PROJECT
WHITEHORSE MINING DISTRICT, Y.T.
FOR
CYPRUS ANVIL MINING CORPORATION

---

1. INTRODUCTION

At the request of Dr. David S. Jennings, Chief Geologist, we have completed a reconnaissance Spectral IP Survey on widely spaced lines at the Tenas Project, on behalf of Cyprus Anvil Mining Corporation. The area of interest chosen for the survey lies to the east of the main mining area at Faro, in the Whitehorse Mining District of the Yukon Territory.

The reconnaissance geologic map of the area shows that favourable host rocks from the Faro District strike roughly east-west across the reconnaissance grid. The spectral IP survey was planned to locate any unknown zones of metallic mineralization that might be present. Further, previous Test Surveys with the Spectral IP technique, in the vicinity of the known ore zones, have shown that the sources of the Spectral IP anomalies detected can often be established as being sulphide

mineralization or graphitic phyllite. This separation is made, based upon the time-constant of the Cole-Cole Dispersion that best approximates the IP effect measured.

2. PRESENTATION OF RESULTS

When the IPV-3 is used in the field, the complete results are stored on tape cassettes, using the CP-1 Computer, which is a major part of the system. These tape cassettes can then be used to plot the data in the field using the HP85, portable computer. In the office, the tape cassettes are used to process the data through an HP9845, portable computer. As outlined in the attached technical paper, the processing consists of the removal of inductive coupling effects from the spectral data and the determination of the electrical parameters of the Cole-Cole dispersion that best fits the measured data.

This processing is applied to the spectral data obtained for each dipole pair along the lines. The various parameters (both measured and calculated) are also plotted in "pseudosection" form by the computer. A copy of all of the relevant data is enclosed in Volume II of the report. Certain spectral plots and pseudosections have been extracted for discussion in this portion of the report.

Line	Electrode Intervals	Dwg. No.
580E	500'	SIP 1104-1 to -3
565E	500'	SIP 1105-1 to -4
550E	500'	SIP 1106-1 to -6
535E	500'	SIP 1107-1 to -11
505E	500'	SIP 1108-1 to -8
475E	500'	SIP 1109-1 to -11
445E	500'	SIP 1110-1 to -9
Baseline 140N	1000'	SIP 1111-1 to -10

Also enclosed with this report is Dwg. SI.P.P. 3109 a plan map of the lines surveyed at a scale of 1" = 833' or 1:10,000. The definite, probable and possible Induced Polarization anomalies are indicated by bars, in the manner shown on the legend, on this plan map as well as on the data plots. These bars represent the surface projection of the anomalous zones as interpreted from the location of the transmitter and receiver electrodes when the anomalous values were measured.

Since the Induced Polarization measurement is essentially an averaging process, as are all potential methods, it is frequently difficult to exactly pinpoint the source of an anomaly. Certainly, no anomaly can be located with more accuracy than the electrode interval length; i.e. when using 500' electrode intervals the position of a narrow sulphide body can only be determined to lie between two stations 500' apart. In order to definitely locate, and fully evaluate, a narrow, shallow source it is necessary to use shorter electrode intervals. In order to locate sources at some depth, larger electrode intervals must be used, with a corresponding increase in the uncertainties of location. Therefore, while the centre of the indicated anomaly probably corresponds fairly well with source, the length of the indicated anomaly along the line should not be taken to represent the exact edges of the anomalous material.

The topographic and geologic information shown on Dwg. SI.P.P. 3109 has been taken from maps made available by the staff of Cyrpus Anvil Mining Corporation.

3. DISCUSSION OF RESULTS

The reconnaissance spectral IP survey at the Tenas Project has given results that are of interest. Definite phase IP anomalies have been detected on all of the lines surveyed; on several lines more than one anomaly was located. Some of the anomalous patterns indicate a shallow source (i.e. anomalous for n = 1). In other cases the results suggest a source at considerable depth.

Line 580E

This is the easternmost line surveyed. There is a shallow anomaly centered at the north end of the data (155N). The source of this anomaly could be better located, and evaluated, by repeating the measurements with shorter electrode intervals and by extending the data to the north. The inversion of the spectral data for D6;N1 gives a time-constant value of 0.45 sec. This does not suggest that graphite is the source.

At the south end of the data there is the suggestion of a deep source at about 120N to 125N. This anomaly cannot be evaluated with the present data; further work would be necessary. The spectral results for D2;N4 gives a moderate apparent resistivity and a time-constant of 4.3 seconds.

The source of the deep anomaly is indicated to lie within, or beneath, the higher resistivity rock unit. The apparent resistivity pseudeosection clearly indicated the contact to be at 150N, near surface. To the north, the apparent resistivities are appreciably lower in magnitude. At some points there are anomalous IP effects within this rock unit; at other places there are none.

This resistivity contact can be easily interpreted on each of the north-south lines we have surveyed. The interpreted contacts have been plotted on the plan map (Dwg. SI.P.P. 3109) and then correlated from line to line.

Line 565E

On this line there is a shallow, narrow, source at about 155N to 160N; this anomaly can be better evaluated only by using shorter electrode intervals. The spectral results for D7;N1 and D7;N3 give time-constants in the range from 0.35 to 2.1 seconds.

The contour pattern suggests a possible second, deeper source, centered at about 150N. This location would be approximately under the northern edge of the high resistivity rock unit. The anomaly pattern is small and sharp; the anomaly shape may suggest that the line passes near the end of a relatively small source. Further detailed measurements would be necessary to better locate, and evaluate, the source.

Line 550E

The deep source on Line 565E may correlate with the much stronger, larger, deep anomaly centered at 155N to 160N on Line 550N. The source of this anomaly appears to lie well within the lower resistivity rock unit. The pattern for this definite, deep source is incomplete. The measurements would have to be extended to the north. The spectral time-constant characteristics for this anomaly are fairly large. However, they are poorly determined and better data is necessary.

There is a slight suggestion in the apparent resistivity data and in the phase shift data, of a second anomaly at considerable depth.

The source would be located beneath the high resistivity rock unit, centered at about 140N to 145N.

Line 535E

There is a similar, very deep anomalous pattern on this line that is somewhat more pronounced than 1500 feet to the east. On Line 535E, the source would have to be centered, at considerable depth, at about 135N to 145N.

The shallow anomaly centered at 155N to 160N on this line is more easily interpreted. The apparent resistivity measured for n = 1 is quite low. The shallow source could be better located, and evaluated, using shorter electrode intervals. The spectral plots for D6;N1, D7;N1; D7;N2 and D8;N3 range from 2.1 seconds to 54 seconds. Measurements with shorter electrode intervals would be more discriminating.

Line 505E

This line lies 3000 feet to the west; the contact with the high resistivity rocks is farther to the south (at about 130N). This interpretation requires an off-set between Line 505E and Line 535E. As we shall discuss later, the measurements along Line 140N Baseline confirm the shift in the contact at about this point.

The apparent resistivity and phase IP data on Line 505E suggest a complex, multiple source in the interval 125N to 150N. It is possible that the survey line is passing more parallel than perpendicular to the source. Further, detailed measurements would be necessary to clarify the location of the source, or sources.

The inversion of the spectral IP plots for the deep anomaly at 125N to 130N show time-constants that range from 0.06 seconds to 0.51 seconds. This result is important, and detailed measurements with

shorter electrode intervals should give rise to more reliable spectra that would permit a better interpretation for the northern portion of the anomaly.

Line 475E

A distance of 3000 feet to the west, the pseudosection for Line 475E indicates two, relatively distinct sources within the lower resistivity rocks. There is a strong, deep source centered at 145N to 150N and a narrow, shallow source centered at 135N to 140N.

The inversion of the spectral plots D4; D6 and D7 shows that the time-constants for these two IP dispersions are fairly small for the shallow source and large for the deeper source.

Detailed measurements are warranted to further investigate the sources of the two anomalies. Better data should lead to better determinations for the time-constant.

Line 445E

The deep anomaly outlined on Line 475E may correlate with the even deeper, stronger anomaly centered at about 135N to 140N on this line. This position for the source would be beneath the edge of the higher resistivity rock unit.

This is one of the more definite deep anomalies located during the reconnaissance survey at Tenas Creek and further investigation is warranted.

The spectral inversion for the dipole pair within the deep anomaly (D4;N2, D4;N4) give time-constants that suggest sulphide mineralization as the source. The measurements at less depth to the north (D5;N1, D7;N2, D7;N3, D8;N1) all give much larger values of time-constant that suggest graphitic material as the source.

Baseline 140N

This east-west line was surveyed using X = 305 meters. The apparent resistivity results show the lower resistivity rock unit to the west of about 530E and the higher resistivity rock unit to the east. This position for the contact agrees relatively well with the off-set previously predicted between Line 505E and Line 535E.

In addition, there is a strong, narrow, shallow resistivity anomaly centered at 510E. There are IP effects here; the pattern suggests that the line crosses the source at approximately right angles and the anomaly correlates with the complex source previously described in Line 505E. The sources should be better located, and evaluated by making measurements using shorter electrode intervals on lines parallel to Baseline 140N.

The spectral plots for the dipole-pair within the anomaly show large values, suggesting that the source may be graphitic. However, the values are poorly determined since the measurements were noisy due to low voltages. Detailed measurements with shorter electrode intervals will give large voltage levels and the spectral plots should be more accurately determined.

4. CONCLUSIONS AND RECOMMENDATIONS

The lines used for the reconnaissance survey at the Tenas Project are 1500 feet and 3000 feet apart. An electrode interval of X = 500 feet was used for the survey and the correlation between lines is possible due to the fact that the patterns show similarities from line to line.

As shown on the plan map, Dwg. No. SI.P.P. 3109, the area of the survey is underlain by volcanic rocks. There is only limited outcrop,

presumably because of recent sediment distributed in the river valley. The contact between high resistivity rocks to the south and lower resistivity rocks to the north, has been interpreted from the data plots and transferred to the plan map. This interpreted contact does not correlate exactly with the approximate contacts shown on the geologic map. It would be worthwhile to discover which of the volcanic rock units correlates with the high resistivity rock unit, some further reconnaissance geologic mapping could be accomplished using straight-forward resistivity techniques.

As shown on the Spectral IP pseudosections, some of the low resistivity rock unit, to the north of the interpreted contact, has broad, weak IP effects. However, there are numerous strong IP anomalies, with associated resistivity lows, within this zone. The anomalies have been shown on the plan map. An attempt has been made to correlate these anomalies from line to line. The correlations have been made, based upon the character of the anomalous values and the indicated depth to the source. Because of the distance between the survey lines, this may not be correct.

In the case of most of the anomalies, the reconnaissance spectral IP results are not definitive enough to permit a discrimination interpretation. The purpose of the reconnaissance survey was primarily to locate anomalous zones; further detailed measurements would be necessary to better locate and evaluate the source of the anomalies. In addition, greater care must be taken to obtain more reliable spectral information on at least one line across each anomalous zone. With accurate spectral IP data for several dipole-dipole pairs in an anomalous pattern, it should be possible to determine the time-constant

of the IP effect from that source.

The nature of the detailed measurements required will depend upon whether the data measured with X = 500' indicates the source to be shallow, or at depth.

a) For the shallow source, the n = 1 measurement with X = 500' is anomalous. The most definte examples from the reconnaissance survey at the Tenas Project are centered at Line 565E, 157+50N; Line 535E, 155N; Line 475E, 137+50N. The detailed measurements should be of three types:

i) The measurements over the anomaly with the spectral system should be repeated with X = 300', and even shorter electrode intervals. The electrode interval should be shortened until the maximum apparent IP effect is not measured for n = 1.

ii) Closely spaced parallel lines should also be surveyed with this short electrode interval.

iii) On one of the lines of this small grid, time should be taken to make an accurate set of spectral measurements. This will be made somewhat easier by the fact that the voltages measured for the short electrode intervals will be larger in magnitude.

b) For the deep sources, the highest IP effects and the lowest apparent resistivities are measured for the larger values of (n). The more definite of the deep anomalies are centered at Line 550E, 155N to 165N; Line 475E, 145N to 155N; Line 445N,

130N to 140N. Because the sources of these anomalies are at depth, they will be difficult to intersect with a single drill hole. Further, the drilling will be expensive. Detailed measurements are necessary, and warranted, to obtain the best location for the source that is possible. Detailed measurements of several types are warranted.

i) The X = 500' measurements should be repeated with the electrode positions shifted 250 feet. This data will confirm the presence of the deep source.

ii) Lines 500 feet and 1000 feet to the east and west of the discovery lines should be surveyed to determine the variations, along strike, of the source. Several of the anomalous patterns for the deep sources, measured with X = 500', suggest that the line may pass near the end of the deep source. The attached theoretical results for sources with infinite strike length show much broader patterns than were measured.

iii) The survey lines necessarily cross the strike of the geologic formation, and the resistivity patterns vary accordingly. When a deep source has been located on several parallel lines, a perpendicular line should be surveyed directly over the source and parallel to its apparent

Fig. I

APPARENT RESISTIVITY

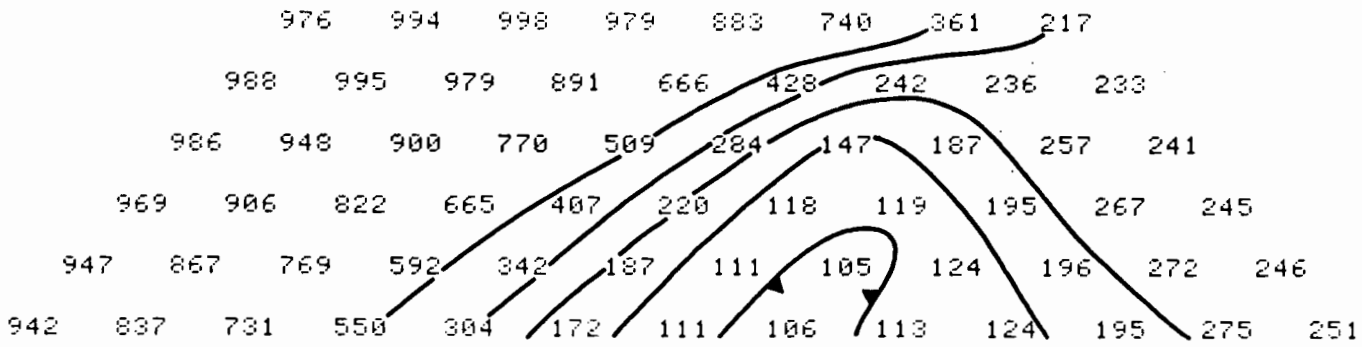

APPARENT METAL FACTOR

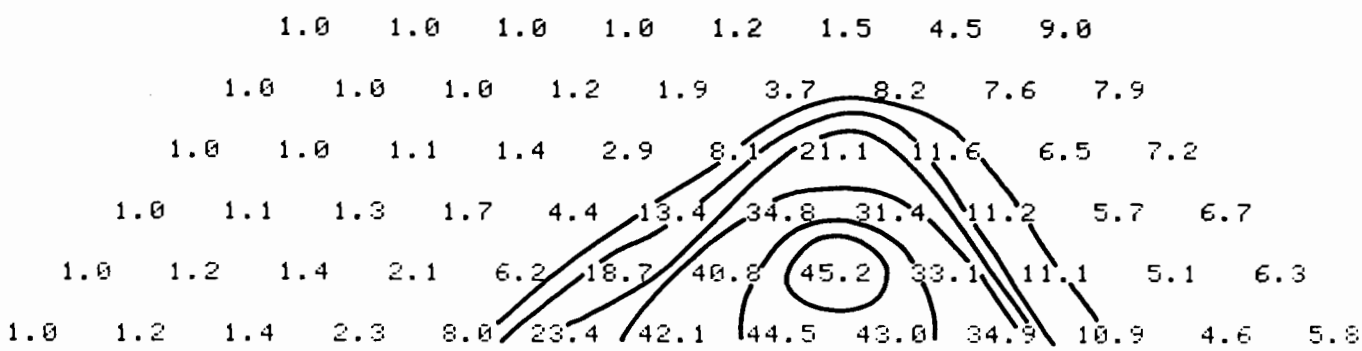

APPARENT PHASE

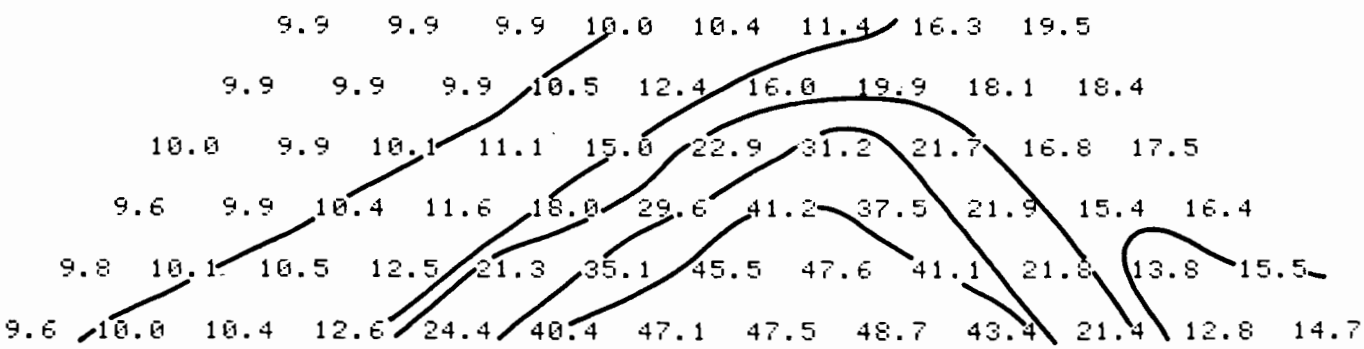

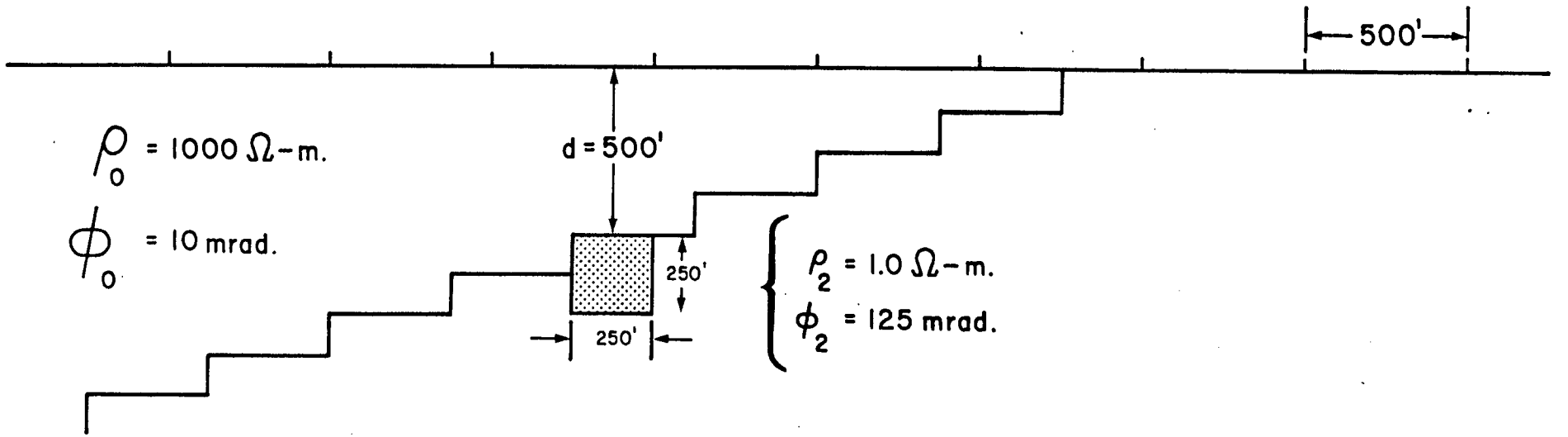

ρ_1 = 200 Ω-m.

ϕ_1 = 20 mrad.

Fig. 1

Fig. II

APPARENT RESISTIVITY

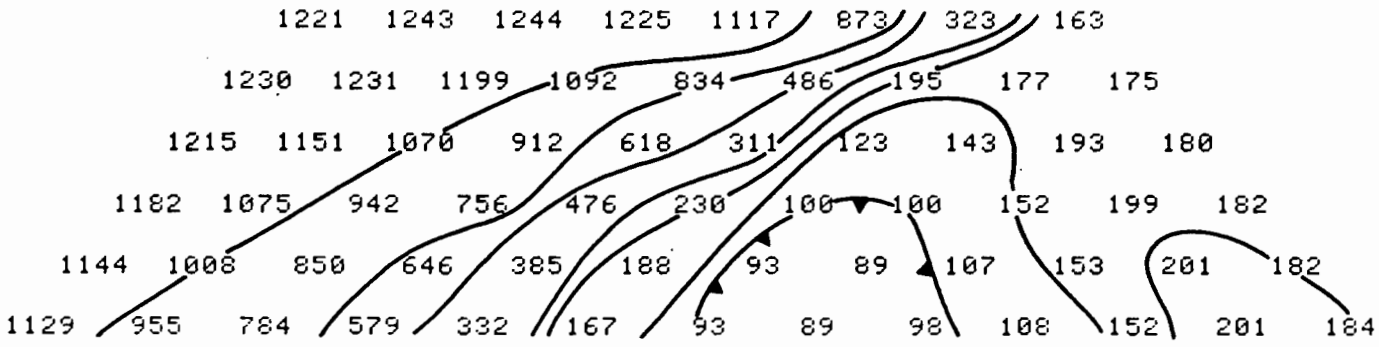

APPARENT METAL FACTOR

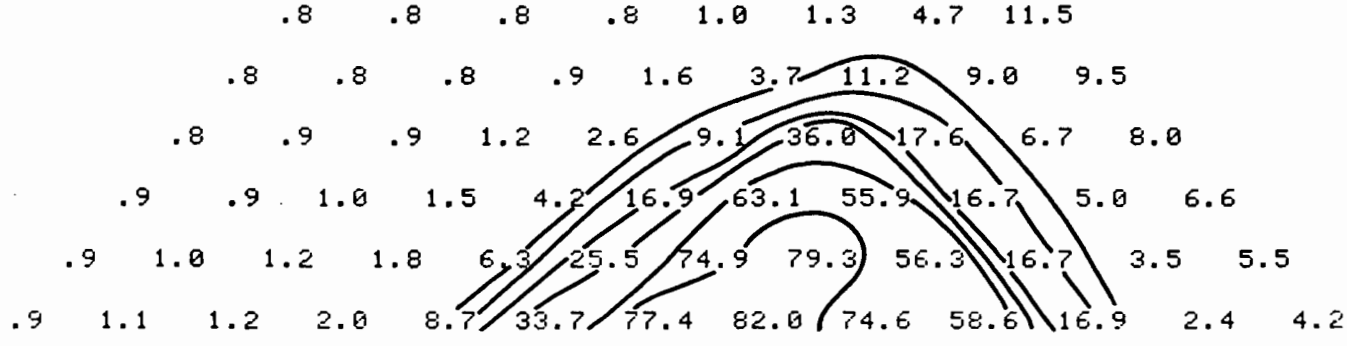

APPARENT PHASE

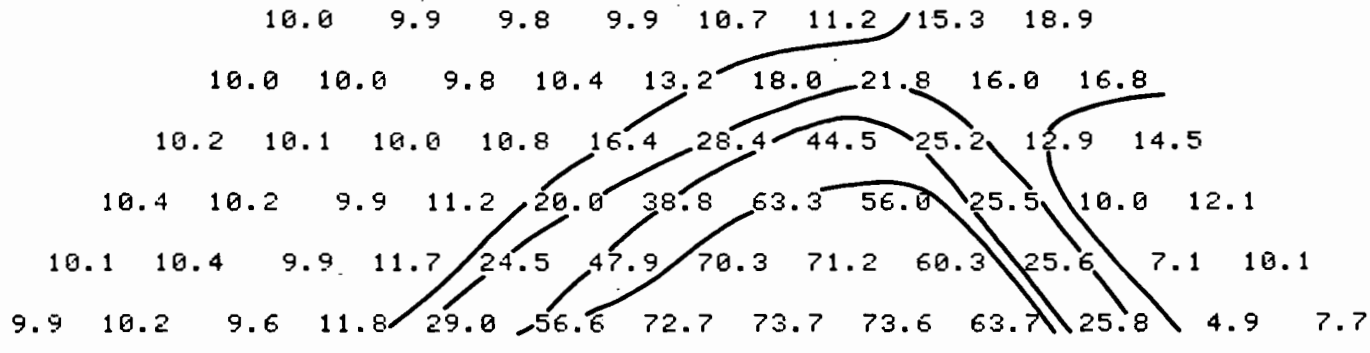

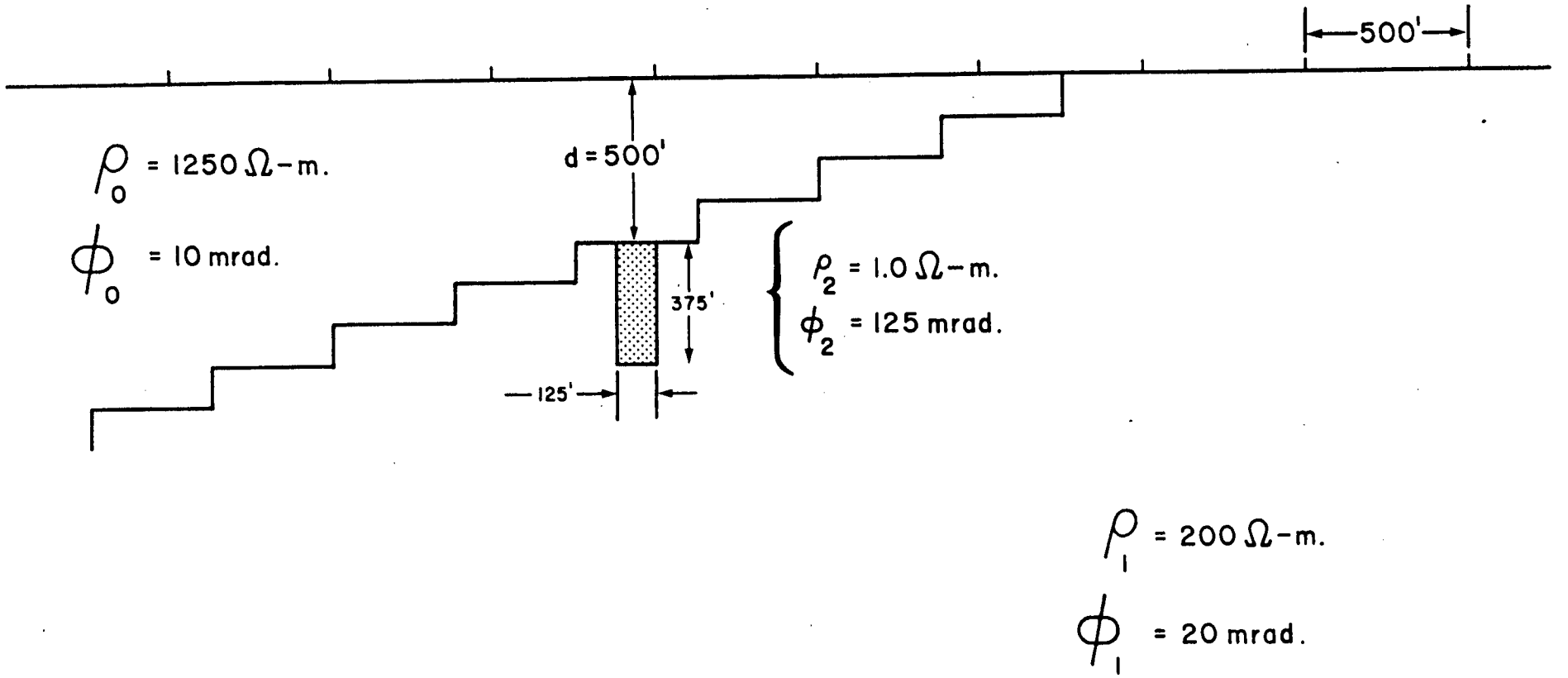
500'
ρ_0 = 1250 Ω-m.
ϕ_0 = 10 mrad.
d = 500'
375'
125'
ρ_2 = 1.0 Ω-m.
ϕ_2 = 125 mrad.
ρ_1 = 200 Ω-m.
ϕ_1 = 20 mrad.

Fig. II

iii) cont'd.

strike. This further data will even better locate the strongest part of the anomaly.

iv) An attempt should be made to measure fully reliable spectral data for the deep sources, on one line. For this check, it may be necessary to use a heavier, more powerful transmitter current source. This may slow the progress of the field work but it should result in interpretable spectral plots.

With this detailed data in hand, it would be possible to locate drill holes to test the sources of the anomalies at the Tenas Project. Further, with good spectral plots it will be possible to make interpretations concerning the time-constant magnitudes for the IP effects from the various sources. These results will provide an excellent test for the usefulness of the spectral IP techniques in reconnaissance exploration in the Anvil Area.

PHOENIX GEOPHYSICS LIMITED

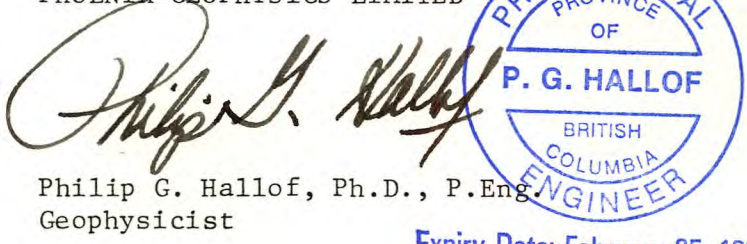

Philip G. Hallof, Ph.D., P.Eng.
Geophysicist

Expiry Date: February 25, 1982

Dated: January 21, 1982

CERTIFICATE

I, Philip George Hallof, of the City of Toronto, Province of Ontario, do hereby certify that:

1. I am a geophysicist residing at Suite 3505, 2045 Lakeshore Blvd. W., Toronto, Ontario.

2. I am a graduate of the Massachusetts Institute of Technology with a B.Sc. Degree (1952) in Geology and Geophysics, and a Ph.D. Degree (1957) in Geophysics.

3. I am a member of the Society of Exploration Geophysicists and the European Association of the Exploration Geophysicists.

4. I am a Professional Geophysicist, registered in the Province of Ontario, the Province of British Columbia and the State of Arizona.

5. I have no direct or indirect interest, nor do I expect to receive any interest directly or indirectly, in the property or securities of Cyprus Anvil Mining Corporation or any affiliate.

6. The statements made in this report are based on a study of published geological literature and unpublished private reports.

7. Permission is granted to use in whole or in part for assessment and qualification requirements but nor for advertising purposes.

Dated at Toronto

This 21st day of January, 1982

Philip G. Hallof, Ph.D., P.Eng.

PROFESSIONAL ENGINEER
PROVINCE OF BRITISH COLUMBIA
P. G. HALLOF

Expiry Date: February 25, 1982

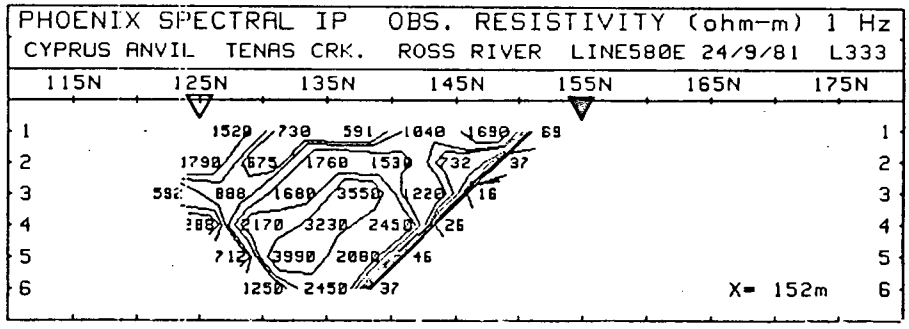
PHOENIX SPECTRAL IP OBS. RESISTIVITY (ohm-m) 1 Hz
CYPRUS ANVIL TENAS CRK. ROSS RIVER LINE580E 24/9/81 L333
115N 125N 135N 145N 155N 165N 175N
1 2 3 4 5 6
1520 730 591 1040 1690 69
1790 675 1760 1530 732 37
592 888 1680 3550 1220 16
388 2170 3230 2450 25
713 3990 2080 46
1250 2450 37
X= 152m

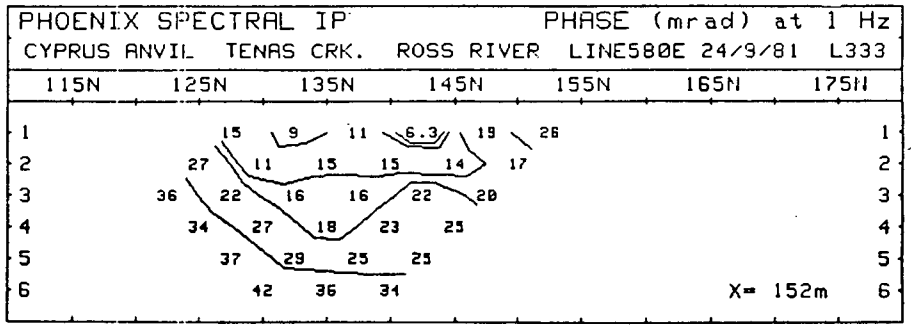
PHOENIX SPECTRAL IP PHASE (mrad) at 1 Hz
CYPRUS ANVIL TENAS CRK. ROSS RIVER LINE580E 24/9/81 L333
115N 125N 135N 145N 155N 165N 175N
1 2 3 4 5 6
15 9 11 6.3 19 26
27 11 15 15 14 17
36 22 16 16 22 20
34 27 18 23 25
37 29 25 25
42 36 34
X= 152m

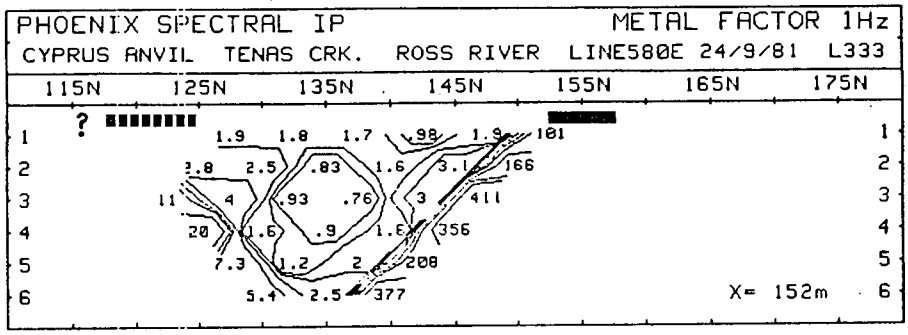
PHOENIX SPECTRAL IP METAL FACTOR 1Hz
CYPRUS ANVIL TENAS CRK. ROSS RIVER LINE580E 24/9/81 L333
115N 125N 135N 145N 155N 165N 175N
1 2 3 4 5 6
1.9 1.8 1.7 .98 1.9 101
3.8 2.5 .83 1.6 3.1 166
11 4 .93 .76 3 411
20 1.6 .9 1.6 356
7.3 1.2 2 208
5.4 2.5 377
X= 152m

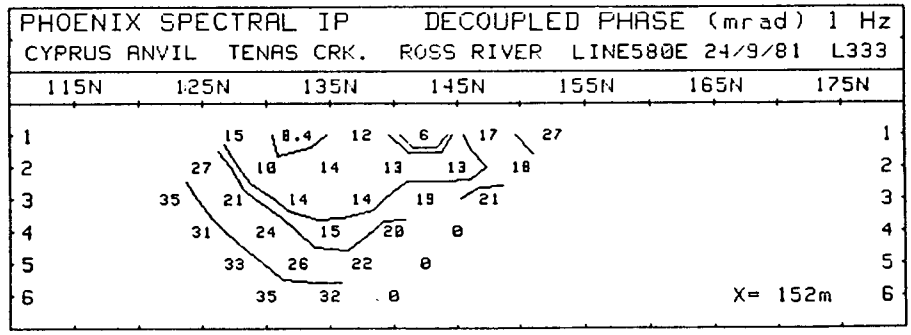
PHOENIX SPECTRAL IP DECOUPLED PHASE (mrad) 1 Hz
CYPRUS ANVIL TENAS CRK. ROSS RIVER LINE580E 24/9/81 L333
115N 125N 135N 145N 155N 165N 175N
1 2 3 4 5 6
15 8.4 12 6 17 27
27 10 14 13 13 18
35 21 14 14 19 21
31 24 15 20 0
33 26 22 0
35 32 0
X= 152m

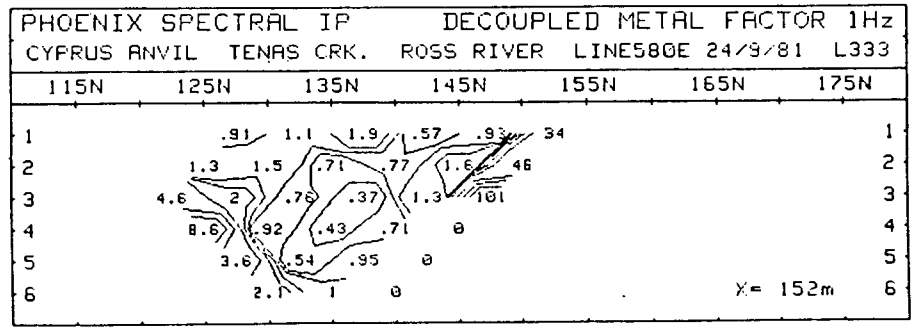
PHOENIX SPECTRAL IP DECOUPLED METAL FACTOR 1Hz
CYPRUS ANVIL TENAS CRK. ROSS RIVER LINE580E 24/9/81 L333
115N 125N 135N 145N 155N 165N 175N
1 2 3 4 5 6
.91 1.1 1.9 .57 .93 34
1.3 1.5 .71 .77 1.6 46
4.6 2 .78 .37 1.3 101
8.6 .92 .43 .71 0
3.6 .54 .95 0
2.1 1 0
X= 152m

DWG. NO. - S.I.P. - 1104 - 2

CYPRUS ANVIL TENAS CRK. ROSS RIVER LINE580E 24/9/81 L333 D= 2 N=4 X=152m

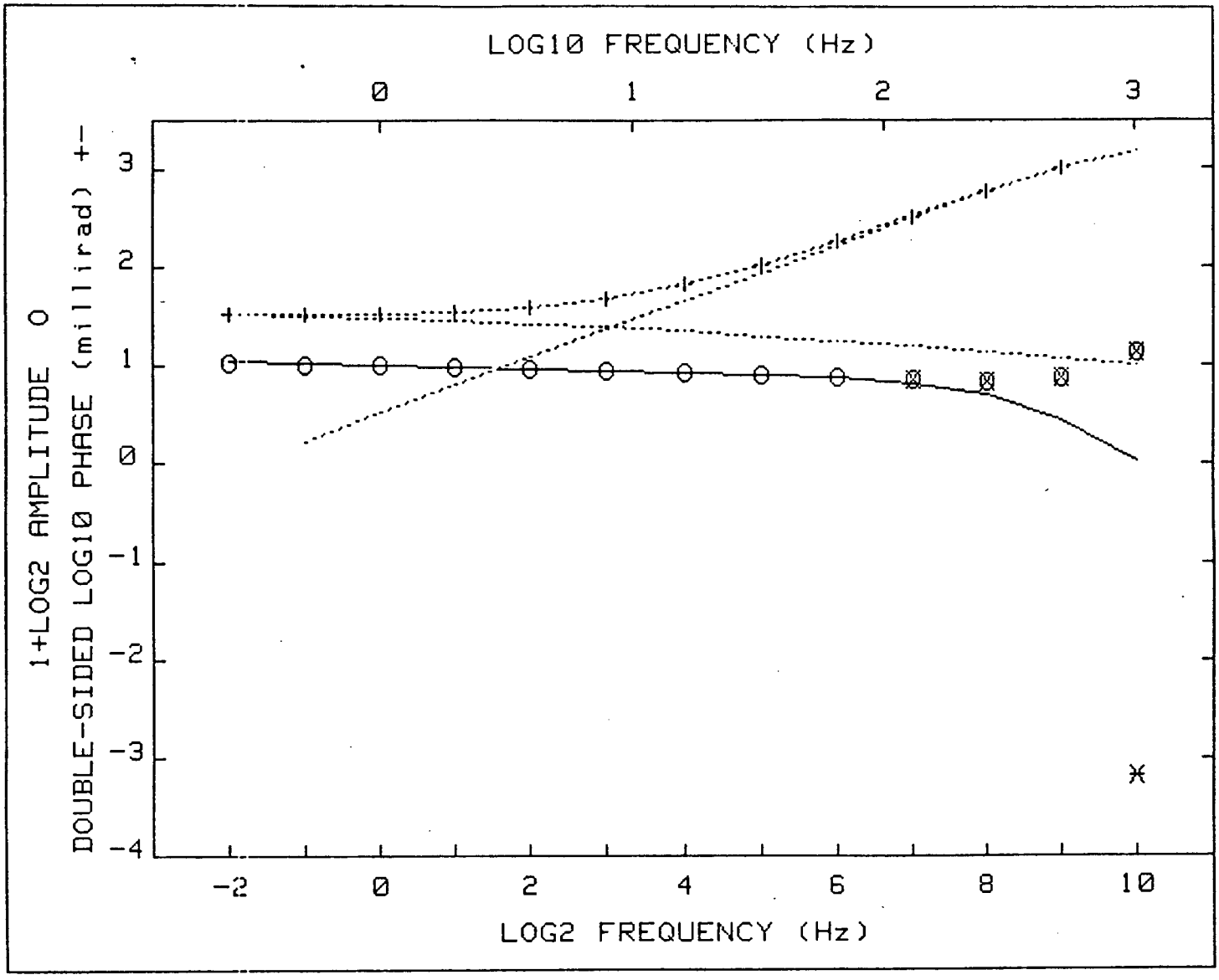

CRL: Number of dispersions= 2
C1=.25 M2=1 fixed

Iter	Lambda	Rchsq	R0	M1	T1	T2	C2
0	1.E-02	.00678	1.265	.301	3.2E+00	3.9E-04	.928
1	1.E-02	.00003	1.250	.290	3.2E+00	2.7E-04	.930
2	1.E-03	.00002	1.253	.291	3.4E+00	2.8E-04	.935
3	1.E-04	.00002	1.259	.293	4.0E+00	2.7E-04	.932
4	1.E-05	.00002	1.262	.294	4.3E+00	2.7E-04	.931

Pct Std Deviations	.8	1.3	28.9	1.3	.6	
Correlation Matrix	1.000					
	.970	1.000				
	.982	.936	1.000			
	-.815	-.783	-.811	1.000		
	-.719	-.603	-.763	.836	1.000	

Apparent Resistivity Measured at 1 Hz is 287.5
Apparent Resistivity Calculated from Inductive Coupling is 410.0

DWG. NO. – S.I.P. – 1104 – 3

CYPRUS ANVIL TENAS CRK. ROSS RIVER LINE580E 24/9/81 L333 D= 6 N=1 X=152m

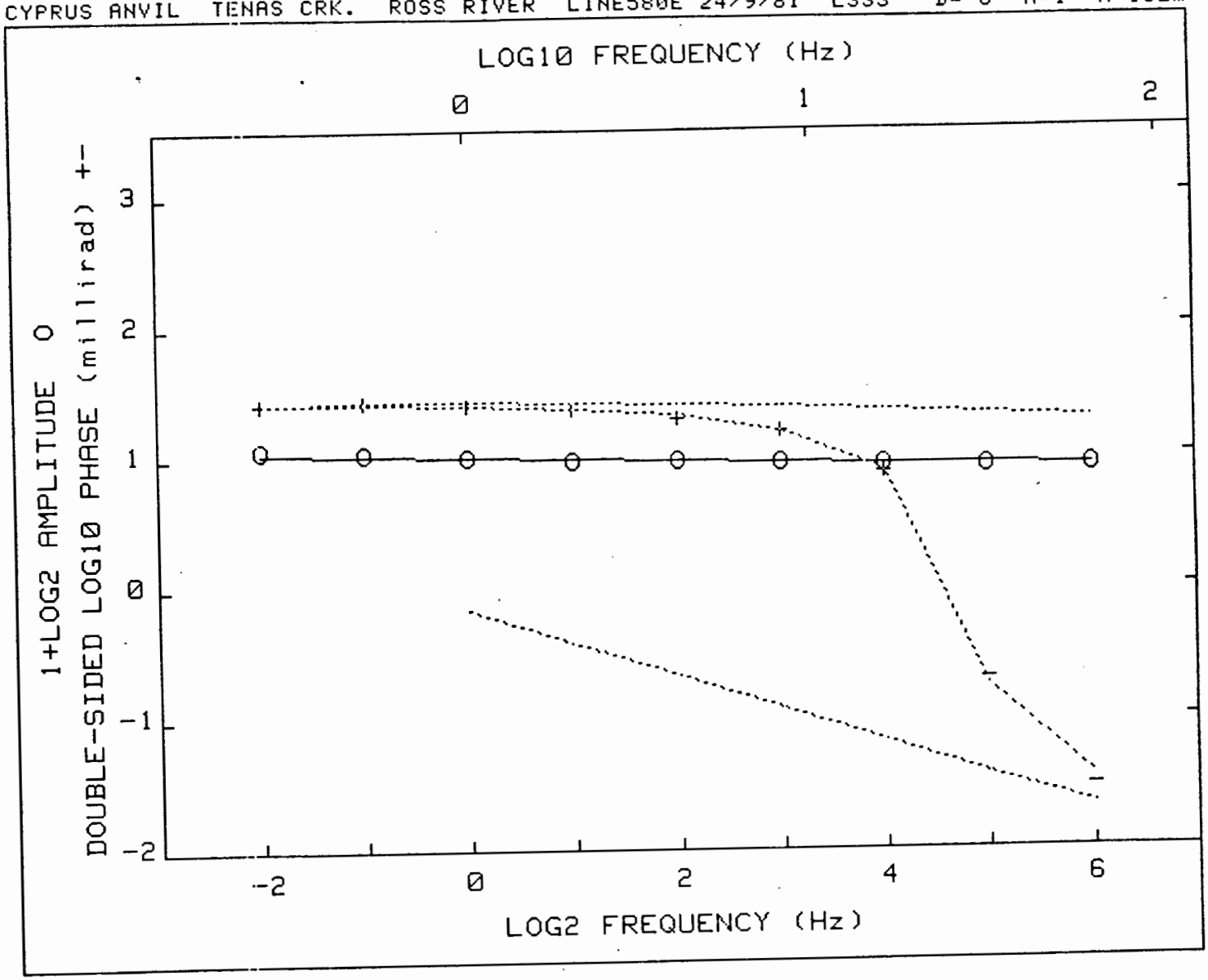

CRL: Number of dispersions= 2 Negative.
C1=.25 M2=1 fixed

Iter	Lambda	Rchsq	R0	M1	T1	T2	C2
0	1.E-02	.00661	1.080	.217	4.9E-01	5.3E-05	.866
1	1.E-02	.00069	1.159	.239	4.6E-01	5.4E-05	.835
2	1.E-02	.00069	1.159	.238	4.5E-01	5.4E-05	.834
Pct Std Deviations			2.0	2.8	195.7	20.1	8.5

Correlation Matrix

1.000					
.162	1.000				
.928	-.059	1.000			
.544	-.535	.690	1.000		
.737	-.428	.875	.949	1.000	

Apparent Resistivity Measured at 1 Hz is 68.96
Apparent Resistivity Calculated from Inductive Coupling is 177.3

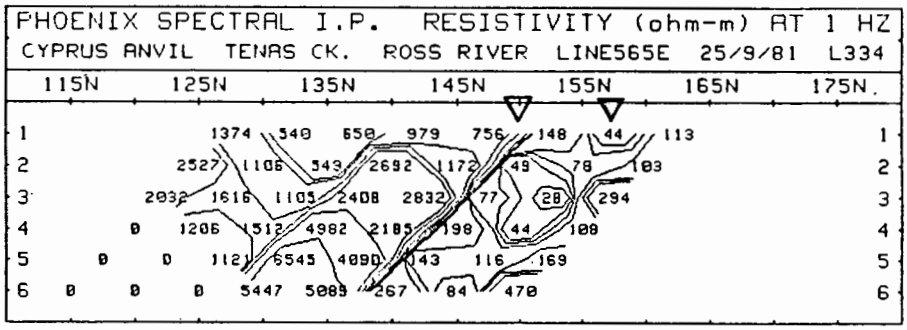
PHOENIX SPECTRAL I.P. RESISTIVITY (ohm-m) AT 1 HZ
CYPRUS ANVIL TENAS CK. ROSS RIVER LINE565E 25/9/81 L334
115N 125N 135N 145N 155N 165N 175N
1 2 3 4 5 6
1374 540 650 979 756 148 44 113
2527 1106 343 2692 1172 49 78 103
2032 1616 1105 2408 2832 77 28 294
0 1206 1512 4982 2185 198 44 108
0 0 112 6545 4090 143 116 169
0 0 0 5447 5089 267 84 470

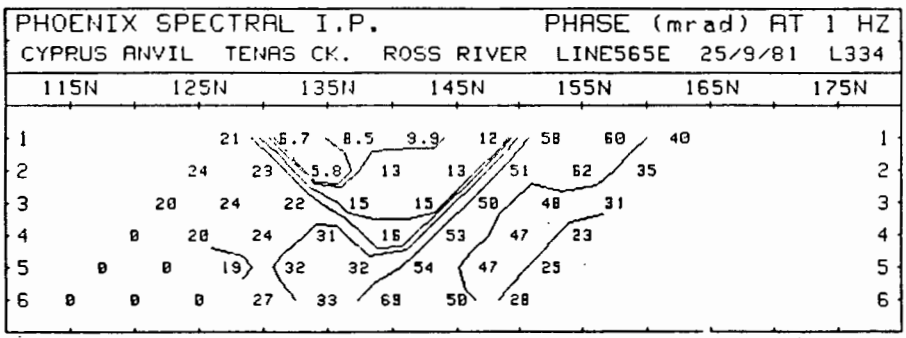
PHOENIX SPECTRAL I.P. PHASE (mrad) AT 1 HZ
CYPRUS ANVIL TENAS CK. ROSS RIVER LINE565E 25/9/81 L334
115N 125N 135N 145N 155N 165N 175N
1 2 3 4 5 6
21 5.7 8.5 9.9 12 58 60 40
24 23 5.8 13 13 51 62 35
20 24 22 15 15 50 48 31
0 20 24 31 16 53 47 23
0 0 19 32 32 54 47 25
0 0 0 27 33 69 50 28

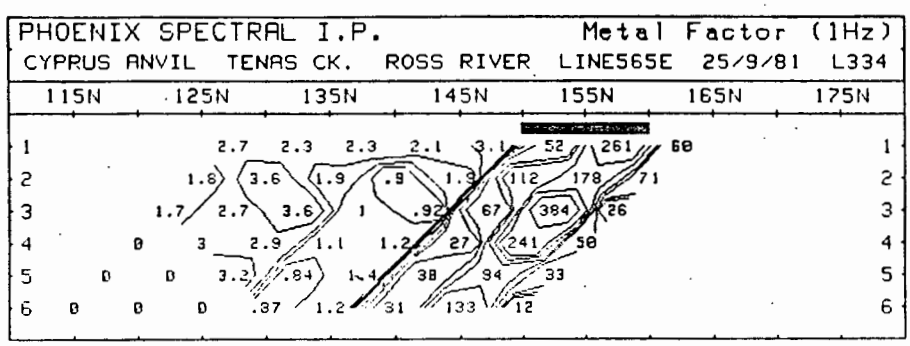
PHOENIX SPECTRAL I.P. Metal Factor (1Hz)
CYPRUS ANVIL TENAS CK. ROSS RIVER LINE565E 25/9/81 L334
115N 125N 135N 145N 155N 165N 175N
1 2 3 4 5 6
2.7 2.3 2.3 2.1 3.1 52 261 60
1.8 3.6 1.9 .9 1.9 112 178 71
1.7 2.7 3.6 1 .92 67 384 26
0 3 2.9 1.1 1.2 27 241 50
0 0 3.2 .84 1.4 38 94 33
0 0 0 .87 1.2 31 133 12

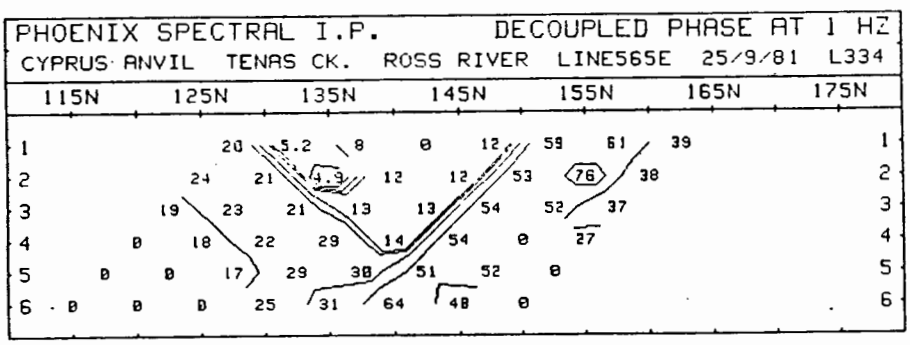
PHOENIX SPECTRAL I.P. DECOUPLED PHASE AT 1 HZ
CYPRUS ANVIL TENAS CK. ROSS RIVER LINE565E 25/9/81 L334
115N 125N 135N 145N 155N 165N 175N
1 2 3 4 5 6
20 5.2 8 0 12 59 61 39
24 21 4.9 12 12 53 76 38
19 23 21 13 13 54 52 37
0 18 22 29 14 54 0 27
0 0 17 29 38 51 52 0
0 0 0 25 31 64 48 0

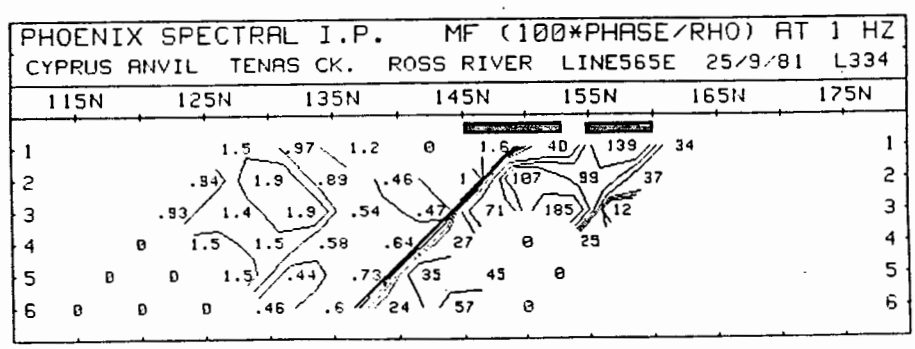
PHOENIX SPECTRAL I.P. MF (100*PHASE/RHO) AT 1 HZ
CYPRUS ANVIL TENAS CK. ROSS RIVER LINE565E 25/9/81 L334
115N 125N 135N 145N 155N 165N 175N
1 2 3 4 5 6
1.5 .97 1.2 0 1.6 40 139 34
.94 1.9 .89 .46 1 107 99 37
.93 1.4 1.9 .54 .47 71 185 12
0 1.5 1.5 .58 .64 27 0 25
0 0 1.5 .44 .73 35 45 0
0 0 0 .46 .6 24 57 0

DWG. NO. - S.I.P. - 1105-2

CYPRUS ANVIL TENAS CK. ROSS RIVER LINE565E 25/9/81 L334 D= 6 N=2 X=152m

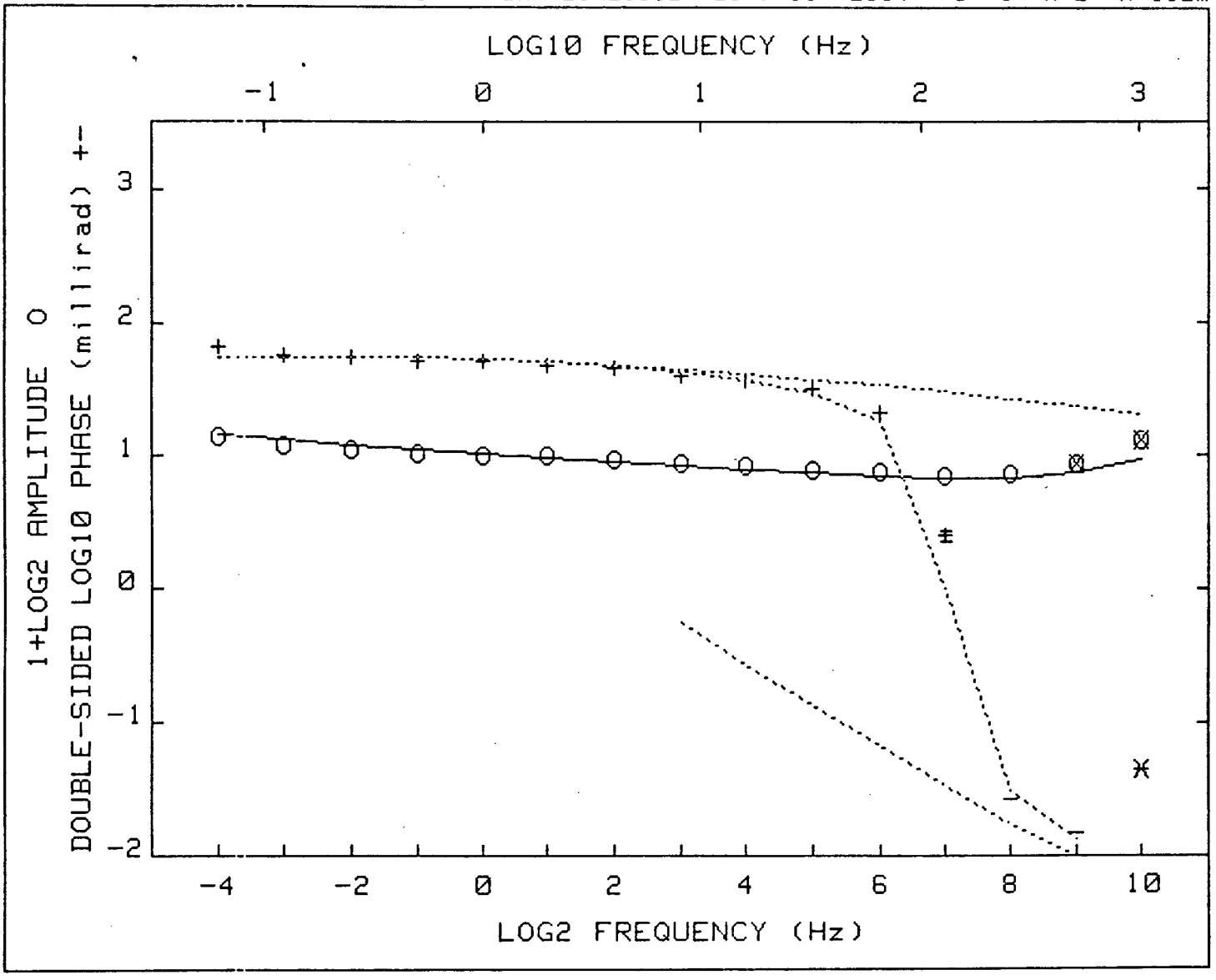

CRL: Number of dispersions= 2 Negative.
C1=.25 C2=1 fixed

Iter	Lambda	Rchsq	R0	M1	T1	M2	T2
0	1.E-02	.00854	1.423	.426	2.6E+00	.165	1.5E-04
1	1.E+03	.00854	1.423	.428	2.6E+00	.165	1.5E-04

Pct Std Deviations	2.9	1.0	99.7	75.5	105.7
Correlation Matrix	1.000				
	.296	1.000			
	.759	.186	1.000		
	.283	-.005	.347	1.000	
	-.384	-.015	-.482	-.977	1.000

Apparent Resistivity Measured at 1 Hz is 49.27
Apparent Resistivity Calculated from Inductive Coupling is 1867

DWG. NO. - S.I.P.-1105-3

CYPRUS ANVIL TENAS CK. ROSS RIVER LINE565E 25/9/81 L334 D= 7 N=1 X=152m

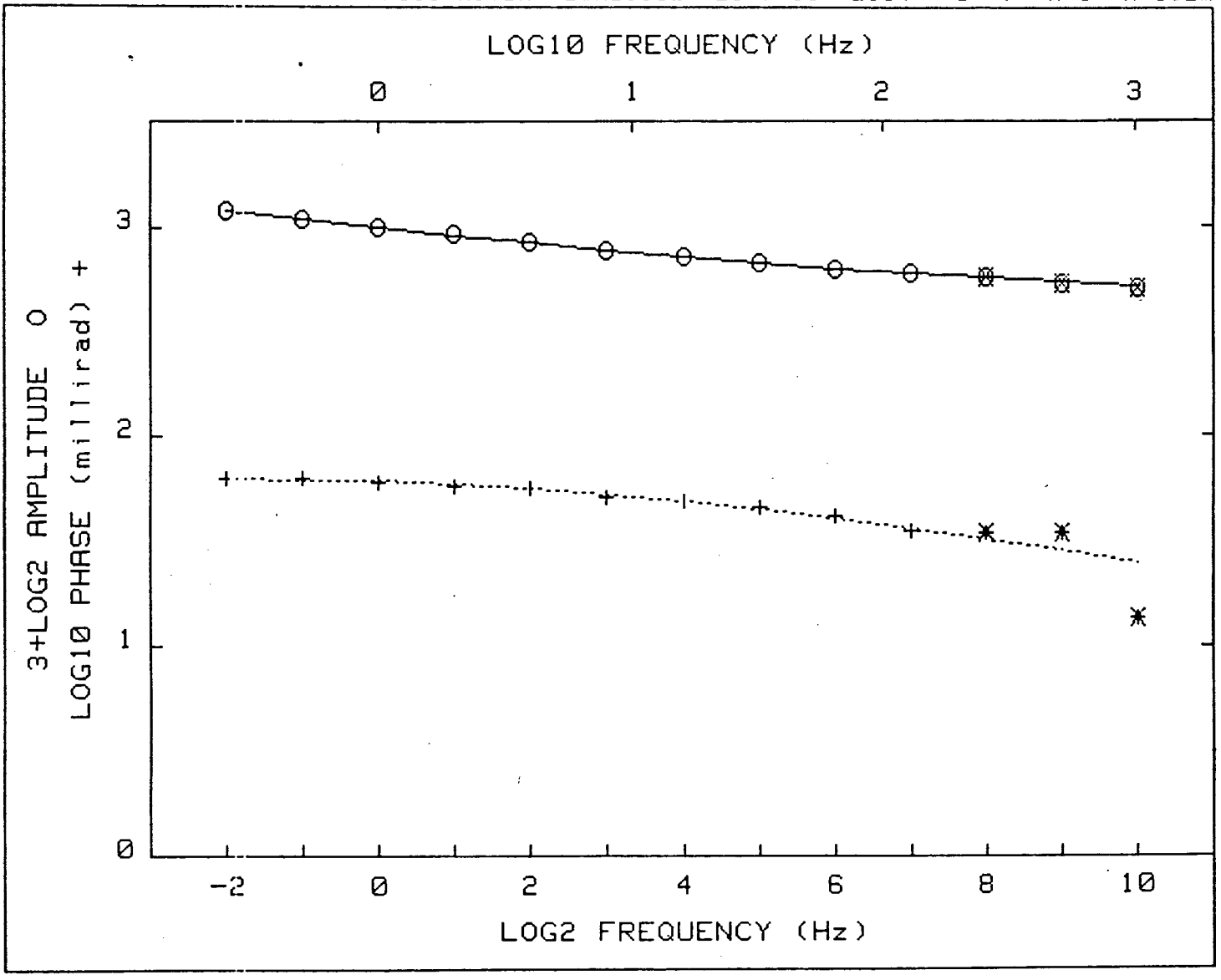

CRL: Number of dispersions= 2 Negative.
C1=.25 M2=0 T2=0 C2=0 fixed

Iter	Lambda	Rchsq	R0	M1	T1
0	1.E-02	.01008	1.280	.405	2.4E+00
1	1.E-02	.00015	1.447	.475	2.2E+00
2	1.E-03	.00004	1.452	.471	2.2E+00
3	1.E-04	.00004	1.451	.471	2.1E+00

Pct Std Deviations	.7	.7	10.6

Correlation Matrix	1.000		
	.952	1.000	
	.950	.890	1.000

Apparent Resistivity Measured at 1 Hz is 43.82
Apparent Resistivity Calculated from Inductive Coupling is 0.000

DWG. NO. - S.I.P. - 1105 - 4

CYPRUS ANVIL TENAS CK. ROSS RIVER LINE565E 25/9/81 L334 D= 7 N=3 X=152m

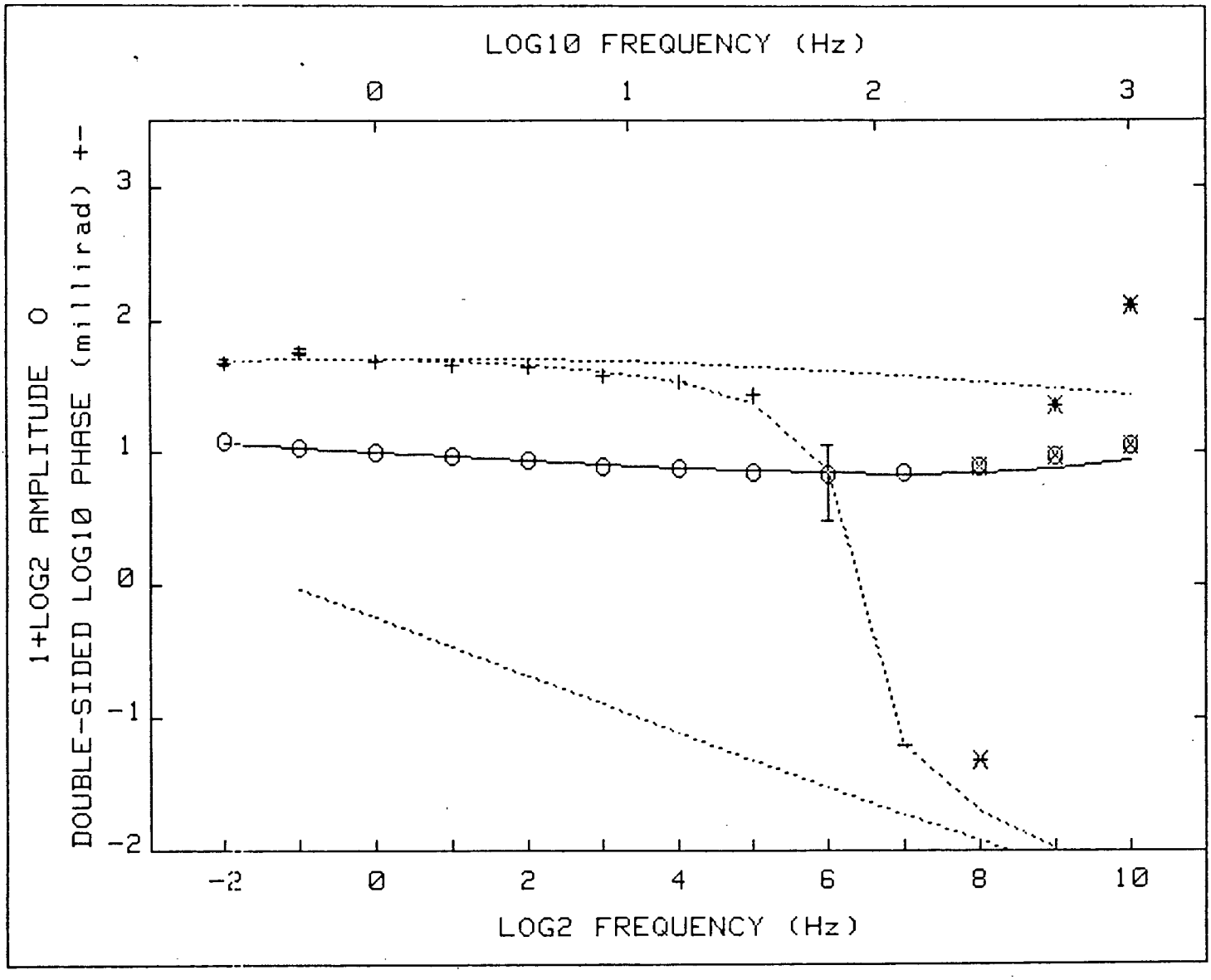

CRL: Number of dispersions= 2 Negative.
C1=.25 M2=1 fixed

Iter	Lambda	Rchsq	R0	M1	T1	T2	C2
0	1.E-02	.00245	1.256	.483	6.3E-02	3.5E-06	.415
1	1.E-02	.00135	1.252	.456	7.0E-02	5.8E-06	.490
2	1.E-03	.00108	1.257	.429	1.1E-01	7.7E-06	.558
3	1.E-04	.00098	1.272	.415	2.0E-01	9.3E-06	.611
4	1.E-05	.00087	1.279	.413	2.5E-01	1.1E-05	.642
5	1.E-06	.00081	1.284	.411	2.9E-01	1.2E-05	.662
6	1.E-07	.00079	1.286	.409	3.2E-01	1.2E-05	.676
7	1.E-08	.00077	1.288	.408	3.4E-01	1.3E-05	.685
8	1.E-09	.00077	1.289	.408	3.5E-01	1.3E-05	.691

Pct Std Deviations	2.4	2.1	98.3	14.3	5.8	
Correlation Matrix	1.000					
	.138	1.000				
	.923	-.156	1.000			
	.077	-.561	.228	1.000		
	.612	-.554	.787	.763	1.000	

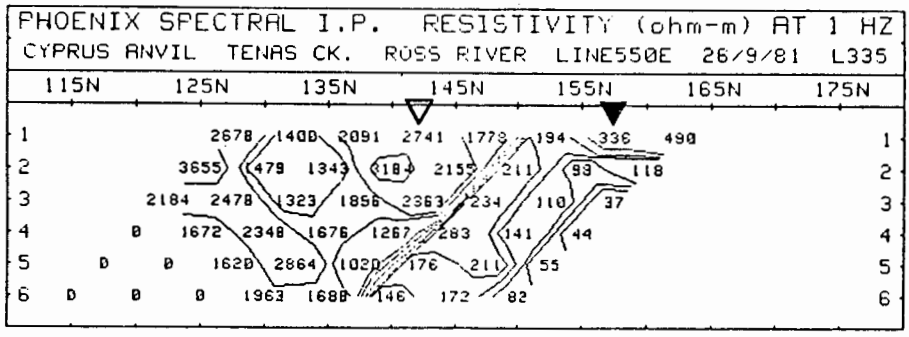
PHOENIX SPECTRAL I.P. RESISTIVITY (ohm-m) AT 1 HZ
CYPRUS ANVIL TENAS CK. ROSS RIVER LINE550E 26/9/81 L335
115N 125N 135N 145N 155N 165N 175N
1 2 3 4 5 6
2678 1400 2091 2741 1773 194 336 490
3655 479 1343 184 2155 211 93 118
2184 2478 1323 1856 2363 234 110 37
0 1672 2348 1676 1267 283 141 44
0 0 1620 2864 1030 176 211 55
0 0 0 1963 1688 146 172 82

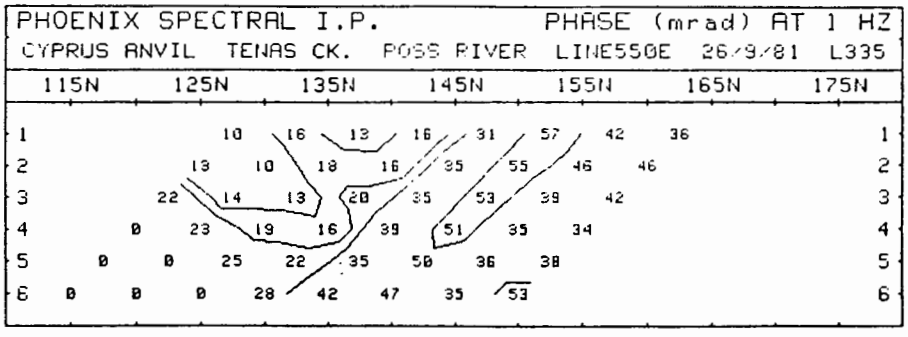
PHOENIX SPECTRAL I.P. PHASE (mrad) AT 1 HZ
CYPRUS ANVIL TENAS CK. ROSS RIVER LINE550E 26/9/81 L335
115N 125N 135N 145N 155N 165N 175N
1 2 3 4 5 6
10 16 13 16 31 57 42 36
13 10 18 16 35 55 46 46
22 14 13 20 35 53 39 42
0 23 19 16 39 51 35 34
0 0 25 22 35 50 36 38
0 0 0 28 42 47 35 53

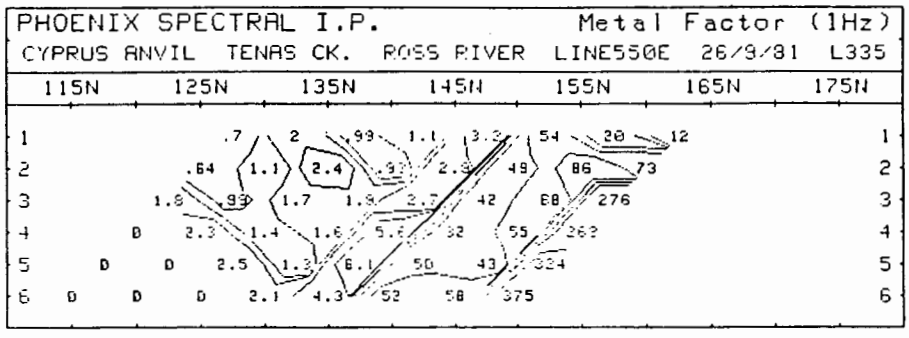
PHOENIX SPECTRAL I.P. Metal Factor (1Hz)
CYPRUS ANVIL TENAS CK. ROSS RIVER LINE550E 26/9/81 L335
115N 125N 135N 145N 155N 165N 175N
1 2 3 4 5 6
.7 2 .99 1.1 3.2 54 20 12
.64 1.1 2.4 .9 2.3 49 86 73
1.8 .99 1.7 1.8 2.7 42 88 276
0 2.3 1.4 1.6 5.6 32 55 262
0 0 2.5 1.3 6.1 50 43 334
0 0 0 2.1 4.3 52 58 375

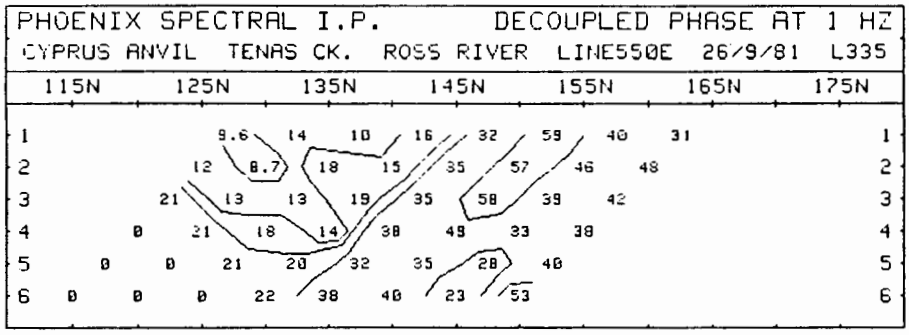
PHOENIX SPECTRAL I.P. DECOUPLED PHASE AT 1 HZ
CYPRUS ANVIL TENAS CK. ROSS RIVER LINE550E 26/9/81 L335
115N 125N 135N 145N 155N 165N 175N
1 2 3 4 5 6
9.6 14 10 16 32 59 40 31
12 8.7 18 15 35 57 46 48
21 13 13 19 35 58 39 42
0 21 18 14 38 48 33 38
0 0 21 20 32 35 28 40
0 0 0 22 38 40 23 53

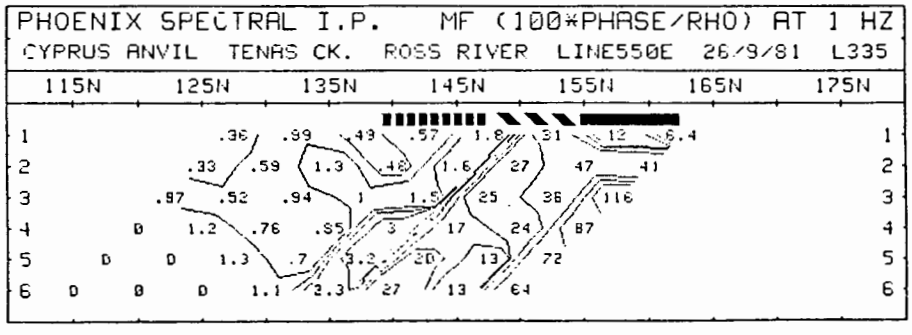
PHOENIX SPECTRAL I.P. MF (100*PHASE/RHO) AT 1 HZ
CYPRUS ANVIL TENAS CK. ROSS RIVER LINE550E 26/9/81 L335
115N 125N 135N 145N 155N 165N 175N
1 2 3 4 5 6
.36 .89 .49 .57 1.8 31 12 6.4
.33 .59 1.3 .48 1.6 27 47 41
.87 .52 .94 1 1.5 25 36 116
0 1.2 .76 .85 3 17 24 87
0 0 1.3 .7 3.2 20 13 72
0 0 0 1.1 2.3 27 13 64

DWG. NO. - S.I.P - 1106 - 2

CYPRUS ANVIL TENAS CK. ROSS RIVER LINE550E 26/9/81 L335 D= 6 N=5 X=152m

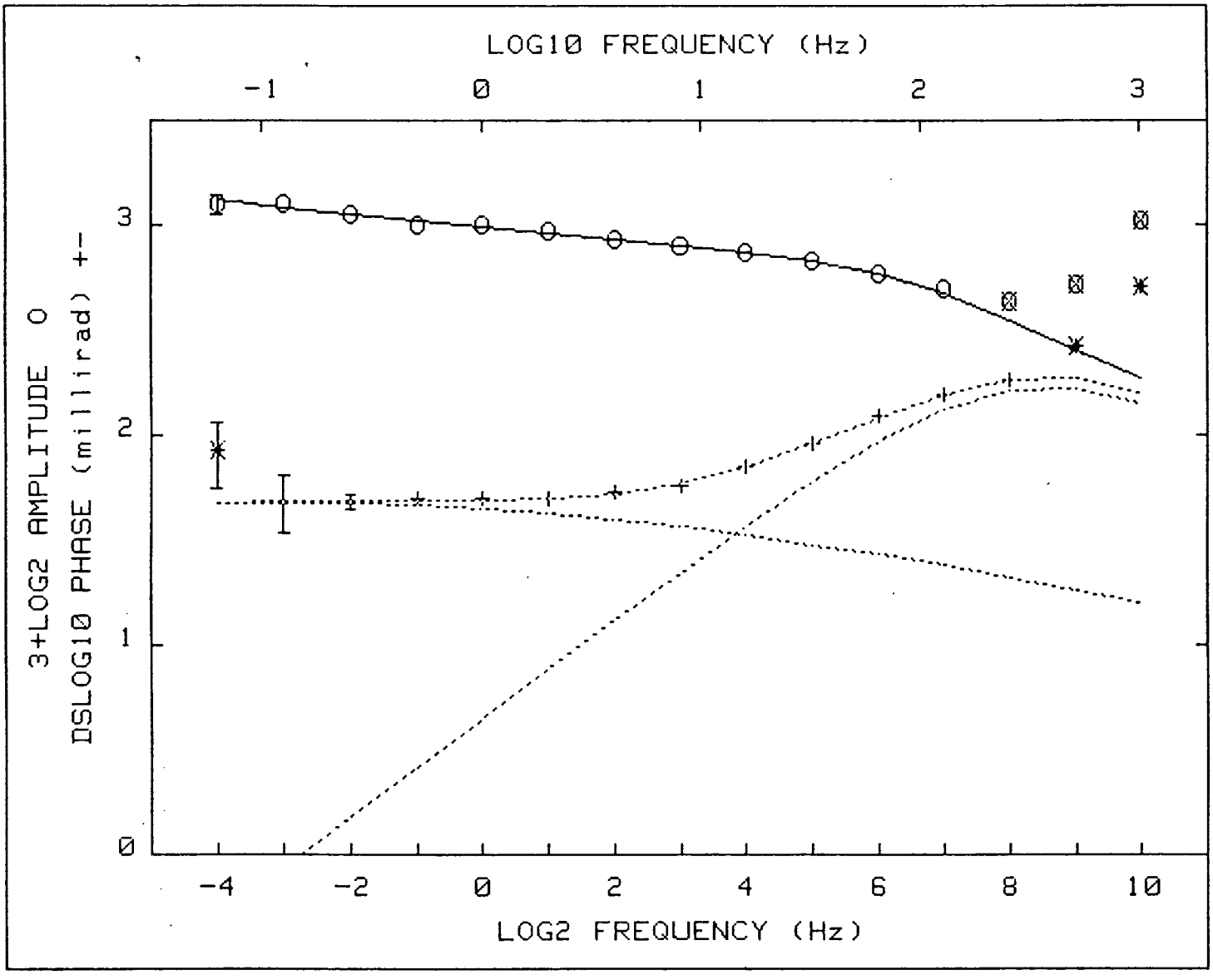

CRL: Number of dispersions= 2
C1=.25 fixed

Iter	Lambda	Rchsq	R0	M1	T1	M2	T2	C2
0	1.E-02	.00025	1.441	.392	1.9E+01	.502	1.2E-04	.578
1	1.E-02	.00023	1.438	.389	1.9E+01	.485	1.3E-04	.568
2	1.E-03	.00020	1.444	.393	1.9E+01	.415	1.9E-04	.591
3	1.E-03	.00018	1.444	.396	1.8E+01	.360	2.7E-04	.622
4	1.E-03	.00016	1.439	.397	1.6E+01	.322	3.5E-04	.652
5	1.E-04	.00014	1.375	.384	5.3E+00	.266	5.6E-04	.729
6	1.E-05	.00012	1.357	.384	3.3E+00	.251	5.9E-04	.763
7	1.E-06	.00012	1.359	.385	3.5E+00	.251	5.9E-04	.763

Pct Std Deviations	2.3	1.5	89.0	10.7	19.4	6.4	
Correlation Matrix	1.000						
	.681	1.000					
	.979	.547	1.000				
	.584	-.028	.672	1.000			
	-.500	.020	-.573	-.971	1.000		
	-.718	-.088	-.796	-.951	.901	1.000	

DWG. NO. - S.I.P. - 1106 - 3

CYPRUS ANVIL TENAS CK. ROSS RIVER LINE550E 26/9/81 L335 D= 6 N=6 X=152m

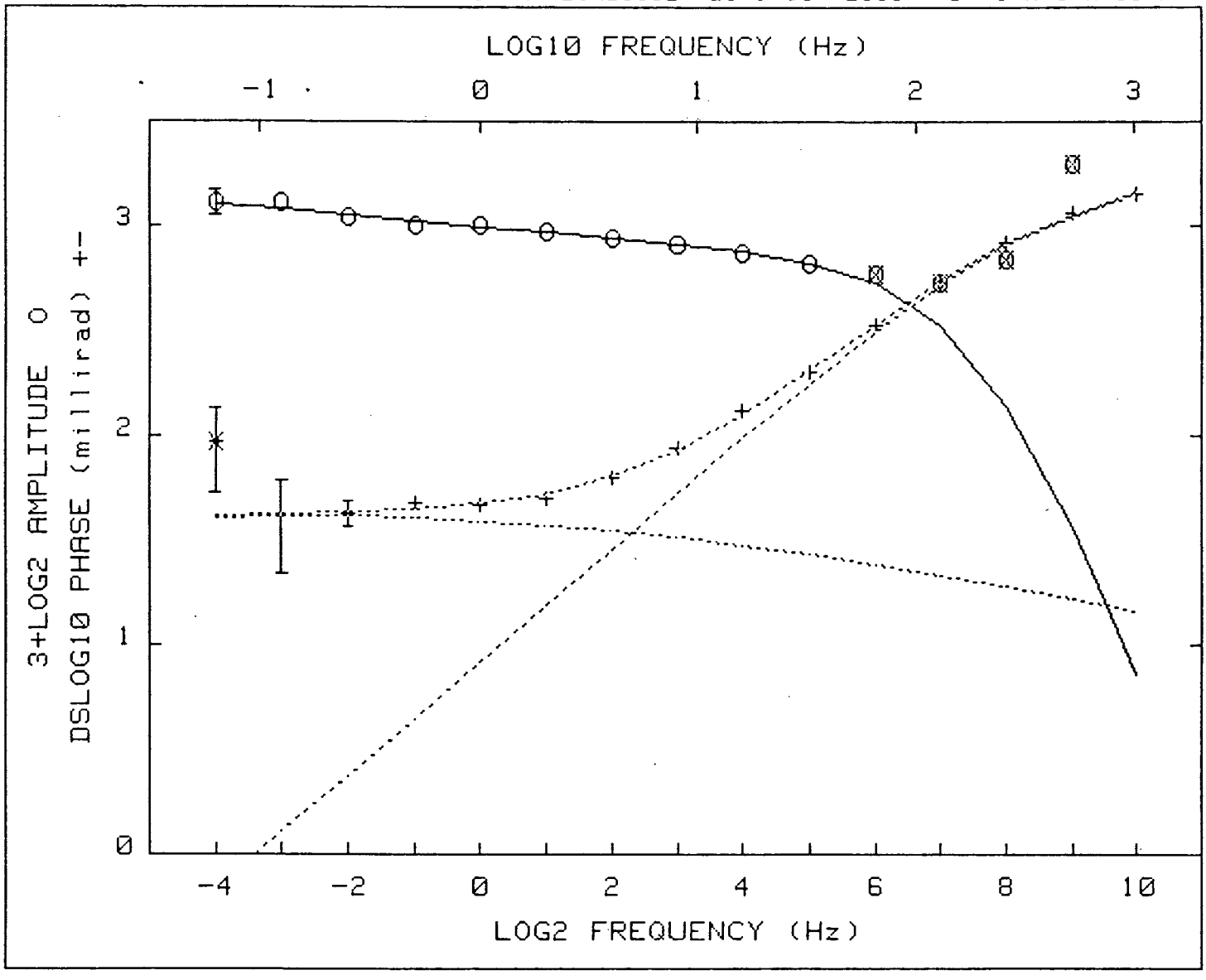

CRL: Number of dispersions= 2
C1=.25 fixed

Iter	Lambda	Rchsq	R0	M1	T1	M2	T2	C2
0	1.E-02	.00024	1.293	.342	2.0E+00	.736	7.2E-04	.887
1	1.E-02	.00022	1.290	.341	2.1E+00	.742	7.1E-04	.877
2	1.E-03	.00022	1.294	.341	2.3E+00	.743	7.1E-04	.874

Pct Std Deviations	2.3	1.9	119.1	2.5	5.6	2.5	
Correlation Matrix	1.000						
	.546	1.000					
	.971	.383	1.000				
	-.025	-.547	.076	1.000			
	-.260	.130	-.298	-.833	1.000		
	-.639	.101	-.715	-.639	.727	1.000	

Apparent Resistivity Measured at 1 Hz is 146.1

Apparent Resistivity Calculated from Inductive Coupling is 338.0

DWG. NO. - S.I.P. - 1106-4

CYPRUS ANVIL TENAS CK. ROSS RIVER LINE550E 26/9/81 L335 D= 8 N=2 X=152m

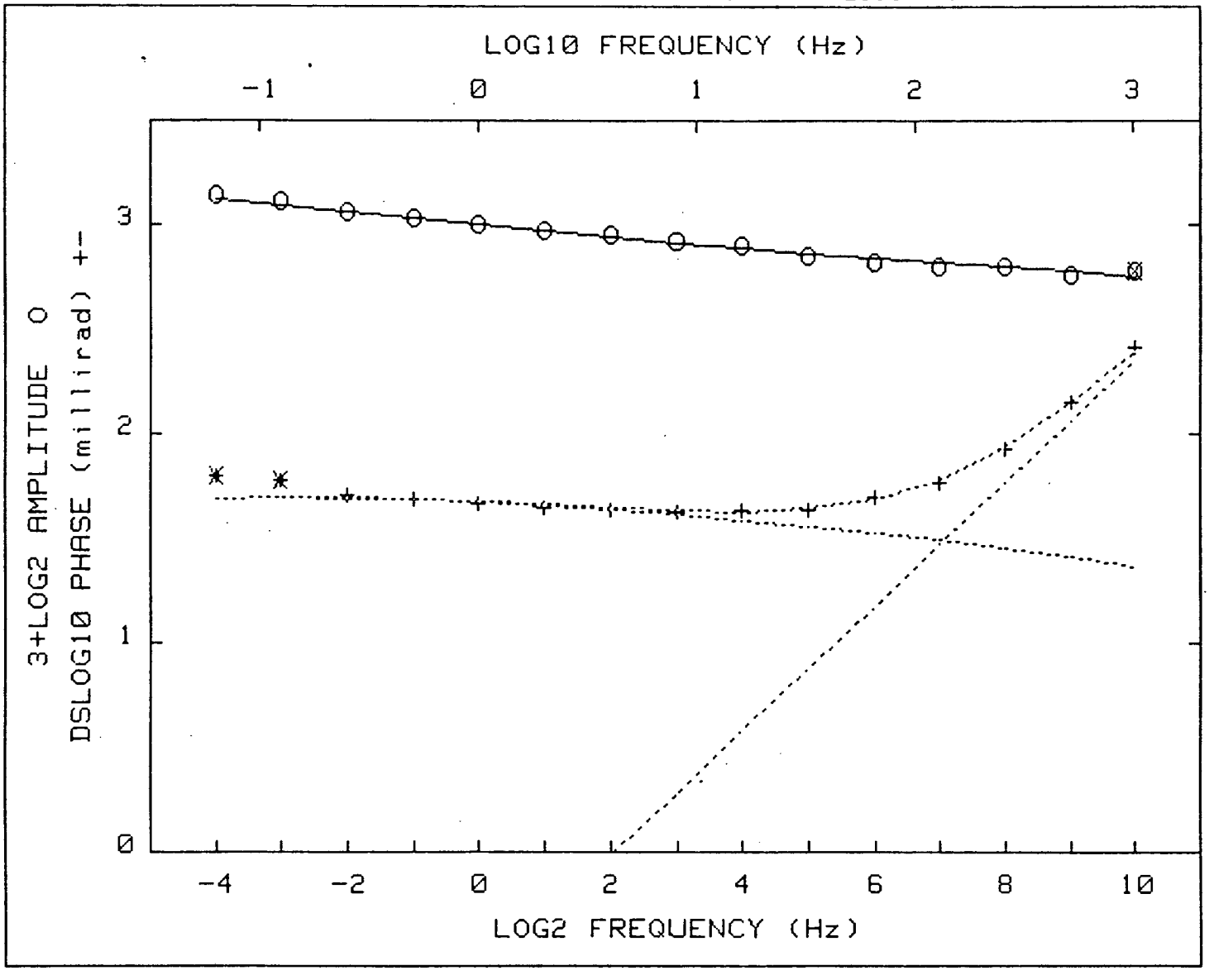

CRL: Number of dispersions= 2
M2=1 fixed

Iter	Lambda	Rchsq	R0	M1	T1	C1	T2	C2
0	1.E-02	.00022	1.345	.393	1.8E+00	.250	2.0E-05	.922
1	1.E-02	.00021	1.354	.404	1.8E+00	.240	2.0E-05	.940
2	1.E-03	.00020	1.383	.424	2.4E+00	.226	2.0E-05	.956
3	1.E-03	.00019	1.401	.433	3.0E+00	.220	2.0E-05	.960
4	1.E-03	.00019	1.417	.441	3.7E+00	.215	2.0E-05	.962
5	1.E-03	.00019	1.430	.448	4.3E+00	.211	2.0E-05	.963
6	1.E-03	.00018	1.442	.454	4.9E+00	.208	2.0E-05	.965
7	1.E-03	.00018	1.453	.459	5.6E+00	.206	2.0E-05	.966

Pct Std Deviations	16.5	28.2	1133.5	34.6	15.6	5.2	
Correlation Matrix	1.000						
	.996	1.000					
	.998	.990	1.000				
	-.988	-.997	-.978	1.000			
	-.816	-.783	-.836	.758	1.000		
	.687	.733	.651	-.759	-.166	1.000	

DWG. NO. - S.I.P. - 1106 - 5

CYPRUS ANVIL TENAS CK. ROSS RIVER LINE550E 26/9/81 L335 D= 8 N=3 X=152m

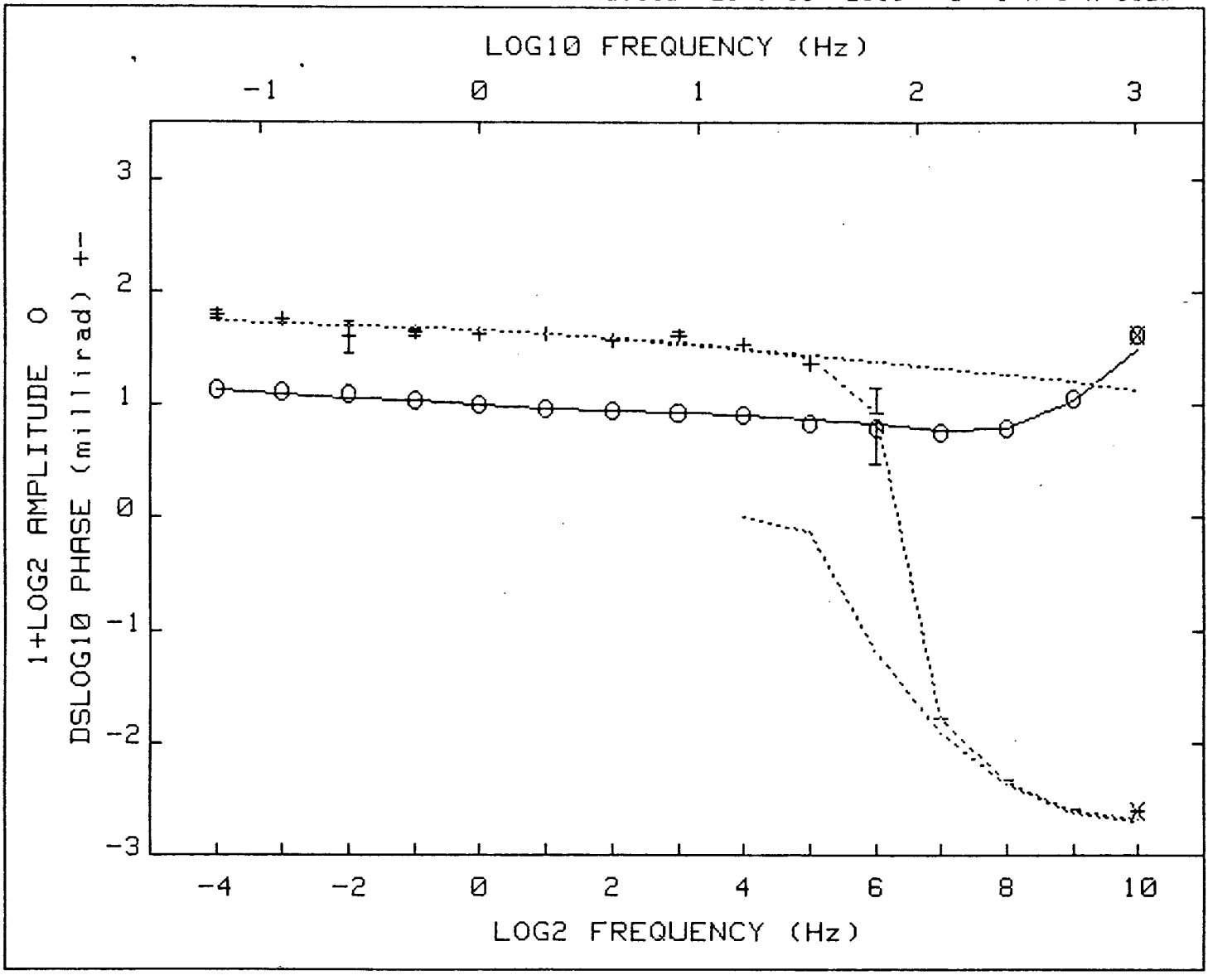

CRL: Number of dispersions= 3 Negative.
C1=.25 C2=1 M3=1 C3=1 fixed

Iter	Lambda	Rchsq	R0	M1	T1	M2	T2	T3
0	1.E-02	.00142	1.466	.418	1.4E+01	.073	1.5E-03	1.0E-04
1	1.E-02	.00142	1.466	.418	1.4E+01	.073	1.5E-03	1.0E-04

Pct Std Deviations	4.9	5.6	131.3	18.6	19.2	10.7	
Correlation Matrix	1.000						
	.974	1.000					
	.965	.922	1.000				
	-.437	-.387	-.463	1.000			
	.397	.317	.467	-.924	1.000		
	-.681	-.632	-.703	.925	-.800	1.000	

Apparent Resistivity Measured at 1 Hz is 36.52

Apparent Resistivity Calculated from Inductive Coupling is 782.6

DWG. NO. - S.I.P - 1106 - 6

CYPRUS ANVIL TENAS CK. ROSS RIVER LINE550E 26/9/81 L335 D= 8 N=4 X=152m

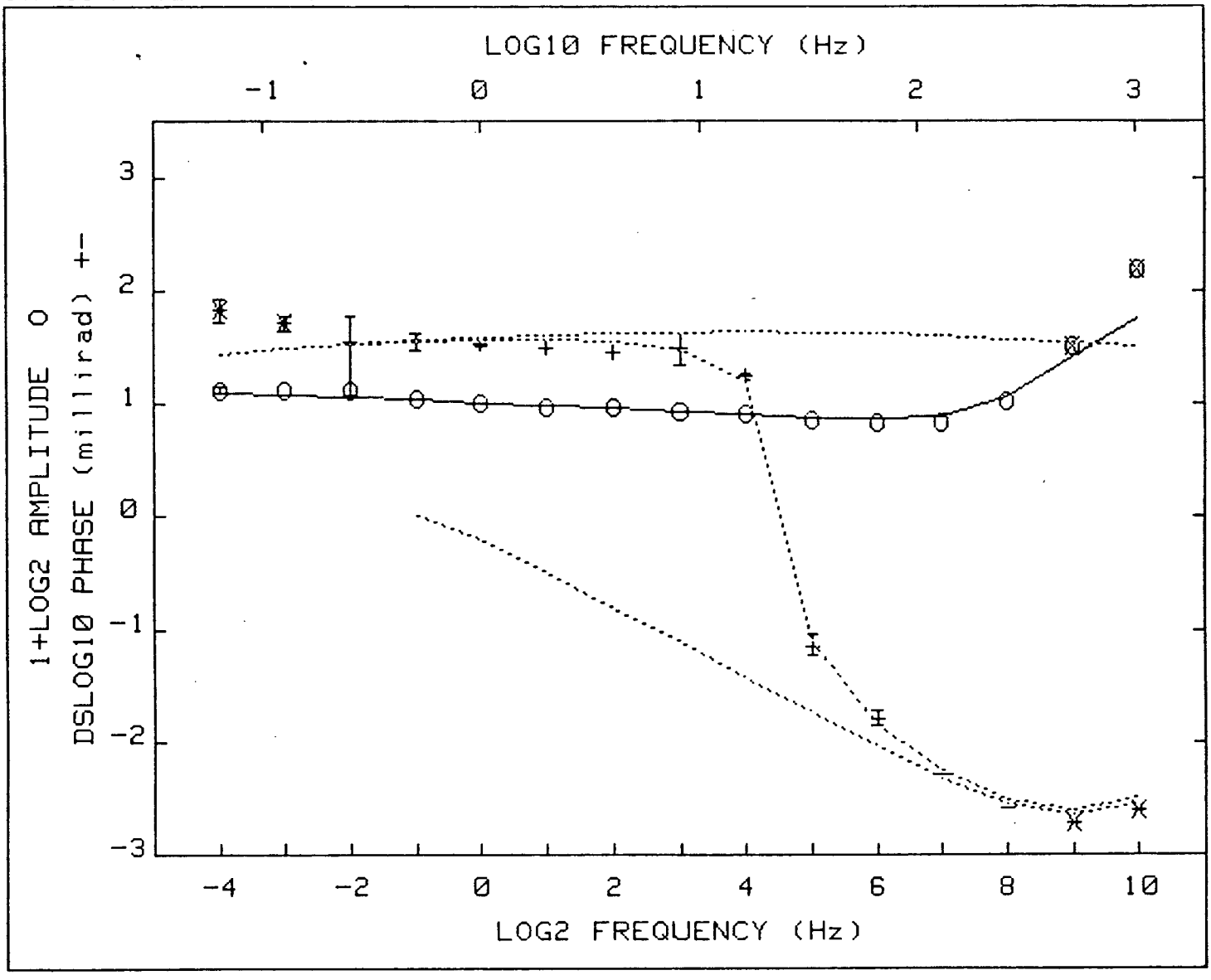

CRL: Number of dispersions= 2 Negative.
C1=.25 M2=1 C2=1 fixed

Iter	Lambda	Rchsq	R0	M1	T1	T2
0	1.E-02	.00660	1.210	.318	3.0E-01	1.9E-04
1	1.E-02	.00340	1.213	.337	1.8E-01	1.8E-04
2	1.E-03	.00267	1.168	.337	4.3E-02	2.1E-04
3	1.E-04	.00244	1.164	.350	2.7E-02	2.2E-04
4	1.E-05	.00244	1.164	.351	2.7E-02	2.2E-04

Pct Std Deviations	2.0	4.8	137.2	7.5	
Correlation Matrix	1.000				
	-.455	1.000			
	.826	-.763	1.000		
	-.674	.885	-.899	1.000	

Apparent Resistivity Measured at 1 Hz is 43.62

Apparent Resistivity Calculated from Inductive Coupling is 642.0

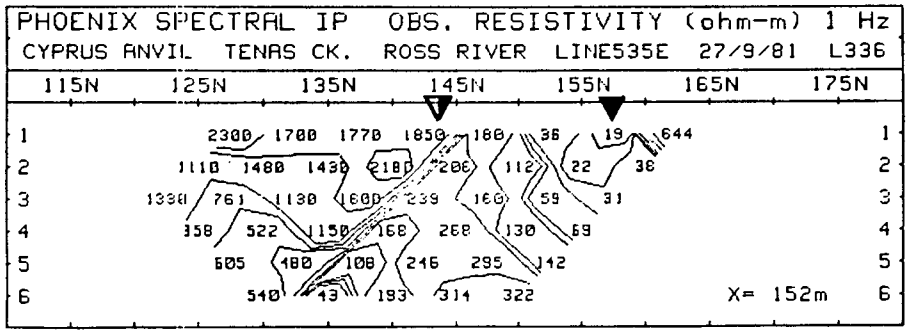
PHOENIX SPECTRAL IP OBS. RESISTIVITY (ohm-m) 1 Hz
CYPRUS ANVIL TENAS CK. ROSS RIVER LINE535E 27/9/81 L336
115N 125N 135N 145N 155N 165N 175N
1 2 3 4 5 6
2300 1700 1770 1850 180 36 19 644
1110 1480 1430 2180 206 112 22 38
1330 761 1130 600 239 160 59 31
358 522 1150 168 268 130 69
505 480 108 246 295 142
540 43 193 314 322
X= 152m

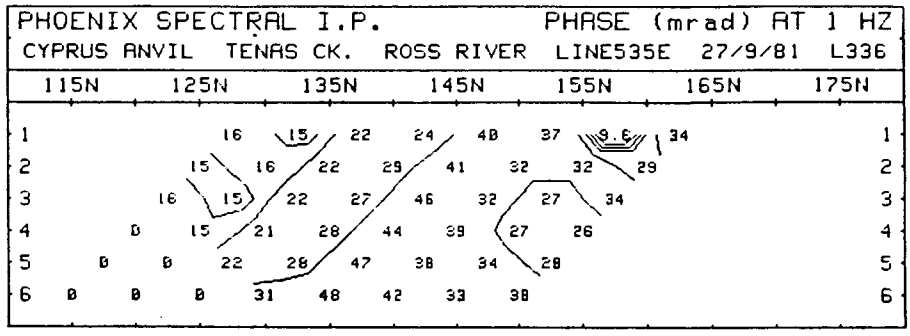
PHOENIX SPECTRAL I.P. PHASE (mrad) AT 1 HZ
CYPRUS ANVIL TENAS CK. ROSS RIVER LINE535E 27/9/81 L336
115N 125N 135N 145N 155N 165N 175N
1 2 3 4 5 6
16 15 22 24 48 37 9.6 34
15 16 22 29 41 32 32 29
16 15 22 27 46 32 27 34
0 15 21 28 44 39 27 26
0 0 22 28 47 38 34 28
0 0 0 31 48 42 33 38

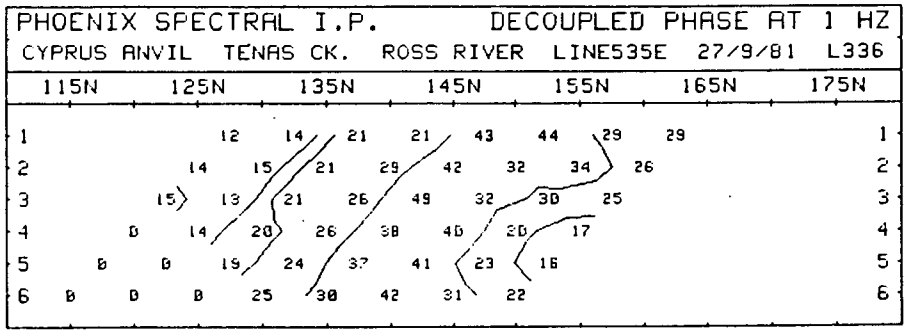
PHOENIX SPECTRAL I.P. DECOUPLED PHASE AT 1 HZ
CYPRUS ANVIL TENAS CK. ROSS RIVER LINE535E 27/9/81 L336
115N 125N 135N 145N 155N 165N 175N
1 2 3 4 5 6
12 14 21 21 43 44 29 29
14 15 21 29 42 32 34 26
15 13 21 26 49 32 30 25
0 14 20 26 38 46 28 17
0 0 19 24 37 41 23 16
0 0 0 25 30 42 31 22

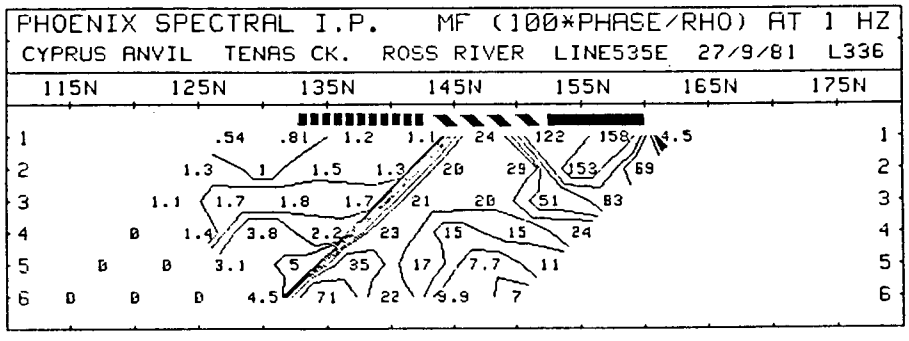
PHOENIX SPECTRAL I.P. MF (100*PHASE/RHO) AT 1 HZ
CYPRUS ANVIL TENAS CK. ROSS RIVER LINE535E 27/9/81 L336
115N 125N 135N 145N 155N 165N 175N
1 2 3 4 5 6
.54 .81 1.2 1.1 24 122 158 4.5
1.3 1 1.5 1.3 20 29 153 69
1.1 1.7 1.8 1.7 21 28 51 83
0 1.4 3.8 2.2 23 15 15 24
0 0 3.1 5 35 17 7.7 11
0 0 0 4.5 71 22 9.9 7

DWG. NO. - S.I.P - 1107 - 2

CYPRUS ANVIL TENAS CK. ROSS RIVER LINE535E 27/9/81 L336 D= 5 N=1 X=152m

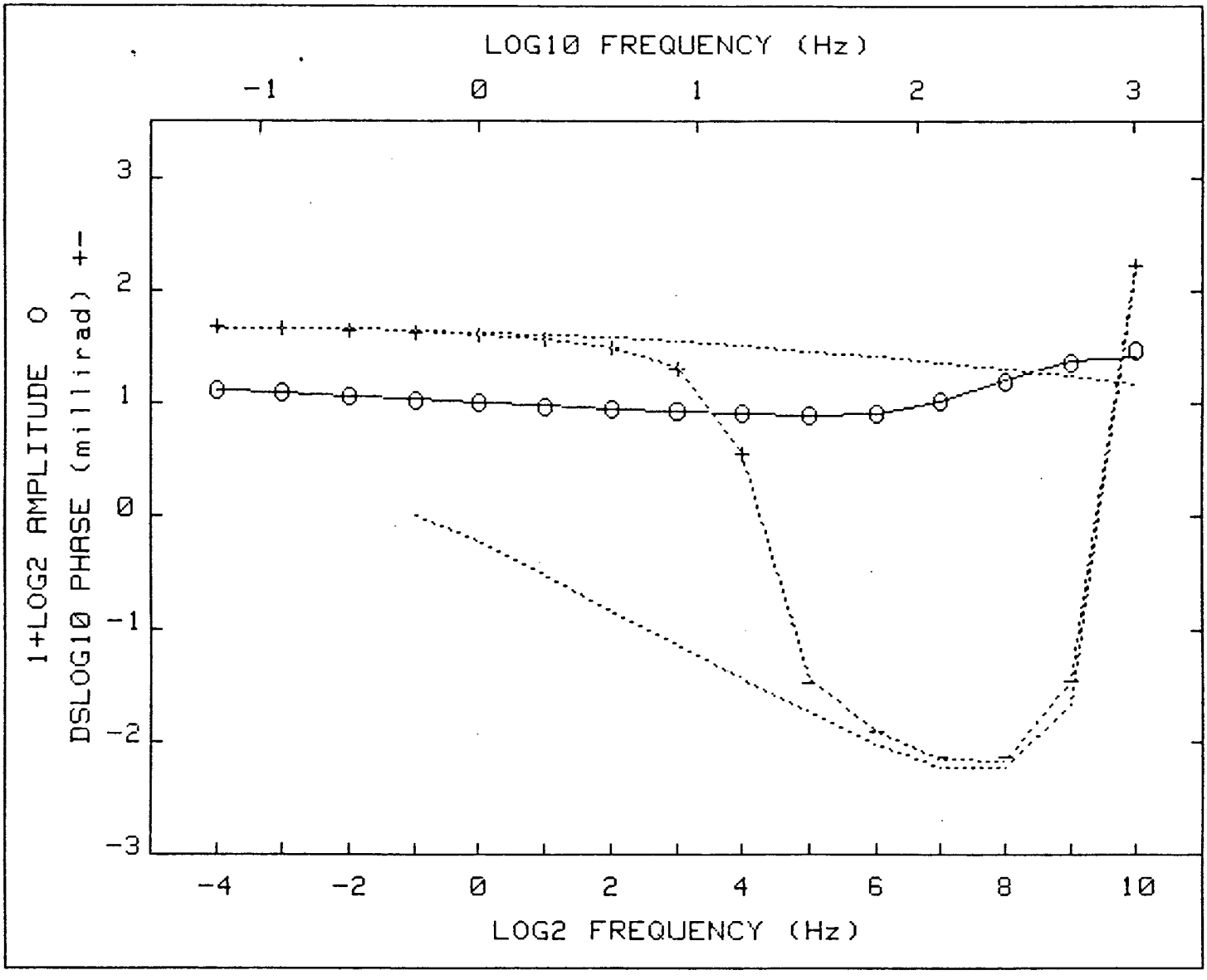

CRL: Number of dispersions= 3 Negative.
C1=.25 M2=1 C2=1 C3=1 fixed

Iter	Lambda	Rchsq	R0	M1	T1	T2	M3	T3
0	1.E-02	.00856	1.506	.456	2.7E+01	3.8E-05	.375	5.8E-04
1	1.E-02	.00077	1.457	.412	1.7E+01	4.2E-05	.385	5.4E-04
2	1.E-03	.00048	1.355	.375	4.9E+00	4.4E-05	.417	5.6E-04
3	1.E-04	.00033	1.349	.372	3.8E+00	4.4E-05	.420	5.7E-04
4	1.E-05	.00033	1.349	.372	3.7E+00	4.4E-05	.420	5.7E-04

	R0	M1	T1	T2	M3	T3
Pct Std Deviations	1.3	1.8	28.9	5.1	3.0	2.3

Correlation Matrix

	1.000					
	.925	1.000				
	.940	.863	1.000			
	-.184	-.210	-.086	1.000		
	-.476	-.442	-.428	.919	1.000	
	-.298	-.168	-.459	-.785	-.534	1.000

Apparent Resistivity Measured at 1 Hz is 179.8

Apparent Resistivity Calculated from Inductive Coupling is 397.5

DWG. NO. – S.I.P. – 1107 – 3

CYPRUS ANVIL TENAS CK. ROSS RIVER LINE535E 27/9/81 L336 D= 5 N=2 X=152m

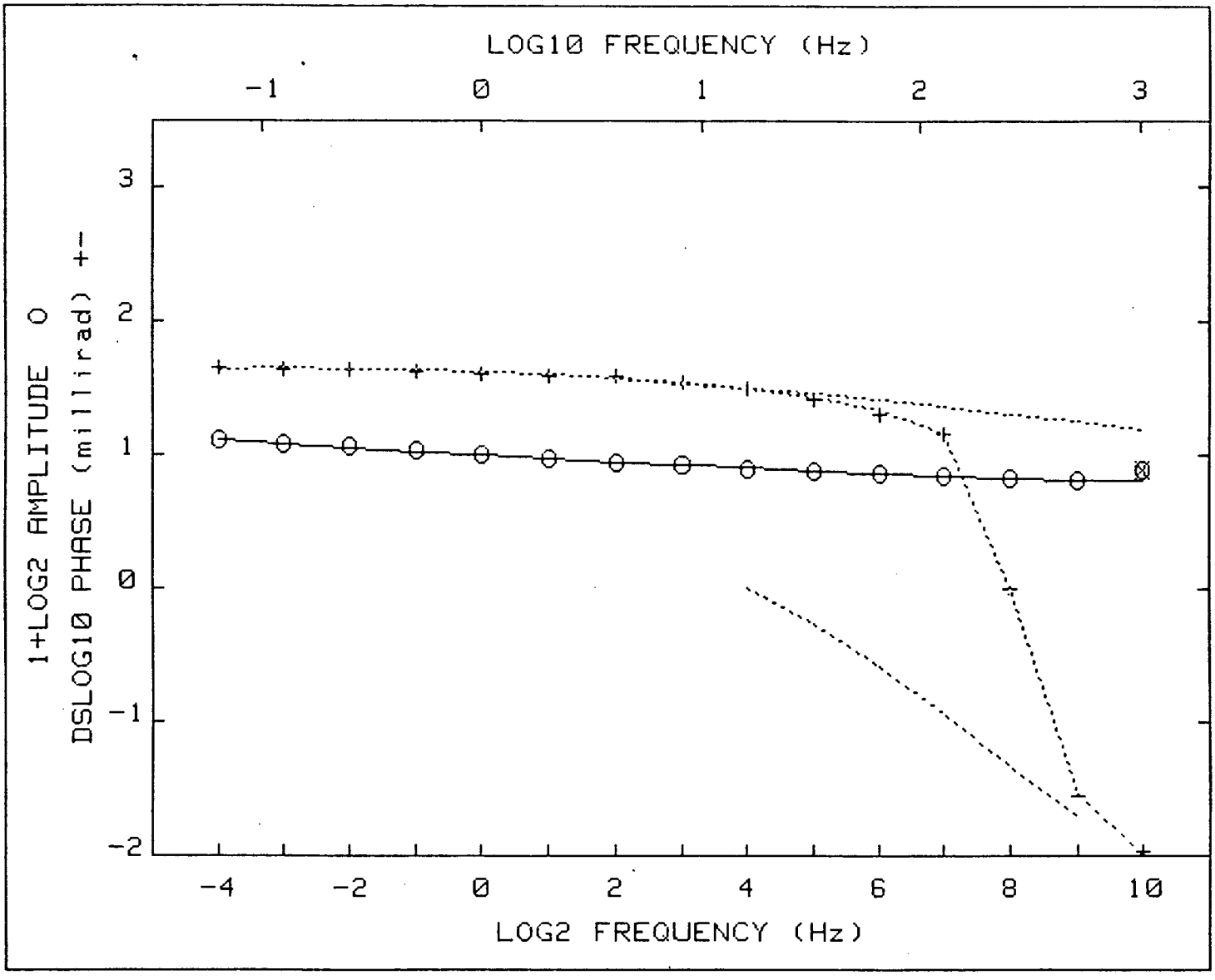

CRL: Number of dispersions= 3 Negative.
C1=.25 C2=1 M3=1 C3=1 fixed

Iter	Lambda	Rchsq	R0	M1	T1	M2	T2	T3
0	1.E-02	.00046	1.317	.357	2.4E+00	.012	8.3E-04	1.3E-05
1	1.E-02	.00019	1.317	.361	2.5E+00	.011	6.0E-04	1.2E-05
2	1.E-03	.00017	1.321	.362	2.7E+00	.011	5.3E-04	1.2E-05
3	1.E-01	.00017	1.321	.362	2.7E+00	.011	5.3E-04	1.2E-05

Pct Std Deviations	.8	1.2	20.6	3.7	15.8	2.4	
Correlation Matrix	1.000						
	.898	1.000					
	.905	.775	1.000				
	-.885	-.986	-.764	1.000			
	.607	.414	.753	-.414	1.000		
	-.765	-.668	-.835	.664	-.578	1.000	

Apparent Resistivity Measured at 1 Hz is 206.3

Apparent Resistivity Calculated from Inductive Coupling is 7673

DWG. NO. - S.I.P - 1107 - 4

CYPRUS ANVIL TENAS CK. ROSS RIVER LINE535E 27/9/81 L336 D= 5 N=3 X=152m

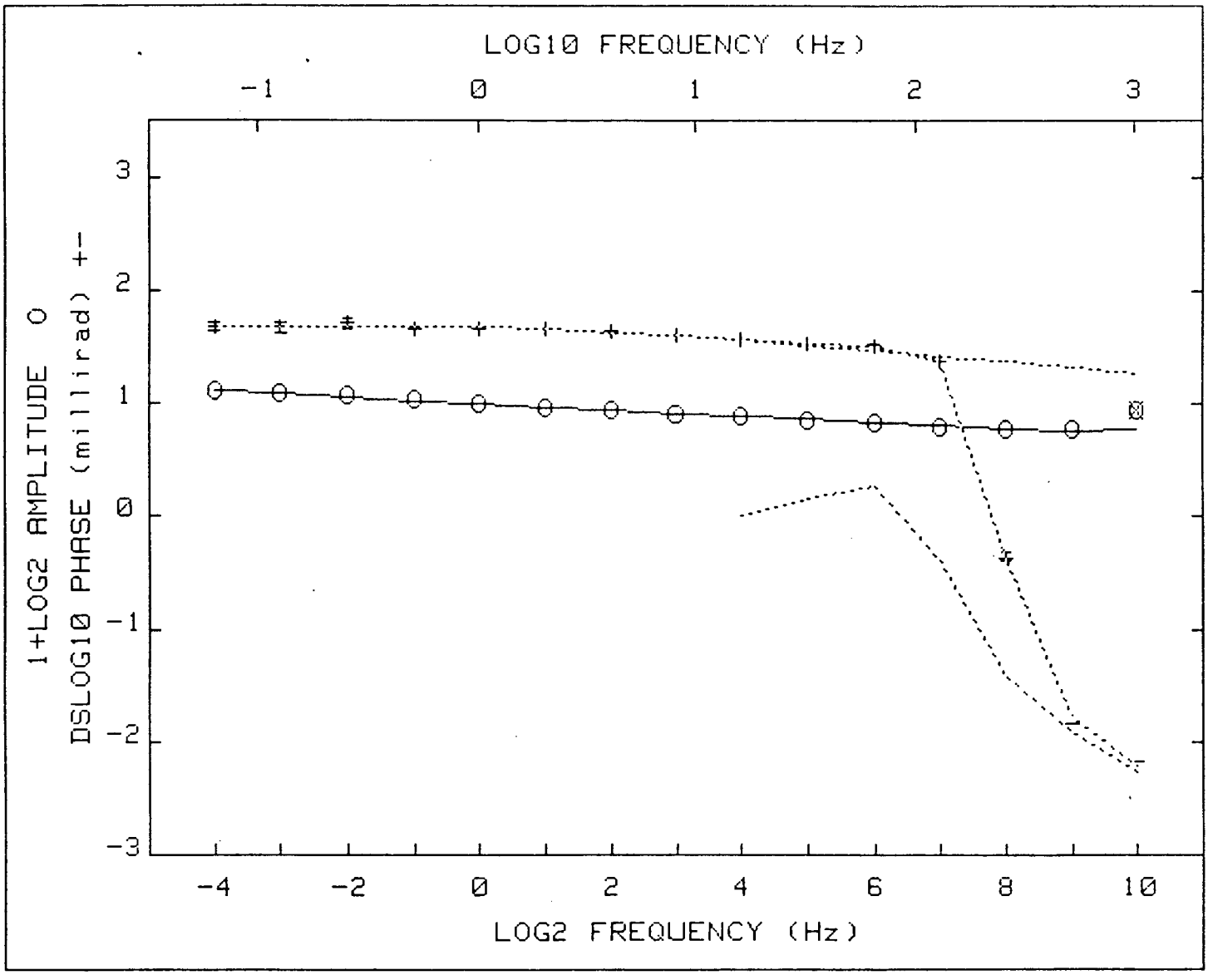

CRL: Number of dispersions= 3 Negative.
C1=.25 C2=1 M3=1 C3=1 fixed

Iter	Lambda	Rchsq	R0	M1	T1	M2	T2	T3
0	1.E-02	.00039	1.355	.387	2.4E+00	.029	8.6E-04	1.9E-05
1	1.E-02	.00031	1.347	.389	2.3E+00	.029	8.5E-04	1.9E-05
2	1.E-03	.00031	1.344	.389	2.2E+00	.029	8.5E-04	1.9E-05

Pct Std Deviations	1.3	1.5	32.3	7.1	9.5	3.7	
Correlation Matrix	1.000						
	.871	1.000					
	.914	.718	1.000				
	.159	-.016	.262	1.000			
	.301	.123	.399	-.353	1.000		
	-.466	-.382	-.505	.644	-.815	1.000	

Apparent Resistivity Measured at 1 Hz is 239.0

Apparent Resistivity Calculated from Inductive Coupling is 3482

CYPRUS ANVIL TENAS CK. ROSS RIVER LINE535E 27/9/81 L336 D= 5 N=4 X=152m

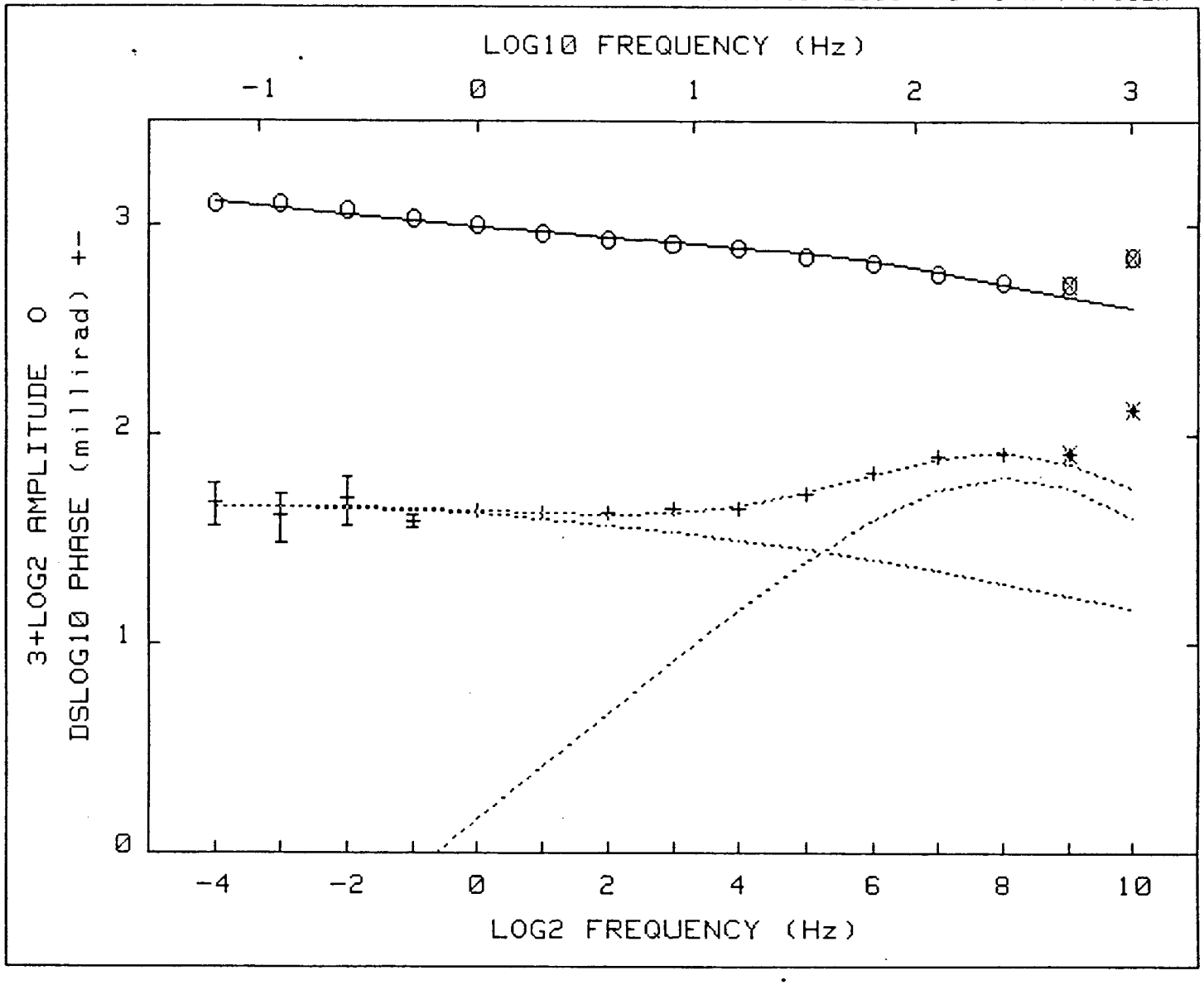

CRL: Number of dispersions= 2
C1=.25 fixed

Iter	Lambda	Rchsq	R0	M1	T1	M2	T2	C2
0	1.E-02	.00059	1.310	.367	1.7E+00	.076	9.3E-04	1.000
1	1.E-02	.00055	1.310	.366	1.8E+00	.082	8.6E-04	.938
2	1.E-03	.00053	1.321	.365	2.4E+00	.091	7.8E-04	.880
3	1.E-04	.00052	1.333	.367	3.2E+00	.097	7.3E-04	.843
4	1.E-05	.00052	1.337	.367	3.5E+00	.099	7.1E-04	.831

Pct Std Deviations	2.4	2.3	101.4	22.2	30.7	13.6	
Correlation Matrix	1.000						
	.712	1.000					
	.948	.522	1.000				
	.547	-.001	.675	1.000			
	-.305	.037	-.389	-.882	1.000		
	-.583	-.032	-.701	-.958	.829	1.000	

Apparent Resistivity Measured at 1 Hz is 167.7

Apparent Resistivity Calculated from Inductive Coupling is 1073

DWG. NO. - S.I.P. - 1107-6

CYPRUS ANVIL TENAS CK. ROSS RIVER LINE535E 27/9/81 L336 D= 5 N=5 X=152m

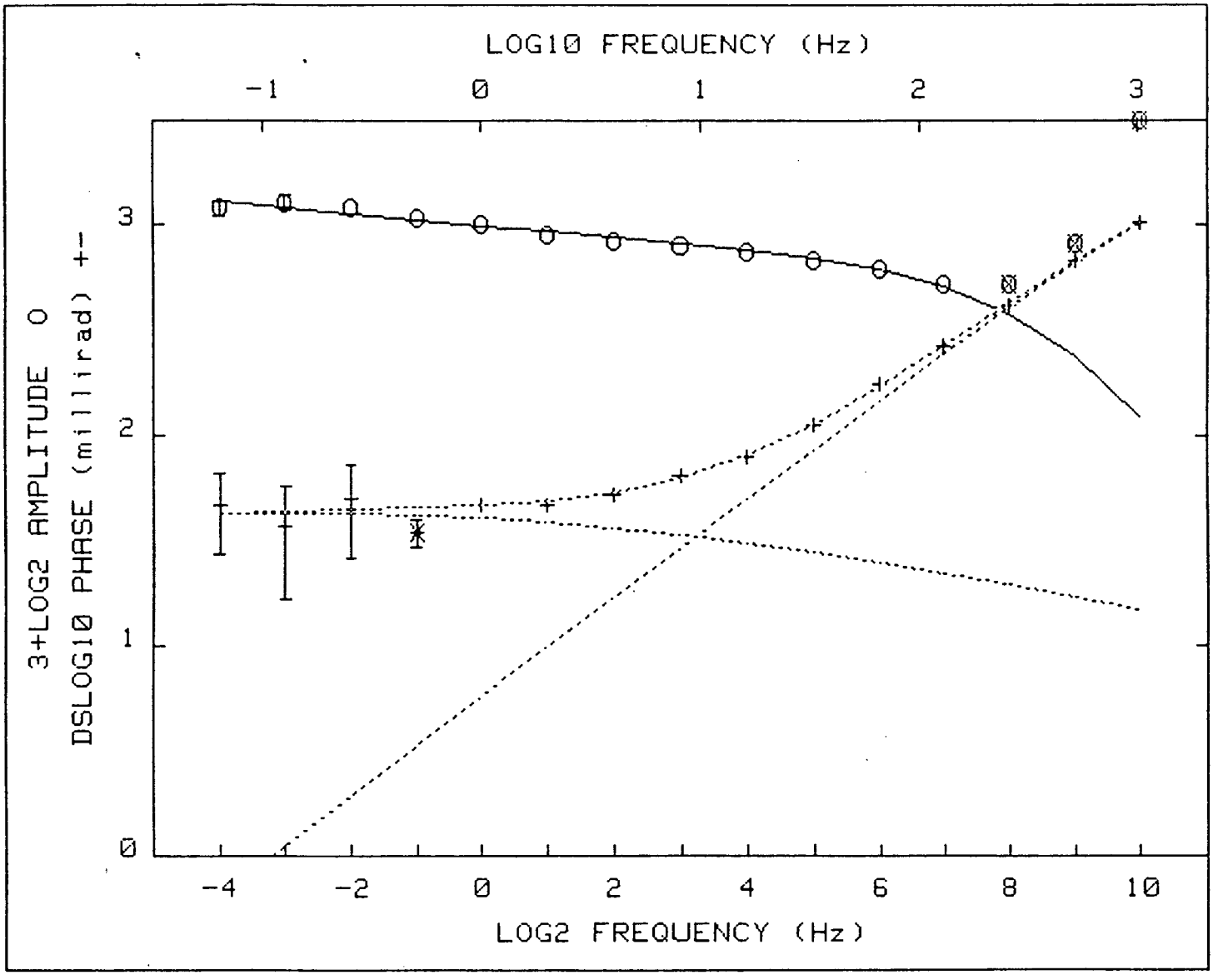

CRL: Number of dispersions= 2
C1=.25 M2=1 fixed

Iter	Lambda	Rchsq	R0	M1	T1	T2	C2
0	1.E-02	.00076	1.321	.342	4.7E+00	1.4E-04	.743
1	1.E-02	.00067	1.332	.354	4.5E+00	1.4E-04	.749
2	1.E-03	.00066	1.320	.353	3.4E+00	1.4E-04	.755
3	1.E-04	.00066	1.309	.351	2.5E+00	1.4E-04	.762
Pct Std Deviations			2.8	2.8	137.3	6.2	3.5

Correlation Matrix

1.000					
.668	1.000				
.949	.471	1.000			
-.599	-.477	-.544	1.000		
-.669	-.080	-.751	.652	1.000	

Apparent Resistivity Measured at 1 Hz is 108.3

Apparent Resistivity Calculated from Inductive Coupling is 558.0

DWG. NO. - S.I.P. - 1107 - 7

CYPRUS ANVIL TENAS CK. ROSS RIVER LINE535E 27/9/81 L336 D= 5 N=6 X=152m

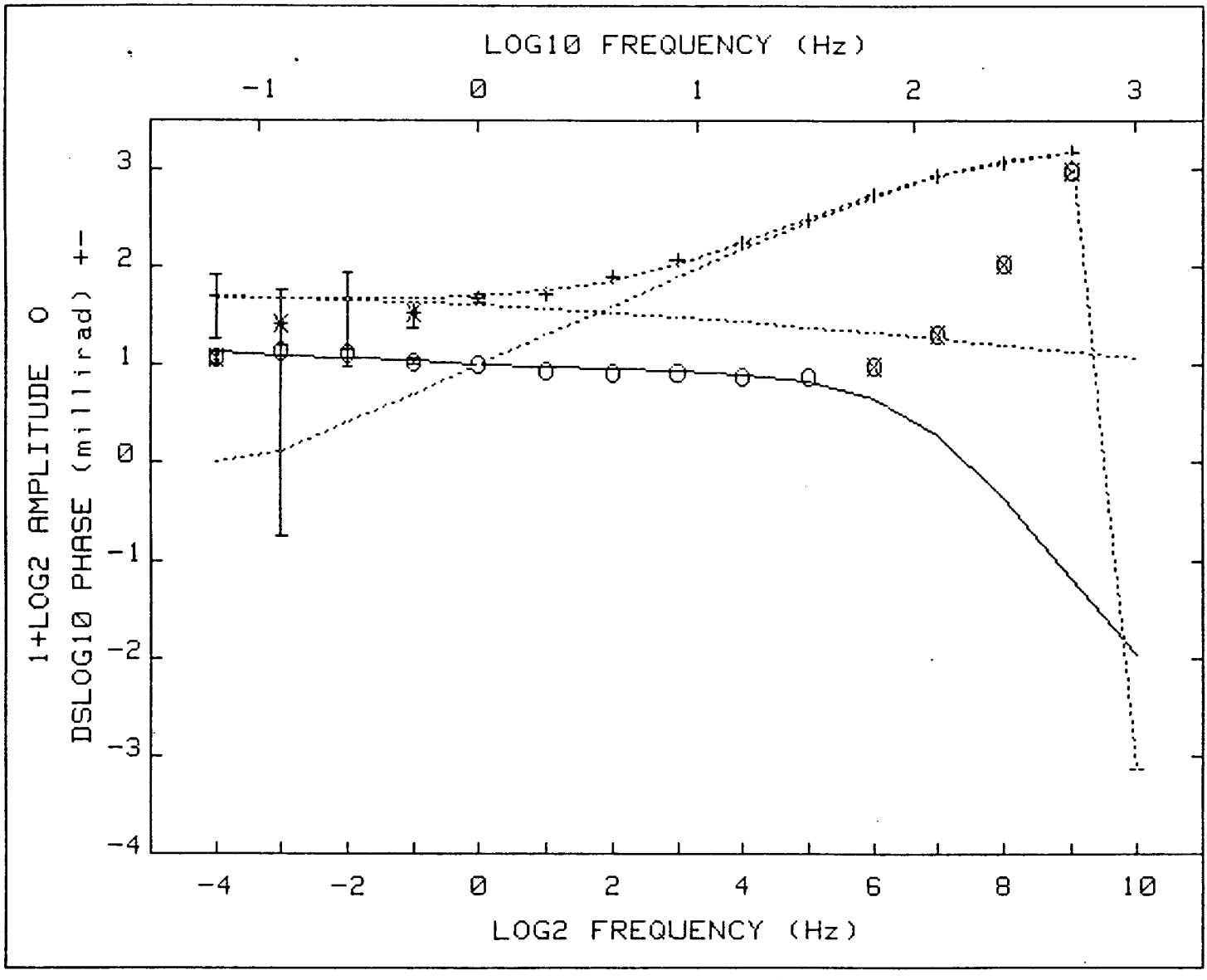

CRL: Number of dispersions= 2
C1=.25 fixed

Iter	Lambda	Rchsq	R0	M1	T1	M2	T2	C2
0	1.E-02	.00087	1.445	.392	1.8E+01	.667	1.4E-03	.953
1	1.E-02	.00085	1.451	.394	1.8E+01	.660	1.4E-03	.957
2	1.E-03	.00085	1.449	.394	1.7E+01	.661	1.4E-03	.958

Pct Std Deviations	7.0	7.7	318.9	5.4	6.6	3.4	
Correlation Matrix	1.000						
	.961	1.000					
	.975	.896	1.000				
	-.869	-.931	-.804	1.000			
	-.070	-.019	-.076	-.276	1.000		
	-.543	-.376	-.611	.128	.573	1.000	

Apparent Resistivity Measured at 1 Hz is 42.72

Apparent Resistivity Calculated from Inductive Coupling is 260.8

DWG. NO. - S.I.P. - 1107-8

CYPRUS ANVIL TENAS CK. ROSS RIVER LINE535E 27/9/81 L336 D= 6 N=1 X=152m

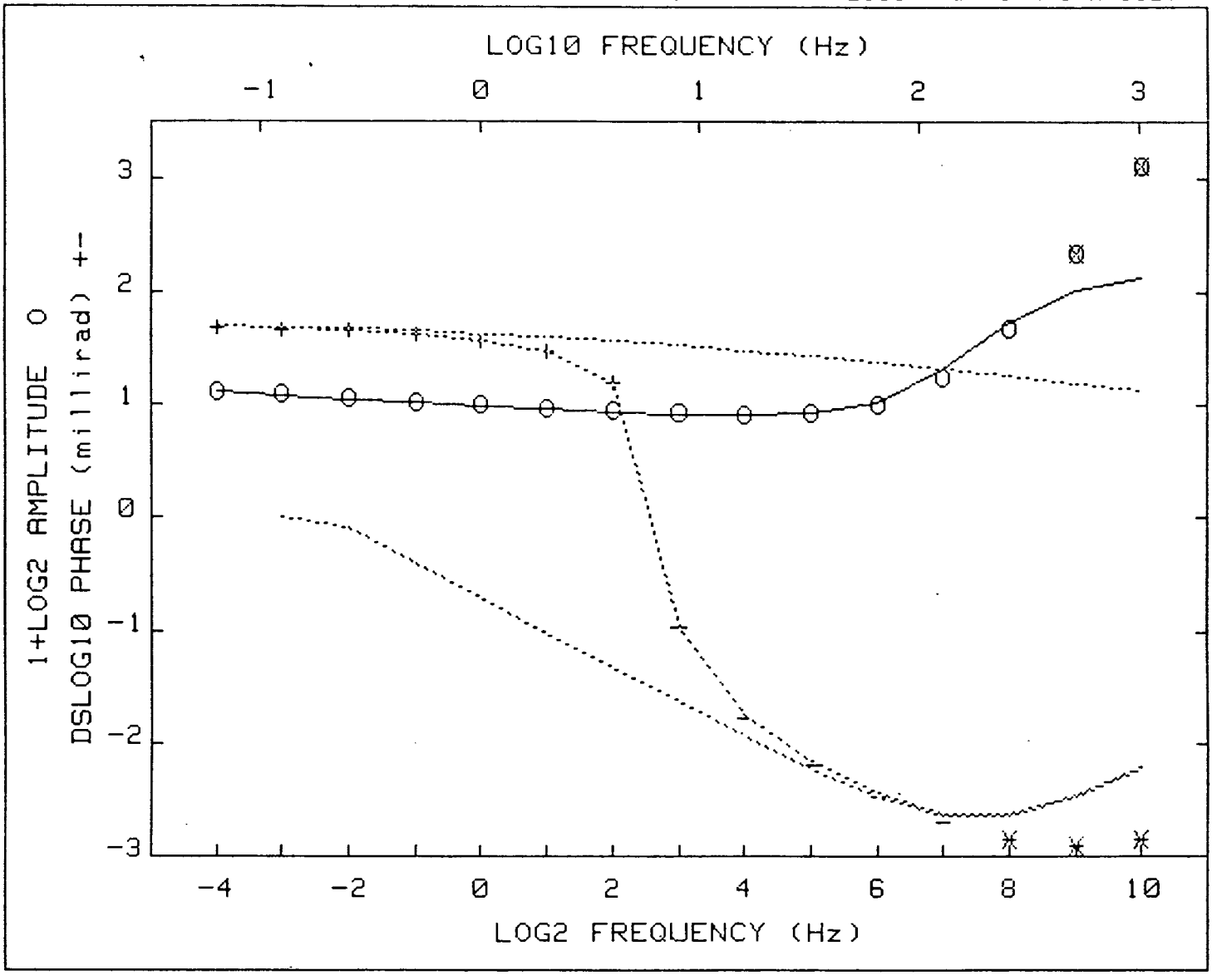

CRL: Number of dispersions= 2 Negative.
C1=.25 M2=1 fixed

Iter	Lambda	Rchsq	R0	M1	T1	T2	C2
0	1.E-02	.00167	1.275	.367	1.0E+00	6.3E-04	.963
1	1.E-02	.00146	1.295	.368	1.5E+00	6.1E-04	.968
2	1.E-03	.00117	1.347	.374	5.0E+00	5.8E-04	.988
3	1.E-04	.00107	1.386	.390	8.7E+00	5.6E-04	.993
4	1.E-05	.00107	1.395	.393	9.4E+00	5.6E-04	.993

Pct Std Deviations	3.6	4.3	103.5	5.8	1.8	
Correlation Matrix	1.000					
	.936	1.000				
	.952	.845	1.000			
	-.786	-.758	-.729	1.000		
	.324	.131	.508	.160	1.000	

Apparent Resistivity Measured at 1 Hz is 35.76

Apparent Resistivity Calculated from Inductive Coupling is 30.36

DWG. NO. - S.I.P - 1107 - 9

CYPRUS ANVIL TENAS CK. ROSS RIVER LINE535E 27/9/81 L336 D= 7 N=1 X=152m

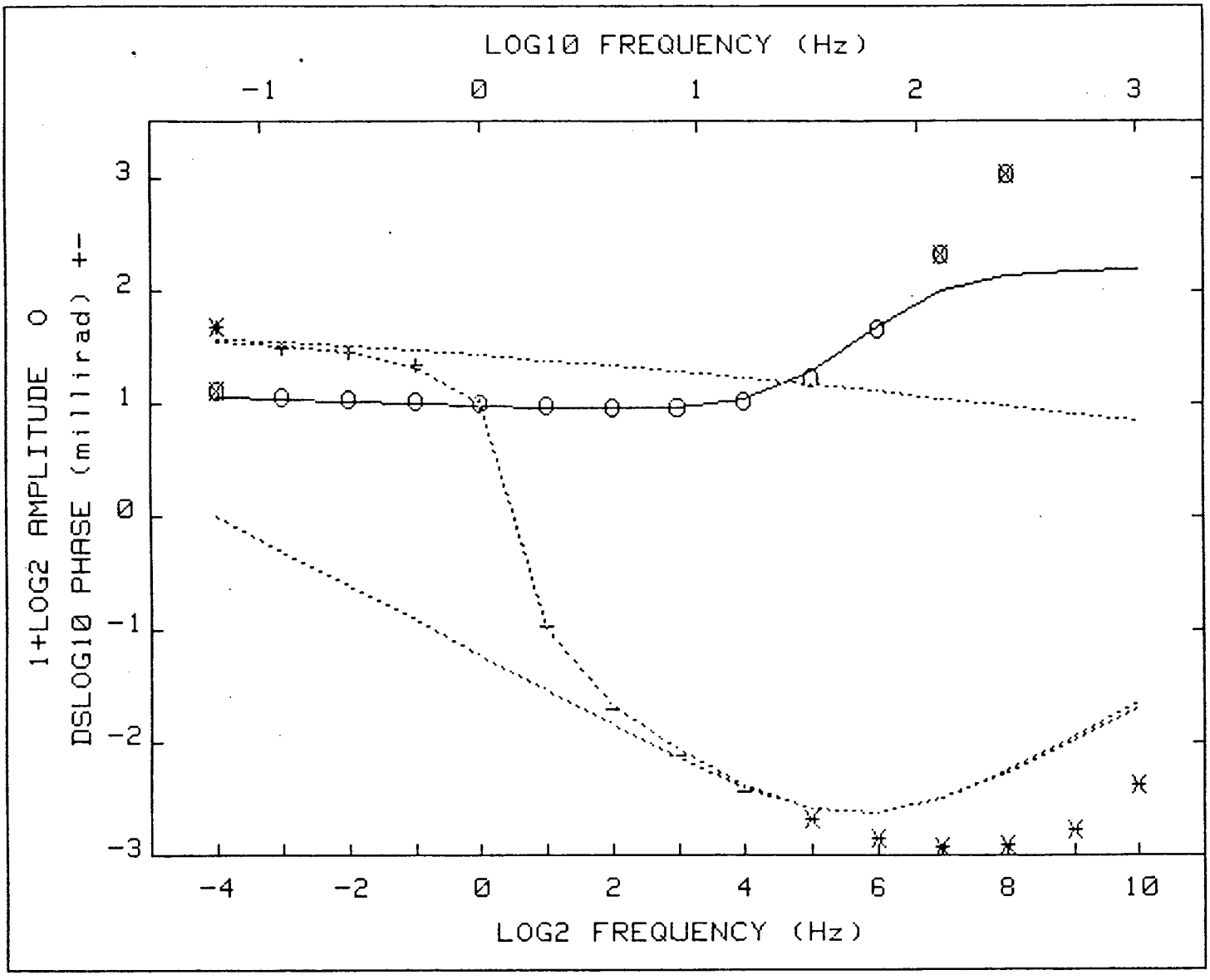

CRL: Number of dispersions= 2 Negative.
C1=.25 M2=1 C2=1 fixed

Iter	Lambda	Rchsq	R0	M1	T1	T2
0	1.E-02	.00123	1.330	.318	4.4E+01	2.0E-03
1	1.E-02	.00113	1.340	.324	4.5E+01	2.0E-03
2	1.E-03	.00112	1.352	.329	5.4E+01	2.0E-03

Pct Std Deviations 7.8 14.5 345.1 10.8

Correlation Matrix

1.000				
.992	1.000			
.992	.988	1.000		
-.967	-.951	-.980	1.000	

Apparent Resistivity Measured at 1 Hz is 18.63

Apparent Resistivity Calculated from Inductive Coupling is 8.816

DWG. NO. - S.I.P. - 1107 - 10

CYPRUS ANVIL TENAS CK. ROSS RIVER LINE535E 27/9/81 L336 D= 7 N=2 X=152m

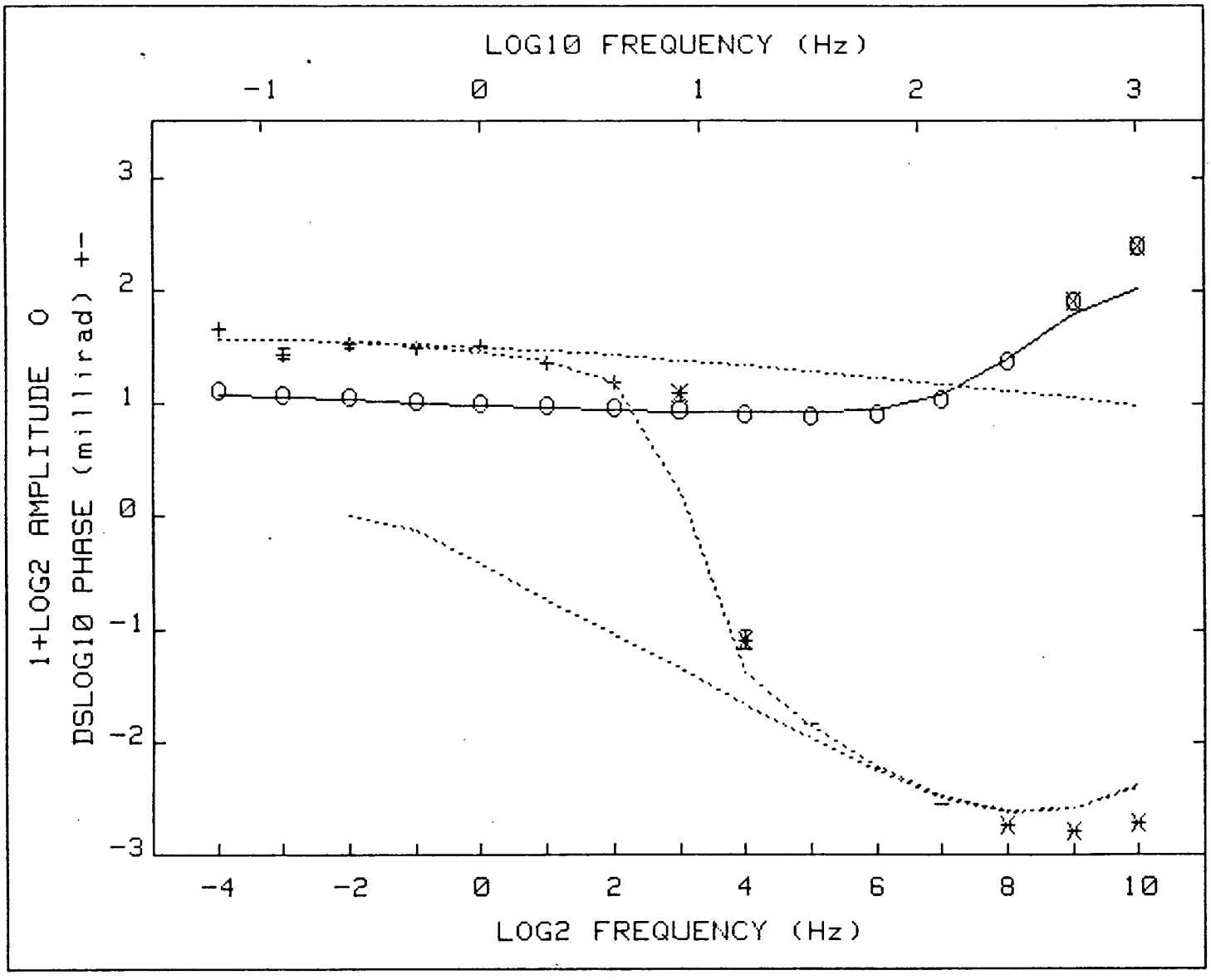

CRL: Number of dispersions= 2 Negative.
C1=.25 M2=1 C2=1 fixed

Iter	Lambda	Rchsq	R0	M1	T1	T2
0	1.E-02	.00337	1.248	.296	2.5E+00	3.1E-04
1	1.E-02	.00225	1.246	.295	3.3E+00	3.5E-04
2	1.E-03	.00211	1.275	.307	6.9E+00	3.4E-04
3	1.E-04	.00208	1.294	.315	9.6E+00	3.3E-04
4	1.E-05	.00208	1.297	.316	1.0E+01	3.3E-04

Pct Std Deviations	4.1	7.3	155.9	7.4	
Correlation Matrix	1.000				
	.957	1.000			
	.953	.925	1.000		
	-.751	-.668	-.760	1.000	

Apparent Resistivity Measured at 1 Hz is 21.92

Apparent Resistivity Calculated from Inductive Coupling is 137.2

DWG. NO. - S.I.P - 1107-11

CYPRUS ANVIL TENAS CK. ROSS RIVER LINE535E 27/9/81 L336 D= 8 N=3 X=152m

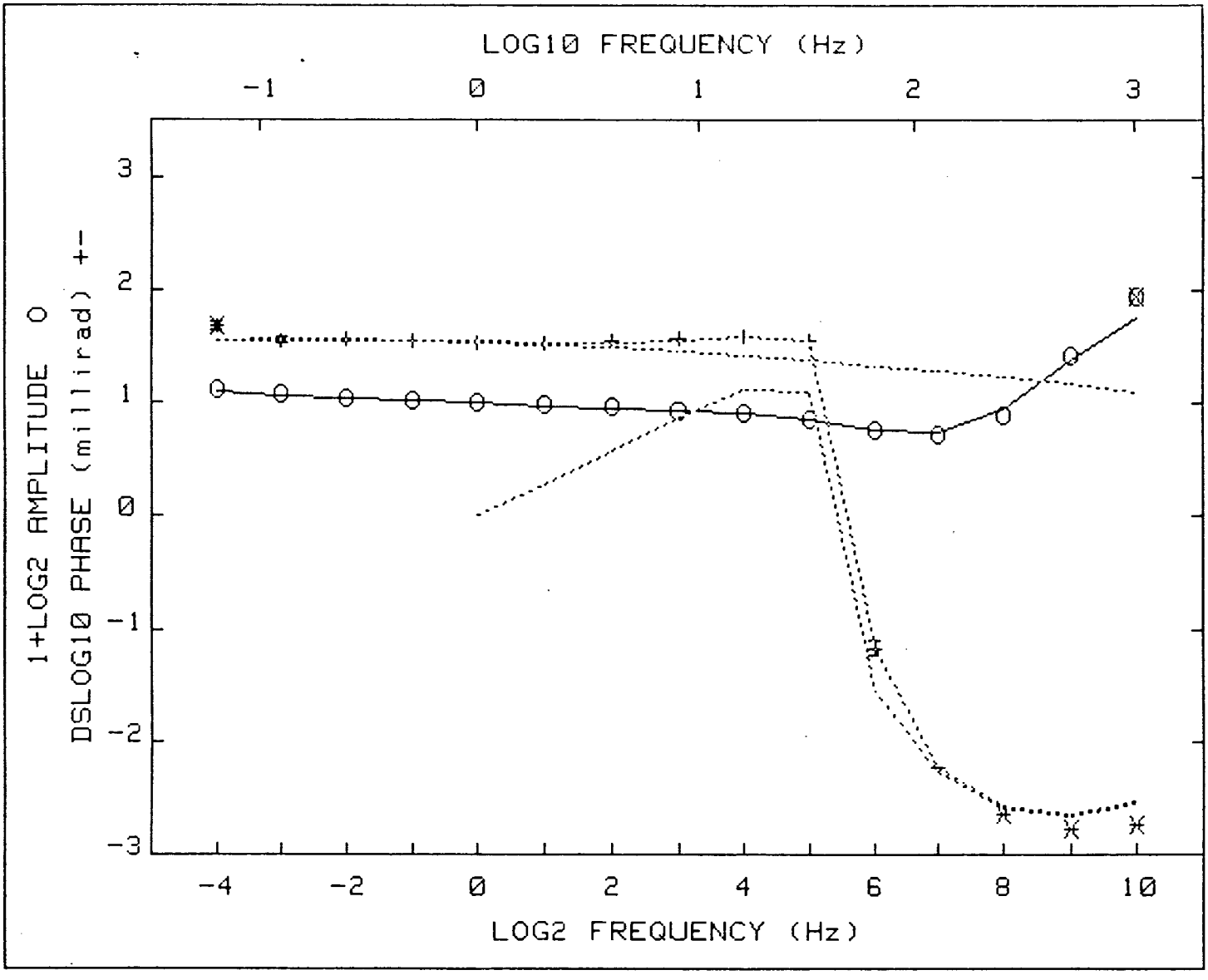

CRL: Number of dispersions= 3 Negative.
C1=.25 C2=1 M3=1 C3=1 fixed

Iter	Lambda	Rchsq	R0	M1	T1	M2	T2	T3
0	1.E-02	.02331	1.478	.476	3.4E+01	.105	2.5E-03	2.0E-04
1	1.E-02	.00238	1.365	.368	2.8E+01	.124	2.8E-03	2.0E-04
2	1.E-03	.00056	1.311	.328	1.1E+01	.126	2.8E-03	2.1E-04
3	1.E-04	.00045	1.243	.300	2.5E+00	.132	2.7E-03	2.3E-04
4	1.E-05	.00040	1.246	.304	2.1E+00	.130	2.6E-03	2.3E-04
5	1.E-02	.00040	1.246	.304	2.1E+00	.130	2.6E-03	2.3E-04

	R0	M1	T1	M2	T2	T3
Pct Std Deviations	1.9	2.6	84.0	6.0	6.0	5.0

Correlation Matrix

1.000						
.875	1.000					
.955	.772	1.000				
-.354	-.270	-.311	1.000			
.483	.233	.520	-.804	1.000		
-.628	-.467	-.620	.931	-.867	1.000	

Apparent Resistivity Measured at 1 Hz is 30.72

Apparent Resistivity Calculated from Inductive Coupling is 248.3

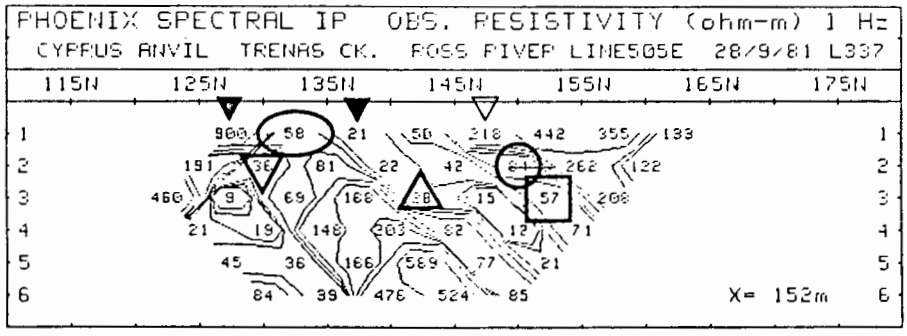
PHOENIX SPECTRAL IP OBS. RESISTIVITY (ohm-m) 1 Hz
CYPRUS ANVIL TRENAS CK. ROSS RIVER LINE505E 28/9/81 L337
115N 125N 135N 145N 155N 165N 175N
X= 152m

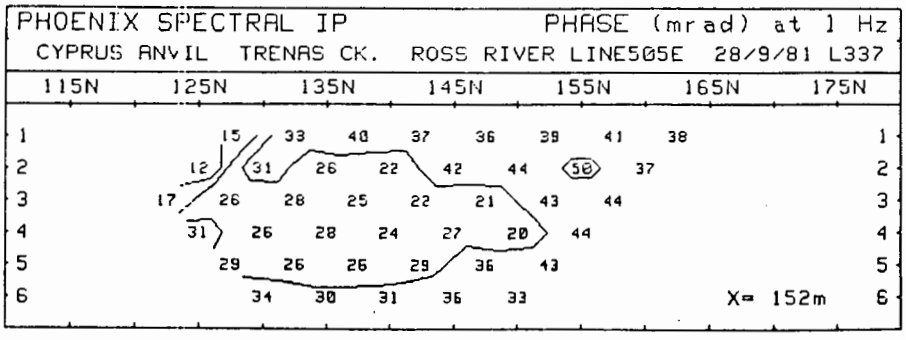
PHOENIX SPECTRAL IP PHASE (mrad) at 1 Hz
CYPRUS ANVIL TRENAS CK. ROSS RIVER LINE505E 28/9/81 L337
115N 125N 135N 145N 155N 165N 175N
X= 152m

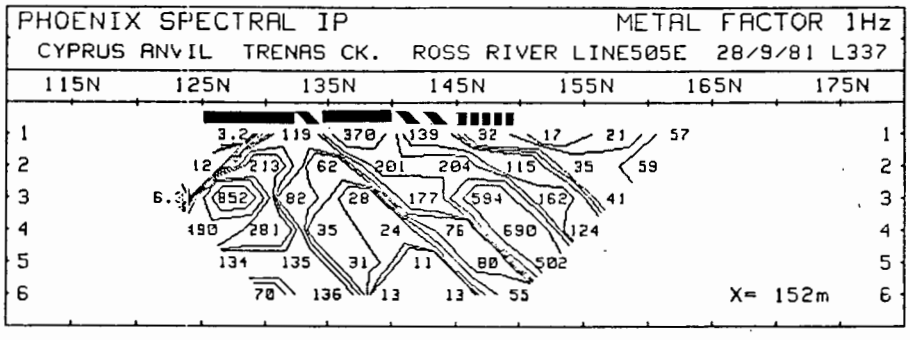
PHOENIX SPECTRAL IP METAL FACTOR 1Hz
CYPRUS ANVIL TRENAS CK. ROSS RIVER LINE505E 28/9/81 L337
115N 125N 135N 145N 155N 165N 175N
X= 152m

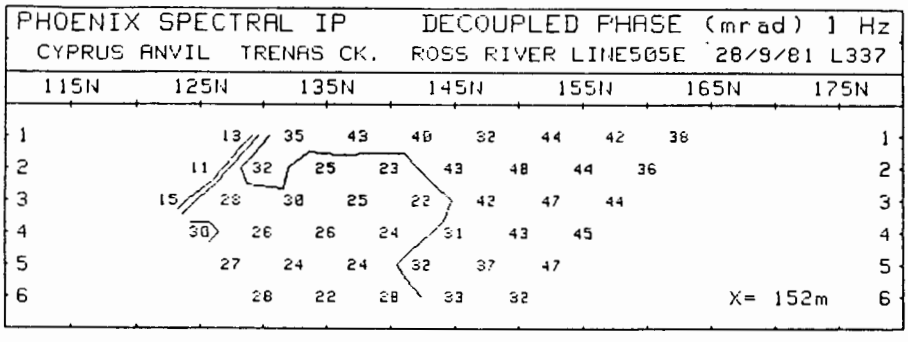
PHOENIX SPECTRAL IP DECOUPLED PHASE (mrad) 1 Hz
CYPRUS ANVIL TRENAS CK. ROSS RIVER LINE505E 28/9/81 L337
115N 125N 135N 145N 155N 165N 175N
X= 152m

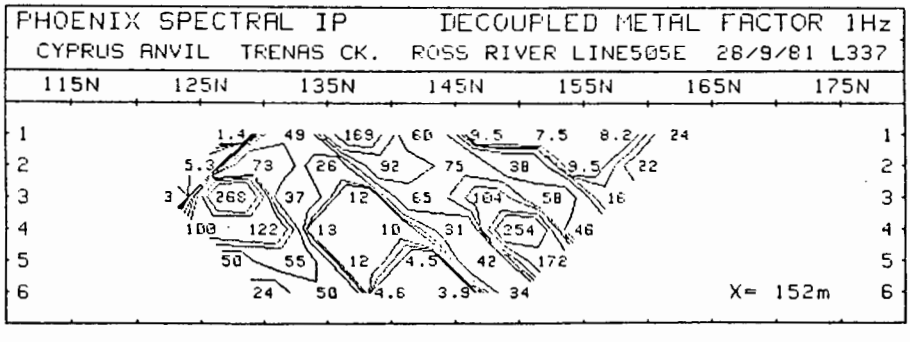
PHOENIX SPECTRAL IP DECOUPLED METAL FACTOR 1Hz
CYPRUS ANVIL TRENAS CK. ROSS RIVER LINE505E 28/9/81 L337
115N 125N 135N 145N 155N 165N 175N
X= 152m

DWG. NO. - S.I.P. - 1108 - 2

CYPRUS ANVIL TRENAS CK. ROSS RIVER LINE505E 28/9/81 L337 D= 2 N=1 X=152m

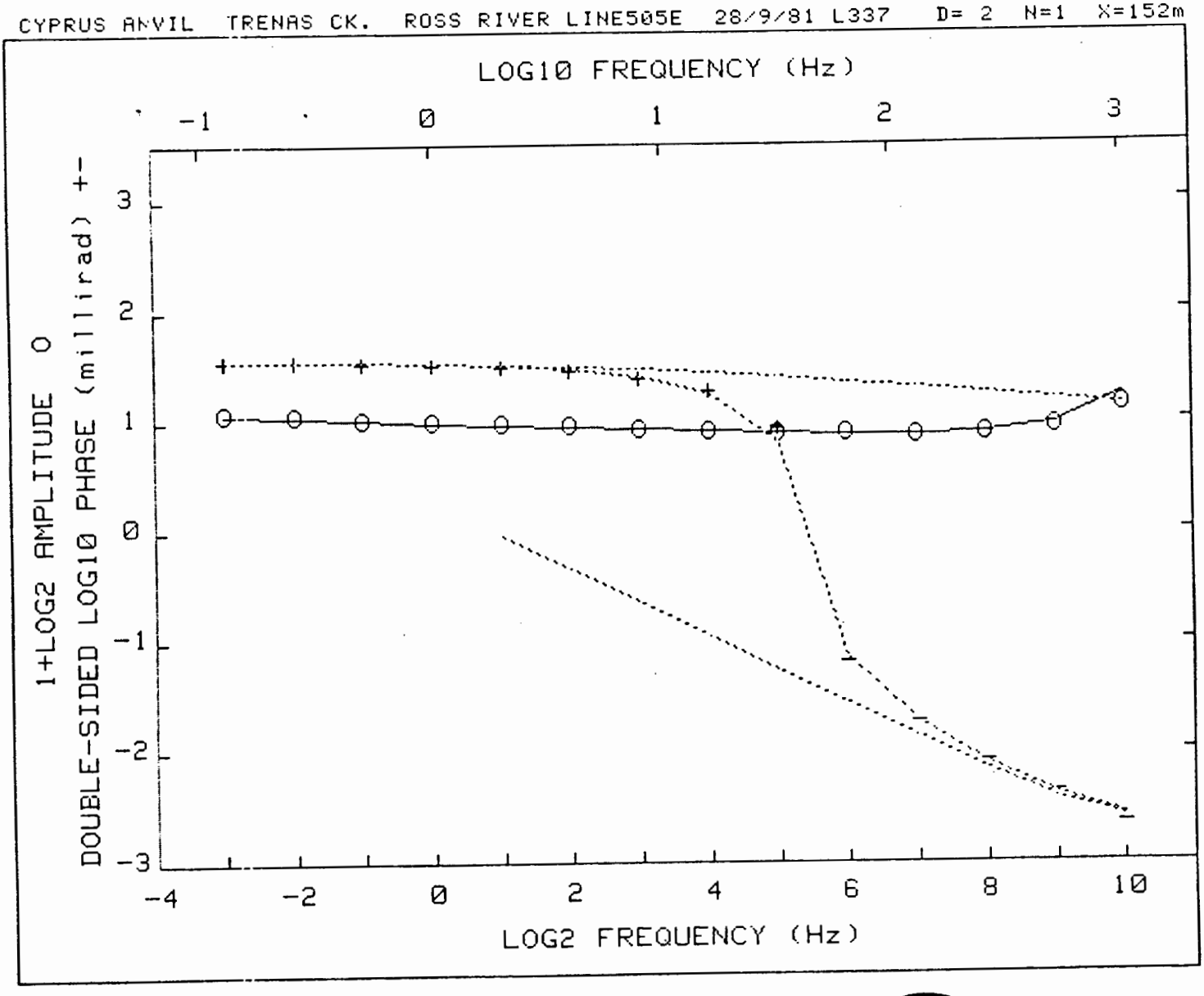

CRL: Number of dispersions= 2 Negative.
C1=.25 M2=1 fixed

Iter	Lambda	Rchsq	R0	M1	T1	T2	C2
0	1.E-02	.21417	1.000	.150	1.0E+00	8.0E-05	1.000
1	1.E-02	.02138	1.175	.244	5.1E+00	4.3E-05	1.000
2	1.E-03	.00510	1.230	.296	1.6E+00	7.3E-05	1.000
3	1.E-04	.00131	1.231	.300	1.6E+00	6.7E-05	1.000
4	1.E+00	.00129	1.234	.302	1.6E+00	6.7E-05	1.000
5	1.E+01	.00123	1.235	.303	1.6E+00	6.7E-05	1.000
6	1.E+01	.00119	1.235	.304	1.6E+00	6.7E-05	1.000
7	1.E+01	.00116	1.236	.304	1.6E+00	6.7E-05	1.000
8	1.E+01	.00114	1.236	.304	1.6E+00	6.7E-05	1.000
9	1.E+01	.00112	1.236	.305	1.6E+00	6.7E-05	1.000

Pct Std Deviations	2.1	3.5	77.7	5.4	2.3	
Correlation Matrix	1.000					
	.885	1.000				
	.916	.781	1.000			
	-.211	-.325	-.083	1.000		
	.471	.215	.668	.620	1.000	

DWG. NO. – S.I.P. – 1108 -3

CYPRUS ANVIL TRENAS CK. ROSS RIVER LINE505E 28/9/81 L337 D= 2 N=2 X=152m

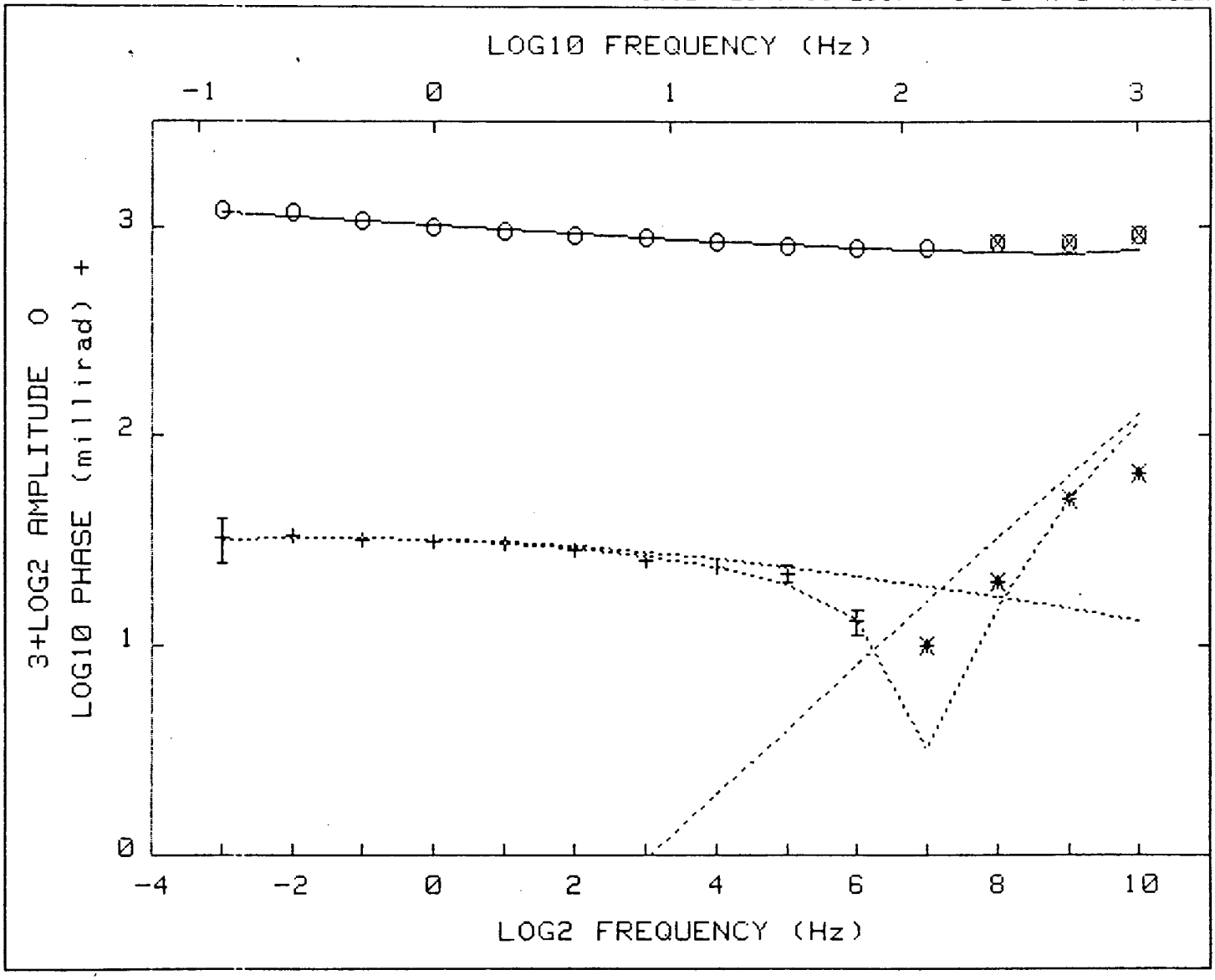

CRL: Number of dispersions= 2 Negative.
C1=.25 M2=1 C2=1 fixed

Iter	Lambda	Rchsq	R0	M1	T1	T2
0	1.E-02	.00164	1.174	.286	1.4E-01	3.4E-05
1	1.E-02	.00076	1.174	.274	2.2E-01	2.6E-05
2	1.E-03	.00040	1.198	.274	6.4E-01	1.8E-05
3	1.E-04	.00029	1.212	.281	9.3E-01	1.6E-05
4	1.E-05	.00029	1.213	.282	9.6E-01	1.5E-05

Pct Std Deviations	.9	1.6	35.1	13.3

Correlation Matrix	1.000			
	.816	1.000		
	.875	.690	1.000	
	-.591	-.287	-.797	1.000

Apparent Resistivity Measured at 1 Hz is 36.20
Apparent Resistivity Calculated from Inductive Coupling is 2961

DWG. NO. - S.I.P - 1108-4

CYPRUS ANVIL TRENAS CK. ROSS RIVER LINE505E 28/9/81 L337 D= 2 N=3 X=152m

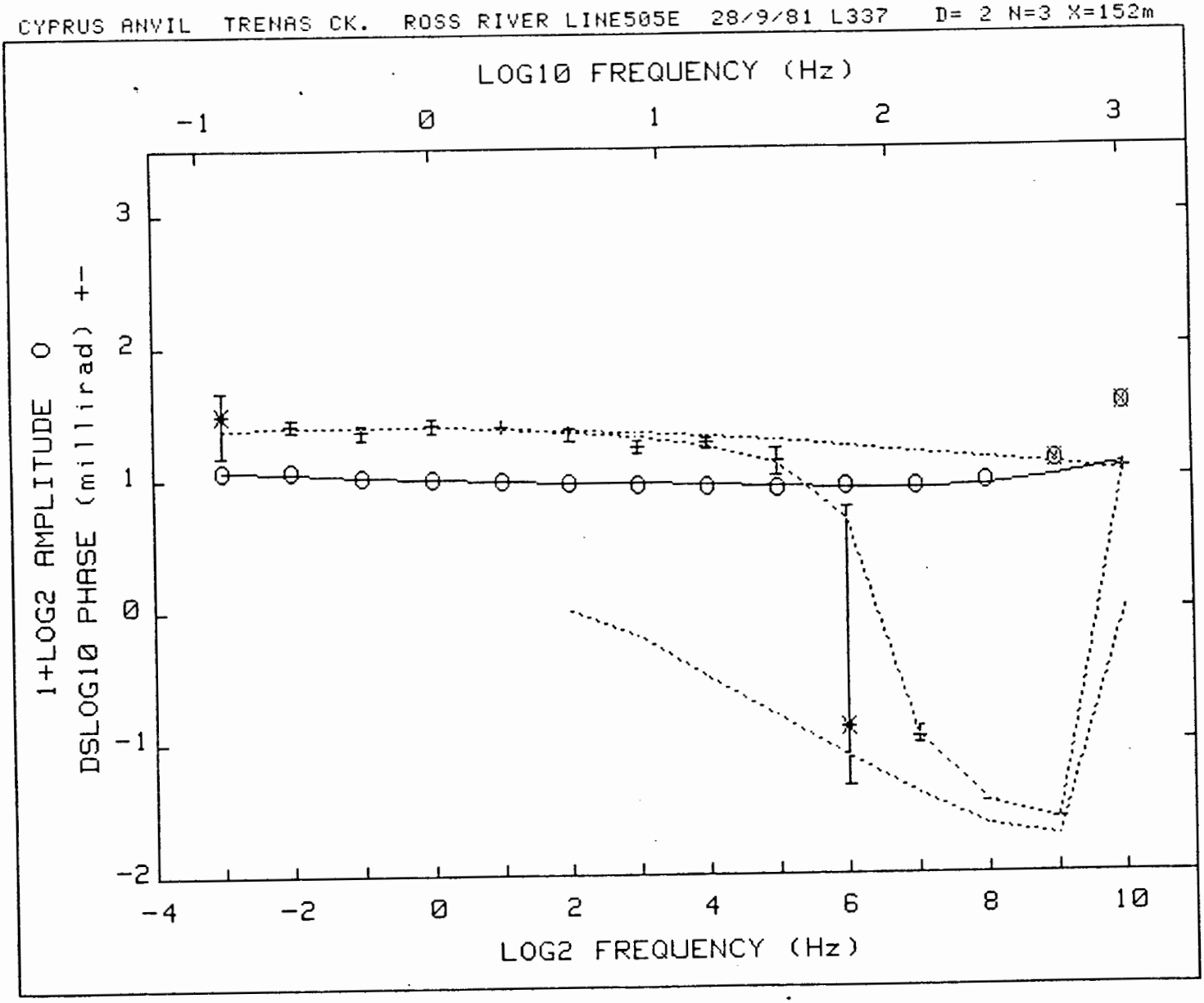

CRL: Number of dispersions= 3 Negative.
C1=.25 M2=1 C2=1 C3=1 fixed

Iter	Lambda	Rchsq	R0	M1	T1	T2	M3	T3
0	1.E-02	.00074	1.167	.224	5.6E-01	1.6E-05	.211	2.0E-04
1	1.E-02	.00067	1.159	.225	5.6E-01	1.6E-05	.210	2.0E-04
2	1.E-03	.00067	1.159	.225	5.6E-01	1.6E-05	.210	2.0E-04

Pct Std Deviations	1.2	2.8	56.7	15.0	13.4	9.5	
Correlation Matrix	1.000						
	.834	1.000					
	.862	.785	1.000				
	.188	.076	.277	1.000			
	.140	.038	.216	.997	1.000		
	-.297	-.168	-.409	-.982	-.970	1.000	

Apparent Resistivity Measured at 1 Hz is 8.980

Apparent Resistivity Calculated from Inductive Coupling is 5251

DWG. NO. - S.I.P. - 1108 - 5

CYPRUS ANVIL TRENAS CK. ROSS RIVER LINE505E 28/9/81 L337 D= 3 N=4 X=152m

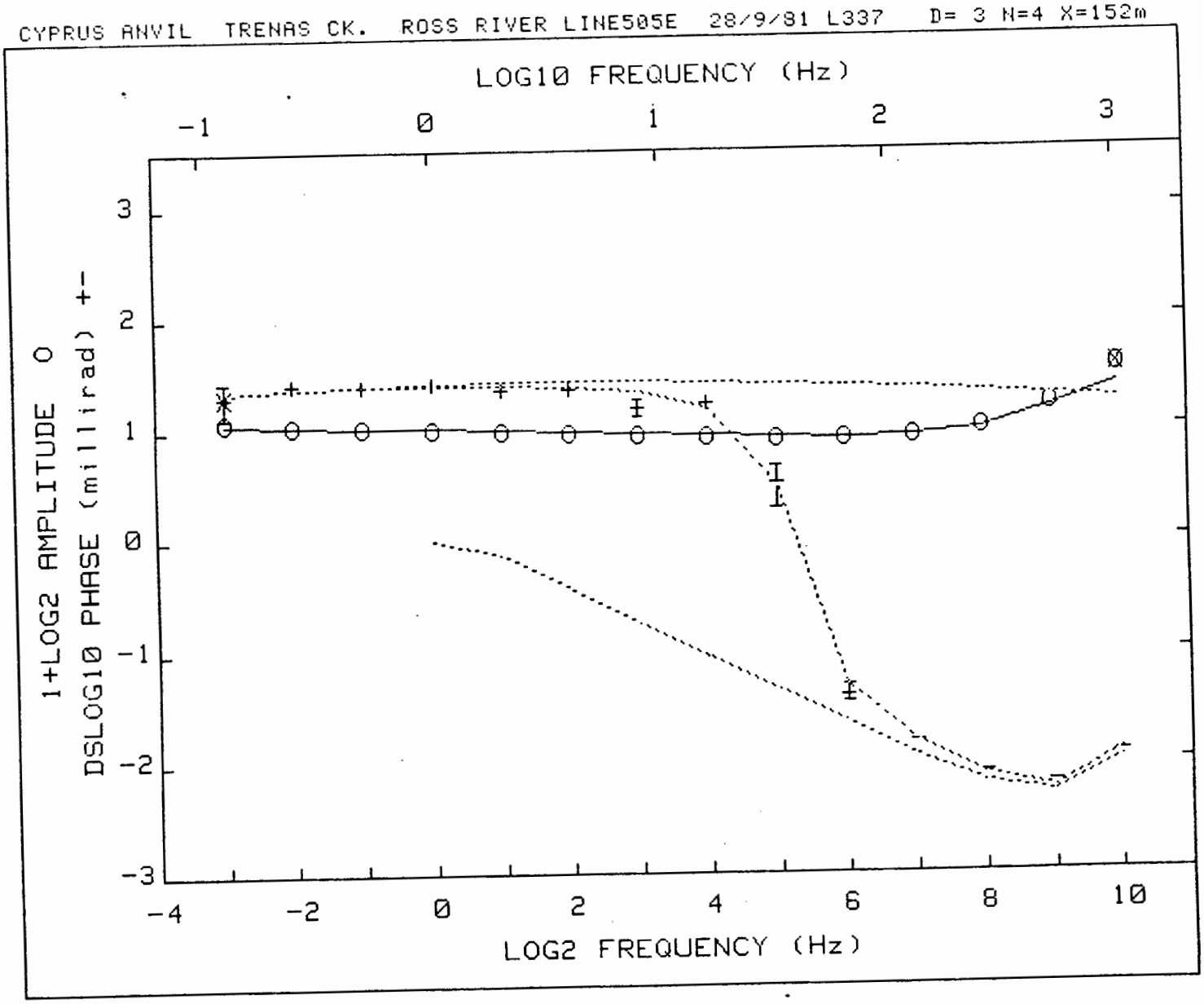

CRL: Number of dispersions= 3 Negative.
C1=.25 M2=1 C2=1 M3=1 C3=1 fixed

Iter	Lambda	Rchsq	R0	M1	T1	T2	T3
0	1.E-02	.00193	1.118	.238	4.2E-02	7.4E-05	1.7E-04
1	1.E-02	.00190	1.120	.238	4.7E-02	7.5E-05	1.7E-04
2	1.E-03	.00188	1.124	.238	5.8E-02	7.5E-05	1.7E-04
3	1.E-04	.00188	1.125	.238	6.1E-02	7.5E-05	1.7E-04

Pct Std Deviations	1.4	2.5	77.1	3.9	3.1

Correlation Matrix

1.000				
.256	1.000			
.752	.044	1.000		
.238	-.093	.372	1.000	
-.396	.436	-.641	.223	1.000

Apparent Resistivity Measured at 1 Hz is 18.77

Apparent Resistivity Calculated from Inductive Coupling is 1857

DWG. NO. - S.I.P. - 1108-6

CYPRUS ANVIL TRENAS CK. ROSS RIVER LINE505E 28/9/81 L337 D= 5 N=3 X=152m

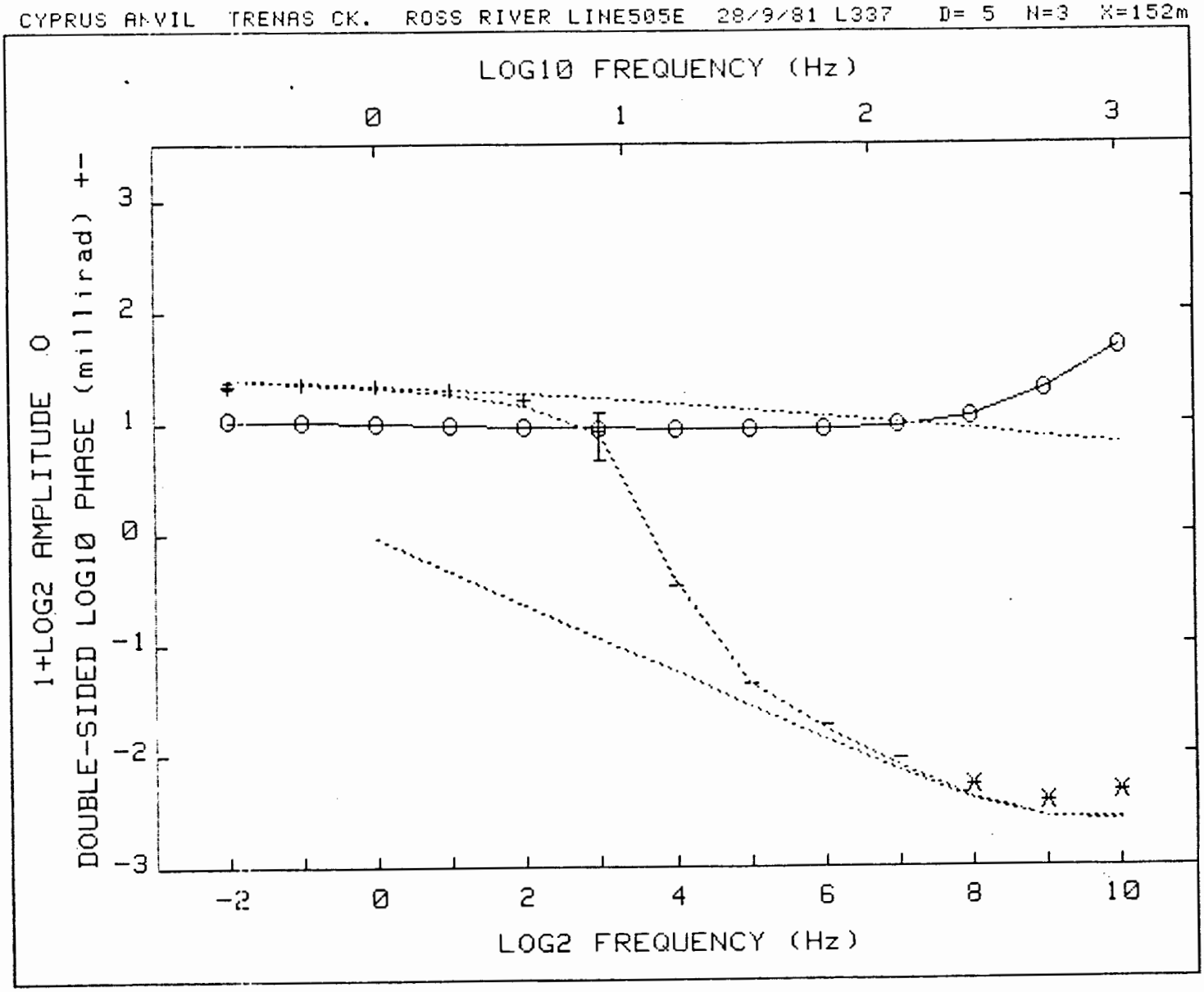

CRL: Number of dispersions= 2 Negative.
C1=.25 M2=1 C2=1 fixed

Iter	Lambda	Rchsq	R0	M1	T1	T2
0	1.E-02	.00097	1.222	.243	1.1E+01	1.4E-04
1	1.E-02	.00097	1.221	.242	1.2E+01	1.4E-04

Pct Std Deviations	3.1	8.7	114.4	5.5
Correlation Matrix	1.000			
	.975	1.000		
	.974	.975	1.000	
	-.904	-.874	-.952	1.000

Apparent Resistivity Measured at 1 Hz is 27.78
Apparent Resistivity Calculated from Inductive Coupling is 613.1

DWG. NO. - S.I.P. - 1108-7

CYPRUS ANVIL TRENAS CK. ROSS RIVER LINE505E 28/9/81 L337 D= 6 N=2 X=152m

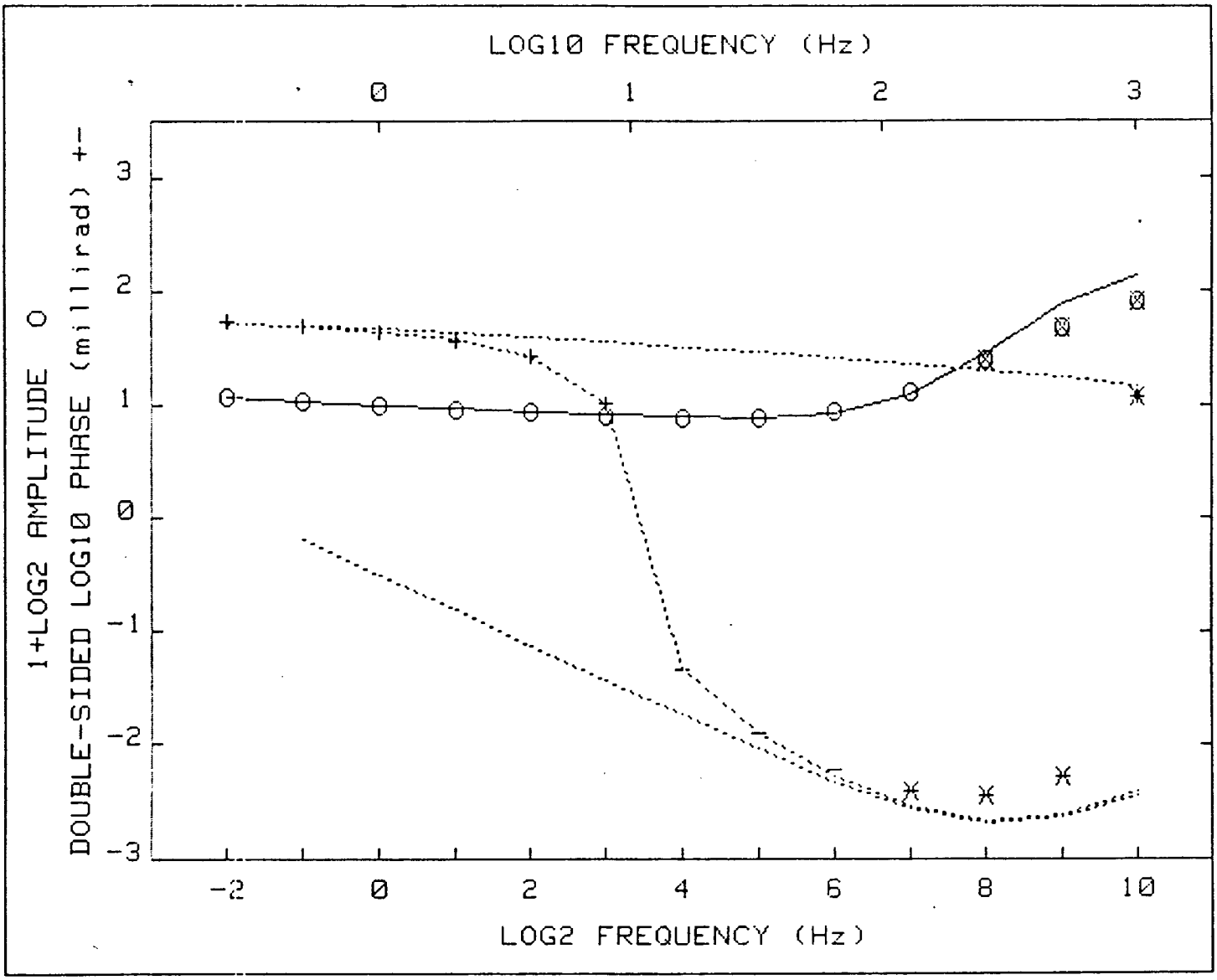

CRL: Number of dispersions= 2 Negative.
C1=.25 M2=1 C2=1 fixed

Iter	Lambda	Rchsq	R0	M1	T1	T2
0	1.E-02	.00045	1.501	.433	1.5E+01	3.2E-04
1	1.E-02	.00037	1.509	.438	1.4E+01	3.3E-04
2	1.E-03	.00037	1.499	.435	1.3E+01	3.4E-04

Pct Std Deviations	4.0	4.5	75.3	5.6

Correlation Matrix

1.000			
.990	1.000		
.987	.977	1.000	
-.942	-.917	-.970	1.000

Apparent Resistivity Measured at 1 Hz is 83.92
Apparent Resistivity Calculated from Inductive Coupling is 135.1

DWG. NO. - S.I.P. - 1108 - 8

CYPRUS ANVIL TRENAS CK. ROSS RIVER LINE505E 28/9/81 L337 D= 7 N=3 X=152m

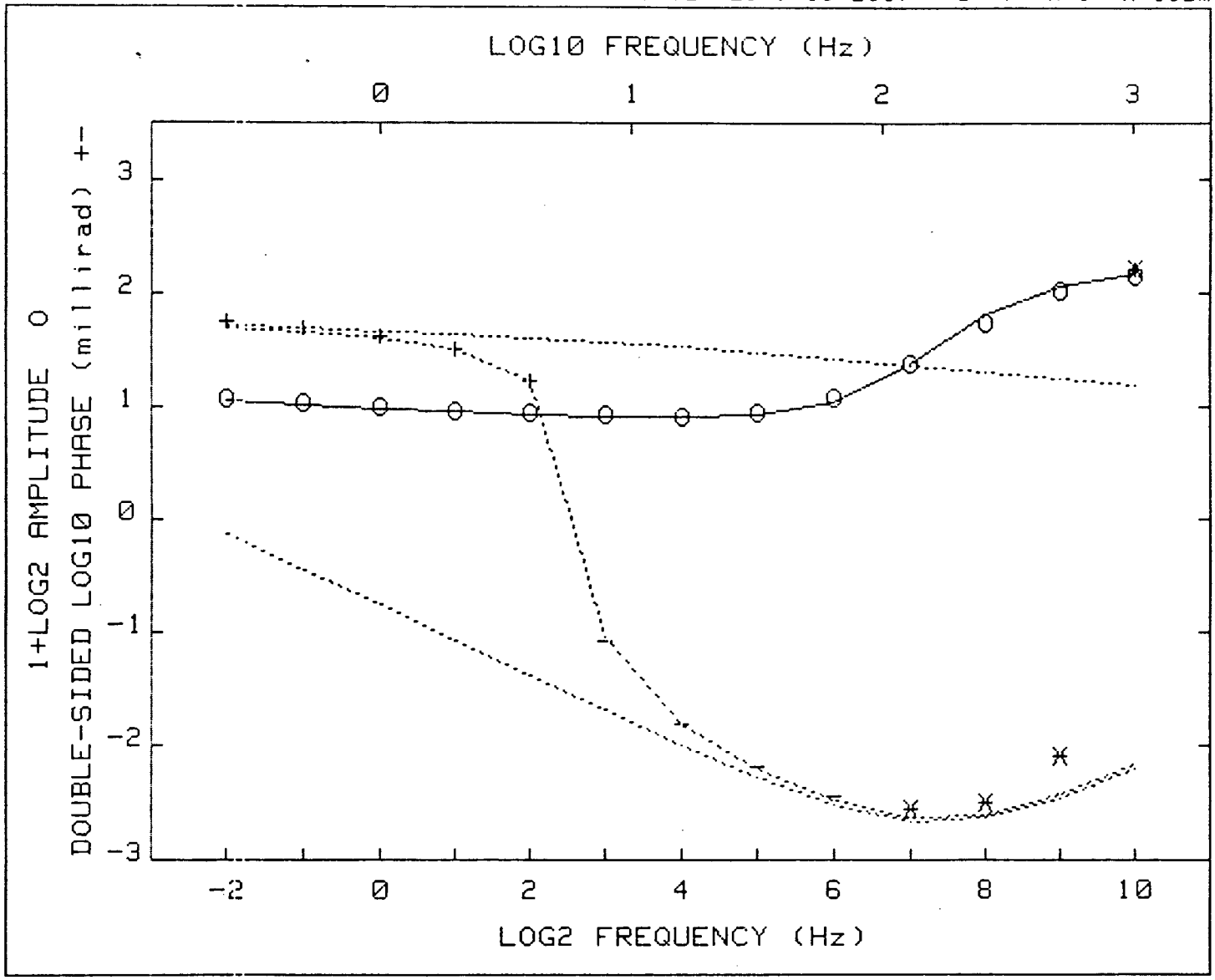

CRL: Number of dispersions= 2 Negative.
C1=.25 M2=1 C2=1 fixed

Iter	Lambda	Rchsq	R0	M1	T1	T2
0	1.E-02	.19193	1.322	.382	1.1E+00	5.1E-04
1	1.E-02	.01035	1.319	.346	4.8E+00	6.8E-04
2	1.E-03	.00126	1.425	.417	9.9E+00	6.1E-04
3	1.E-04	.00101	1.428	.415	7.7E+00	6.2E-04
4	1.E-02	.00101	1.428	.415	7.8E+00	6.3E-04

Pct Std Deviations	2.7	3.4	62.7	4.7	
Correlation Matrix	1.000				
	.930	1.000			
	.947	.865	1.000		
	-.855	-.705	-.934	1.000	

Apparent Resistivity Measured at 1 Hz is 56.88
Apparent Resistivity Calculated from Inductive Coupling is 136.3

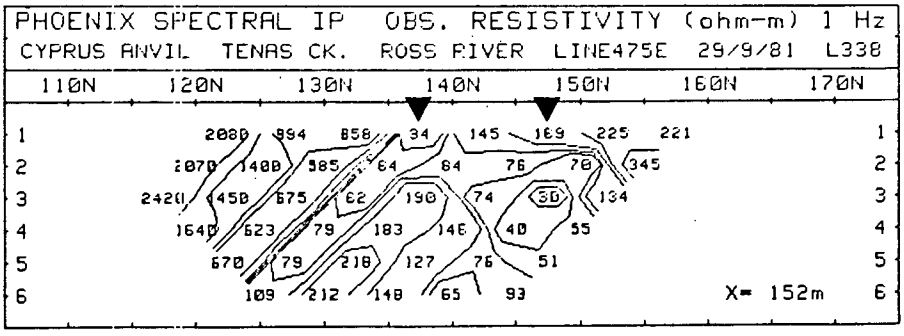
PHOENIX SPECTRAL IP OBS. RESISTIVITY (ohm-m) 1 Hz
CYPRUS ANVIL TENAS CK. ROSS RIVER LINE475E 29/9/81 L338
110N 120N 130N 140N 150N 160N 170N
X= 152m

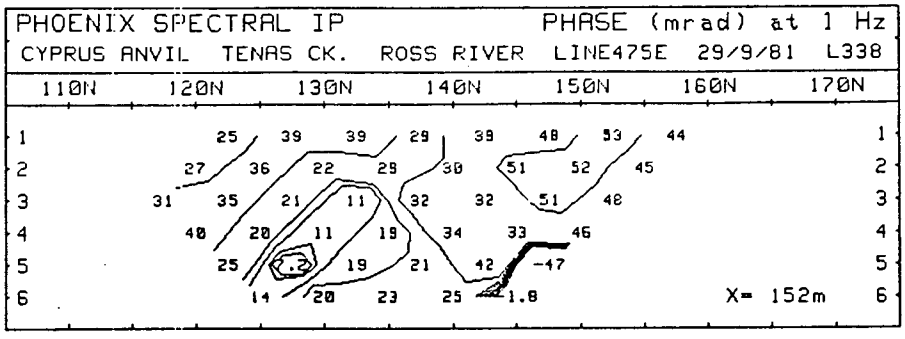
PHOENIX SPECTRAL IP PHASE (mrad) at 1 Hz
CYPRUS ANVIL TENAS CK. ROSS RIVER LINE475E 29/9/81 L338
110N 120N 130N 140N 150N 160N 170N
X= 152m

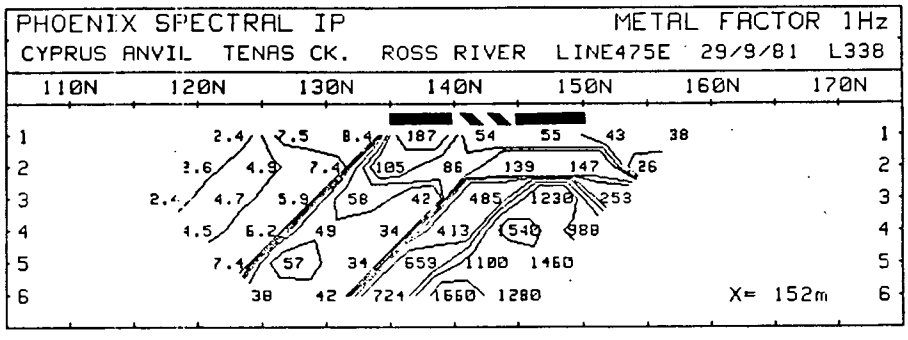
PHOENIX SPECTRAL IP METAL FACTOR 1Hz
CYPRUS ANVIL TENAS CK. ROSS RIVER LINE475E 29/9/81 L338
110N 120N 130N 140N 150N 160N 170N
X= 152m

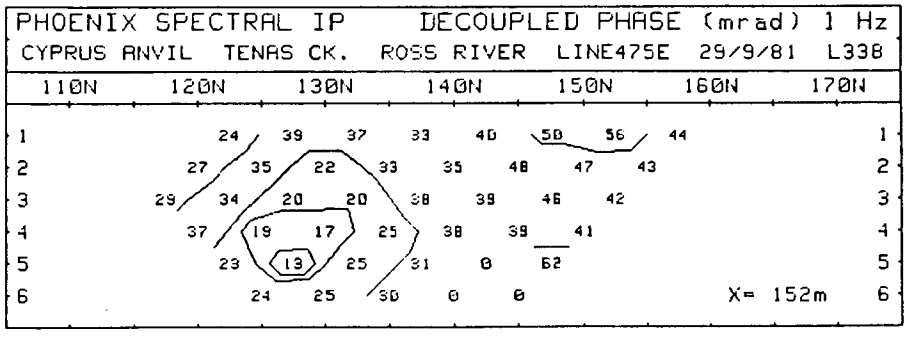
PHOENIX SPECTRAL IP DECOUPLED PHASE (mrad) 1 Hz
CYPRUS ANVIL TENAS CK. ROSS RIVER LINE475E 29/9/81 L338
110N 120N 130N 140N 150N 160N 170N
X= 152m

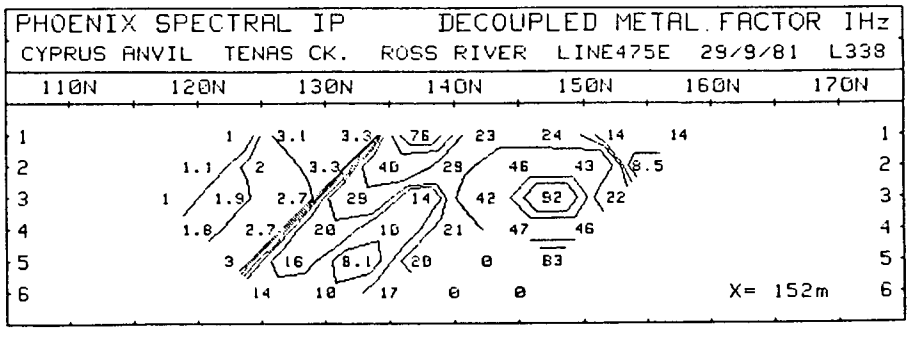
PHOENIX SPECTRAL IP DECOUPLED METAL FACTOR 1Hz
CYPRUS ANVIL TENAS CK. ROSS RIVER LINE475E 29/9/81 L338
110N 120N 130N 140N 150N 160N 170N
X= 152m

DWG. NO. - S.I.P. - 1109-2

CYPRUS ANVIL TENAS CK. ROSS RIVER LINE475E 29/9/81 L338 D= 4 N=1 X=152m

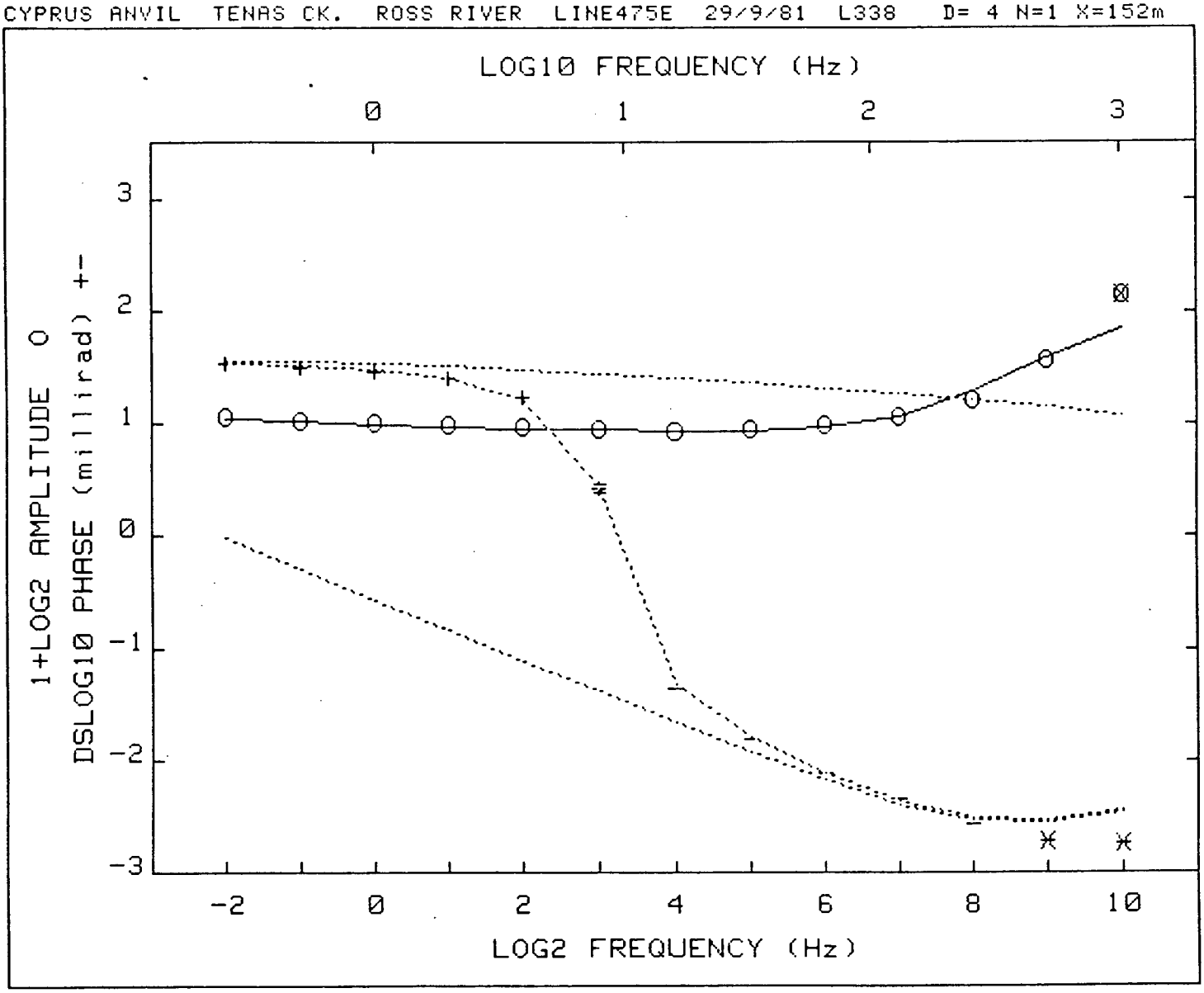

CRL: Number of dispersions= 2 Negative.
C1=.25 M2=1 fixed

Iter	Lambda	Rchsq	R0	M1	T1	T2	C2
0	1.E-02	.00087	1.260	.305	3.8E+00	2.5E-04	.911
1	1.E-01	.00085	1.260	.307	3.8E+00	2.4E-04	.906
2	1.E-02	.00082	1.260	.307	3.7E+00	2.4E-04	.903
3	1.E-03	.00081	1.252	.304	3.1E+00	2.4E-04	.901
4	1.E-04	.00081	1.242	.300	2.4E+00	2.4E-04	.897

Pct Std Deviations	3.7	5.9	183.9	6.3	1.7	
Correlation Matrix	1.000					
	.957	1.000				
	.969	.909	1.000			
	-.827	-.807	-.785	1.000		
	.615	.463	.749	-.240	1.000	

Apparent Resistivity Measured at 1 Hz is 34.16

Apparent Resistivity Calculated from Inductive Coupling is 50.30

DWG. NO. - S.I.P. - 1109 - 3

CYPRUS ANVIL TENAS CK. ROSS RIVER. LINE475E 29/9/81 L338 D= 4 N=2 X=152m

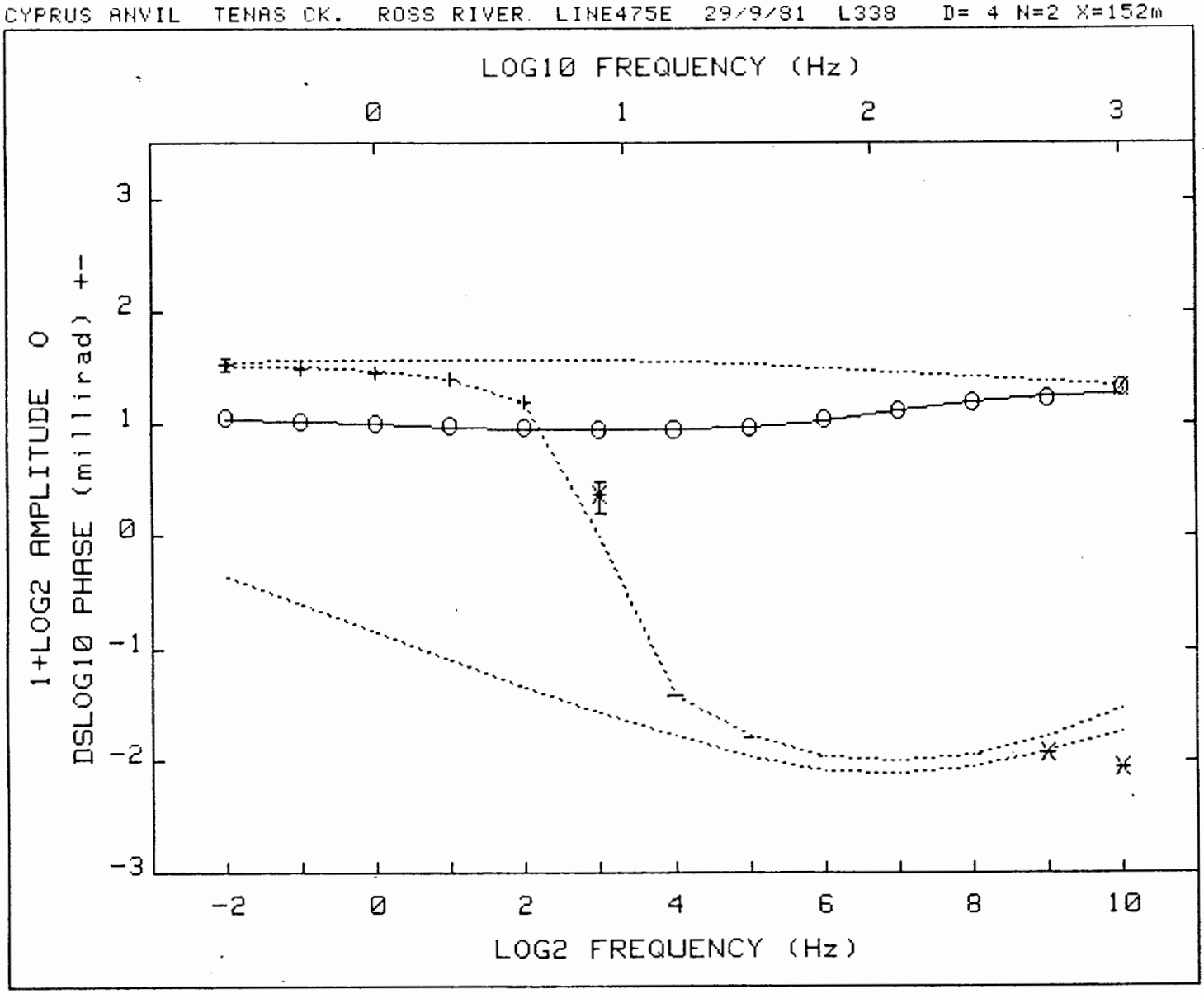

CRL: Number of dispersions= 2 Negative.
C1=.25 fixed

Iter	Lambda	Rchsq	R0	M1	T1	M2	T2	C2
0	1.E-02	.00064	1.320	.332	1.0E+01	.232	1.3E-03	.899
1	1.E-02	.00061	1.313	.330	8.7E+00	.235	1.3E-03	.895
2	1.E-03	.00043	1.256	.309	3.0E+00	.254	1.3E-03	.876
3	1.E-03	.00030	1.229	.302	1.4E+00	.268	1.3E-03	.859
4	1.E-03	.00024	1.212	.302	7.5E-01	.280	1.3E-03	.844
5	1.E-03	.00021	1.202	.303	4.9E-01	.290	1.3E-03	.833
6	1.E-04	.00019	1.181	.308	2.1E-01	.311	1.2E-03	.810
7	1.E-05	.00018	1.178	.314	1.6E-01	.318	1.2E-03	.803
8	1.E+00	.00018	1.178	.314	1.6E-01	.318	1.2E-03	.803

Pct Std Deviations	1.2	4.2	108.0	7.0	4.6	3.2	
Correlation Matrix	1.000						
	-.747	1.000					
	.935	-.910	1.000				
	-.826	.949	-.940	1.000			
	.326	-.554	.435	-.672	1.000		
	.664	-.941	.830	-.936	.738	1.000	

CYPRUS ANVIL TENAS CK. ROSS RIVER LINE475E 29/9/81 L338 D= 4 N=3 X=152m

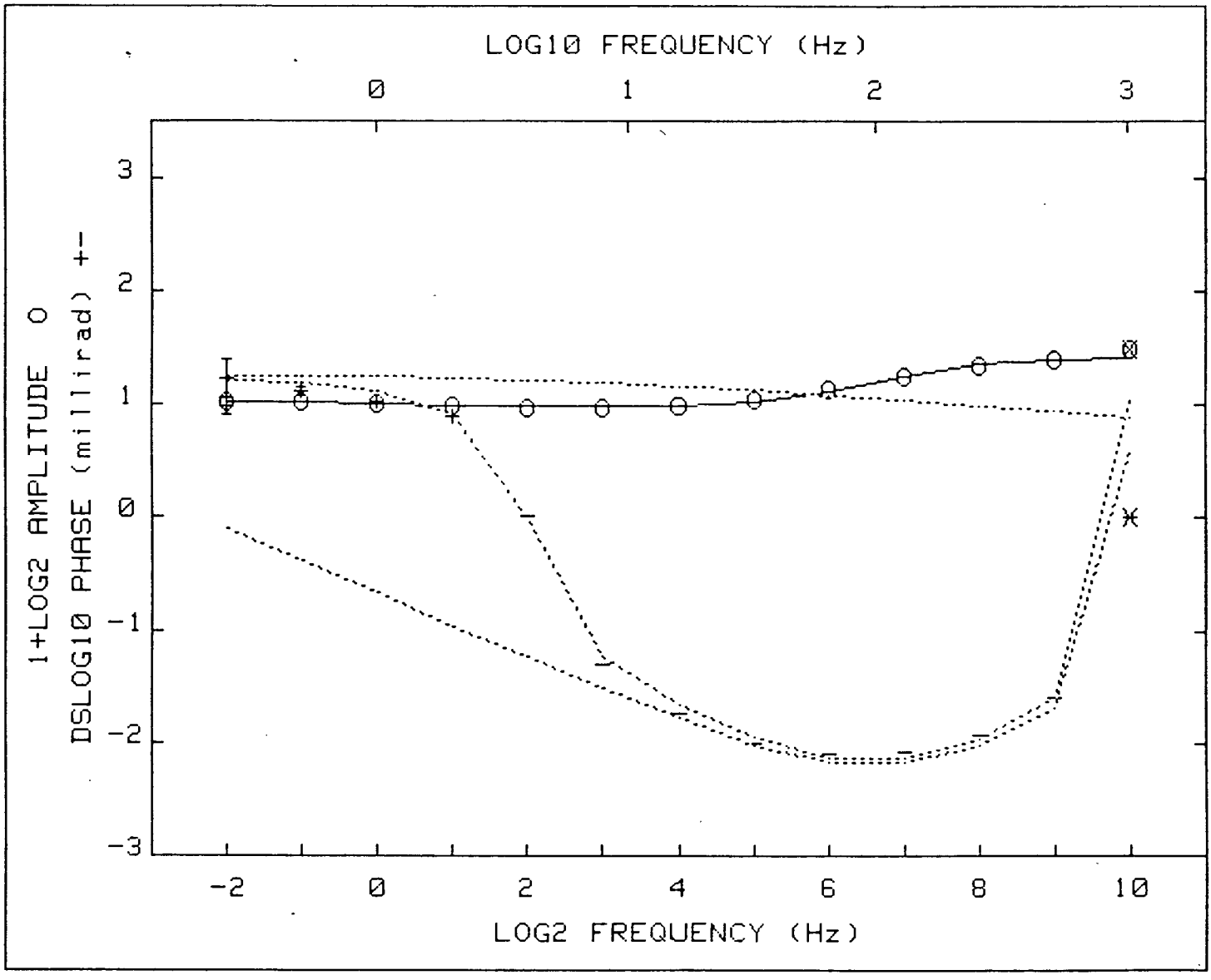

CRL: Number of dispersions= 3 Negative.
C1=.25 M2=1 C2=1 fixed

Iter	Lambda	Rchsq	R0	M1	T1	T2	M3	T3	C3
0	1.E-02	.00170	1.106	.164	5.4E-01	8.2E-06	.366	1.4E-03	.932
1	1.E+03	.00170	1.106	.164	5.4E-01	8.2E-06	.366	1.4E-03	.932

Pct Std Deviations	1.6	5.3	244.4	87.3	11.1	13.4	5.6	
Correlation Matrix	1.000							
	.063	1.000						
	.793	-.282	1.000					
	-.500	.461	-.686	1.000				
	-.616	.456	-.796	.939	1.000			
	.498	-.441	.701	-.949	-.930	1.000		
	.607	-.618	.915	-.801	-.857	.820	1.000	

Apparent Resistivity Measured at 1 Hz is 61.53

Apparent Resistivity Calculated from Inductive Coupling is 134.9

DWG. NO. - S.I.P - 1109-5

CYPRUS ANVIL TENAS CK. ROSS RIVER LINE475E 29/9/81 L338 D= 4 N=4 X=152m

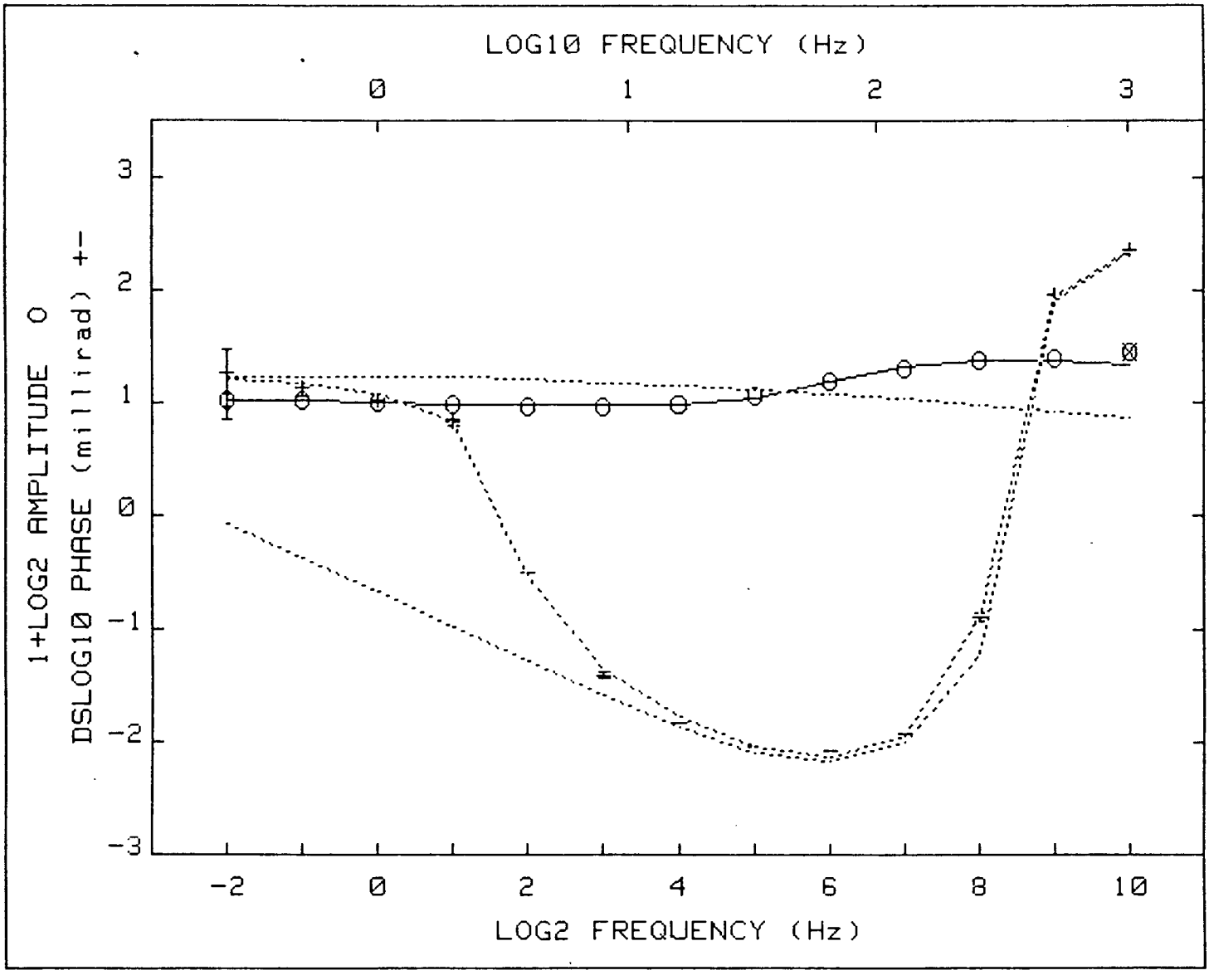

CRL: Number of dispersions= 3 Negative.
C1=.25 M2=1 C2=1 C3=1 fixed

Iter	Lambda	Rchsq	R0	M1	T1	T2	M3	T3
0	1.E-02	.00124	1.107	.159	4.6E-01	4.6E-05	.345	2.2E-03
1	1.E-02	.00118	1.100	.158	4.6E-01	4.6E-05	.343	2.2E-03
2	1.E-03	.00118	1.100	.158	4.7E-01	4.6E-05	.343	2.2E-03

Pct Std Deviations	1.7	3.3	207.7	5.9	4.3	3.4	

Correlation Matrix

1.000						
.575	1.000					
.899	.524	1.000				
-.104	-.149	-.024	1.000			
-.729	-.290	-.781	.577	1.000		
-.440	.039	-.584	-.704	.134	1.000	

Apparent Resistivity Measured at 1 Hz is 79.48

Apparent Resistivity Calculated from Inductive Coupling is 188.8

DWG. NO. - S.I.P - 1109 - 6

CYPRUS ANVIL TENAS CK. ROSS RIVER LINE475E 29/9/81 L338 D= 4 N=5 X=152m

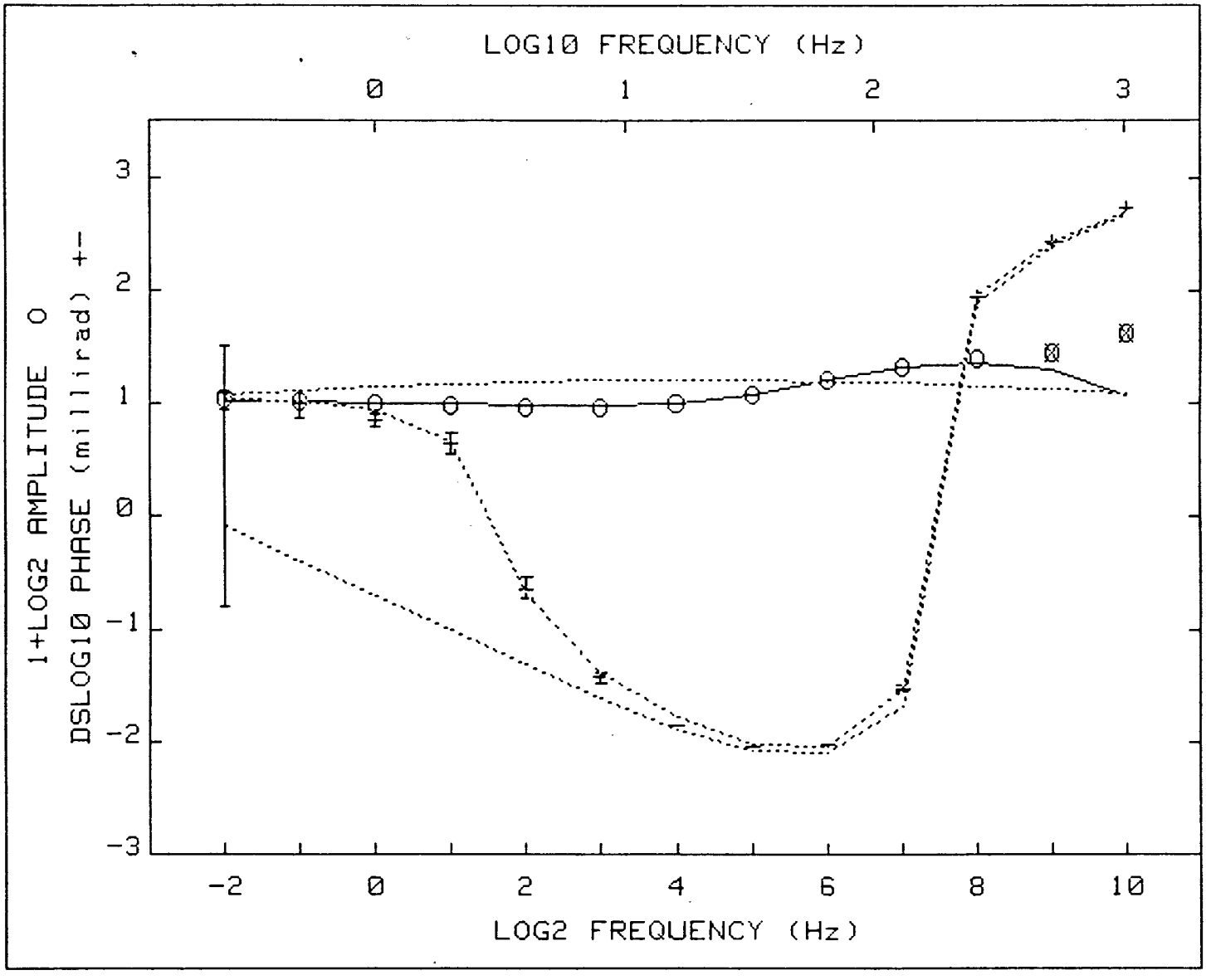

CRL: Number of dispersions= 3 Negative.
C1=.25 M2=1 C2=1 C3=1 fixed

Iter	Lambda	Rchsq	R0	M1	T1	T2	M3	T3
0	1.E-02	.00183	1.069	.130	1.0E-01	1.2E-04	.354	2.3E-03
1	1.E-02	.00181	1.068	.130	8.6E-02	1.2E-04	.355	2.3E-03
2	1.E-03	.00172	1.062	.134	3.8E-02	1.2E-04	.360	2.4E-03
3	1.E-04	.00167	1.056	.144	1.4E-02	1.2E-04	.367	2.4E-03
4	1.E-05	.00161	1.056	.148	1.2E-02	1.2E-04	.368	2.4E-03
5	1.E-06	.00160	1.056	.149	1.1E-02	1.2E-04	.369	2.4E-03

Pct Std Deviations	1.1	16.8	402.1	7.5	4.8	4.3	
Correlation Matrix	1.000						
	-.612	1.000					
	.646	-.978	1.000				
	.034	-.218	.195	1.000			
	-.456	.605	-.597	.575	1.000		
	-.276	.624	-.553	-.745	-.148	1.000	

Apparent Resistivity Measured at 1 Hz is 78.65

Apparent Resistivity Calculated from Inductive Coupling is 222.8

DWG. NO. - S.I.P. - 1109-7

CYPRUS ANVIL TENAS CK. ROSS RIVER LINE475E 29/9/81 L338 D= 4 N=6 X=152m

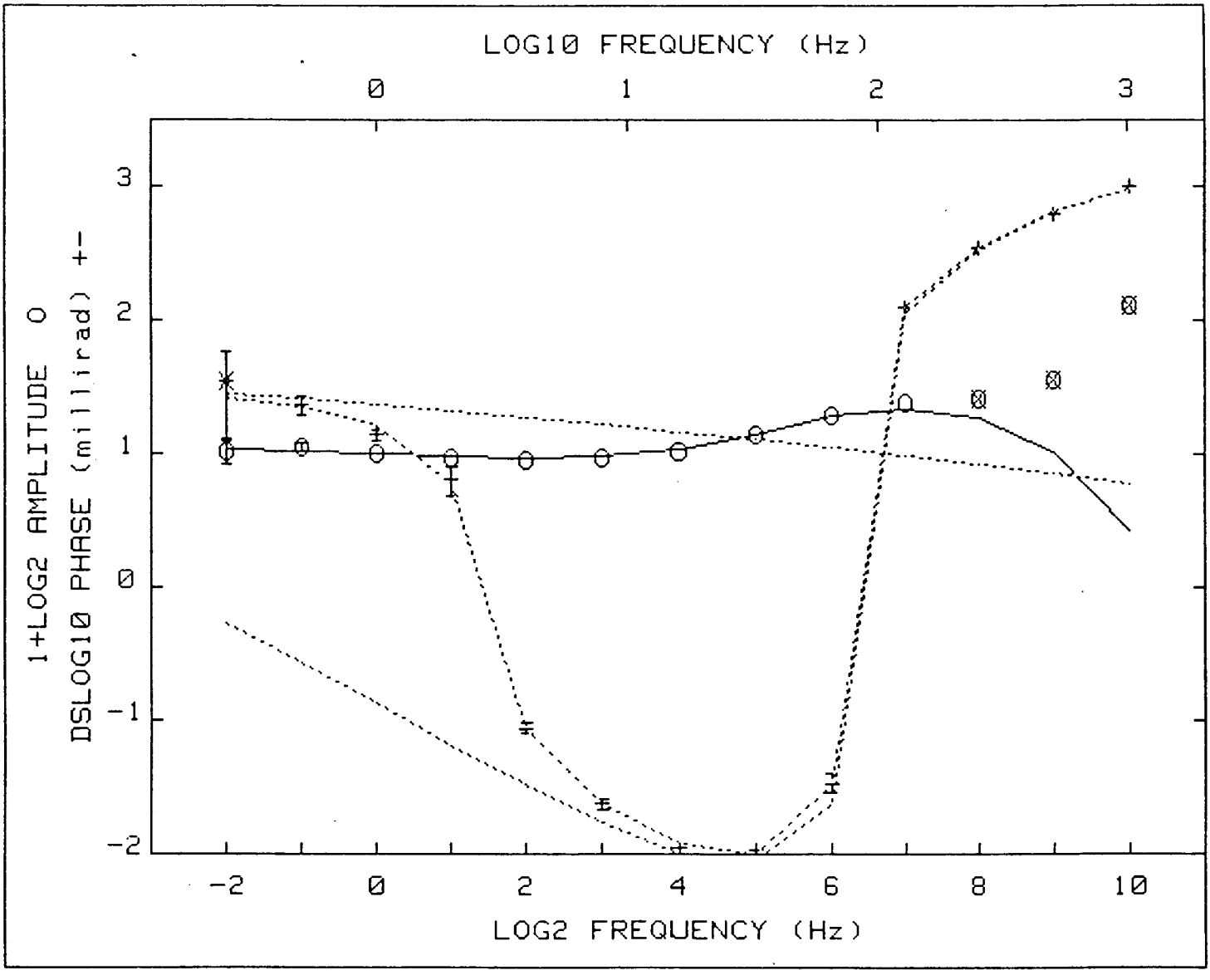

CRL: Number of dispersions= 3 Negative.
C1=.25 M2=1 C2=1 C3=1 fixed

Iter	Lambda	Rchsq	R0	M1	T1	T2	M3	T3
0	1.E-02	.00118	1.621	.422	9.0E+02	2.0E-04	.241	3.9E-03
1	1.E-02	.00101	1.572	.405	7.8E+02	2.1E-04	.245	3.9E-03
2	1.E-03	.00087	1.439	.357	2.6E+02	2.3E-04	.271	3.9E-03
3	1.E-04	.00083	1.311	.299	5.9E+01	2.6E-04	.306	3.8E-03
4	1.E-05	.00065	1.318	.296	5.1E+01	2.6E-04	.307	3.8E-03
5	1.E-06	.00065	1.318	.296	5.1E+01	2.6E-04	.308	3.8E-03

Pct Std Deviations	4.3	9.7	134.3	7.5	6.1	2.6	
Correlation Matrix	1.000						
	.988	1.000					
	.983	.980	1.000				
	-.750	-.752	-.727	1.000			
	-.867	-.862	-.962	.959	1.000		
	-.066	-.035	-.143	-.468	-.286	1.000	

Apparent Resistivity Measured at 1 Hz is 108.8

Apparent Resistivity Calculated from Inductive Coupling is 232.6

DWG. NO. - S.I.P - 1109 - 8

CYPRUS ANVIL TENAS CK. ROSS RIVER LINE475E 29/9/81 L338 D= 6 N=2 X=152m

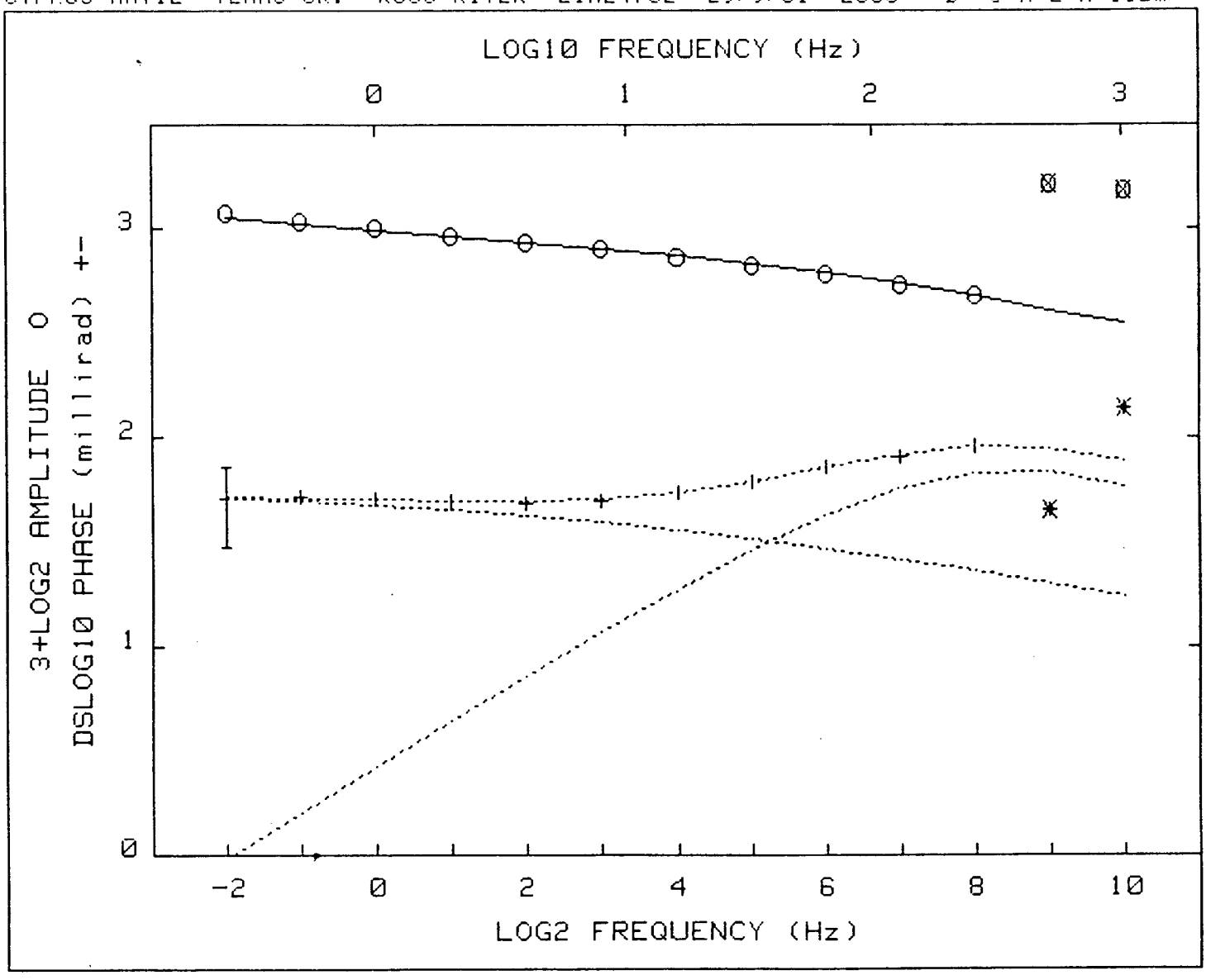

CRL: Number of dispersions= 2
C1=.25 fixed

Iter	Lambda	Rchsq	R0	M1	T1	M2	T2	C2
0	1.E-02	.00010	1.379	.405	3.4E+00	.123	5.3E-04	.711
1	1.E+03	.00010	1.379	.405	3.4E+00	.123	5.3E-04	.711

Pct Std Deviations	3.2	2.1	125.1	21.3	32.9	12.7	
Correlation Matrix	1.000						
	.832	1.000					
	.984	.742	1.000				
	.717	.287	.787	1.000			
	-.535	-.150	-.598	-.946	1.000		
	-.770	-.344	-.833	-.983	.901	1.000	

Apparent Resistivity Measured at 1 Hz is 75.78

Apparent Resistivity Calculated from Inductive Coupling is 206.9

DWG. NO. - S.I.P. - 1109 -9

CYPRUS ANVIL TENAS CK. ROSS RIVER LINE475E 29/9/81 L338 D= 6 N=3 X=152m

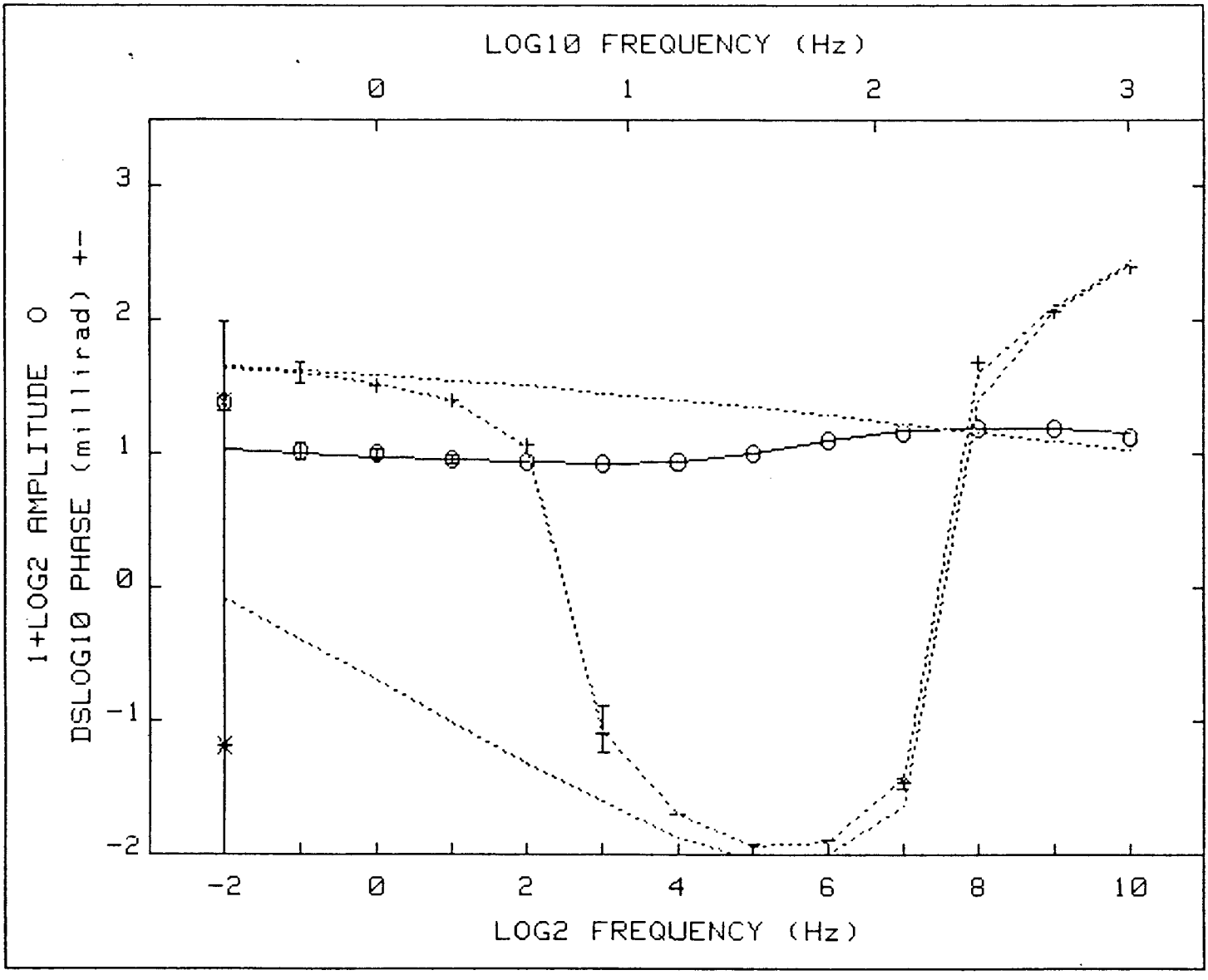

CRL: Number of dispersions= 3 Negative.
C1=.25 M2=1 C2=1 C3=1 fixed

Iter	Lambda	Rchsq	R0	M1	T1	T2	M3	T3
0	1.E-02	.00086	1.476	.413	3.9E+01	3.4E-05	.174	3.3E-03
1	1.E-02	.00085	1.470	.411	3.8E+01	3.4E-05	.174	3.3E-03

Pct Std Deviations	13.5	18.0	525.4	13.1	16.1	2.7	
Correlation Matrix	1.000						
	.998	1.000					
	.996	.994	1.000				
	-.948	-.948	-.941	1.000			
	-.989	-.986	-.992	.963	1.000		
	-.460	-.444	-.496	.263	.428	1.000	

Apparent Resistivity Measured at 1 Hz is 73.62

Apparent Resistivity Calculated from Inductive Coupling is 150.2

DWG. NO. – S.I.P. – 1109 – 10

CYPRUS ANVIL TENAS CK. ROSS RIVER LINE475E 29/9/81 L338 D= 7 N=2 X=152m

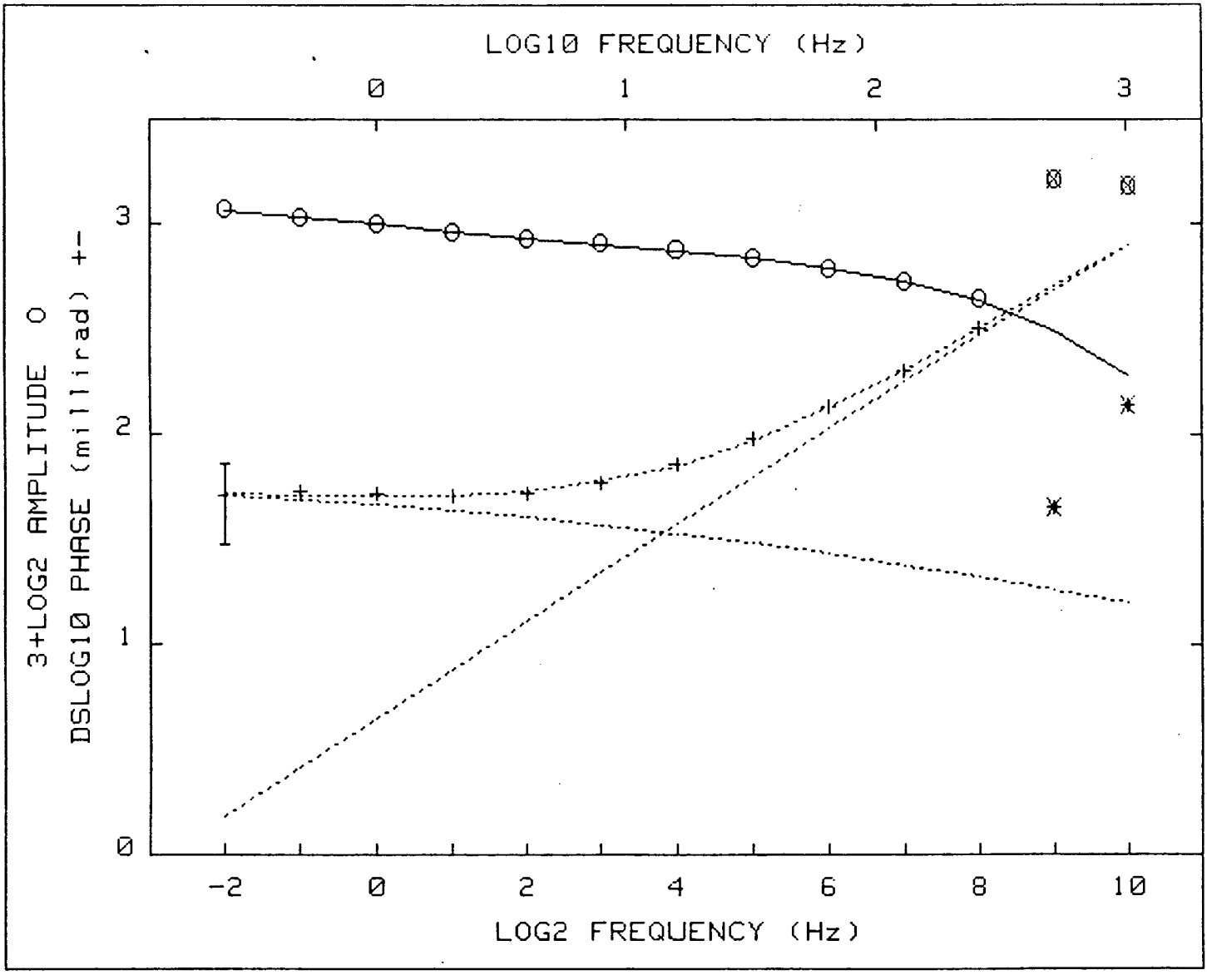

CRL: Number of dispersions= 2
C1=.25 M2=1 fixed

Iter	Lambda	Rchsq	R0	M1	T1	T2	C2
0	1.E-02	.00011	1.543	.445	2.8E+01	6.5E-05	.715
1	1.E-02	.00011	1.540	.443	2.8E+01	6.4E-05	.709
2	1.E-03	.00010	1.520	.437	2.2E+01	6.6E-05	.713
3	1.E-04	.00009	1.440	.414	9.1E+00	7.4E-05	.733
4	1.E-05	.00008	1.415	.408	6.0E+00	7.7E-05	.745
5	1.E-06	.00007	1.417	.408	6.0E+00	7.7E-05	.745

Pct Std Deviations	2.6	2.5	71.0	7.0	2.4	
Correlation Matrix	1.000					
	.964	1.000				
	.985	.917	1.000			
	-.790	-.679	-.824	1.000		
	-.708	-.539	-.774	.945	1.000	

Apparent Resistivity Measured at 1 Hz is 70.25

Apparent Resistivity Calculated from Inductive Coupling is 213.1

CYPRUS ANVIL TENAS CK. ROSS RIVER LINE475E 29/9/81 L338 D= 7 N=3 X=152m

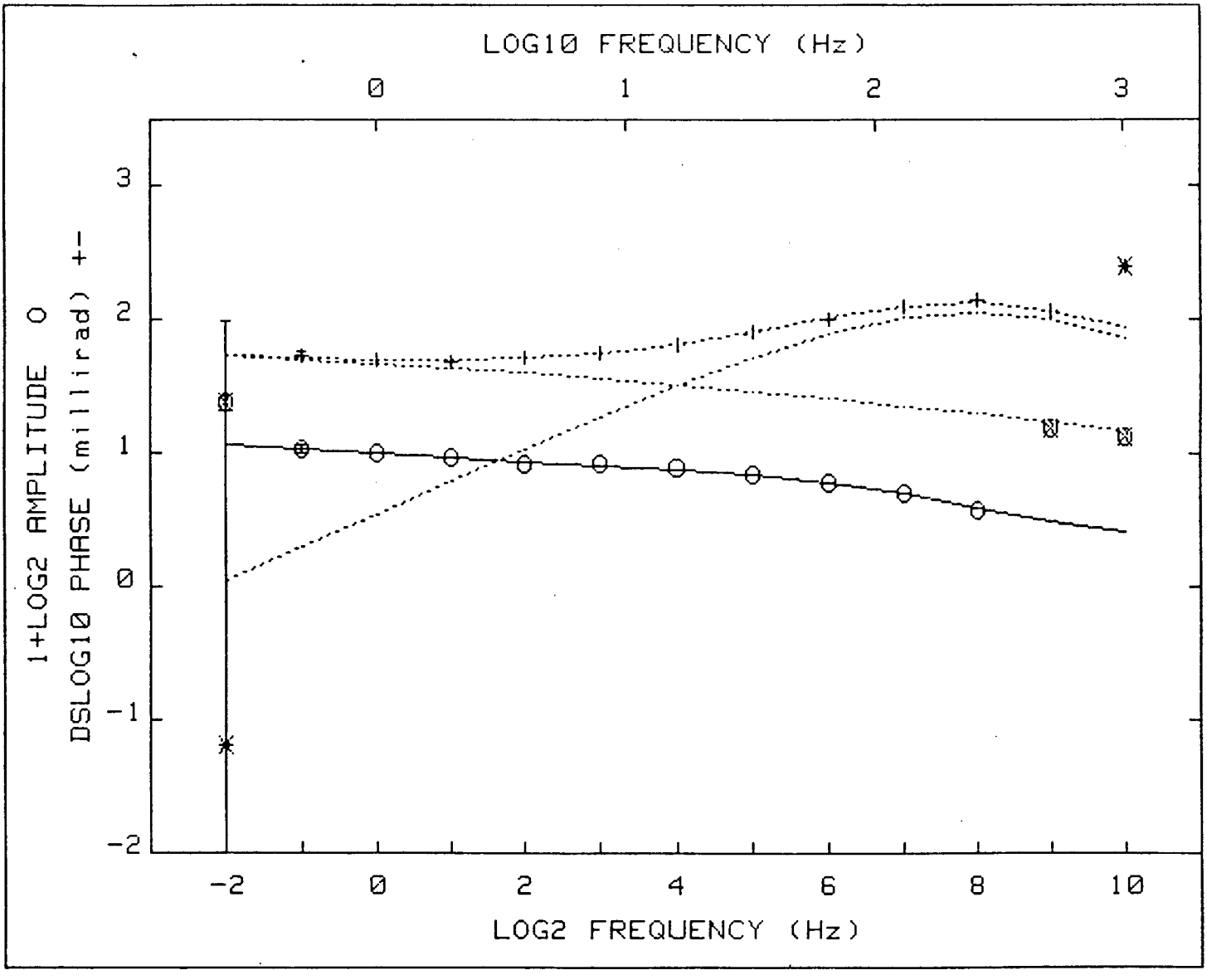

CRL: Number of dispersions= 2
C1=.25 fixed

Iter	Lambda	Rchsq	R0	M1	T1	M2	T2	C2
0	1.E-02	.00043	1.679	.486	7.7E+01	.169	7.1E-04	.727
1	1.E-02	.00019	1.682	.487	7.7E+01	.155	8.4E-04	.749
2	1.E-03	.00017	1.682	.488	7.2E+01	.151	8.8E-04	.770
3	1.E-04	.00016	1.618	.471	4.4E+01	.154	8.7E-04	.777
4	1.E-04	.00016	1.576	.459	3.0E+01	.156	8.7E-04	.784
5	1.E-05	.00016	1.509	.440	1.6E+01	.159	8.7E-04	.795
6	1.E-06	.00016	1.499	.437	1.4E+01	.158	8.7E-04	.800

Pct Std Deviations	9.3	9.5	322.7	4.7	5.2	4.8	
Correlation Matrix	1.000						
	.995	1.000					
	.995	.984	1.000				
	-.556	-.618	-.499	1.000			
	.107	.120	.094	-.509	1.000		
	-.713	-.658	-.751	-.123	.315	1.000	

Apparent Resistivity Measured at 1 Hz is 29.75

Apparent Resistivity Calculated from Inductive Coupling is 292.5

PHOENIX SPECTRAL I.P. RESISTIVITY (ohm-m) AT 1 HZ
CYPRUS ANVIL TENAS CK. ROSS RIVER LINE445E 30/9/81 L339

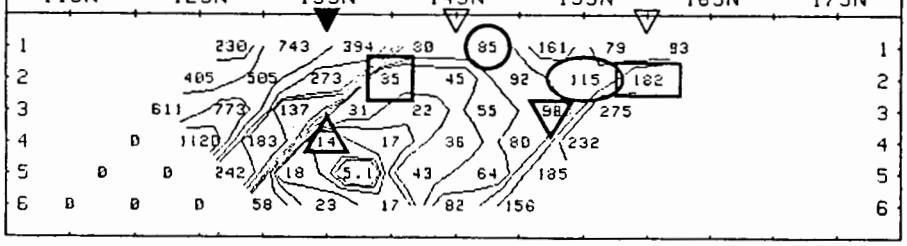

PHOENIX SPECTRAL I.P. PHASE (mrad) AT 1 HZ
CYPRUS ANVIL TENAS CK. ROSS RIVER LINE445E 30/9/81 L339

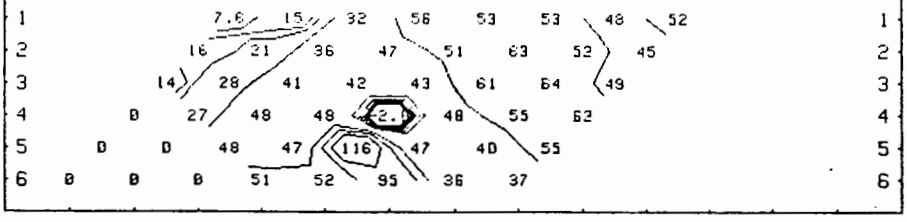

PHOENIX SPECTRAL I.P. Metal Factor (1Hz)
CYPRUS ANVIL TENAS CK. ROSS RIVER LINE445E 30/9/81 L339

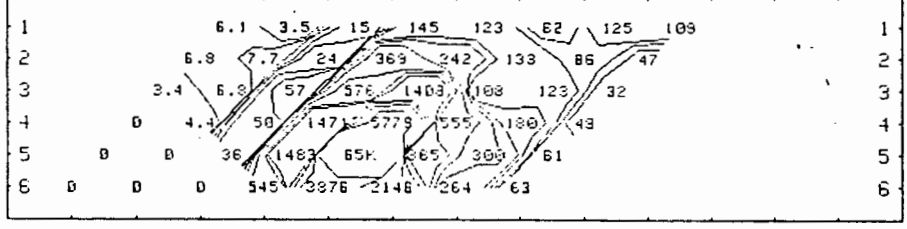

PHOENIX SPECTRAL I.P. DECOUPLED PHASE AT 1 HZ
CYPRUS ANVIL TENAS CK. ROSS RIVER LINE445E 30/9/81 L339

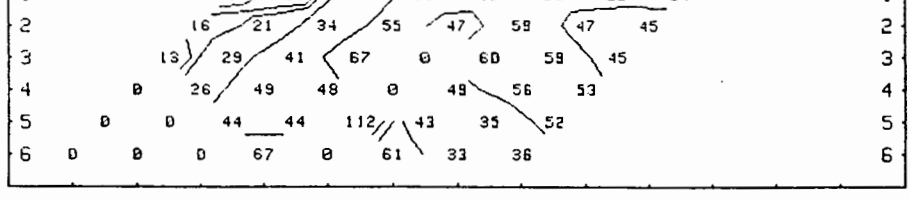

PHOENIX SPECTRAL I.P. MF (100*PHASE/RHO) AT 1 HZ
CYPRUS ANVIL TENAS CK. ROSS RIVER LINE445E 30/9/81 L339

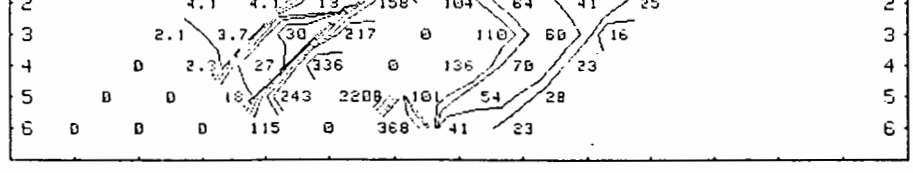

DWG. NO. – S.I.P. – 1110 – 2

CYPRUS ANVIL TENAS CK. ROSS RIVER LINE445E 30/9/81 L339 D= 4 N=2 X=152m

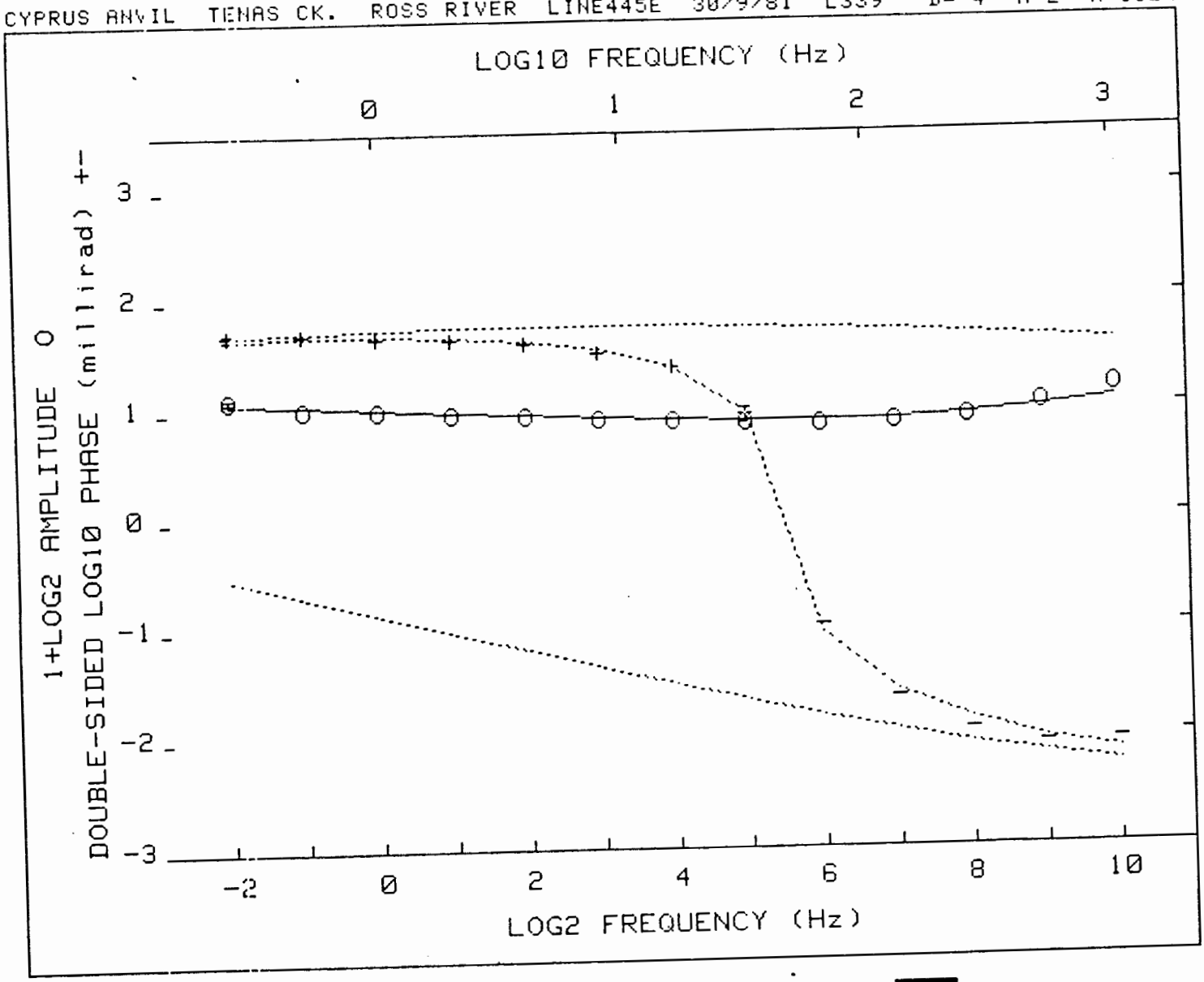

CRL: Number of dispersions= 2 Negative.
C1=.25 M2=1 fixed

Iter	Lambda	Rchsq	R0	M1	T1	T2	C2
0	1.E-02	.58558	1.399	.458	1.0E+00	2.2E-04	.976
1	1.E-02	.02733	1.138	.278	2.0E-01	4.8E-05	.881
2	1.E-03	.00769	1.242	.416	9.3E-02	2.0E-05	.616
3	1.E-04	.00376	1.254	.447	6.1E-02	1.4E-05	.513
4	1.E-05	.00363	1.267	.436	9.9E-02	1.3E-05	.522
5	1.E-06	.00363	1.265	.441	9.0E-02	1.3E-05	.518
Pct Std Deviations			4.2	12.7	453.2	27.6	12.7

Correlation Matrix

1.000					
-.615	1.000				
.893	-.877	1.000			
-.791	.500	-.763	1.000		
.602	-.958	.841	-.332	1.000	

Apparent Resistivity Measured at 1 Hz is 34.74
Apparent Resistivity Calculated from Inductive Coupling is 212.8

DWG. NO. - S.I.P - 1110 - 3

CYPRUS ANVIL TENAS CK. ROSS RIVER LINE445E 30/9/81 L339 D= 4 N=4 X=152m

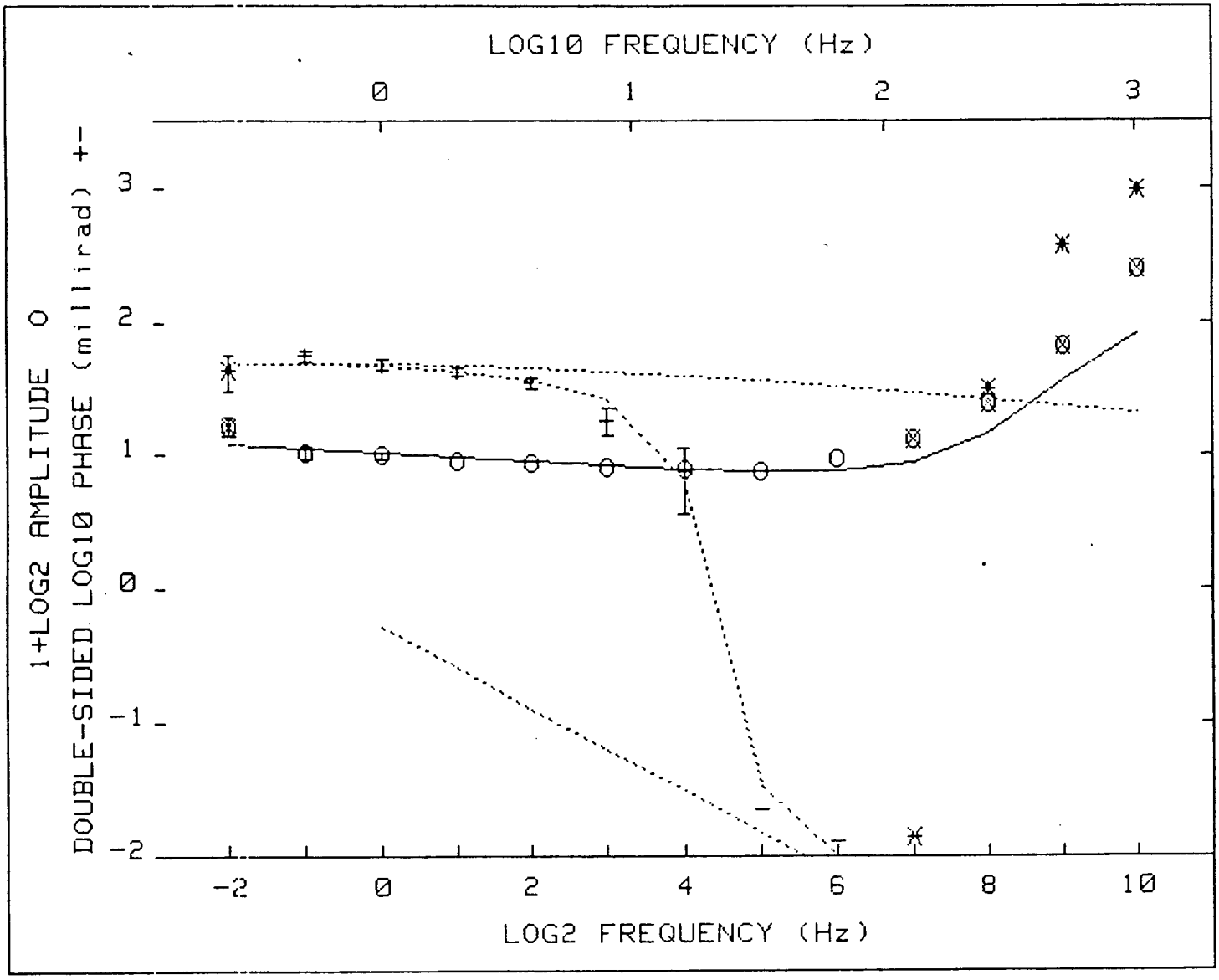

CRL: Number of dispersions= 2 Negative.
C1=.25 M2=1 C2=1 fixed

Iter	Lambda	Rchsq	R0	M1	T1	T2
0	1.E-02	.00739	1.323	.385	1.0E+00	2.3E-04
1	1.E-02	.00734	1.335	.391	1.1E+00	2.3E-04

Pct Std Deviations 10.8 12.2 790.7 23.3

Correlation Matrix

1.000			
.944	1.000		
.962	.900	1.000	
-.861	-.730	-.946	1.000

Apparent Resistivity Measured at 1 Hz is 14.40
Apparent Resistivity Calculated from Inductive Coupling is 606.0

DWG. NO. - SIP - 1110 - 5

CYPRUS ANVIL TENAS CK. ROSS RIVER LINE445E 30/9/81 L339 D= 5 N=5, X=152m

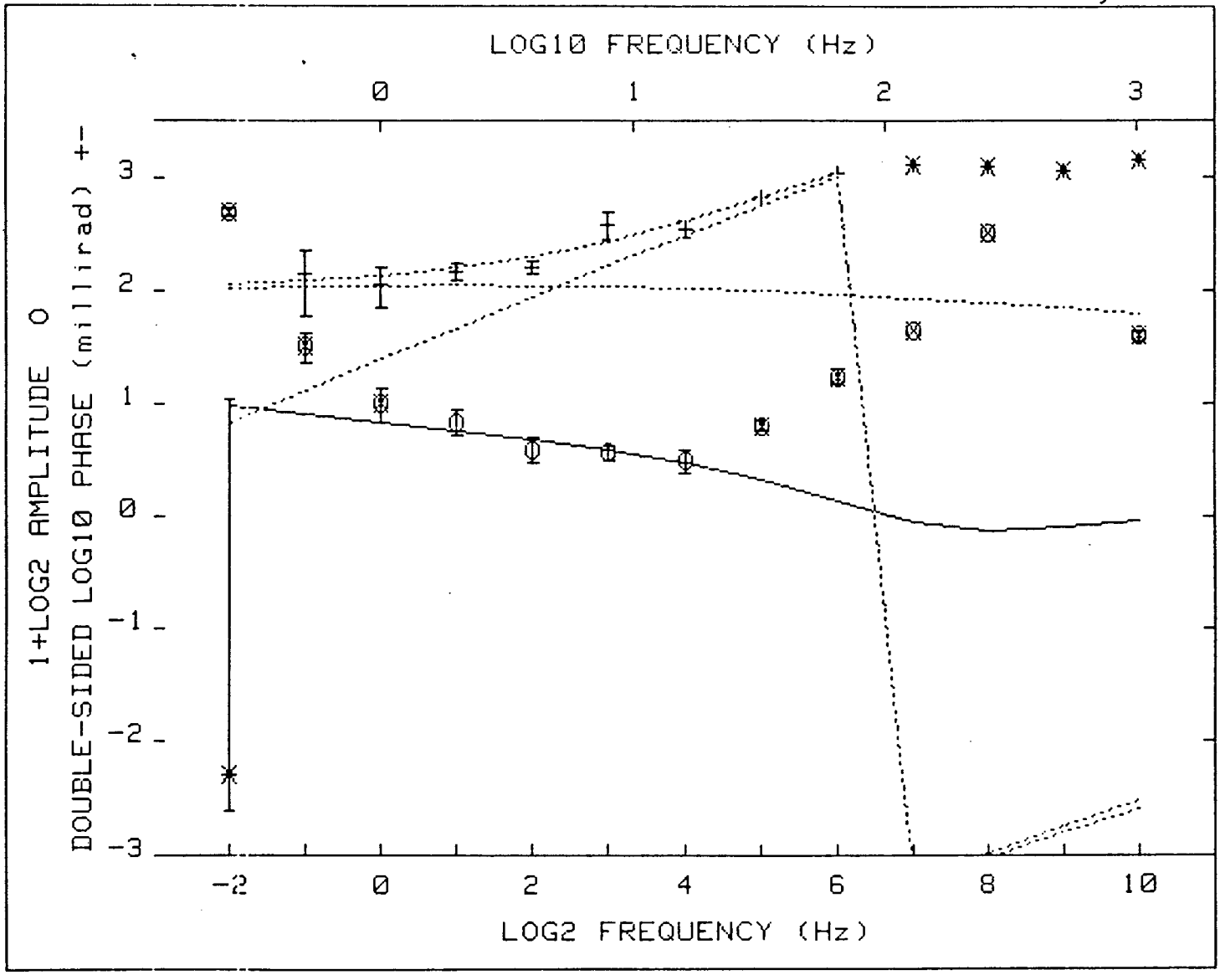

CRL: Number of dispersions= 2
T1=1 C1=.25 fixed

Iter	Lambda	Rchsq	R0	M1	M2	T2	C2
0	1.E-02	.07482	1.540	.690	.241	2.0E-03	.878
1	1.E-02	.01022	1.612	.725	.523	3.0E-03	.948
2	1.E-03	.00829	1.543	.690	.629	2.1E-03	.879
3	1.E-04	.00826	1.539	.687	.708	1.7E-03	.863
Pct Std Deviations			14.8	23.8	999.9	999.9	72.5

Correlation Matrix

1.000					
.950	1.000				
-.707	-.797	1.000			
.650	.748	-.995	1.000		
.743	.865	-.963	.955	1.000	

Apparent Resistivity Measured at 1 Hz is 5.060
Apparent Resistivity Calculated from Inductive Coupling is 99.74

CYPRUS ANVIL TENAS CK. ROSS RIVER LINE445E 30/9/81 L339 D= 7 N=2 X=152m

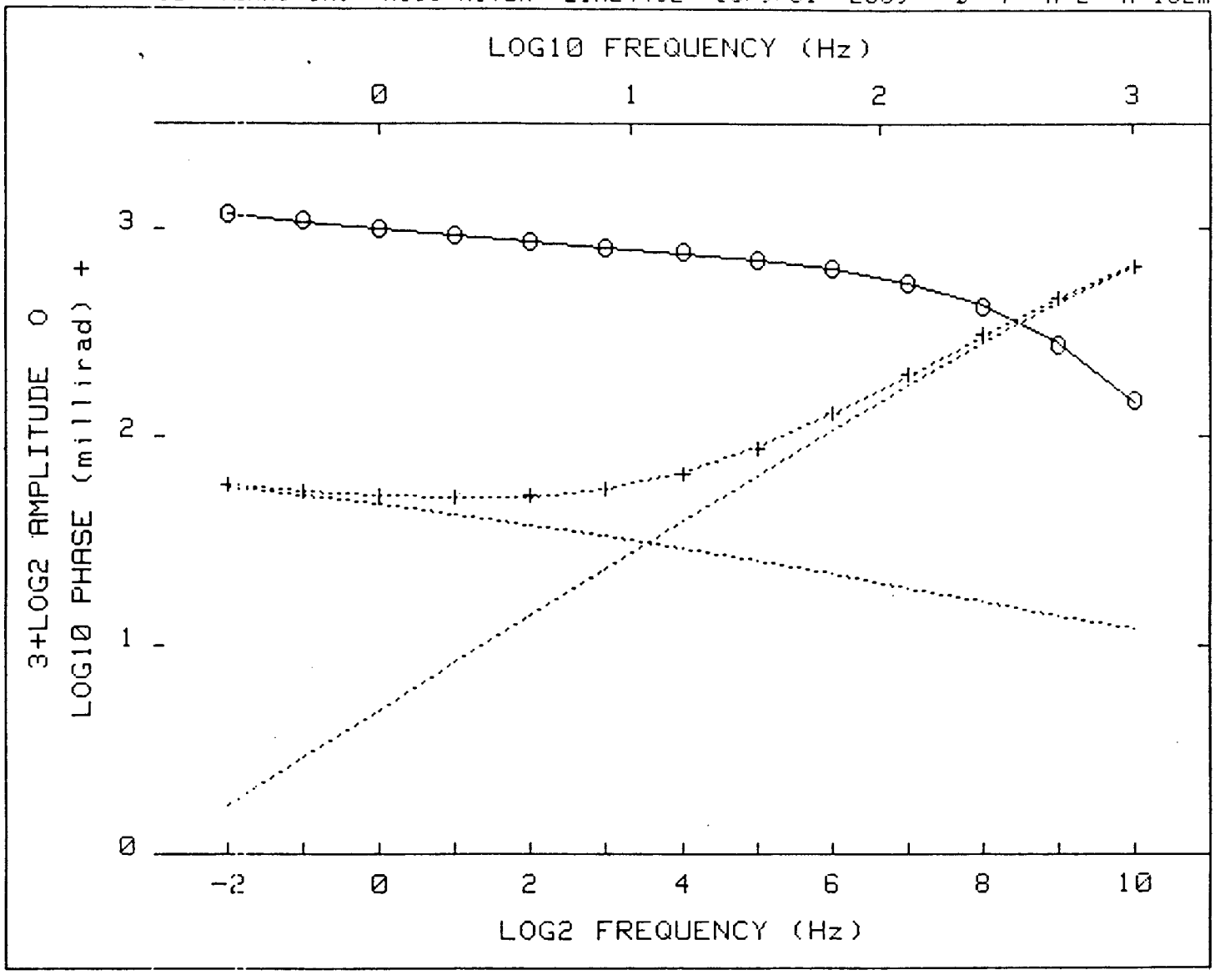

CRL: Number of dispersions= 2
C1=.25 fixed

Iter	Lambda	Rchsq	R0	M1	T1	M2	T2	C2
0	1.E-02	.01086	1.949	.577	1.2E+02	.337	3.2E-04	.830
1	1.E-02	.00123	1.772	.518	1.3E+02	.479	1.7E-04	.736
2	1.E-03	.00007	1.787	.517	1.4E+02	.579	1.2E-04	.731
3	1.E-04	.00004	1.819	.526	1.7E+02	.577	1.2E-04	.737
4	1.E-05	.00004	1.845	.532	2.0E+02	.571	1.2E-04	.736

Pct Std Deviations	5.7	4.7	82.6	4.8	3.9	1.2	
Correlation Matrix	1.000						
	.999	1.000					
	.997	.994	1.000				
	-.919	-.924	-.903	1.000			
	-.406	-.394	-.434	.034	1.000		
	-.675	-.653	-.704	.412	.817	1.000	

Apparent Resistivity Measured at 1 Hz is 115.5
Apparent Resistivity Calculated from Inductive Coupling is 231.8

DWG. NO. – SIP – 1110 – 7

CYPRUS ANVIL TENAS CK. ROSS RIVER LINE445E 30/9/81 L339 D= 7 N=3 X=152m

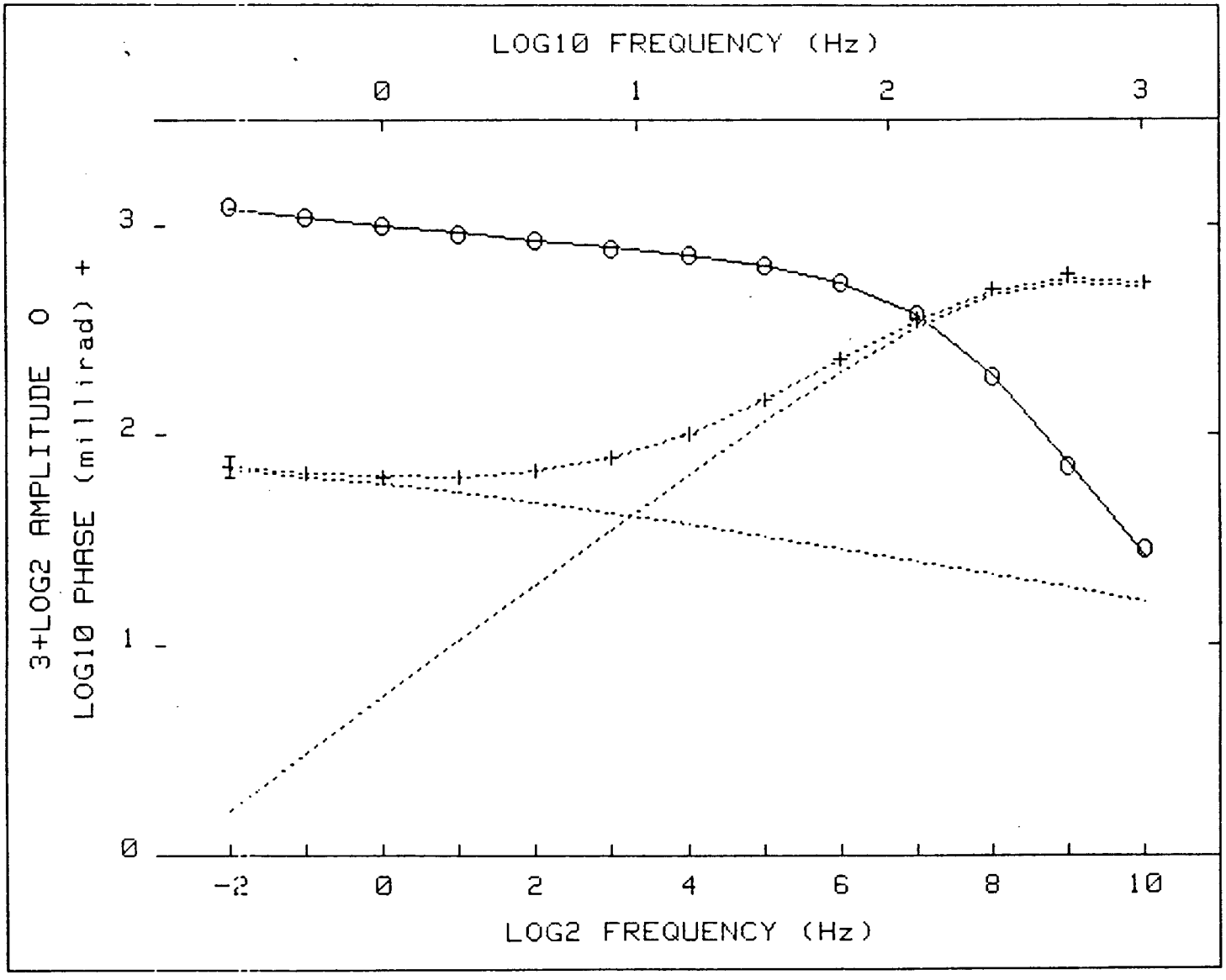

CRL: Number of dispersions= 2
C1=.25 fixed

Iter	Lambda	Rchsq	R0	M1	T1	M2	T2	C2
0	1.E-02	.06770	1.845	.532	2.0E+02	.571	1.2E-04	.736
1	1.E-02	.03069	1.893	.549	2.1E+02	.296	6.1E-04	.641
2	1.E-03	.00487	2.070	.625	1.3E+02	.295	6.2E-04	.987
3	1.E-04	.00187	1.749	.548	4.3E+01	.365	6.4E-04	.875
4	1.E-05	.00010	1.877	.560	8.7E+01	.348	6.4E-04	.858
5	1.E-06	.00010	1.898	.564	9.6E+01	.344	6.4E-04	.859
Pct Std Deviations			7.7	5.4	123.2	6.6	1.6	1.1

Correlation Matrix

1.000						
.998	1.000					
.996	.990	1.000				
-.985	-.990	-.974	1.000			
.175	.166	.171	-.262	1.000		
-.610	-.581	-.642	.491	.208	1.000	

Apparent Resistivity Measured at 1 Hz is 98.24
Apparent Resistivity Calculated from Inductive Coupling is 236.8

DWG. NO. - S.I.P - 1110 - 8

CYPRUS ANVIL TENAS CK. ROSS RIVER LINE445E 30/9/81 L339 D= 8 N=1 X=152m

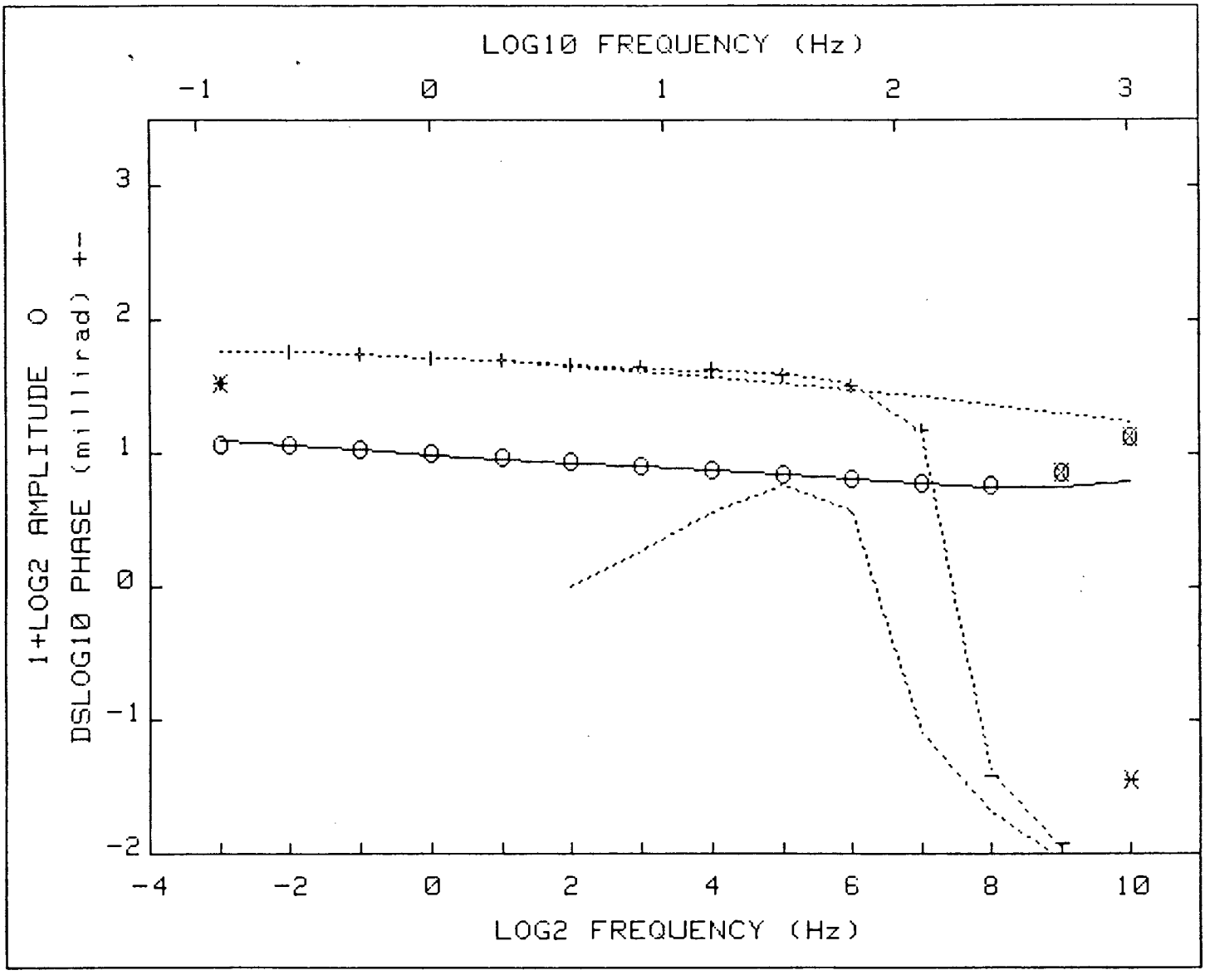

CRL: Number of dispersions= 3 Negative.
C1=.25 C2=1 M3=1 C3=1 fixed

Iter	Lambda	Rchsq	R0	M1	T1	M2	T2	T3
0	1.E-02	.02227	1.301	.297	5.5E+00	.100	1.0E-02	1.9E-05
1	1.E-01	.01454	1.405	.437	5.2E+00	.048	8.2E-03	1.8E-05
2	1.E-02	.00222	1.455	.453	4.4E+00	.021	4.7E-03	2.0E-05
3	1.E-03	.00048	1.434	.441	3.7E+00	.016	2.2E-03	2.1E-05
4	1.E-04	.00035	1.478	.448	7.2E+00	.022	2.1E-03	2.1E-05
5	1.E-05	.00029	1.492	.453	8.2E+00	.021	2.2E-03	2.0E-05
6	1.E-06	.00029	1.491	.453	8.1E+00	.021	2.2E-03	2.0E-05

Pct Std Deviations	3.9	3.8	85.5	8.4	11.1	5.8	
Correlation Matrix	1.000						
	.985	1.000					
	.984	.954	1.000				
	.546	.442	.635	1.000			
	.366	.297	.416	.461	1.000		
	-.906	-.880	-.917	-.451	-.586	1.000	

Apparent Resistivity Measured at 1 Hz is 92.59

Apparent Resistivity Calculated from Inductive Coupling is 846.2

CYPRUS ANVIL TENAS CK. ROSS RIVER LINE445E 30/9/81 L339 D= 8 N=2 X=152m

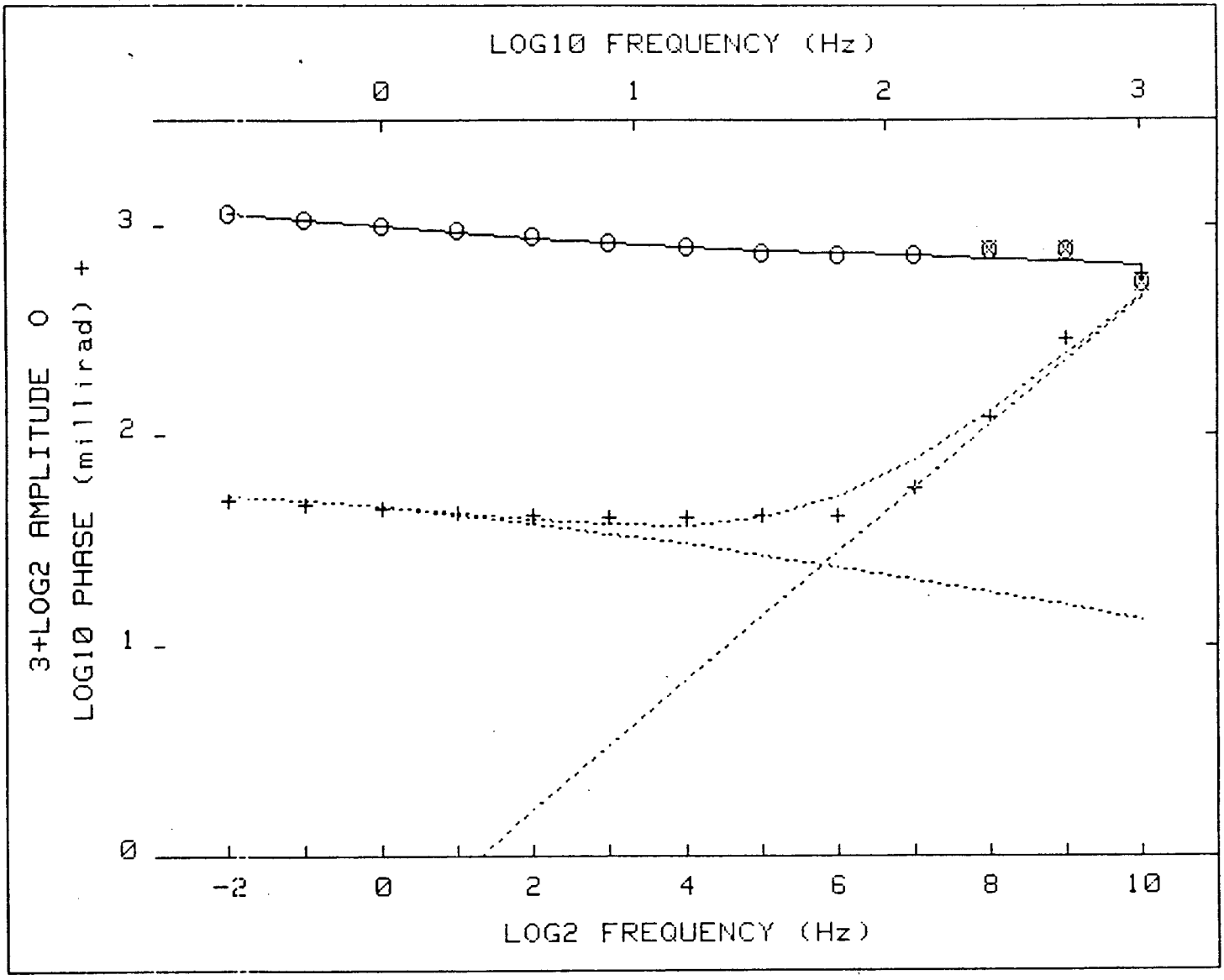

CRL: Number of dispersions= 2
C1=.25 M2=1 C2=1 fixed

Iter	Lambda	Rchsq	R0	M1	T1	T2
0	1.E-02	.00248	1.502	.433	2.1E+01	4.2E-05
1	1.E-02	.00248	1.503	.433	2.1E+01	4.2E-05

Pct Std Deviations	11.2	13.6	350.1	11.0	
Correlation Matrix	1.000				
	.992	1.000			
	.983	.975	1.000		
	-.769	-.787	-.729	1.000	

Apparent Resistivity Measured at 1 Hz is 181.6
Apparent Resistivity Calculated from Inductive Coupling is 1079

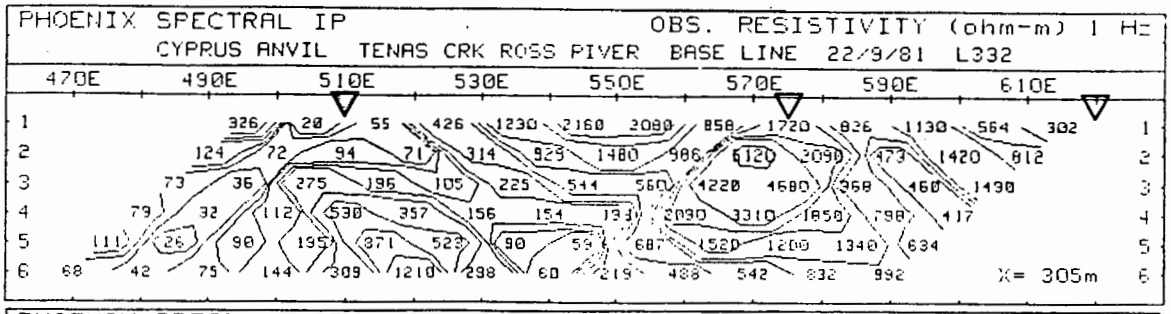
PHOENIX SPECTRAL IP
OBS. RESISTIVITY (ohm-m) 1 Hz
CYPRUS ANVIL TENAS CRK ROSS RIVER BASE LINE 22/9/81 L332
470E 490E 510E 530E 550E 570E 590E 610E
X= 305m

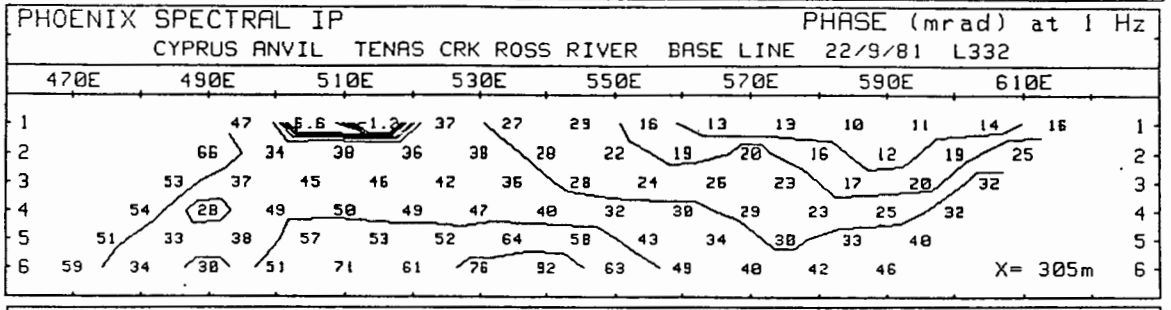
PHOENIX SPECTRAL IP
PHASE (mrad) at 1 Hz
CYPRUS ANVIL TENAS CRK ROSS RIVER BASE LINE 22/9/81 L332
470E 490E 510E 530E 550E 570E 590E 610E
X= 305m

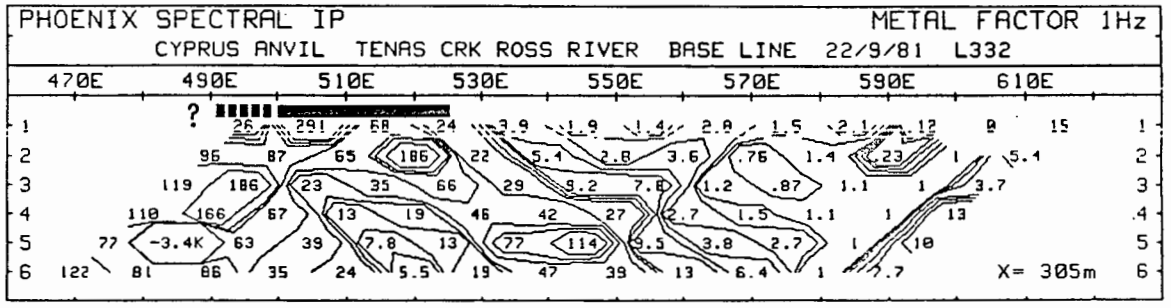
PHOENIX SPECTRAL IP
METAL FACTOR 1Hz
CYPRUS ANVIL TENAS CRK ROSS RIVER BASE LINE 22/9/81 L332
470E 490E 510E 530E 550E 570E 590E 610E
X= 305m

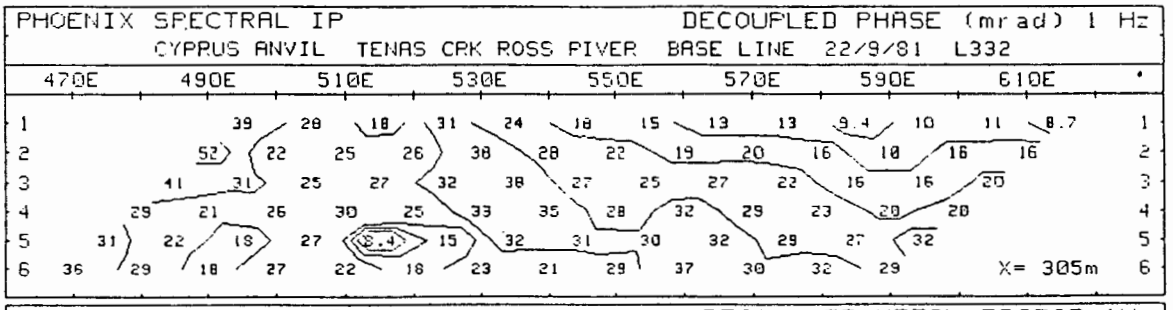
PHOENIX SPECTRAL IP
DECOUPLED PHASE (mrad) 1 Hz
CYPRUS ANVIL TENAS CRK ROSS RIVER BASE LINE 22/9/81 L332
470E 490E 510E 530E 550E 570E 590E 610E
X= 305m

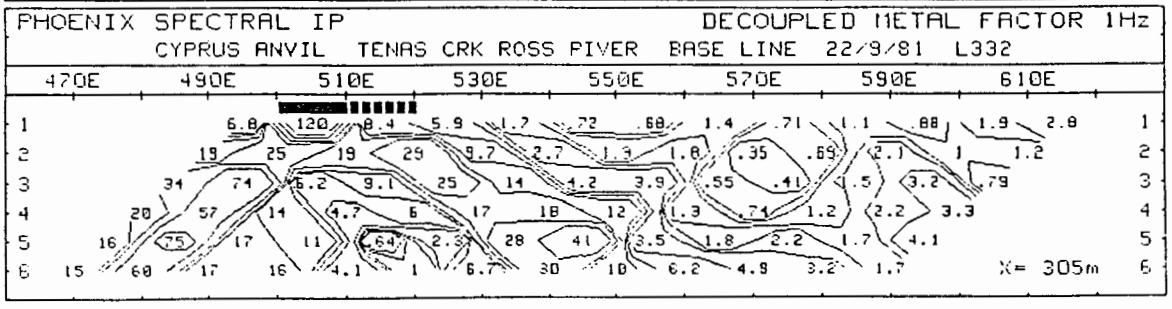
PHOENIX SPECTRAL IP
DECOUPLED METAL FACTOR 1Hz
CYPRUS ANVIL TENAS CRK ROSS RIVER BASE LINE 22/9/81 L332
470E 490E 510E 530E 550E 570E 590E 610E
X= 305m

DWG. NO. - S.I.P - IIII - 2

CYPRUS ANVIL TENAS CRK ROSS RIVER BASE LINE 22/9/81 L332 D= 2 N=1 X=305m

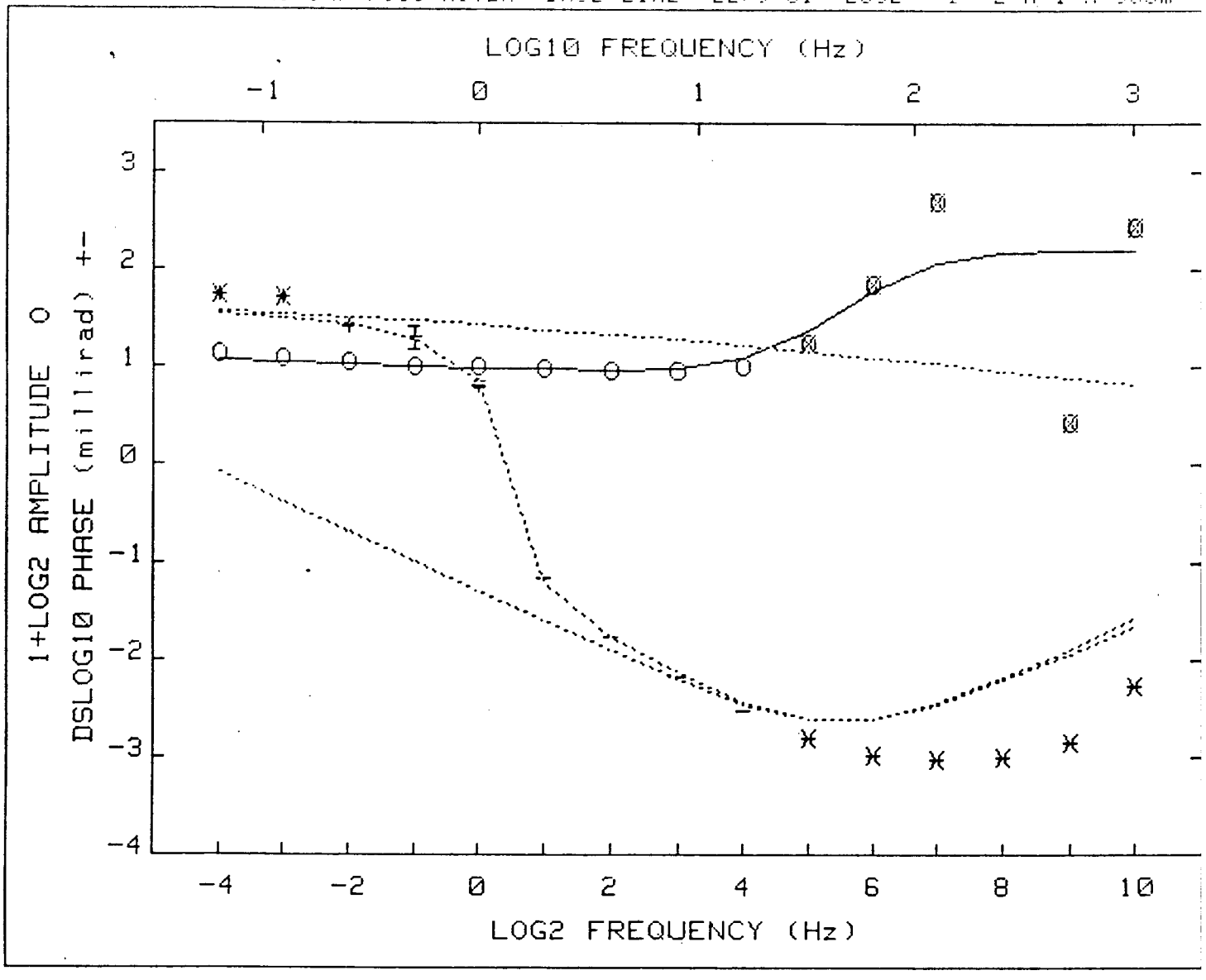

CRL: Number of dispersions= 2 Negative.
C1=.25 M2=1 C2=1 fixed

Iter	Lambda	Rchsq	R0	M1	T1	T2
0	1.E-02	.00246	1.379	.337	6.8E+01	2.3E-03
1	1.E-02	.00246	1.383	.338	7.0E+01	2.3E-03

Pct Std Deviations	24.7	47.8	5792.4	32.6	
Correlation Matrix	1.000				
	.998	1.000			
	.997	.997	1.000		
	-.984	-.980	-.991	1.000	

Apparent Resistivity Measured at 1 Hz is 20.17

Apparent Resistivity Calculated from Inductive Coupling is 30.55

DWG. NO. - S.I.P. - IIII - 3

CYPRUS ANVIL TENAS CRK ROSS RIVER BASE LINE 22/9/81 L332 D= 2 N=2 X=305m

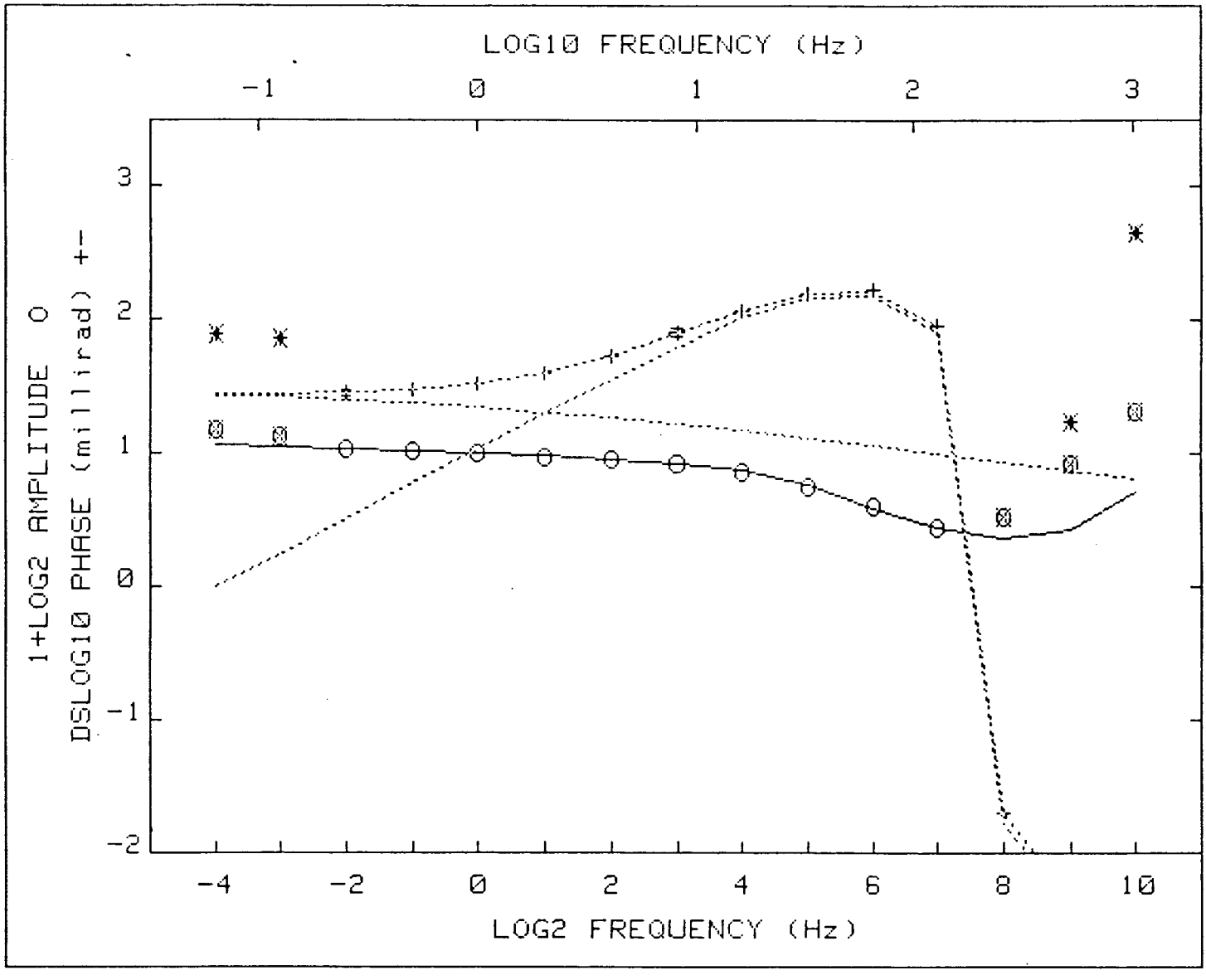

CRL: Number of dispersions= 3 Negative.
C1=.25 M3=1 C3=1 fixed

Iter	Lambda	Rchsq	R0	M1	T1	M2	T2	C2	T3
0	1.E-02	.00011	1.231	.246	1.3E+01	.280	3.4E-03	.879	5.5E-05
1	1.E-02	.00011	1.231	.247	1.3E+01	.280	3.4E-03	.879	5.5E-05
Pct Std Deviations			5.3	12.0	482.5	2.6	2.8	2.4	4.9

Correlation Matrix

1.000							
.994	1.000						
.995	.983	1.000					
-.571	-.636	-.520	1.000				
-.064	-.043	-.089	-.510	1.000			
-.753	-.697	-.789	-.048	.478	1.000		
-.826	-.850	-.802	.872	-.447	.321	1.000	

Apparent Resistivity Measured at 1 Hz is 72.23

Apparent Resistivity Calculated from Inductive Coupling is 3329

DWG. NO. - S.I.P - IIII - 4

CYPRUS ANVIL TENAS CRK ROSS RIVER BASE LINE 22/9/81 L332 D= 2 N=3 X=305m

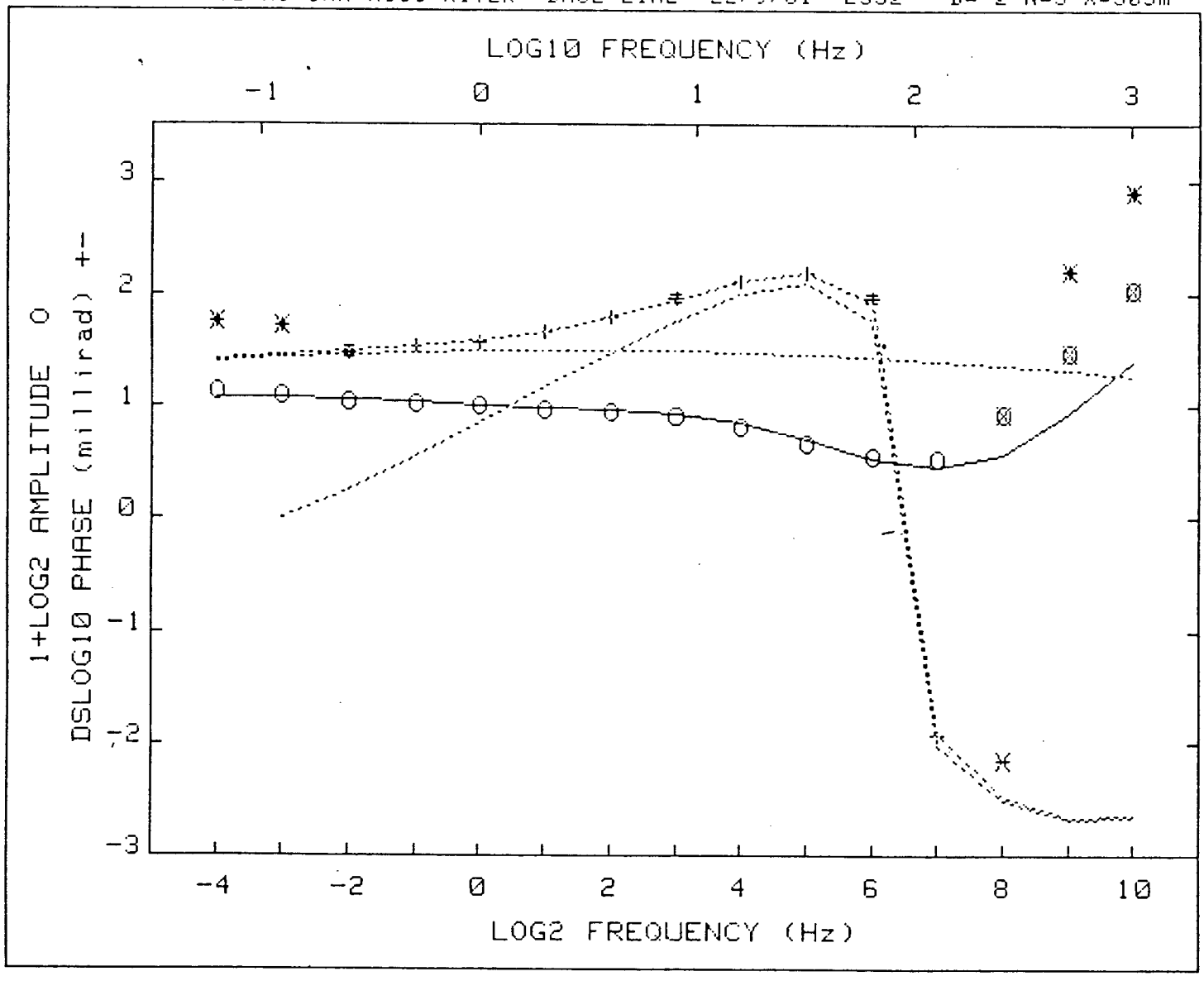

CRL: Number of dispersions= 3 Negative.
C1=.25 C2=1 M3=1 C3=1 fixed

Iter	Lambda	Rchsq	R0	M1	T1	M2	T2	T3
0	1.E-02	.00114	1.148	.269	1.1E-01	.232	4.9E-03	1.6E-04
1	1.E-02	.00109	1.156	.271	1.1E-01	.232	5.0E-03	1.6E-04
2	1.E-03	.00109	1.156	.271	1.1E-01	.232	5.0E-03	1.6E-04

Pct Std Deviations	2.9	12.8	823.8	5.2	7.7	9.9	

Correlation Matrix

1.000						
-.805	1.000					
.948	-.929	1.000				
.547	-.737	.636	1.000			
.452	-.611	.519	.211	1.000		
-.783	.807	-.838	-.309	-.772	1.000	

Apparent Resistivity Measured at 1 Hz is 35.75

Apparent Resistivity Calculated from Inductive Coupling is 2203

DWG. NO. – S.I.P. – IIII –5

CYPRUS ANVIL TENAS CRK ROSS RIVER BASE LINE 22/9/81 L332 D= 2 N=4 X=305m

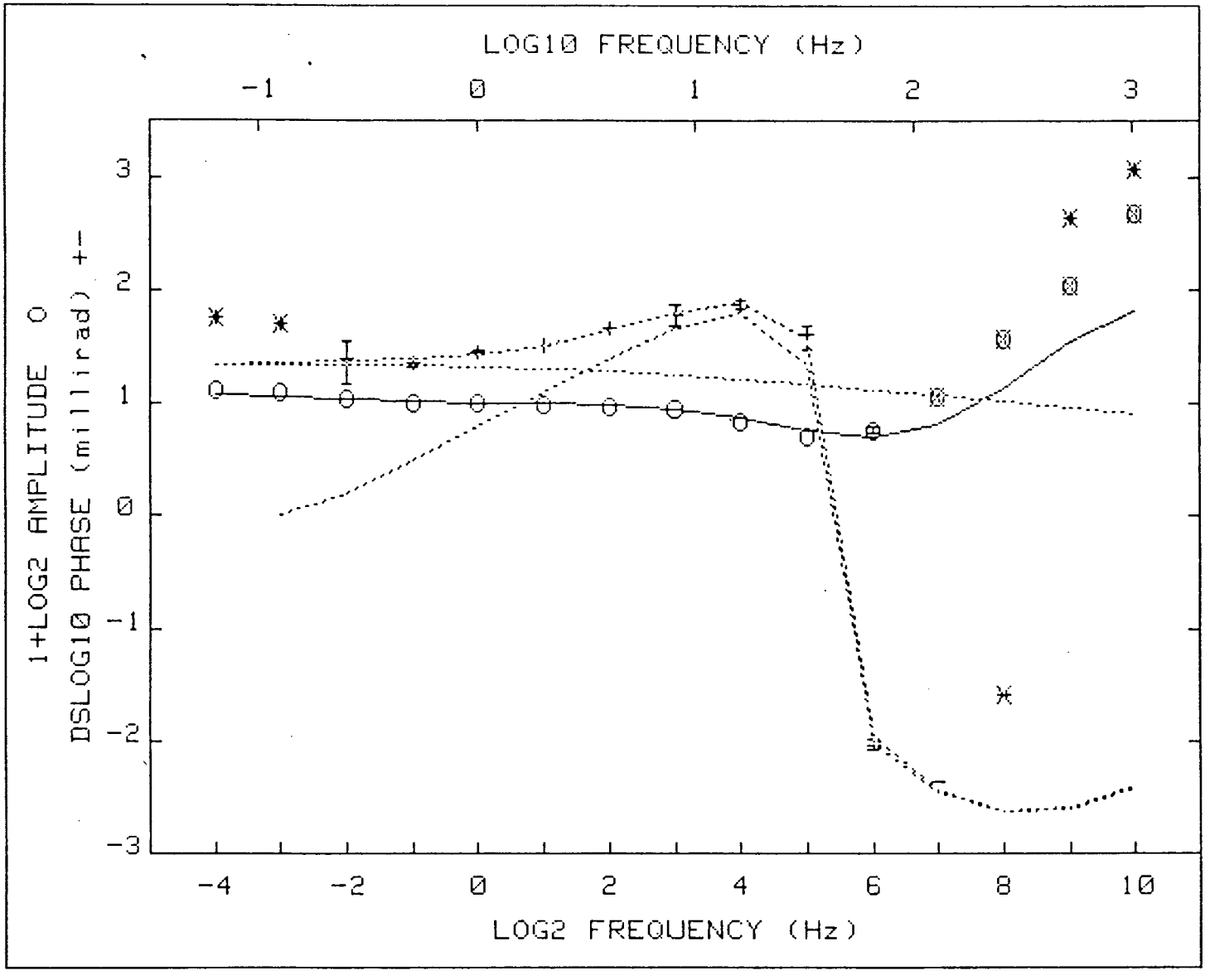

CRL: Number of dispersions= 3 Negative.
C1=.25 C2=1 M3=1 C3=1 fixed

Iter	Lambda	Rchsq	R0	M1	T1	M2	T2	T3
0	1.E-02	.00229	1.135	.198	1.3E+00	.172	7.0E-03	3.3E-04
1	1.E-02	.00197	1.152	.199	1.3E+00	.169	7.1E-03	3.3E-04
2	1.E-03	.00197	1.153	.199	1.4E+00	.169	7.1E-03	3.3E-04

Pct Std Deviations	6.5	10.6	4113.6	6.2	11.4	14.0	

Correlation Matrix

1.000						
.837	1.000					
.980	.767	1.000				
-.212	-.349	-.183	1.000			
.560	.247	.606	-.394	1.000		
-.800	-.610	-.822	.604	-.792	1.000	

Apparent Resistivity Measured at 1 Hz is 32.32

Apparent Resistivity Calculated from Inductive Coupling is 1720

CYPRUS ANVIL TENAS CRK ROSS RIVER BASE LINE 22/9/81 L332 D= 2 N=5 X=305m

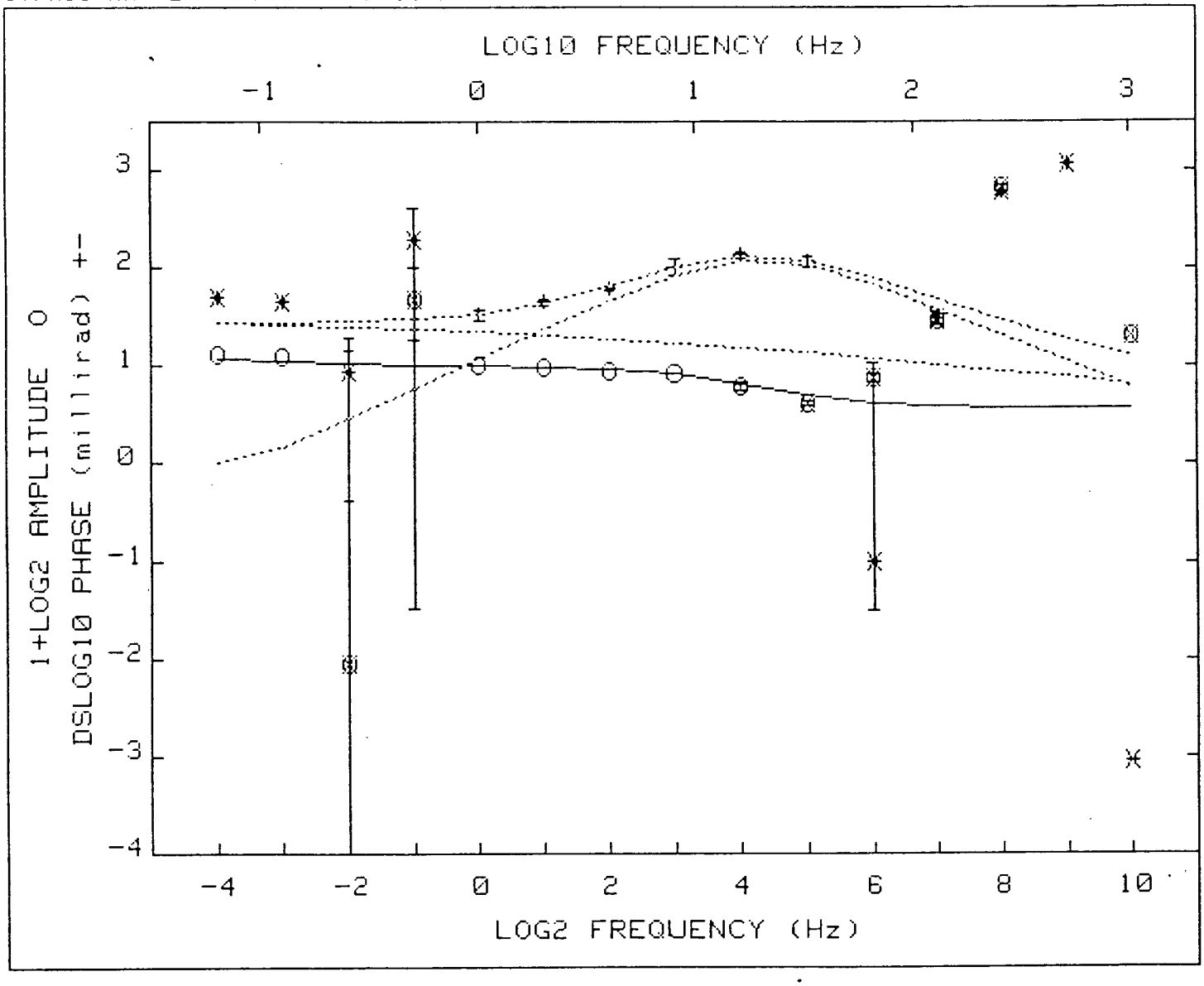

CRL: Number of dispersions= 2
C1=.25 C2=1 fixed

Iter	Lambda	Rchsq	R0	M1	T1	M2	T2
0	1.E-02	.00100	1.231	.247	1.0E+01	.166	9.1E-03
1	1.E-02	.00099	1.222	.243	1.0E+01	.164	9.3E-03
2	1.E-03	.00099	1.225	.244	1.1E+01	.164	9.4E-03

Pct Std Deviations	54.5	208.7	9999.9	35.0	9.7	
Correlation Matrix	1.000					
	.999	1.000				
	.999	.996	1.000			
	-.982	-.986	-.975	1.000		
	.381	.356	.403	-.367	1.000	

Apparent Resistivity Measured at 1 Hz is 25.80

Apparent Resistivity Calculated from Inductive Coupling is 517.9

DWG. NO. - S.I.P. - IIII - 7

CYPRUS ANVIL TENAS CRK ROSS RIVER BASE LINE 22/9/81 L332 D= 2 N=6 X=305m

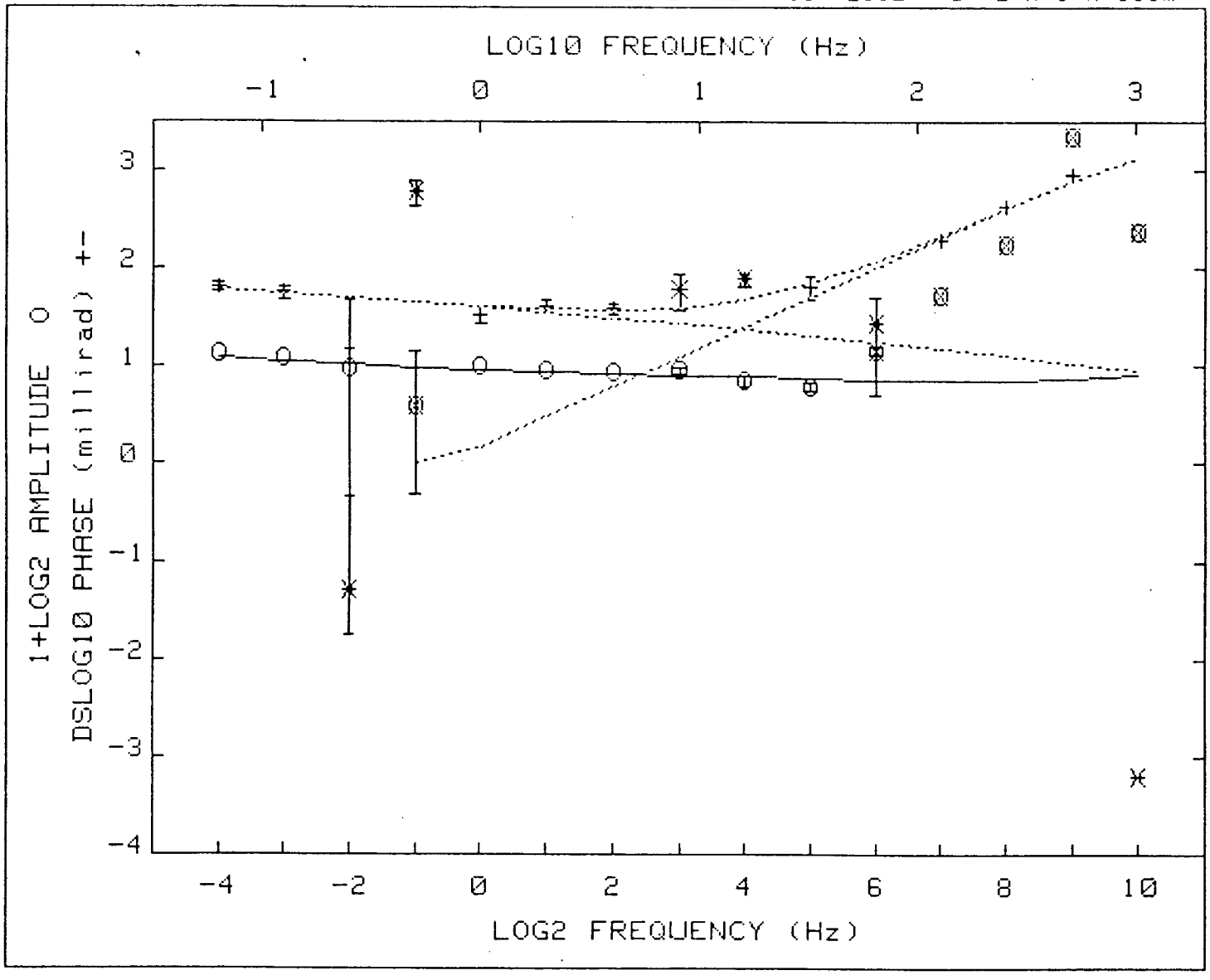

CRL: Number of dispersions= 2
C1=.25 M2=1 C2=1 fixed

Iter	Lambda	Rchsq	R0	M1	T1	T2
0	1.E-02	.00303	1.905	.544	6.9E+02	1.2E-04
1	1.E-02	.00300	1.905	.544	7.0E+02	1.2E-04
Pct Std Deviations			34.3	27.2	1555.9	33.2

Correlation Matrix

1.000				
.998	1.000			
.993	.990	1.000		
-.964	-.967	-.951	1.000	

Apparent Resistivity Measured at 1 Hz is 41.58

Apparent Resistivity Calculated from Inductive Coupling is 9120

DWG. NO. - S.I.P - IIII - 8

CYPRUS ANVIL TENAS CRK ROSS RIVER BASE LINE 22/9/81 L332 D= 3 N=2 X=305m

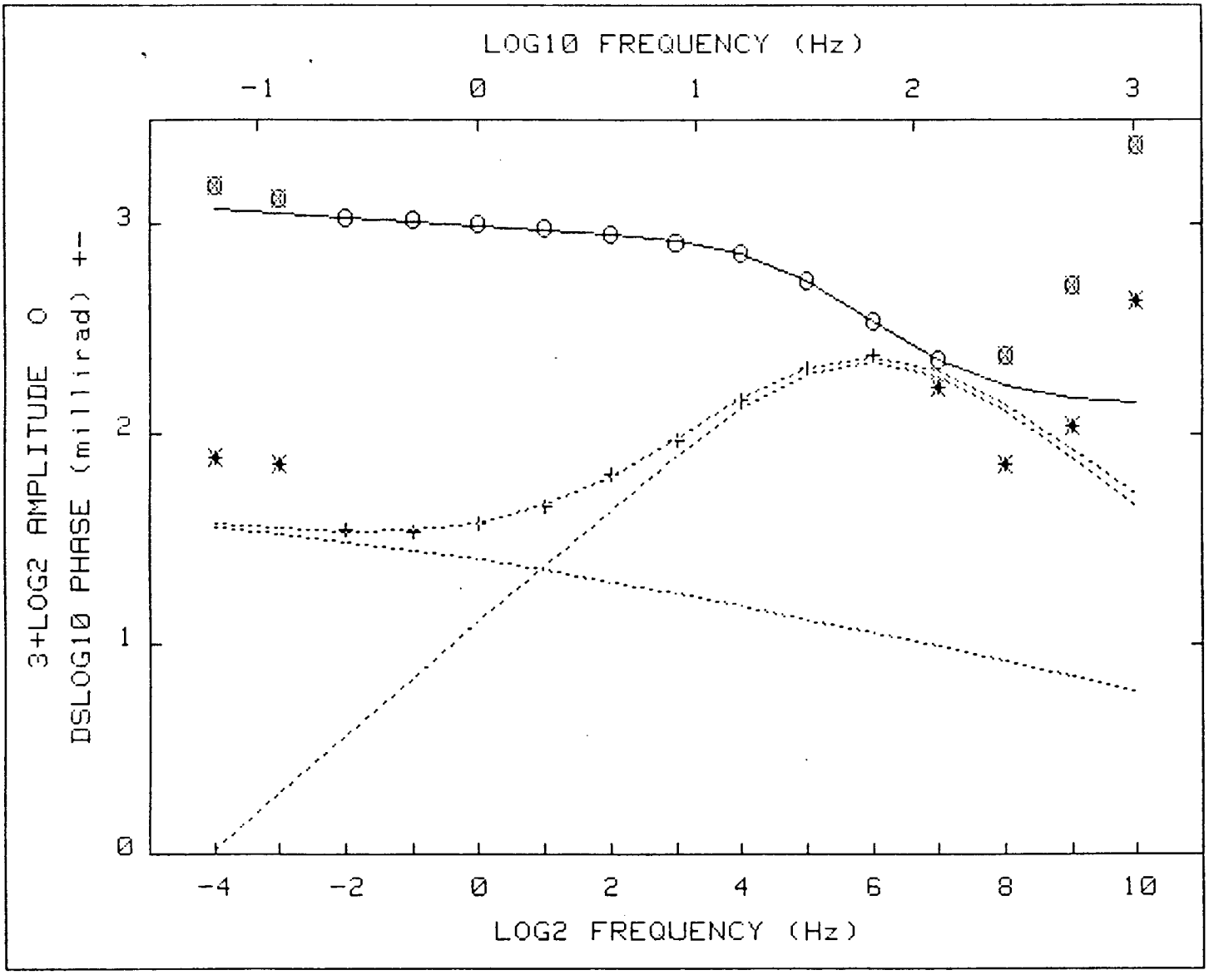

CRL: Number of dispersions= 2
C1=.25 fixed

Iter	Lambda	Rchsq	R0	M1	T1	M2	T2	C2
0	1.E-02	.00004	1.430	.352	1.6E+02	.274	3.6E-03	.894
1	1.E-02	.00004	1.430	.352	1.6E+02	.274	3.5E-03	.893
2	1.E-03	.00004	1.432	.353	1.6E+02	.274	3.5E-03	.893

Pct Std Deviations	9.9	17.2	423.4	7.3	3.3	1.9	
Correlation Matrix	1.000						
	1.000	1.000					
	.999	.997	1.000				
	-.960	-.964	-.950	1.000			
	-.342	-.336	-.363	.094	1.000		
	-.764	-.753	-.786	.573	.746	1.000	

Apparent Resistivity Measured at 1 Hz is 93.99

Apparent Resistivity Calculated from Inductive Coupling is 131.2

DWG. NO. - S.I.P. - IIII - 9

CYPRUS ANVIL TENAS CRK ROSS RIVER BASE LINE 22/9/81 L332 D= 4 N=2 X=305m

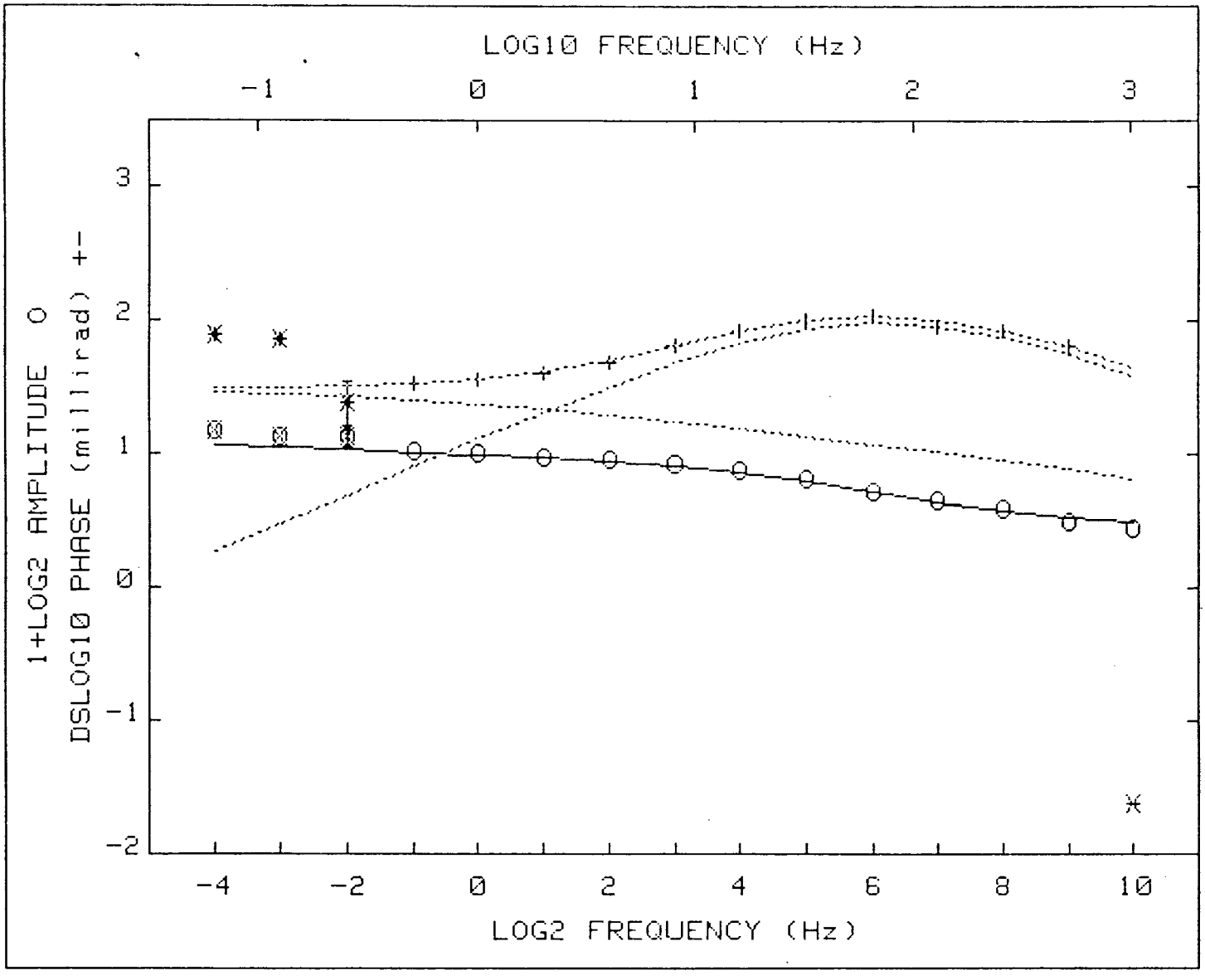

CRL: Number of dispersions= 2
C1=.25 fixed

Iter	Lambda	Rchsq	R0	M1	T1	M2	T2	C2
0	1.E-02	.00054	1.265	.272	1.7E+01	.197	2.8E-03	.715
1	1.E-02	.00052	1.258	.265	1.7E+01	.201	2.8E-03	.702
2	1.E-03	.00052	1.259	.265	1.9E+01	.202	2.8E-03	.701

Pct Std Deviations	37.3	96.2	9999.9	11.0	10.5	10.3	
Correlation Matrix	1.000						
	.998	1.000					
	.998	.994	1.000				
	-.830	-.861	-.802	1.000			
	.754	.730	.769	-.480	1.000		
	-.880	-.855	-.900	.502	-.738	1.000	

Apparent Resistivity Measured at 1 Hz is 71.01

Apparent Resistivity Calculated from Inductive Coupling is 89.73

DWG. NO. - S.I.P. - 1111-10

CYPRUS ANVIL TENAS CRK PASS RIVER BASE LINE 22/9/81 L332 D= 5 N=3 X=305m

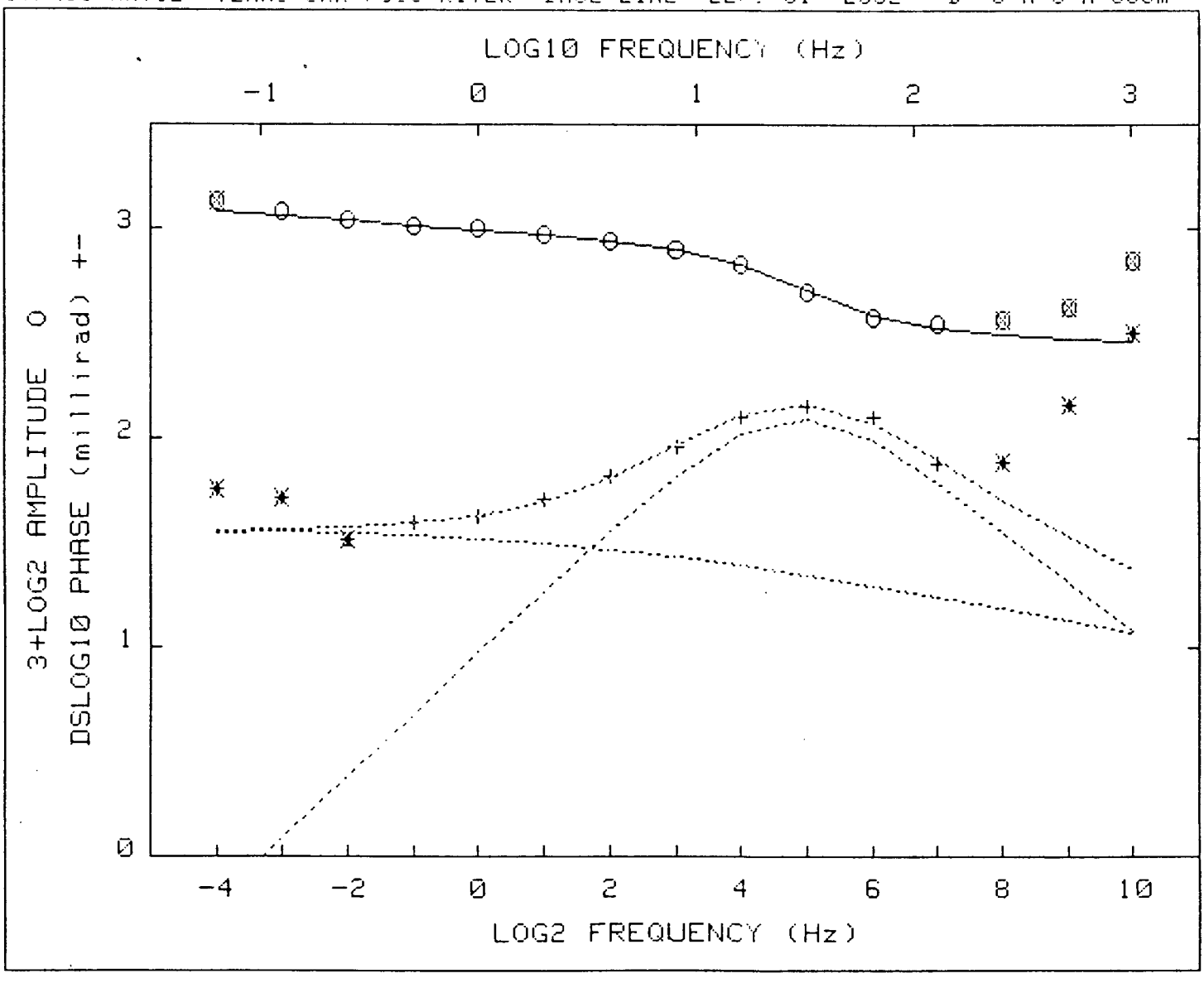

CRL: Number of dispersions= 2
C1=.25 fixed

Iter	Lambda	Rchsq	F0	M1	T1	M2	T2	C2
0	1.E-02	.00023	1.2E1	.297	3.0E+00	.174	5.2E-03	.937
1	1.E-02	.00020	1.2E5	.303	3.0E+00	.169	5.3E-03	.963
2	1.E-03	.00020	1.2E5	.303	3.0E+00	.169	5.3E-03	.963

Pct Std Deviations	11.5	13.2	3758.0	5.1	2.9	5.7	
Correlation Matrix	1.000						
	.981	1.000					
	.957	.966	1.000				
	.663	.546	.730	1.000			
	.012	-.042	.049	.203	1.000		
	-.893	-.817	-.919	-.872	-.082	1.000	

Apparent Resistivity Measured at 1 Hz is 105.1

Apparent Resistivity Calculated from Inductive Coupling is 286.6

RECENT AND FUTURE ADVANCES IN THE INDUCED POLARIZATION METHOD

by

Philip G. Hallof, Ph.D., and William H. Pelton, Ph.D.

Prepared for Presentation
at the Prospectors and Developers Convention
Royal York Hotel, Toronto
March 8th to March 11th, 1981

- -

RECENT AND FUTURE ADVANCES IN THE INDUCED POLARIZATION METHOD

BY

Philip G. Hallof, Ph.D., and William H. Pelton, Ph.D.

INTRODUCTION

The induced polarization (IP) method was introduced into Canadian exploration practice in the period from 1955 to 1960. Two measurement techniques were widely used, the pulse-transient method (time domain) and the variable frequency method (frequency domain). In the fifteen years following 1960, striking improvements were made in both frequency domain and time domain IP equipment, but only limited progress was made in a better understanding of the IP phenomenon, its source, and how to use it.

However, in the five year period since 1975, considerable progress has been made in our understanding of the IP method. Beginning with an understanding of the exact equivalence of the IP measurements in the phase-domain, the frequency-domain and the time-domain (see Figure 1), we have progressed to the study of the IP effect over the entire frequency range of interest. These studies have led to a greatly advanced understanding of the IP method in at least three important areas:-

i) Our understanding of the IP phenomenon itself has been vastly increased. A greater knowledge of the source of the IP effect and its detailed behavior has suggested additional uses for the method, beyond the simple detection of anomalies.

ii) A better idea of what we wanted to measure, and modern solid-state electronics, have resulted in greatly improved measurement techniques and instrumentation.

iii) The advent of smaller, less expensive digital computers has greatly helped with the interpretation of IP field data. Rapid forward problem solutions and the possibility of direct inversion of IP field data have made it possible for the geophysicists to give the exploration geologist a much better picture of just what the source of a particular IP anomaly might be.

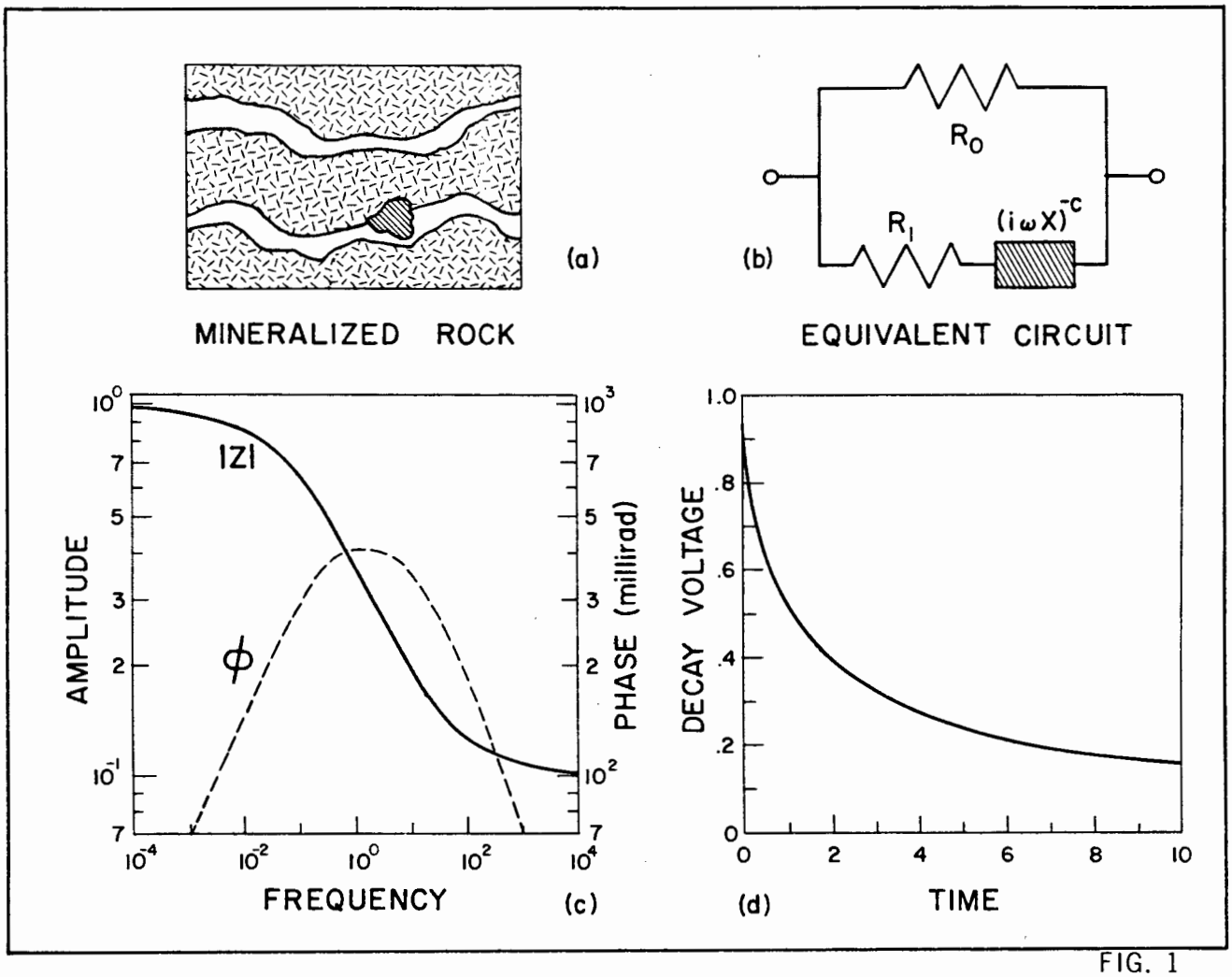

FIG. 1

WHAT IS THE NATURE OF THE IP EFFECT

Spectral induced polarization measurements (the measurement of the phase shifts over a wide frequency range) in open-pit mines, gave the first information concerning the detailed nature of the IP phenomenon. It became clear that four parameters, not just two (resistivity and IP

effect) were necessary to completely describe the IP effect.

The equation shown on Figure 2 and Figure 3 is formally known as the Cole-Cole Dispersion Equation; the four electrical parameters are:

Ro - the dc resistivity value

m - the IP effect (in non-dimensional form)

τ - the time constant of the IP effect

c - the exponent of the frequency (ω)

Since the very beginning of our experience with spectral IP measurements, we have found that these four parameters, and the Cole-Cole equation will adequately describe any IP effect that has been measured. The first measurements were made using one meter electrode intervals, within open-pit mines. The circles on Figure 4 and Figure 5 show the data points measured over massive graphite and massive sulphides at the Anvil Mine. As the solid line curves on the drawings show, the measured data points can be almost exactly replaced using a Cole-Cole Dispersion.

The four parameters obtained by the computer inversion of the graphite data are typical of those that have been measured over all graphite deposits. The IP effect is very large and the time constant (τ) is much greater than 1.0 seconds.

Large IP effects are also measured over massive sulphide sources. However, invariably the time constant value for (τ) is less than 1.0 seconds. The measurements shown on Figure 6 are for a massive sulphide source at the Kidd Creek Mine; again there is a large IP effect, and a small time constant.

The critical frequency (Fc) for a Cole-Cole Dispersion is defined as that frequency for which the maximum phase-shift is measured. An examination of the equation and curves in Figure 2 shows that as the time-constant (τ) is increased by a factor of ten, the critical frequency (Fc) will decrease by a factor of ten. Therefore, we can expect that for the spectral IP response of polarizable sources (Fc) will be inversely proportional to (τ).

An understanding of the physical parameters that affect the time-constant (τ) of a spectral IP response has come from two areas of research. One is the study of the spectral IP response from artificial rocks; these samples are prepared using metallic particles of known material and size (see Figure 8 for example). The second line of attack has been to formulate the mathematical expressions that might describe the macro-characteristics of conduction in a mineralized rock, with certain simplifying assumptions. Initially spherical particles were assumed for this work and an example of the predicted spectral results is shown on Figure 7.

We have shown these two different sets of data, because they are very similar in character. Further, they show the same result that all of

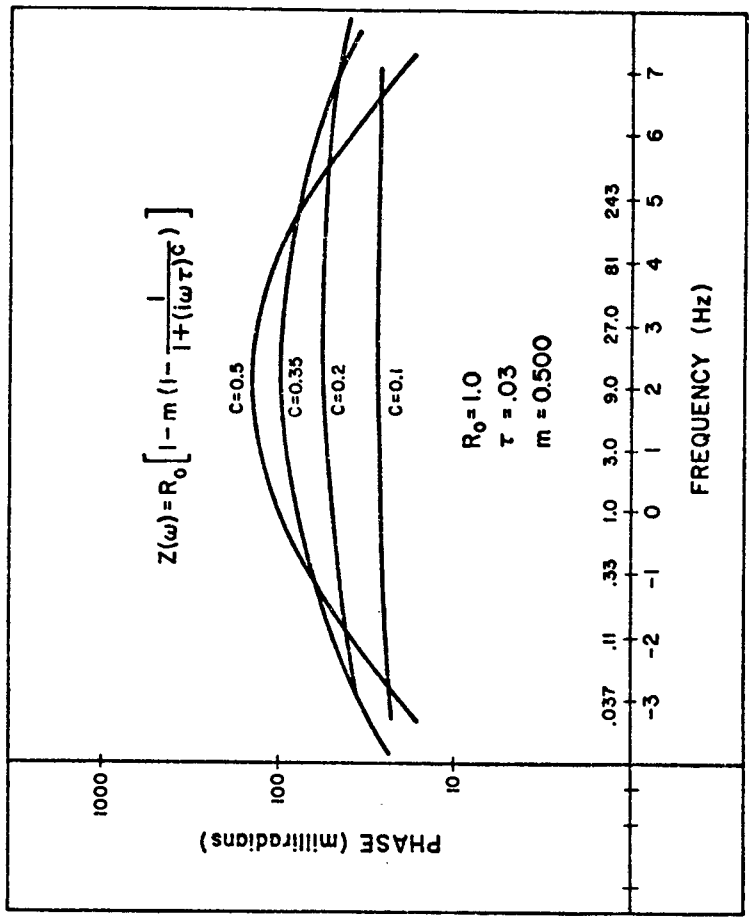
$Z(\omega)=R_0\left[1-m\left(1-\frac{1}{1+(i\omega\tau)^c}\right)\right]$
C=0.5
C=0.35
C=0.2
C=0.1
R_0=1.0
τ = .03
m = 0.500
FREQUENCY (Hz)
PHASE (milliradians)

FIG. 3

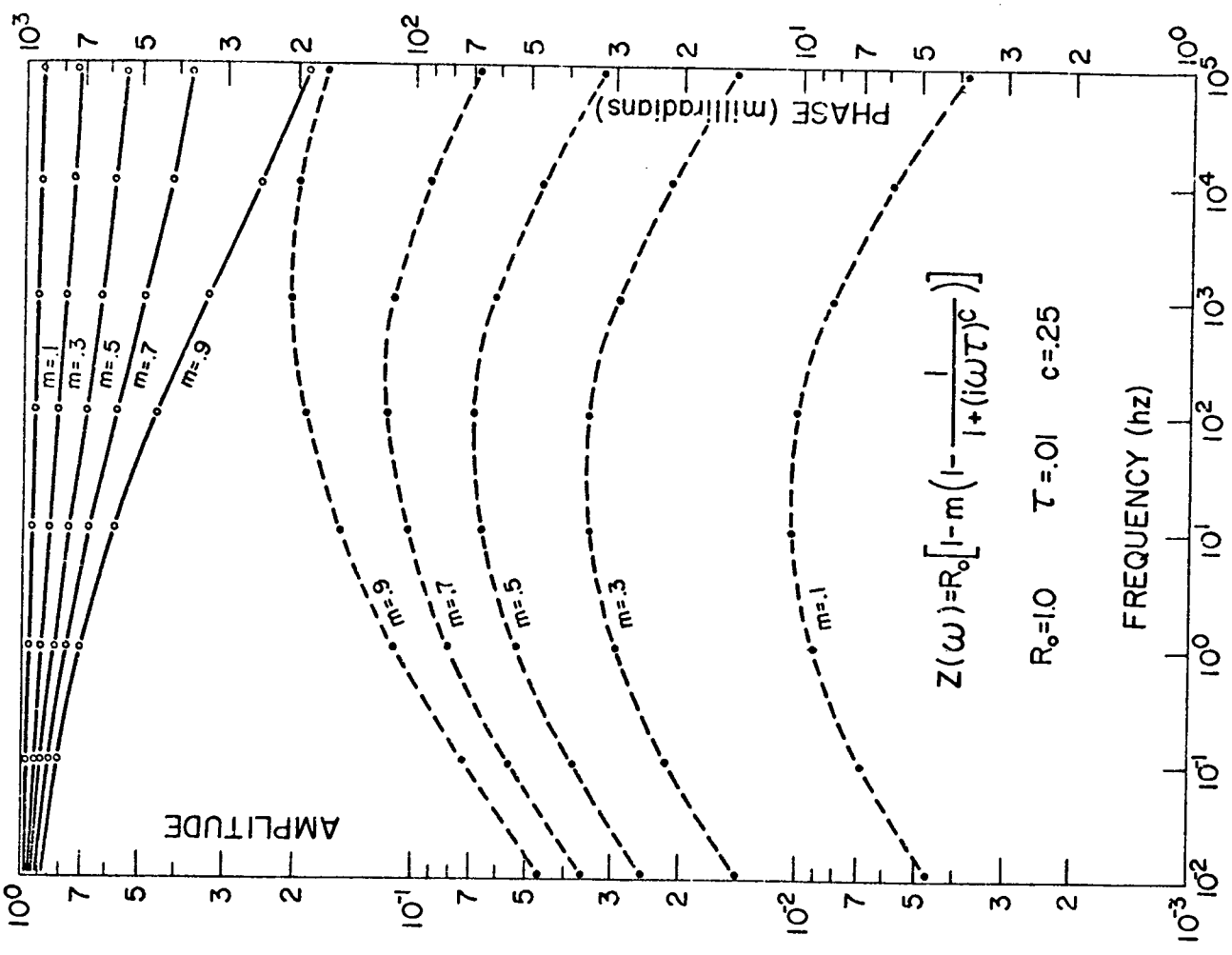
AMPLITUDE
PHASE (milliradians)
$Z(\omega)=R_0\left[1-m\left(1-\frac{1}{1+(i\omega\tau)^c}\right)\right]$
R_0=1.0 τ=.01 c=.25
FREQUENCY (hz)
m=.1
m=.3
m=.5
m=.7
m=.9

FIG. 2

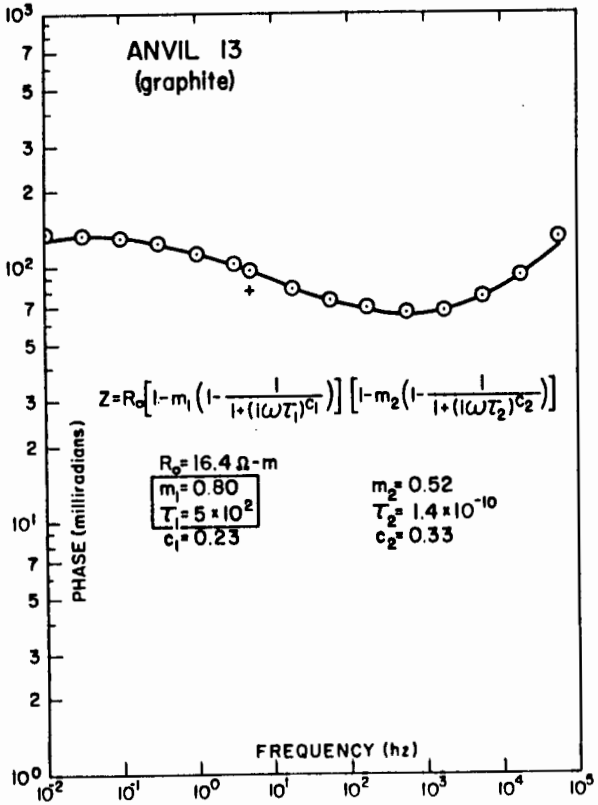

FIG. 4

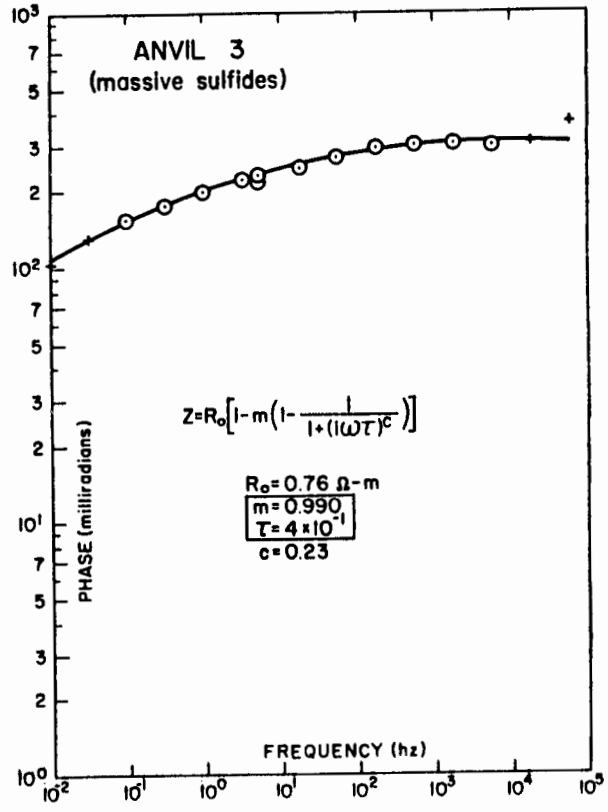

FIG. 5

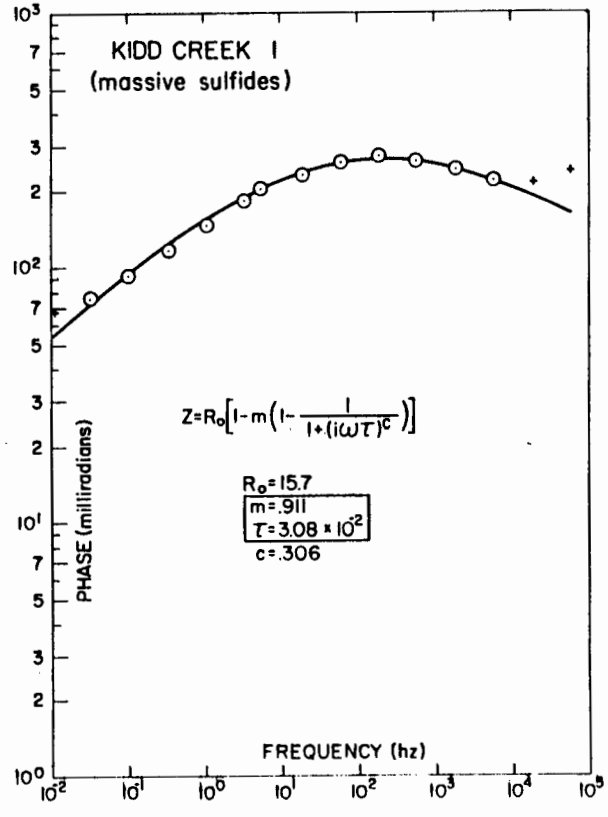

FIG. 6

THEORETICAL RESULTS FOR VARIATION IN GRAIN SIZE OF POLARIZABLE PARTICLE

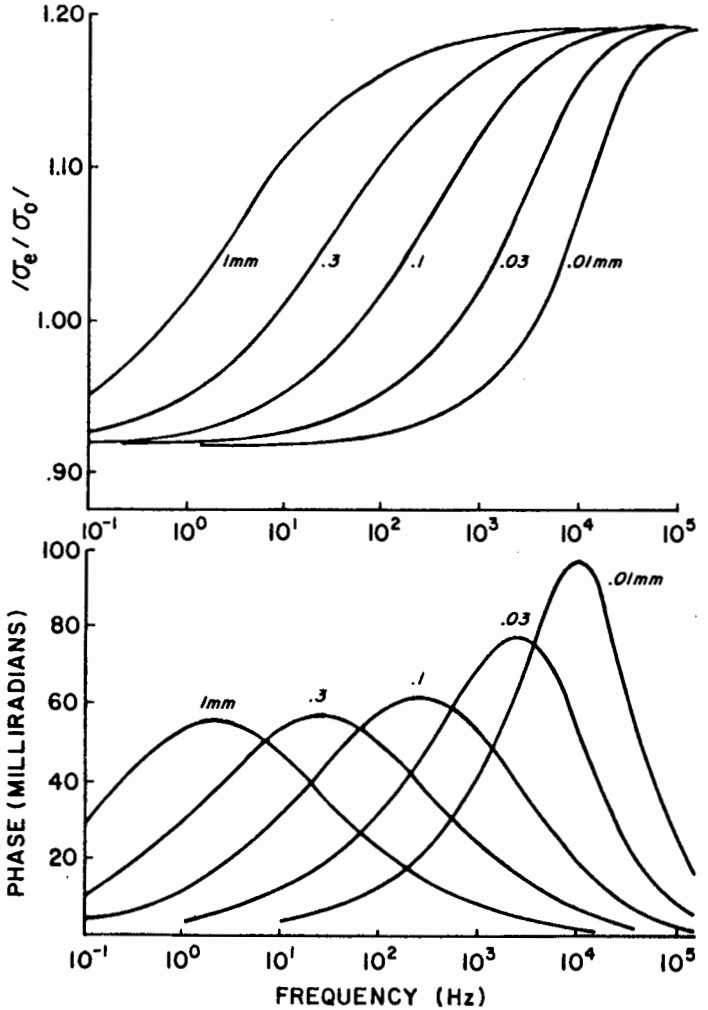

from Wong

FIG. 7

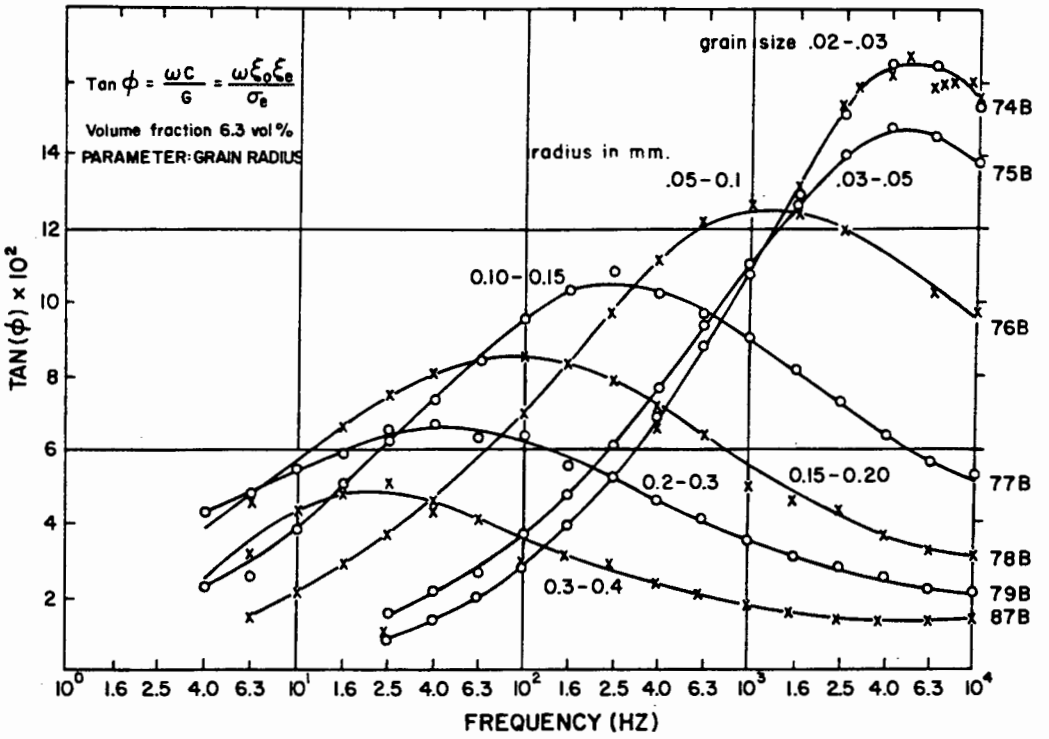

from Wong
data by Grissemann

FIG. 8

our research has shown. The time-constant (τ) of a spectral IP dispersion curve is directly related to the physical size of the metallic particles that are the source of the IP effect. The critical (Fc) is therefore inversely related to the grain-size. Thus, for all of the massive sulphide deposits for which we have spectral measurements, the effective grain-size of the polarizable particles is appreciably smaller than that for graphite sources.

There is one additional test we have devised to confirm the validity of the electrochemical model we have developed to describe the detailed nature of the IP phenomenon. The spectral IP results for a single mineral electrode (pyrite, chalcopyrite, bornite, galena, etc.) immersed in distilled water can be measured, and then inverted using the computer. This inversion determines the various electrical parameters that describe the electrical transfer function for that particular mineral. These electrical parameters, and the analytically determined concentrations of the metal cation in the solution after steady-state current flow has been achieved, can be used to calculate the reaction valence (total number of electrons involved) of the chemical reaction at the interface. This measured value of the reaction valence can be compared to the various values that would be possible from various chemical reactions.

In past research, these measured numbers have not agreed within an order of magnitude with those predicted by the commonly accepted dissolution reaction equations for the various sulphide minerals. The results we have achieved for galena (Figure 10) and chalcopyrite (Figure 9) are typical of the work that has been done recently. The measured values of the reaction valence give much closer agreement to the predicted valence than was previously the case. For chalcopyrite, the predicted reaction varies with the copper ion concentration, and the agreement is still quite acceptable.

With the success of the above described research, has come the implication that we may now understand the IP phenomenon well enough to use some of our knowledge in a predictive way. The resistivity and phase-shift data plotted in the pseudo-section format on Figure 11 are from the Kennedy Property near Winnemucca, Nevada. The results suggest a broad, weak IP anomaly that might be due to a "porphyry copper" type source containing a small concentration of metallic mineralization. However, one notices immediately that the phase-shifts measured at 9.0 Hz are the same magnitude as those measured at 0.11 Hz (a factor of 3^{-4} lower in frequency). This is the same Spectral IP characteristic that was previously measured at the Brenda Mine in British Columbia.

This unusual circumstance is confirmed by the spectral plots for two typical dipole pairs, shown in Figure 12 and Figure 13. With the inductive coupling effects removed by computer inversion, the phase-shift vs. frequency curve is very flat over a frequency range of 3^{8}Hz. This requires a very low (c_1) value of 0.125 (see Figure 3); more importantly, a value of IP effect (m) in excess of 0.500 is necessary. Therefore, although the measured phase-shifts are low in magnitude, the true IP effect within the source material must be large. This should not be considered to be a weak anomaly.

CHALCOPYRITE

$[CuSO_4]$ 0	10^{-5}	10^{-4}	10^{-3}	Reaction Valence
4.6				
3.5	1.5	.95	.53	Measured
3.6				
4.0	1.33	1.33		Actual

$$CuFeS_2 \longleftrightarrow Cu^{2+} + Fe^{2+} + 2S + 4e^-$$

$$\frac{2}{3}\,CuFeS_2 + Cu^{2+} + \frac{4}{3}e^- \longleftrightarrow \frac{1}{3}\,Cu_5FeS_4 + \frac{1}{3}\,Fe^{2+}$$

(Wadsworth, 1980)

FIG. 9

GALENA

[NaCl] 0.10	Reaction Valence
1.6	
1.6	Measured
2.0	Actual

$$PbS \longleftrightarrow Pb^{2+} + S^0 + 2e^-$$

(Sato, 1960)

FIG. 10

W A BOWES KENNEDY AREA WINNEMUCCA NEVADA X=200 JUNE 1979

Apparent Resistivity(ohm-m)

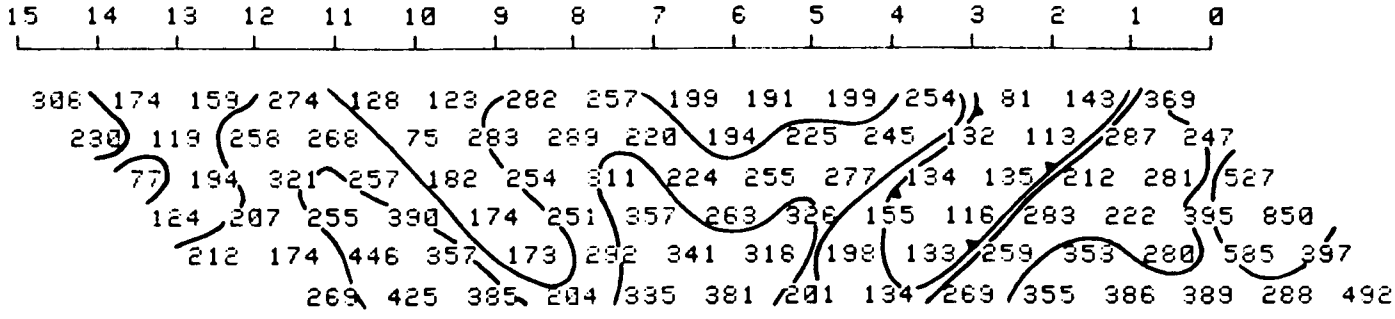

Decoupled Phase(mrad) 9 Hz

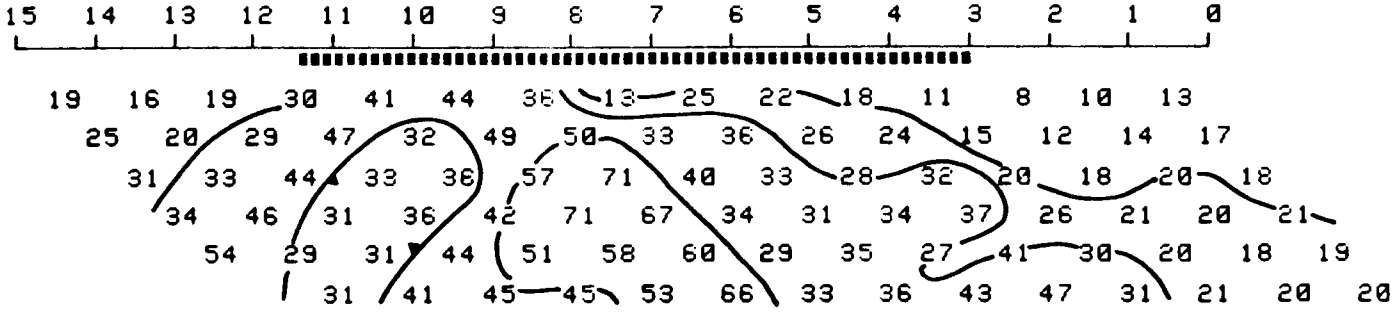

Decoupled Phase(mrad) .1111 Hz

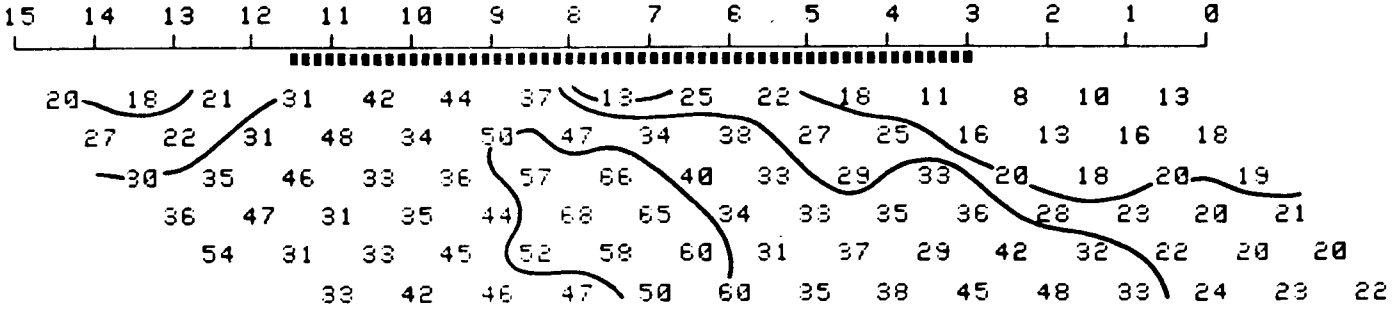

FIG. 11

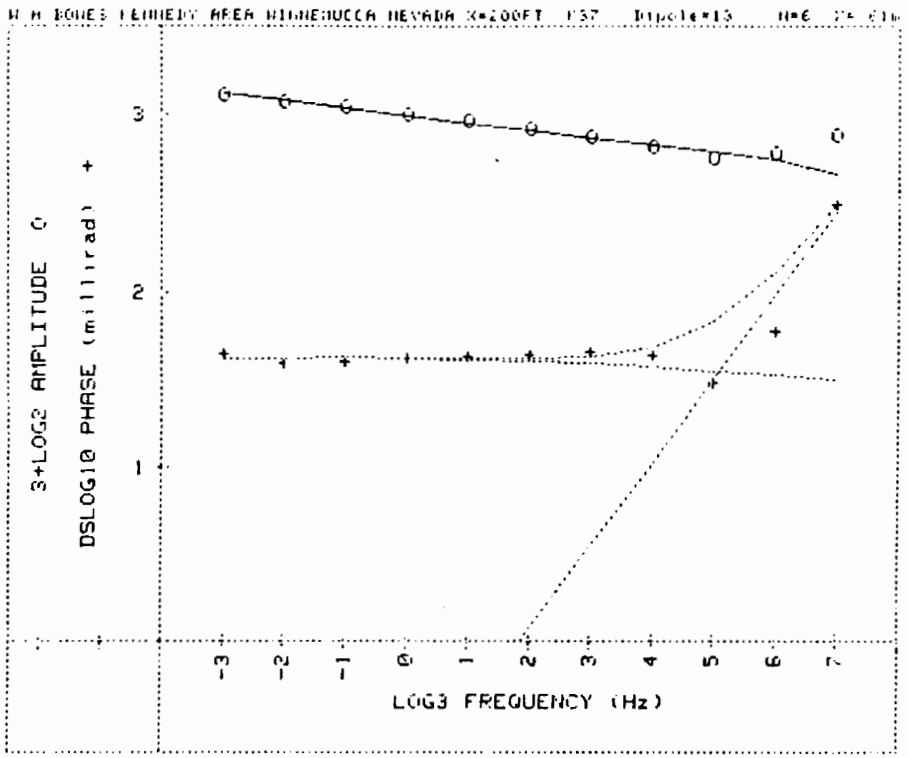

Iter	Lambda	Rchsq	P0	M1	T1	C1	M2	T2	C2
0	1.E-02	.00068	1.599	.567	2.0E+01	.125	1.000	2.0E-05	.992
1	1.E-01	.00064	1.599	.566	2.0E+01	.125	1.000	2.1E-05	1.000
2	1.E+00	.00063	1.596	.584	2.0E+01	.125	1.000	2.1E-05	1.000
3	1.E+00	.00063	1.595	.583	2.0E+01	.125	1.000	2.1E-05	1.000

Pct Std Deviations	5.4	1.6	499.4	0.0	0.0	10.5	9.8	
Correlation Matrix	1.0000							
	.5235	1.0000						
	.9782	.3667	1.0000					
	0.0000	0.0000	0.0000	0.0000				
	0.0000	0.0000	0.0000	0.0000	0.0000			
	-.3604	.0864	-.3990	0.0000	0.0000	1.0000		
	-.6447	.0924	-.7125	0.0000	0.0000	.7305	1.0000	

Apparent Resistivity Measured at 1 Hz is 425

Apparent Resistivity Calculated from Inductive Coupling is 2117

FIG. 12

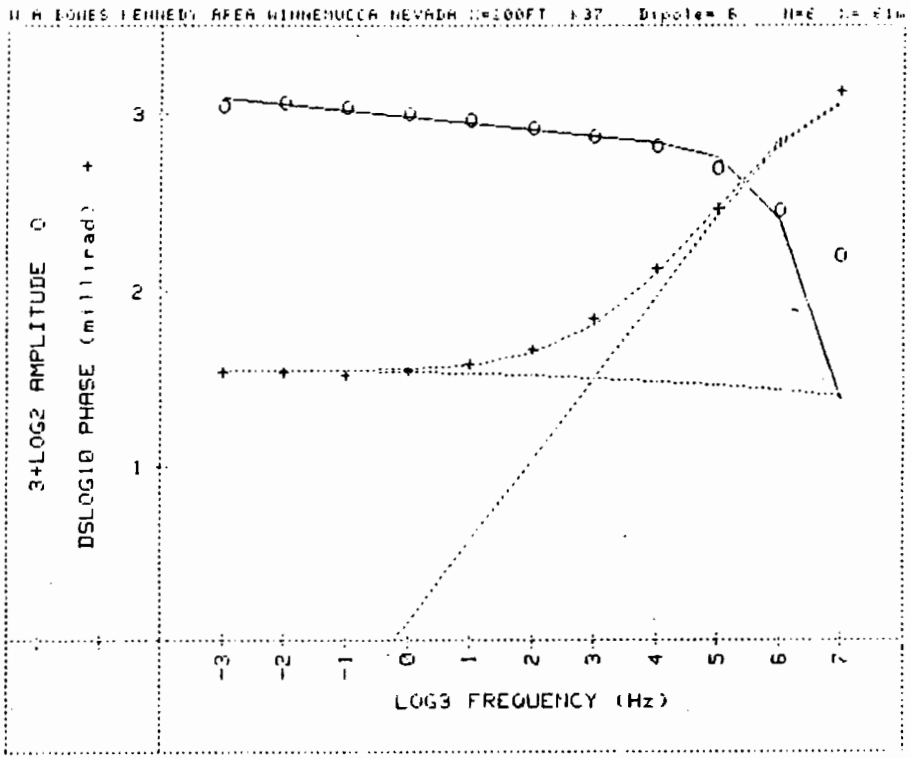

Iter	Lambda	Rchsq	P0	M1	T1	C1	M2	T2	C2
0	1.E-02	.00102	1.482	.517	2.0E+01	.125	1.000	1.8E-04	.977
1	1.E-02	.00162	1.481	.518	1.9E+01	.125	1.000	1.8E-04	.978

Pct Std Deviations	6.7	2.6	1243.0	0.0	0.0	5.4	2.8	
Correlation Matrix	1.0000							
	.6234	1.0000						
	.9768	.4657	1.0000					
	0.0000	0.0000	0.0000	0.0000				
	0.0000	0.0000	0.0000	0.0000	0.0000			
	.1989	.0726	.2067	0.0000	0.0000	1.0000		
	-.4224	.0478	-.4586	0.0000	0.0000	.4189	1.0000	

Apparent Resistivity Measured at 1 Hz is 201

Apparent Resistivity Calculated from Inductive Coupling is 235

FIG. 13

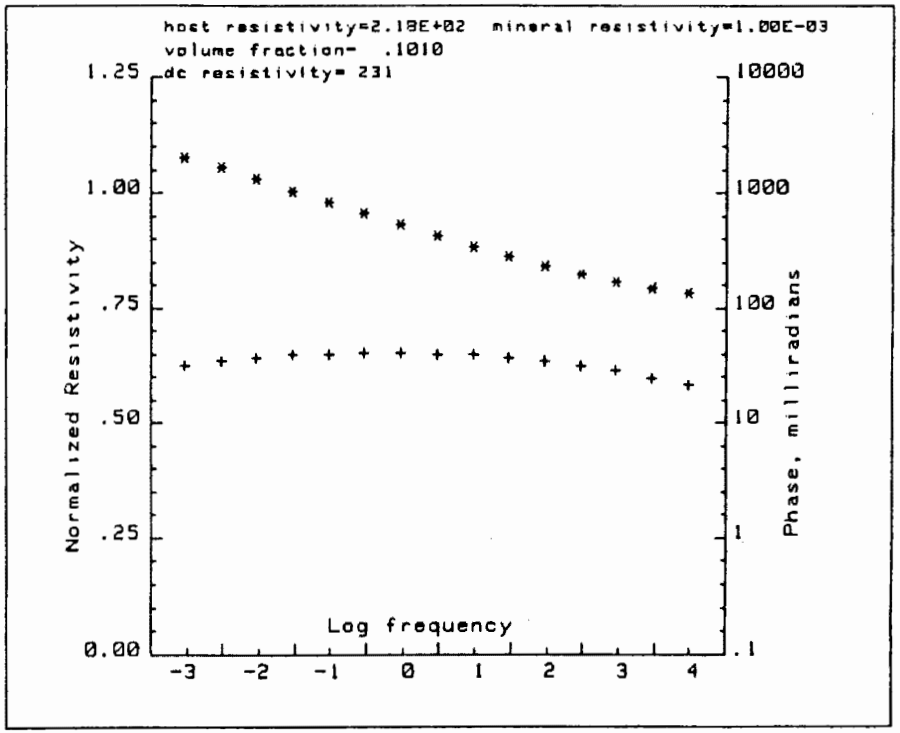
host resistivity=2.18E+02 mineral resistivity=1.00E-03
volume fraction= .1010
dc resistivity= 231
Normalized Resistivity
Phase, milliradians
Log frequency
1.25
1.00
.75
.50
.25
0.00
10000
1000
100
10
1
.1
-3
-2
-1
0
1
2
3
4

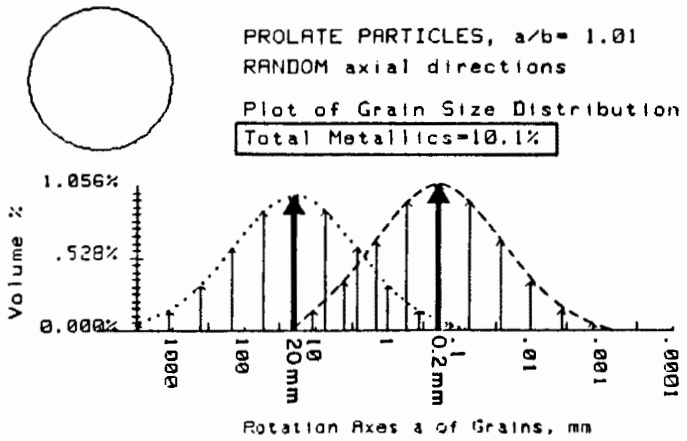
PROLATE PARTICLES, a/b= 1.01
RANDOM axial directions
Plot of Grain Size Distribution
Total Metallics=10.1%
Volume %
1.056%
.528%
0.000%
1000
100
20mm
10
1
0.2mm
.1
.01
.001
.0001
Rotation Axes a of Grains, mm

FIG. 14

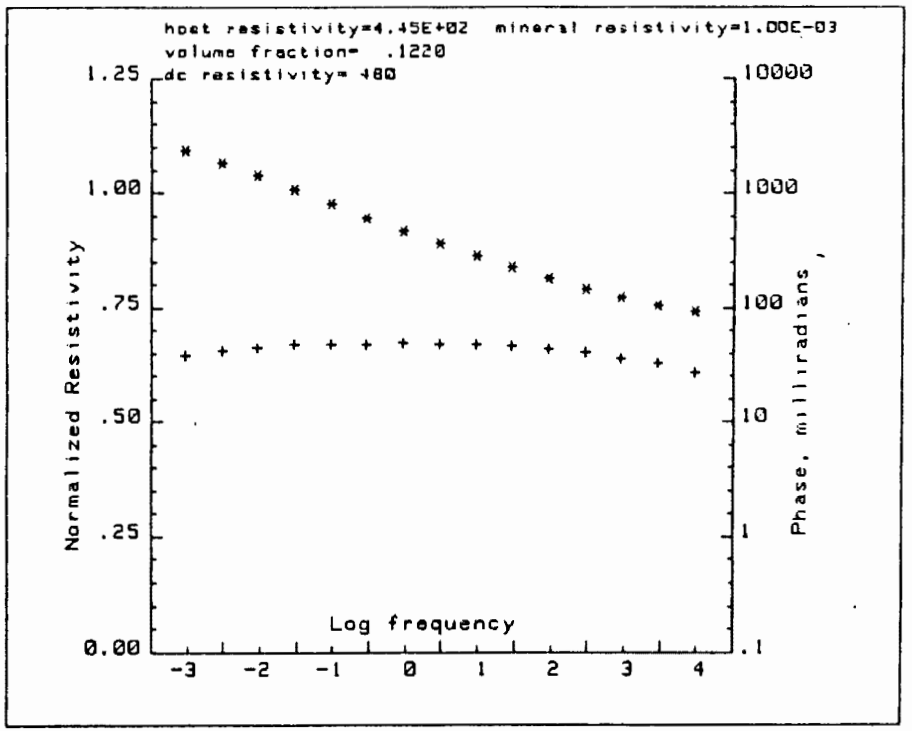
host resistivity=4.45E+02 mineral resistivity=1.00E-03
volume fraction= .1220
dc resistivity= 480
Normalized Resistivity
Phase, milliradians
Log frequency
1.25
1.00
.75
.50
.25
0.00
10000
1000
100
10
1
.1
-3
-2
-1
0
1
2
3
4

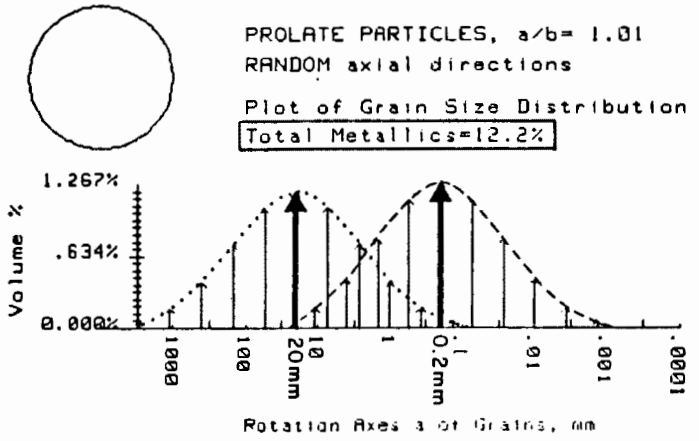
PROLATE PARTICLES, a/b= 1.01
RANDOM axial directions
Plot of Grain Size Distribution
Total Metallics=12.2%
Volume %
1.267%
.634%
0.000%
1000
100
20mm
10
1
0.2mm
.1
.01
.001
.0001
Rotation Axes a of Grains, mm

FIG. 15

We used these results in our first attempt to predict the nature of the mineralization that is the source of the "weak" anomaly shown in Figure 11. The mathematical formula used to predict the spectra shown in Figure 7 has been expanded to include prolate and oblate spheroids, as well as spheres, of metallic material. By a trial and error process, the spectra shown in Figure 14 and Figure 15 were generated as being a "good fit" to the measured data.

The chosen parameters for the sources are probably not unique; however, some valid points can be drawn from the calculation presented.

i) the flat spectrum (small c value) cannot be obtained from a single grain-size (time-constant) population. There must be at least two different grain-size populations present.

ii) Although the two grain-size distributions, with mean values of 20mm and 0.2mm, are probably not exactly correct, a difference of at least two orders of magnitude is necessary to produce the value c = 0.125.

iii) Despite the low magnitude for the IP field anomaly, the true IP effect within the source is large ($m_1 > 0.500$) and this results in a fairly high concentration of metallic mineralization predicted for the source (10 - 12% total metallic mineralization).

The first drill hole at the Kennedy Project is now nearing completion; it was collared at approximately station No. 5 along the line of data shown in Figure 11. There was metallic mineralization throughout the drill hole, with an increase below about 75-80 meters of depth.

Throughout the entire length of the drill hole (in excess of 250 meters), there were two different types of mineralization present. There were veinlets (large grain-size) that might, or might not, contain quartz. All of the veinlets contained chalcopyrite or molybdenite or chalcopyrite with molybdenite; some pyrite was also present. There was also fine-grained disseminated metallic magnetite throughout the hole (the small grain-sized source). The magnetite contains appreciable gold value; there is enough gold present to give detectable assays throughout the length of the hole.

We do not have enough information to determine if the total concentration of metallic mineralization approaches 10 to 12 percent. However, in other respects the source of the IP anomaly does seem to approximate that predicted by the spectral IP analysis.

IMPROVED MEASUREMENT TECHNIQUES AND INSTRUMENTATION

The much publicized "explosion" in solid-state, semi-conductor

electronic components has produced as many changes in the geophysical instrumentation industry as it has in other phases of modern life. Beginning with diodes and transistors and now including complex microprocessor chips, there has been a bewildering number of improvements in this industry. They have resulted in a major reduction in the size of, and the power requirements of (smaller battery packs), geophysical field instruments; at the same time the reliability, digital data storage capability and analysis capability have been almost infinitely increased.

The Phoenix IPV-2, Prospecting Phase IP system is an example of one of the least complicated units that can be engineered with modern electronics. The types of features that can now be made available are:

i) Microprocessor-controlled signal stacking of each measurement to give almost infinite noise rejection through coherent detection.

ii) Matched, heated crystal clocks give phase stability between current source and voltmeter without connecting cable.

iii) Dual-channel electronics permits two separate voltages to be measured simultaneously.

iv) Digital readout of magnitude and phase-shift of measured voltage at either channel.

v) Five frequency capability (0.11, 0.33, 1.0, 3.0, 9.0 Hz) permits limited analysis of spectral character of any anomaly.

vi) Appreciable increase in survey speed over either frequency-domain or time-domain IP systems.

By completing a reconnaissance survey with a single frequency (typically 0.33 Hz or 1.0 Hz) it is possible to achieve the lowest cost possible for IP field surveys. However, once an anomaly is detected, the IPV-2 can be used to make detailed measurements that give some feeling for the character of the spectral response of the source.

If detailed measurements are made at only two frequencies, it is possible to make some statement about the critical frequency (Fc) of the IP spectrum from the source. On Figure 17 and Figure 18 are shown the detailed phase-IP measurements made using X = 100' and 0.33 Hz over two anomalies previously located by a reconnaissance IP survey using larger electrode intervals. On both Line 18E and Line 15E the anomalous pattern indicates a relatively narrow source, with some depth to the top.

During the detailed survey with X = 100', several of the anomalous values in each anomalous pattern were measured at both 0.33 Hz and 3.0 Hz.

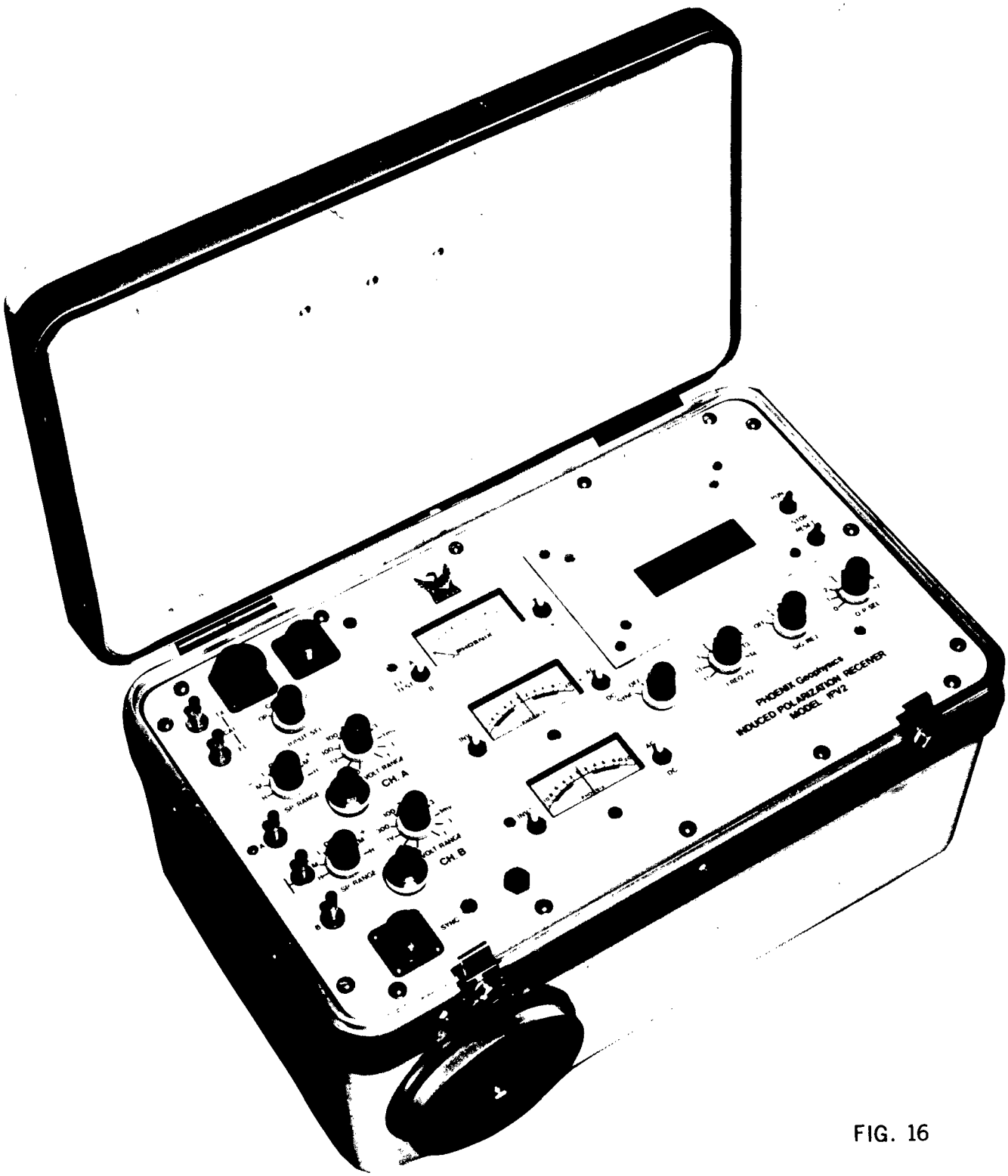
PHOENIX Geophysics
INDUCED POLARIZATION RECEIVER
MODEL IPV2
CH. A
CH. B

FIG. 16

PRICE COMPANY BLOCK NO.8 PROPERTY
IPV-2 PHASE IP TEST

LINE-18E

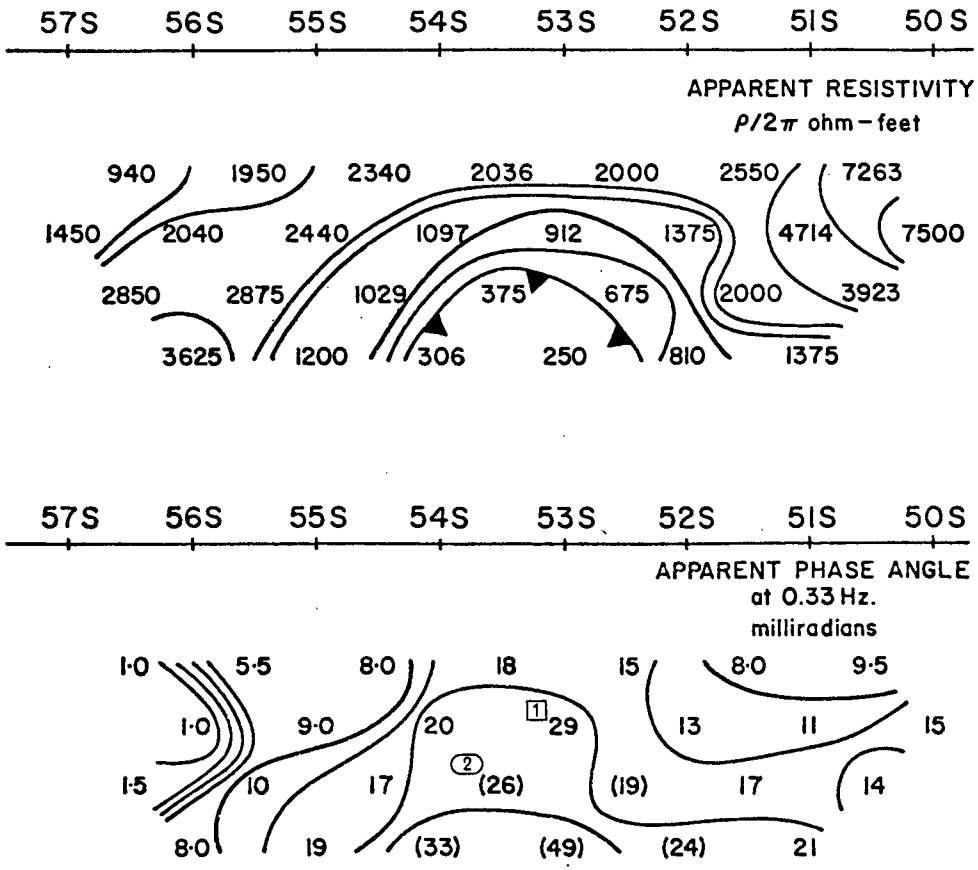

FIG. 17

PRICE COMPANY BLOCK NO.8 PROPERTY
IPV-2 PHASE IP TEST

LINE-15E

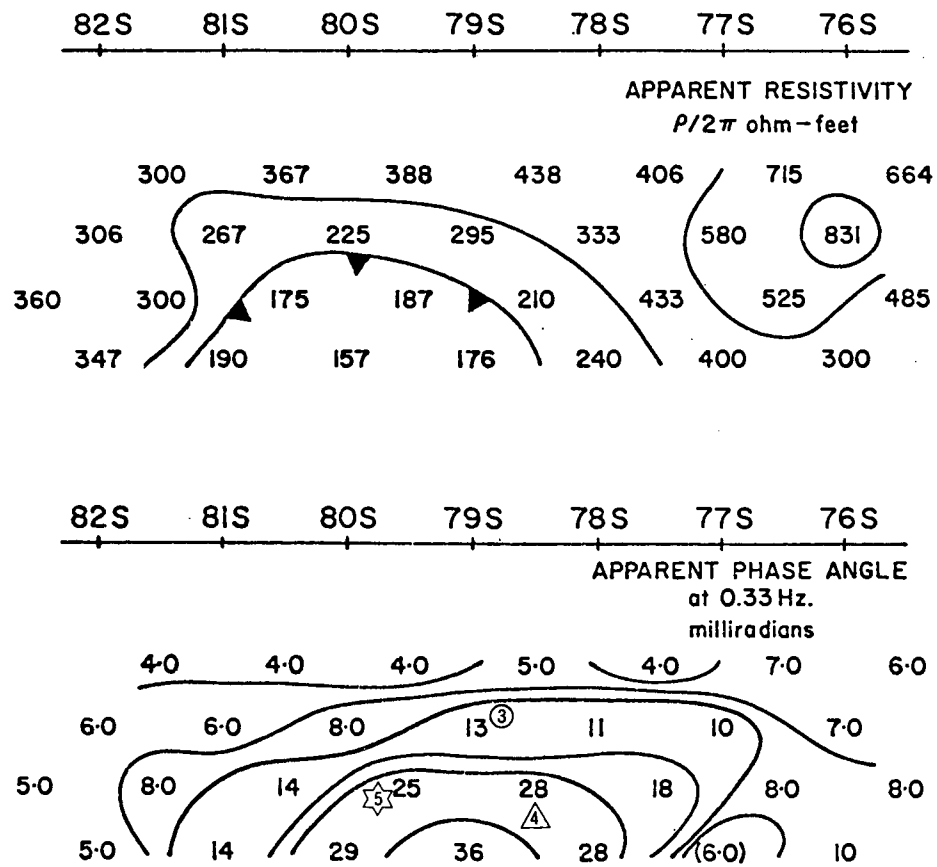

FIG. 18

The results are shown on Figure 19 and Figure 20. On Line 18E, the apparent phase values measured increase with frequency, indicating a value for Fc above 3.0 Hz. On Line 15E the apparent phase values were decreasing with frequency, indicating a value for Fc that is below 0.33 Hz.

The relationship we have established between the critical frequency (Fc) - the time constant (τ) - and the grain-size of the polarizable particles, coupled with our experience over known zones suggests that the grain-size of the source of the anomaly on Line 18E is appreciably smaller than the grain-size of the source of the anomaly on Line 15E.

Our expectation that the large grain-size source is more likely to be graphite is confirmed by the drilling of the two anomalies. The anomaly on Line 18E was found to be due to massive sulphide mineralization; the source of the anomaly located on Line 15E was a graphitic tuff zone, with small concentrations of pyrite.

If field time is taken to make measurements at all five frequencies, it is possible to make a more formal presentation of the spectral characteristics of two anomalies. On Figure 21, is shown a computer-plotted pseudo-section of a single line of phase IP data. The plot shows the apparent resistivity value and the apparent phase value (1.0 Hz) measured for each dipole pair. At the lower part of the data plot is shown the short (five frequency) spectrum (normalized to the value at 1.0 Hz) for each dipole pair.

In this case, the two anomalous zones had a considerable strike length, in an area where the surface was largely covered. The electrical parameters of the two sources were much the same; however, as shown on Figure 21, the source of Zone I is clearly different from the source of Zone II. From drilling, it is known that Zone I is due to a broad, irregular zone of pyrite and sphalerite (with appreciable silver) in a tuffaceous rock unit. The source of Zone II is pyrrhotite in an adjoining andesite rock unit.

Another example of a difference in spectral character is shown in Figure 22. In this location, the source of Zone A had been traced for a considerable distance along strike. Zone B was detected only on two adjacent lines. The difference in spectral character strongly suggests that Zone B is not merely a greater width to the mineralized zone that is the source of Zone A.

The Phoenix IPV-3, Spectral IP Receiver is the most advanced induced polarization receiver ever put into field operation (Figure 23). It completely replaces a truck-mounted system that was assembled largely from off-the-shelf computers, voltmeters, oscilloscopes, etc. The entire system is controlled by the Phoenix CP-1, geophysical computer, that was designed especially for this function. Through an FM-modulated link, the CP-1 also controls the spectral IP current source. Some of the more important features of the IPV-3 are:

i) Six simultaneous voltage channels plus current monitor.

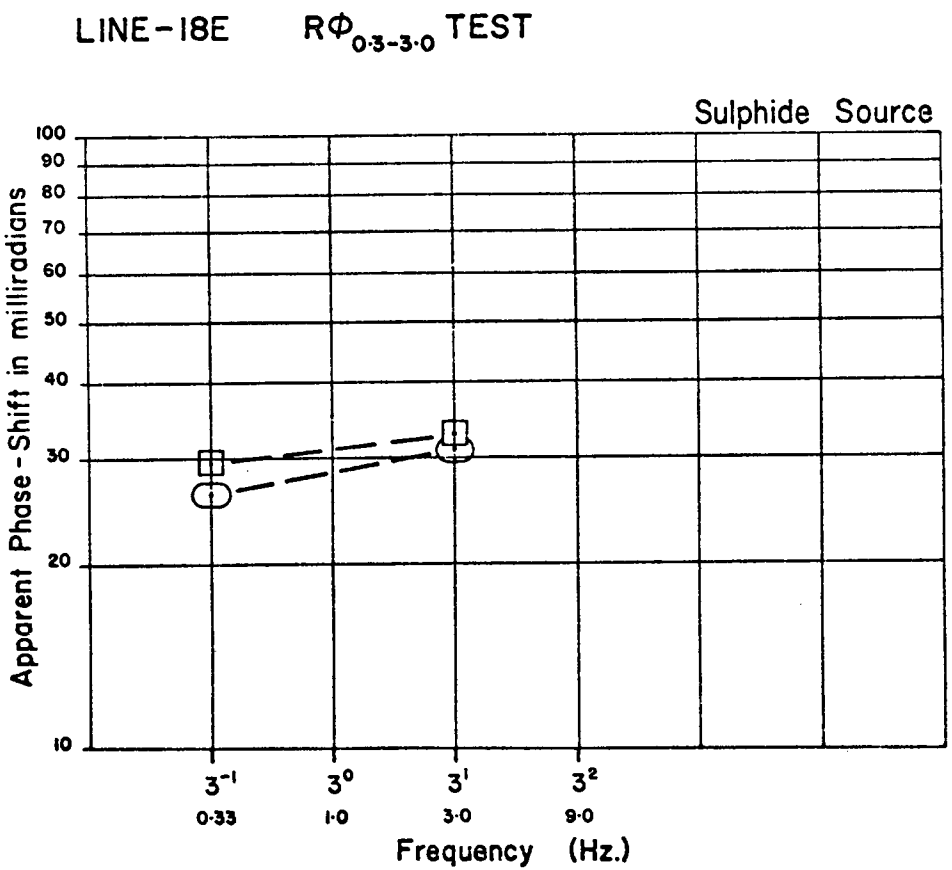
LINE-18E RΦ0·3-3·0 TEST
Sulphide Source
Apparent Phase-Shift in milliradians
100
90
80
70
60
50
40
30
20
10
3-1 0·33
3⁰ 1·0
3¹ 3·0
3² 9·0
Frequency (Hz.)

FIG. 19

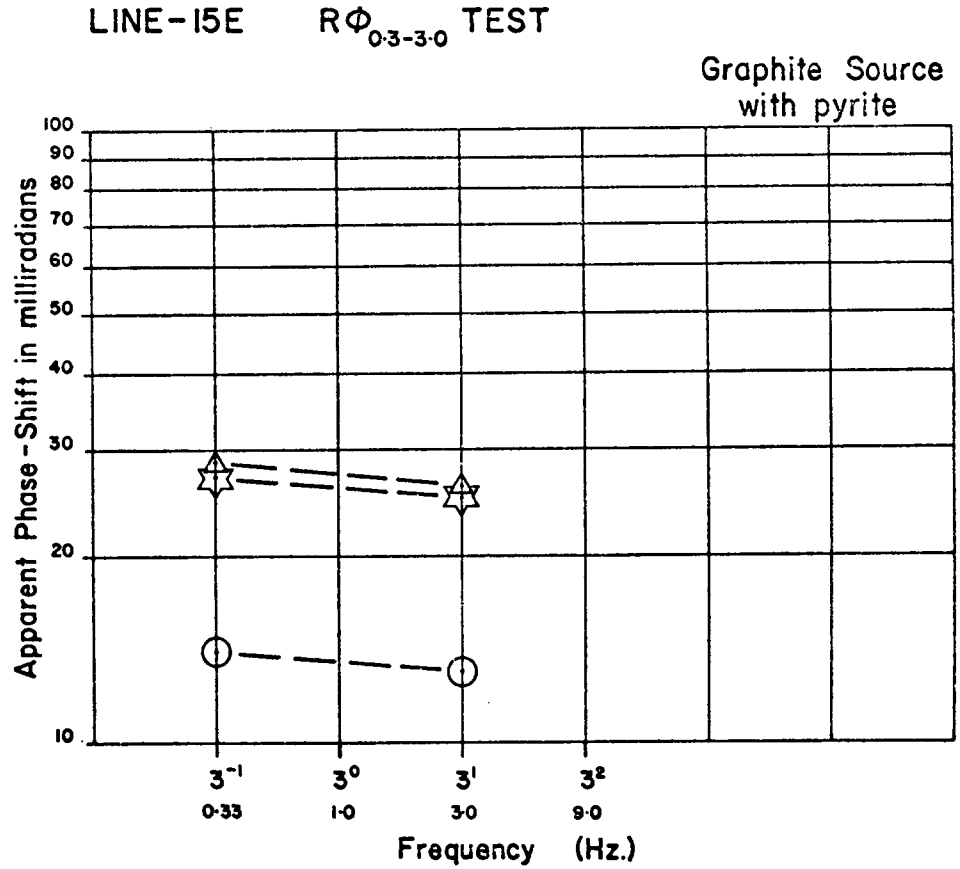
LINE-15E RΦ0·3-3·0 TEST
Graphite Source with pyrite
Apparent Phase-Shift in milliradians
100
90
80
70
60
50
40
30
20
10
3-1 0·33
3⁰ 1·0
3¹ 3·0
3² 9·0
Frequency (Hz.)

FIG. 20

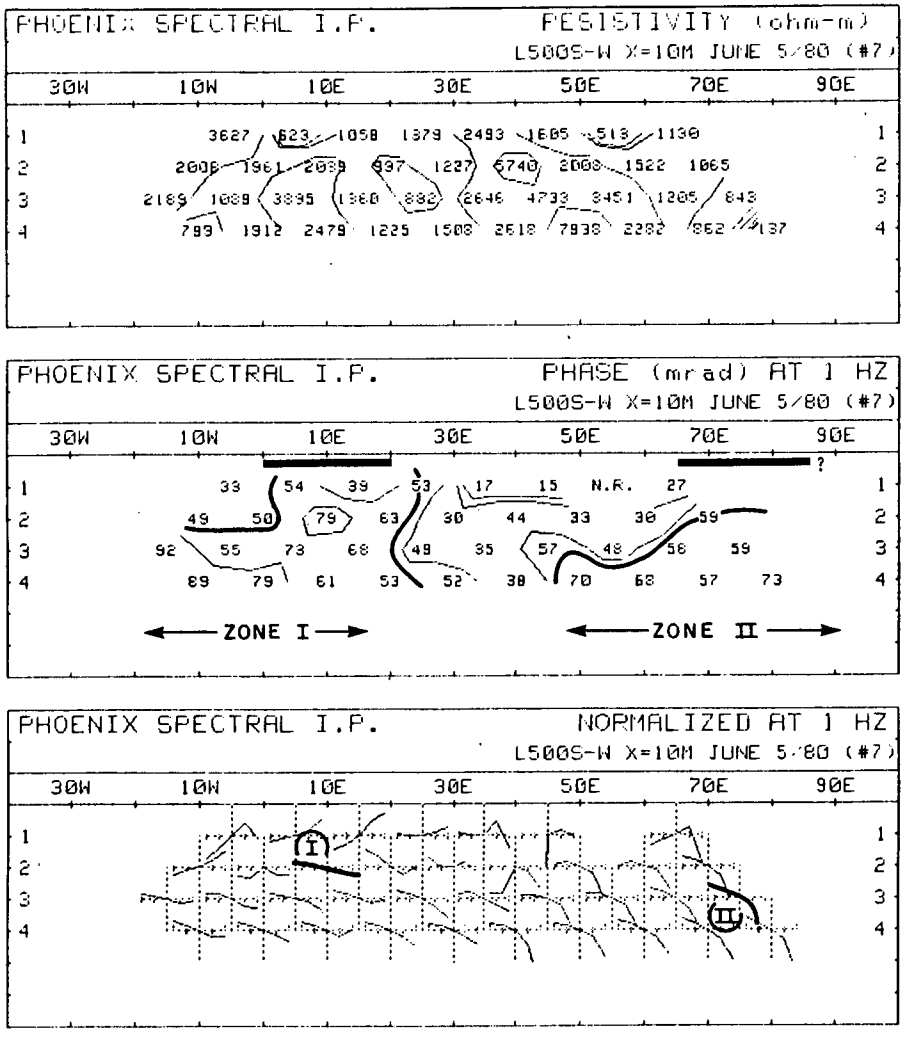
PHOENIX SPECTRAL I.P.
RESISTIVITY (ohm-m)
L500S-W X=10M JUNE 5/80 (#7)
30W 10W 10E 30E 50E 70E 90E
PHOENIX SPECTRAL I.P.
PHASE (mrad) AT 1 HZ
L500S-W X=10M JUNE 5/80 (#7)
ZONE I
ZONE II
PHOENIX SPECTRAL I.P.
NORMALIZED AT 1 HZ
L500S-W X=10M JUNE 5/80 (#7)
I
II

FIG. 21

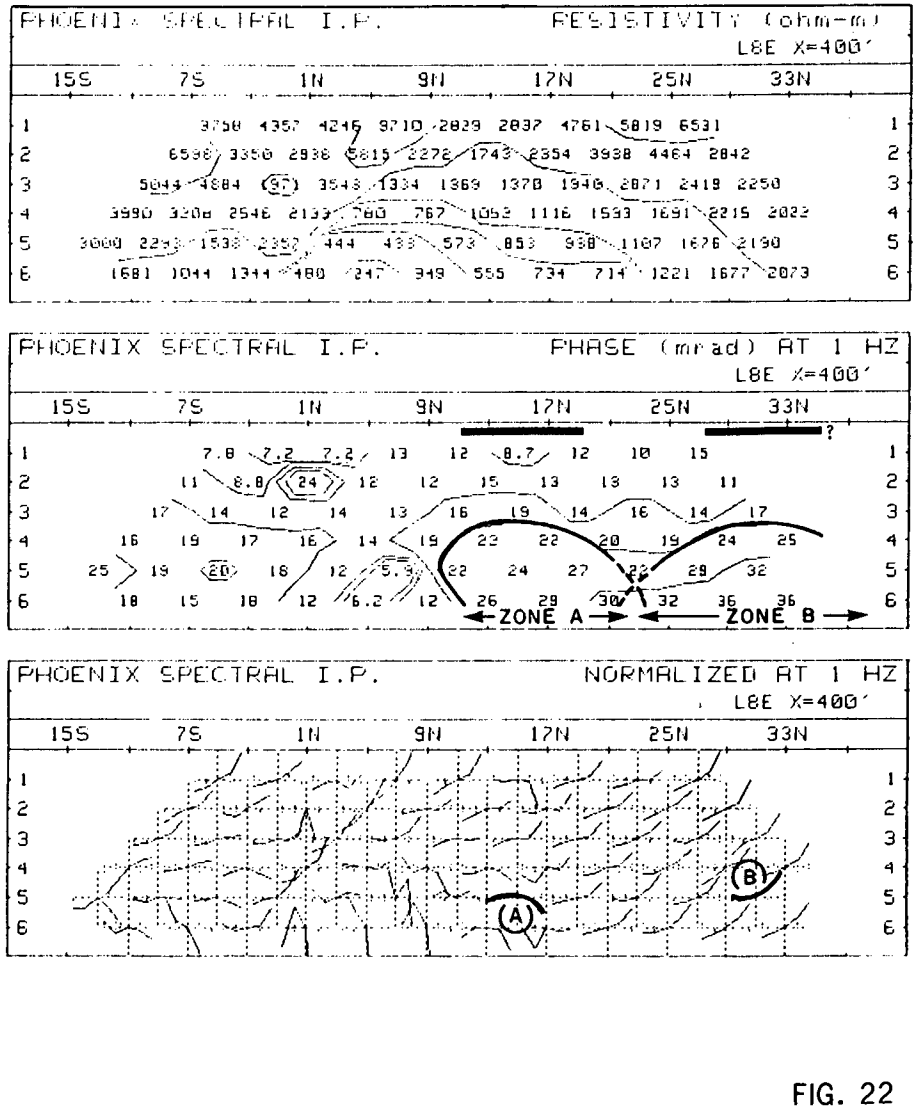
PHOENIX SPECTRAL I.P.
RESISTIVITY (ohm-m)
L8E X=400'
15S 7S 1N 9N 17N 25N 33N
PHOENIX SPECTRAL I.P.
PHASE (mrad) AT 1 HZ
L8E X=400'
ZONE A
ZONE B
PHOENIX SPECTRAL I.P.
NORMALIZED AT 1 HZ
L8E X=400'
A
B

FIG. 22

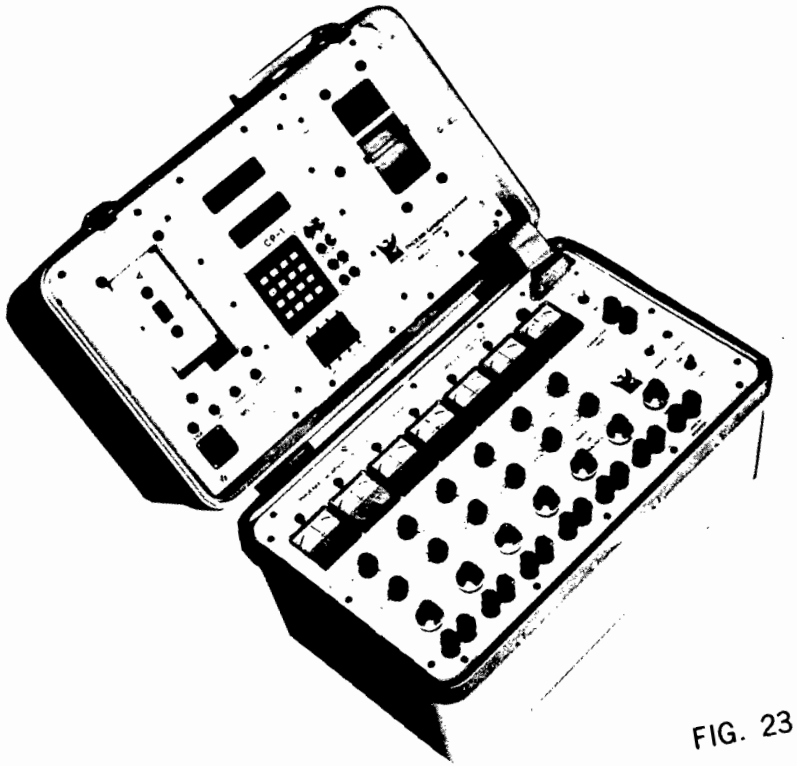

FIG. 23

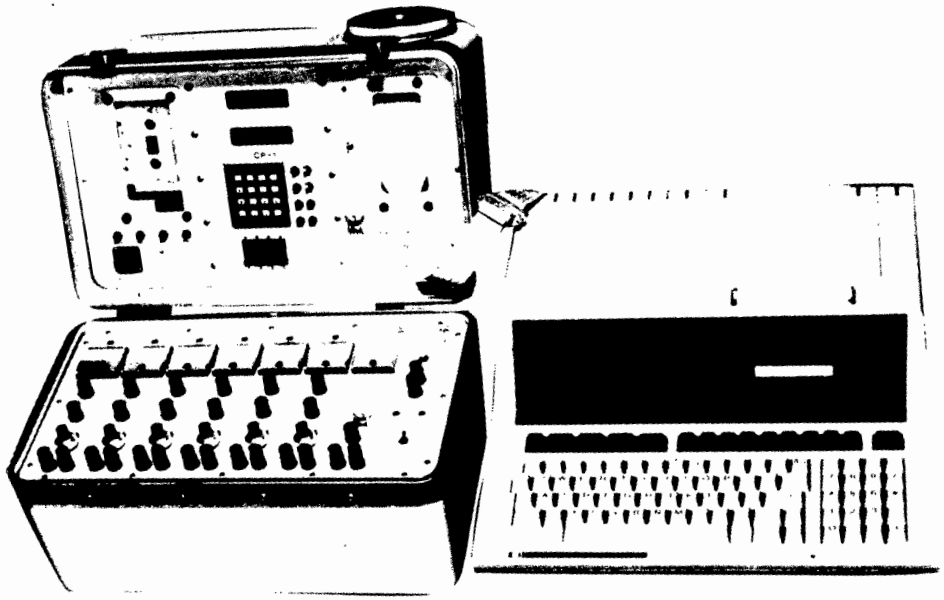

FIG. 24

ii) Frequency range from 2^{-14} Hz (0.00006 Hz) to 2^{+16} Hz (65,536 Hz) with automatic scanning programmable through CP-1.

iii) Real time de-convolution and coherent filtering via use of CP-1.

iv) Field Data available through digital read-out and recorded on paper tape and tape cassette.

v) Field results directly transferrable from tape cassette through CP-1 and interface to computer for analysis and interpretation. (Figure 24).

By using the IPV-3 and the HP=85 computer in the field, the geophysicist has at his disposal all of the interpretational power of the spectral IP method. As shown on Figure 25 it is possible to remove the inductive coupling effects from the broad-band spectral IP results. When this information is removed, it is possible to invert the remaining, decoupled IP spectra and determine the apparent values of Ro, m, τ, c for that particular dipole-pair measurement.

For the spectra shown in Figure 25, the values are m = 0.172; c = 0.376; τ = 0.044 sec.; these parameters suggest a small grain-size, and in fact the source is a massive sulphide zone in New Brunswick. The parameter values obtained by inverting the spectral curve from all of the anomalous dipole pairs were essentially the same; we have found this to be universally true if the anomaly is due to a single, more-or-less uniform source.

For the spectral curve shown in Figure 26, the parameter values of the source are m = 0.509; c = 0.180; τ = 540 seconds. The large time-constant confirms the large grain-size for the graphite zone that is the source of the anomaly.

For IP measurements with large electrode intervals in areas of low resistivity (high conductivity) inductive coupling effects will completely distort IP field data. This can happen even for low frequency measurements (in the variable frequency method) or long time delay measurements (in the time domain technique). When the inductive coupling effects are removed from the spectral curve for each dipole pair (as in Figure 12 and Figure 25) the pseudo-section can be reconstructed using the decoupled data.

The data pseudo-section shown in Figure 27 is from the Elura Deposit near Cobar, New South Wales. The resistivity results show a deep, variable high conductivity surface layer. The phase IP measurements at 3.0 Hz with X = 100 meters are completely dominated by inductive coupling effects that essentially depend only upon the electrode separation (n). However, when the inductive effects are removed from the data for each dipole pair, the pseudo-section clearly shows the presence of the massive sulphide zone, at depth, at approximately station 2500E.

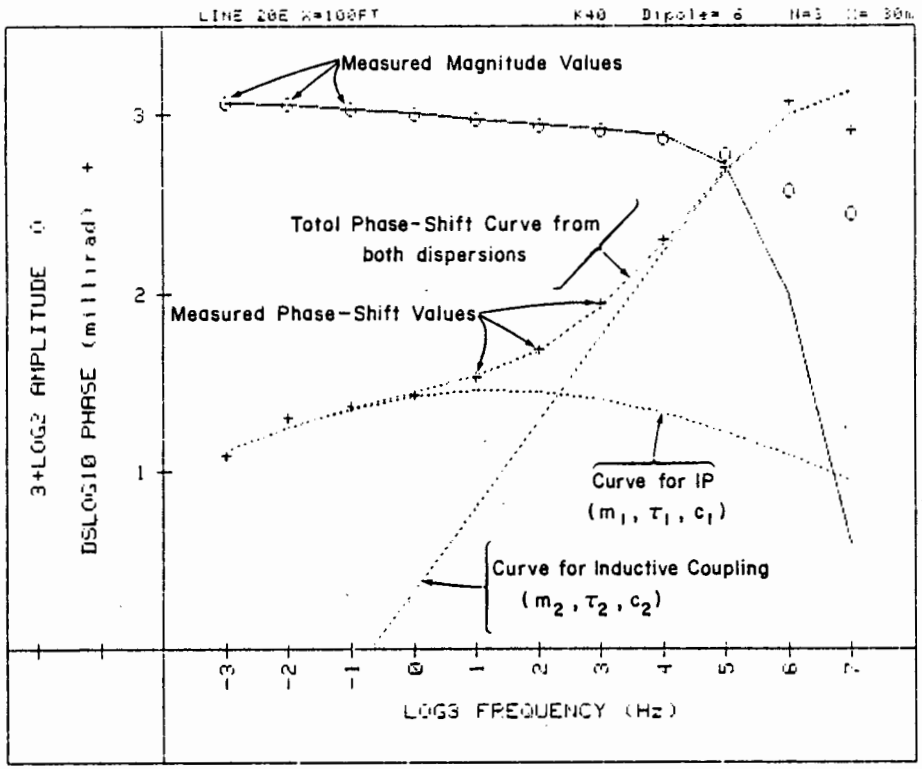

				IP EFFECT			INDUCTIVE COUPLING EFFECT		
Iter	Lambda	Rchsq	R0	M1	T1	C1	M2	T2	C2
0	1.E-02	.03405	1.089	.221	4.0E-02	.329	1.000	1.1E-04	1.000
1	1.E-02	.00168	1.063	.196	2.5E-02	.373	1.000	3.6E-04	1.000
2	1.E-03	.00068	1.072	.186	3.1E-02	.355	1.000	3.3E-04	1.000
3	1.E-04	.00067	1.071	.174	4.3E-02	.373	1.000	3.4E-04	1.000
4	1.E-05	.00066	1.071	.172	4.4E-02	.376	1.000	3.4E-04	1.000
Pct Std Deviations			.8	16.4	84.2	13.5	0.0	5.5	0.0

Correlation Matrix

1.0000							
.5173	1.0000						
-.4289	-.9715	1.0000					
-.5302	-.9438	.8971	1.0000				
0.0000	0.0000	0.0000	0.0000	0.0000			
-.2093	-.6596	.6657	.5348	0.0000	1.0000		
0.0000	0.0000	0.0000	0.0000	0.0000	0.0000	0.0000	

Apparent Resistivity Measured at 1 Hz is 78

Apparent Resistivity Calculated from Inductive Coupling is 10

FIG. 25

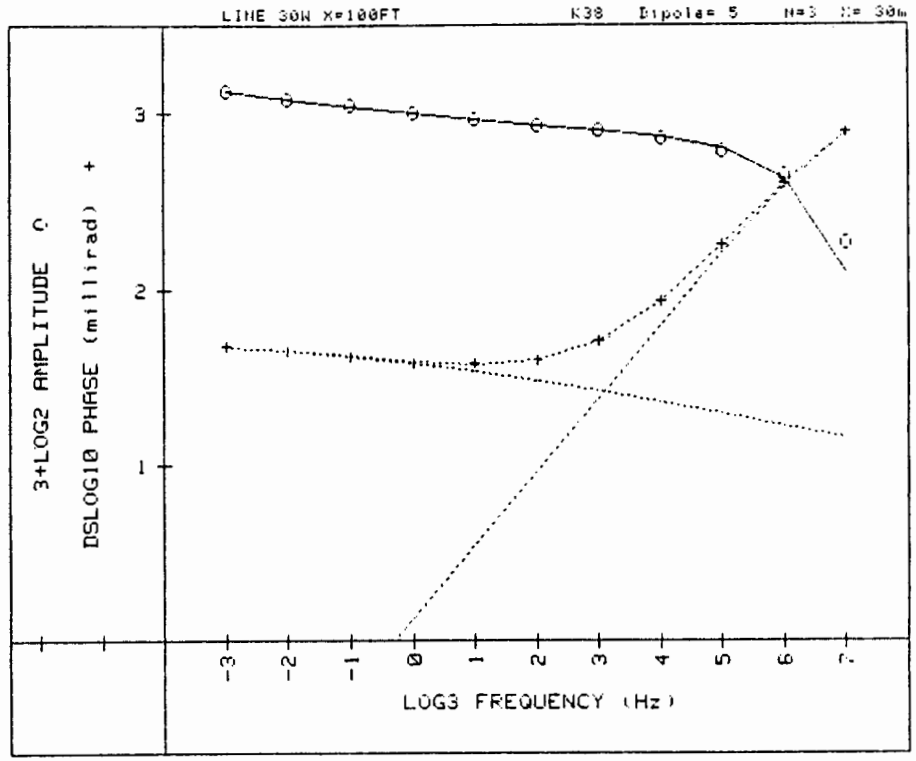

Iter	Lambda	Rchsq	R0	M1	T1	C1	M2	T2	C2
0	1.E-02	.01496	1.776	.571	1.2E+02	.180	1.000	1.5E-04	.970
1	1.E-02	.00083	1.569	.483	1.3E+02	.180	1.000	9.3E-05	.883
2	1.E-03	.00008	1.616	.487	1.9E+02	.180	1.000	8.8E-05	.891
3	1.E-04	.00006	1.677	.502	4.0E+02	.180	1.000	8.7E-05	.882
4	1.E-05	.00005	1.704	.508	5.3E+02	.180	1.000	8.7E-05	.879
5	1.E-06	.00005	1.707	.509	5.4E+02	.180	1.000	8.7E-05	.879
Pct Std Deviations			2.4	2.0	53.1	0.0	0.0	2.0	1.0

Correlation Matrix

1.0000						
.9916	1.0000					
.9885	.9710	1.0000				
0.0000	0.0000	0.0000	0.0000			
0.0000	0.0000	0.0000	0.0000	0.0000		
-.1166	-.0389	-.1282	0.0000	0.0000	1.0000	
-.4909	-.4268	-.5273	0.0000	0.0000	.7128	1.0000

Apparent Resistivity Measured at 1 Hz is 231

Apparent Resistivity Calculated from Inductive Coupling is 26

FIG. 26

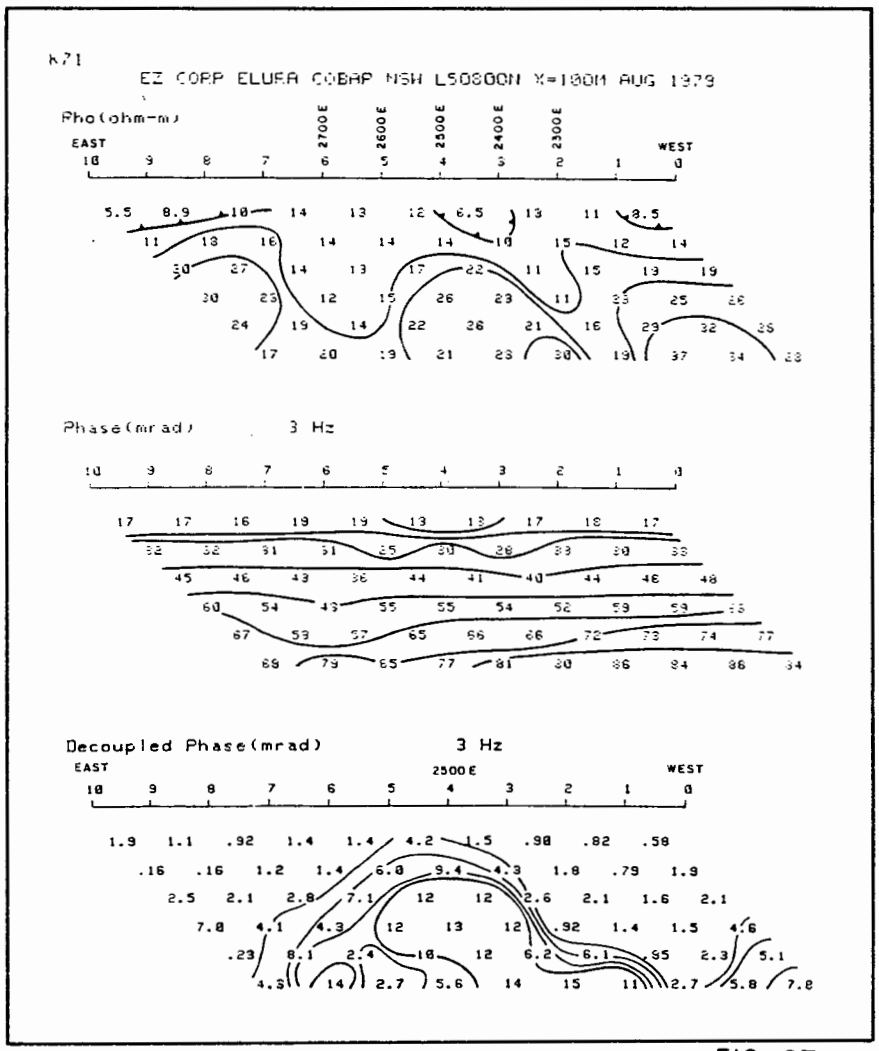

FIG. 27

COMPUTER ASSISTED INTERPRETATION OF IP DATA

The increased size, storage capability and speed of the modern digital computer has been a big boon to the exploration geophysicist. Forward problem solutions for potential methods (gravity, magnetics, etc.) have been available for some time. Recently, numerical modelling methods and large, very fast computers have made similar forward problem solutions available for applied field geophysics such as resistivity and induced polarization.

The forward problem solution shown in Figure 28 is for a fairly normal, dipping source. (The geometry is Two-Dimensional). The patterns of the induced polarization and resistivity pseudo-sections are similar to those we have previously seen from field data over dipping sources.

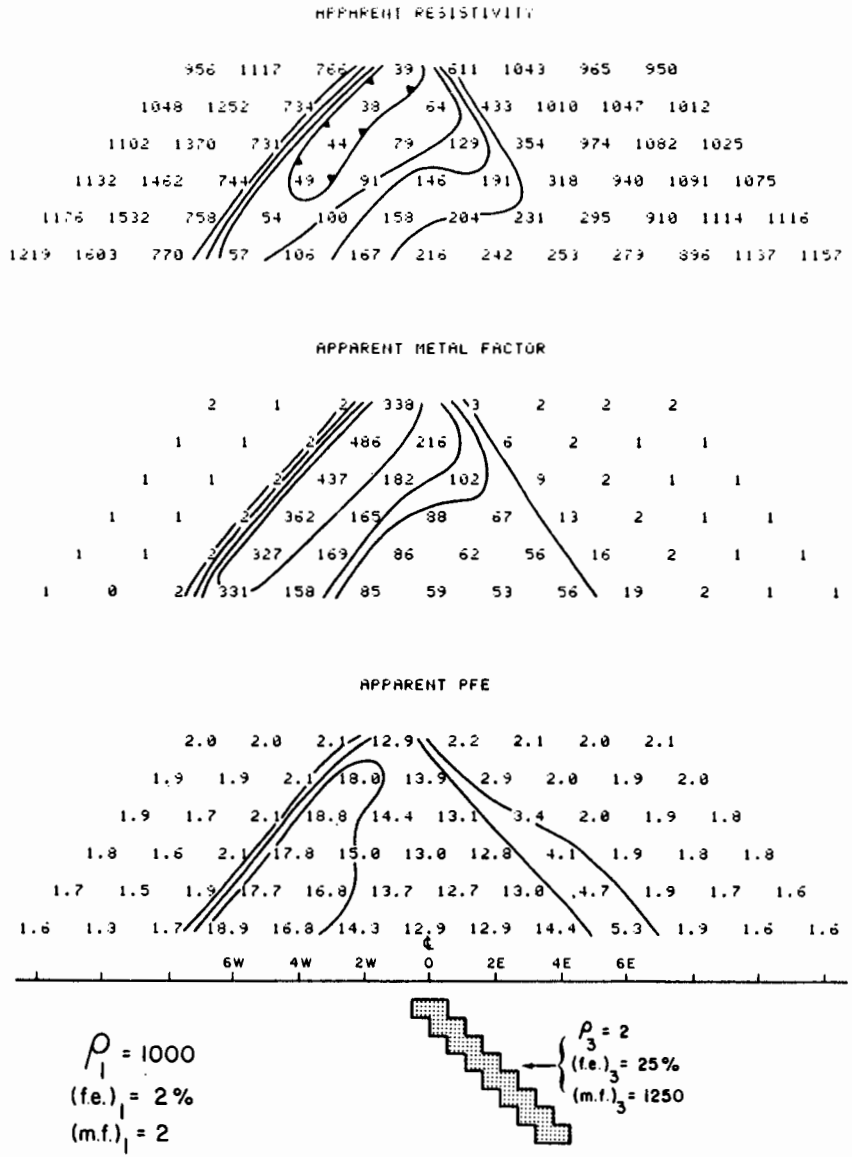
APPARENT RESISTIVITY
956 1117 766 39 611 1043 965 950
1048 1252 734 38 64 433 1010 1047 1012
1102 1370 731 44 79 129 354 974 1082 1025
1132 1462 744 49 91 146 191 318 940 1091 1075
1176 1532 758 54 100 158 204 231 295 910 1114 1116
1219 1603 770 57 106 167 216 242 253 279 896 1137 1157
APPARENT METAL FACTOR
2 1 2 338 3 2 2 2
1 1 2 486 216 6 2 1 1
1 1 2 437 182 102 9 2 1 1
1 1 2 362 165 88 67 13 2 1 1
1 1 2 327 169 86 62 56 16 2 1 1
1 0 2 331 158 85 59 53 56 19 2 1 1
APPARENT PFE
2.0 2.0 2.1 12.9 2.2 2.1 2.0 2.1
1.9 1.9 2.1 18.0 13.9 2.9 2.0 1.9 2.0
1.9 1.7 2.1 18.8 14.4 13.1 3.4 2.0 1.9 1.8
1.8 1.6 2.1 17.8 15.0 13.0 12.8 4.1 1.9 1.8 1.8
1.7 1.5 1.9 17.7 16.8 13.7 12.7 13.0 4.7 1.9 1.7 1.6
1.6 1.3 1.7 18.9 16.8 14.3 12.9 12.9 14.4 5.3 1.9 1.6 1.6
6W 4W 2W 0 2E 4E 6E
ρ1 = 1000
(f.e.)1 = 2%
(m.f.)1 = 2
ρ3 = 2
(f.e.)3 = 25%
(m.f.)3 = 1250

FIG. 28

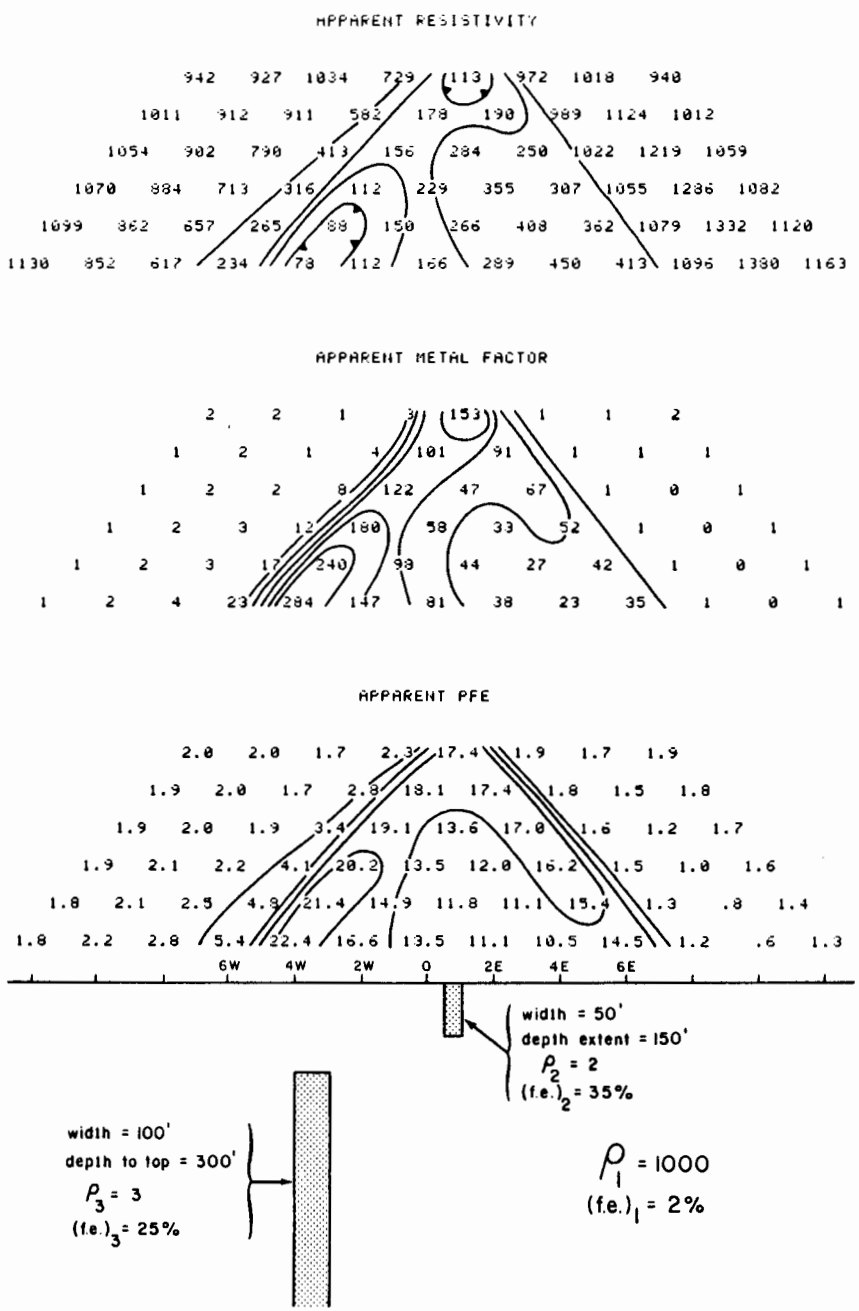
APPARENT RESISTIVITY
942 927 1034 729 113 972 1018 940
1011 912 911 582 178 190 989 1124 1012
1054 902 790 413 156 284 250 1022 1219 1059
1070 884 713 316 112 229 355 307 1055 1286 1082
1099 862 657 265 88 150 266 408 362 1079 1332 1120
1130 852 617 234 78 112 166 289 450 413 1096 1380 1163
APPARENT METAL FACTOR
2 2 1 3 153 1 1 2
1 2 1 4 101 91 1 1 1
1 2 2 8 122 47 67 1 0 1
1 2 3 12 180 58 33 52 1 0 1
1 2 3 17 240 98 44 27 42 1 0 1
1 2 4 23 284 147 81 38 23 35 1 0 1
APPARENT PFE
2.0 2.0 1.7 2.3 17.4 1.9 1.7 1.9
1.9 2.0 1.7 2.8 18.1 17.4 1.8 1.5 1.8
1.9 2.0 1.9 3.4 19.1 13.6 17.0 1.6 1.2 1.7
1.9 2.1 2.2 4.1 20.2 13.5 12.0 16.2 1.5 1.0 1.6
1.8 2.1 2.5 4.8 21.4 14.9 11.8 11.1 15.4 1.3 .8 1.4
1.8 2.2 2.8 5.4 22.4 16.6 13.5 11.1 10.5 14.5 1.2 .6 1.3
6W 4W 2W 0 2E 4E 6E
width = 50'
depth extent = 150'
ρ2 = 2
(f.e.)2 = 35%
width = 100'
depth to top = 300'
ρ3 = 3
(f.e.)3 = 25%
ρ1 = 1000
(f.e.)1 = 2%

FIG. 29

Recently however, we had occasion to try to interpret a field anomaly that was very similar to that shown in Figure 29. The presence of the shallow, limited depth extent source was known from previous drilling. By the trial and error method, we were able to show that the pattern (which is very similar to that in Figure 28) need not have originated from a dipping source.

By limiting the solutions somewhat, it is possible to create computer programs to do the inverse problem. That is, the computer accepts the field data as input and as output gives the vertical, tabular source that gives the best "least square fit" to that data. For comparison, the computer also outputs the pseudo-section data that would be measured for the source it has chosen.

The simplest problem is for resistivity data alone. The results shown in Figure 30 are from a geothermal exploration program in which the resistivity survey was completed using X = 250 meters. The large, deep resistivity low was measured on the side of an extinct volcano, under recent lava flows. The computer inversion gives a major, poorly determined, conductor (with a high conductivity times width product) at a depth of 350 to 400 meters. This data was used to show the geologist that the source of the resistivity anomaly could be a good geothermal target.

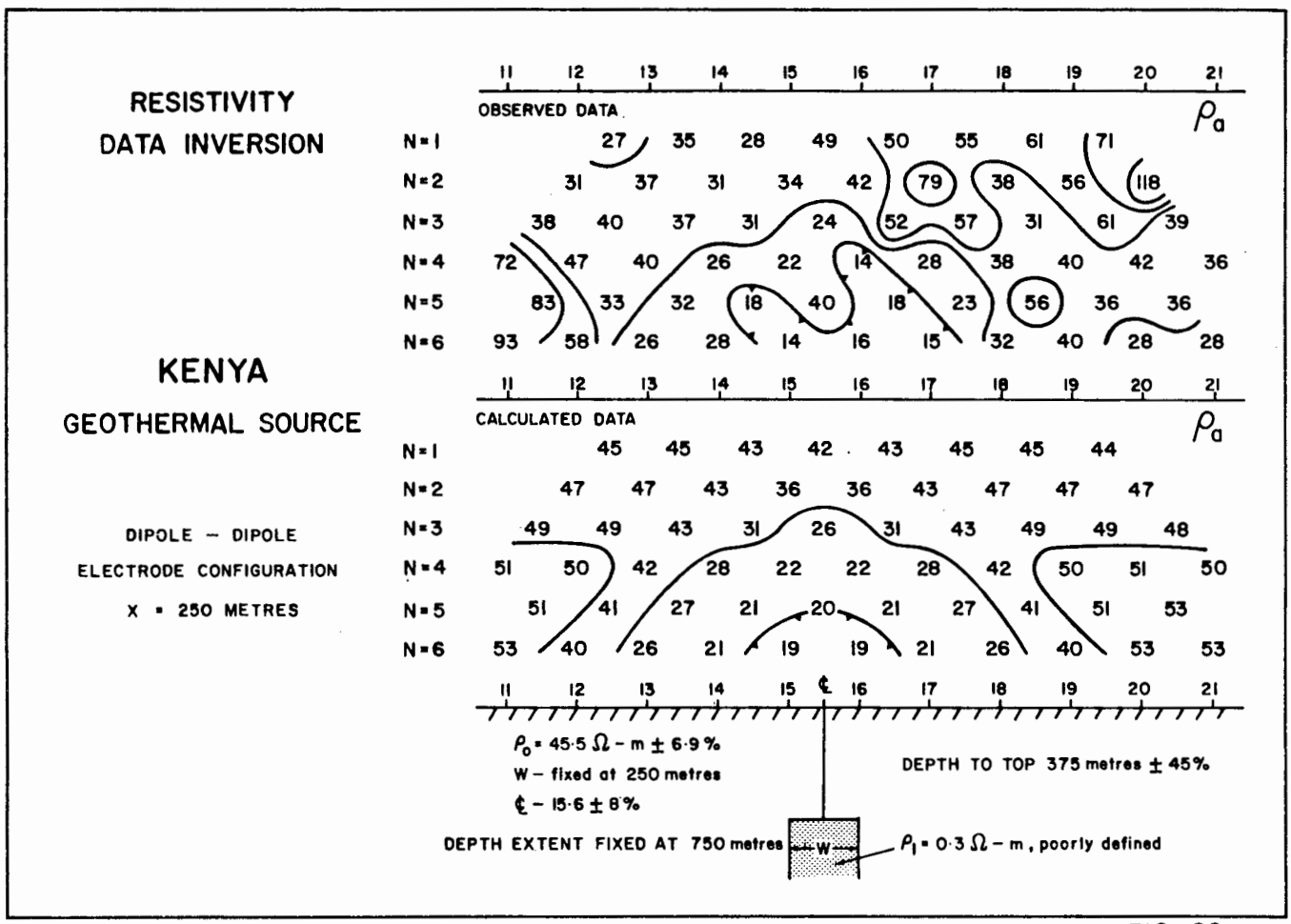

FIG. 30

The example shown in Figure 31 and Figure 32 is from the Pine Point Area. The computer inversion shows that in this case the source has a poor resistivity contrast with the surrounding limestones. However, the IP effect is quite anomalous.

If there is conductive overburden present, and the source itself is conductive, the inversions will be more complex. The data shown on Figure 33 and Figure 34 were measured with X = 100 feet, in an area where the depth of overburden was determined to be about fifty feet. The calculated results give a "good fit" to the measured data, and the source described by this inversion is a typical Canadian Shield, massive sulphide deposit.

The inversion program can also be used to show that two dissimilar anomalies can in fact be due to the same type of source. The inversions of the IP data shown in Figure 35 and Figure 36 are those for the field data previously shown in Figure 17 and Figure 18. The background resistivities are very different, and the depths to the top of the sources are different by a factor of three. However, the indicated source parameters are much the same. As we saw previously, the spectral characteristics of the IP anomaly from the two sources are quite different.

The use of the computer inversion techniques make it possible to obtain an estimate of the source parameters, even in situations in which an unusual geologic environment would make it difficult to interpret the data. The field results shown in Figure 37 are from a deeply buried source in a highly conductive environment. The rocks in which the survey was completed were porous, and filled with saline water. However, the inversion output on Figure 38 shows the source is not unlike that determined in Figure 34.

WHAT OF THE FUTURE?

There seems to be almost no limit to the future development of the induced polarization method. As the orebodies for which we search become deeper, and more difficult to detect, we will need all of the help we can get.

A simple extension of what we are now doing should lead to the following examples in the next twelve to twenty-four months.

a) The computer can be used to store parameters obtained by the computer inversions of spectral IP data. Therefore, it will be possible to correlate the electrical parameters (m, τ, c) of all sources known in a given geographical area or a certain geologic environment. For a new, unknown source, the computer could be asked to output the probability that the unknown source will be due to metallic mineralization of a certain type.

The data shown in Figure 39 was a first attempt at such a correlation. On the plot are shown the IP effect vs. Time-Constant (m, vs.τ) coordinates for a few massive sulphide

PINE POINT, N-38A, X=200FT

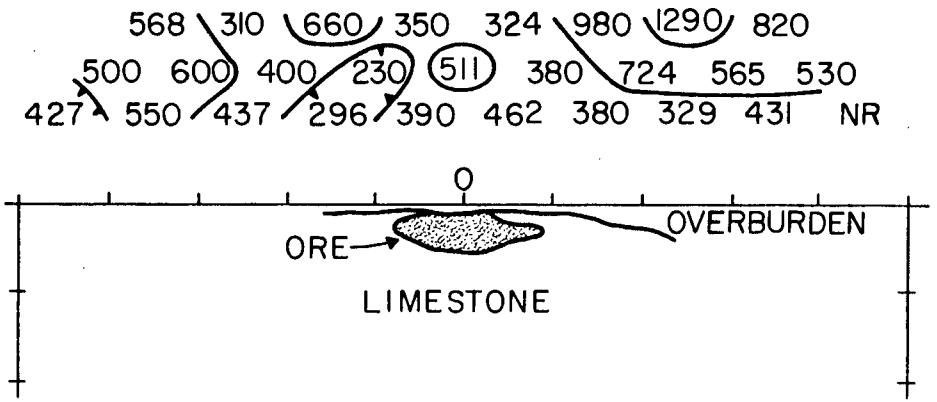

PINE POINT, N-38A, X=200 FT

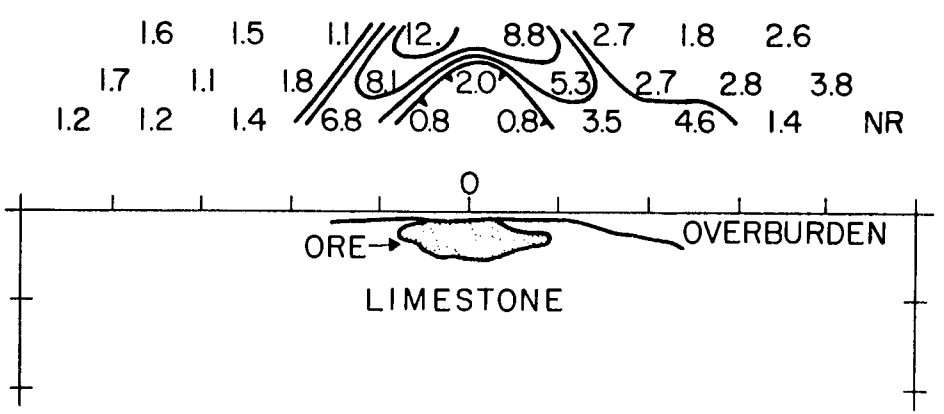

RESISTIVITY MODEL

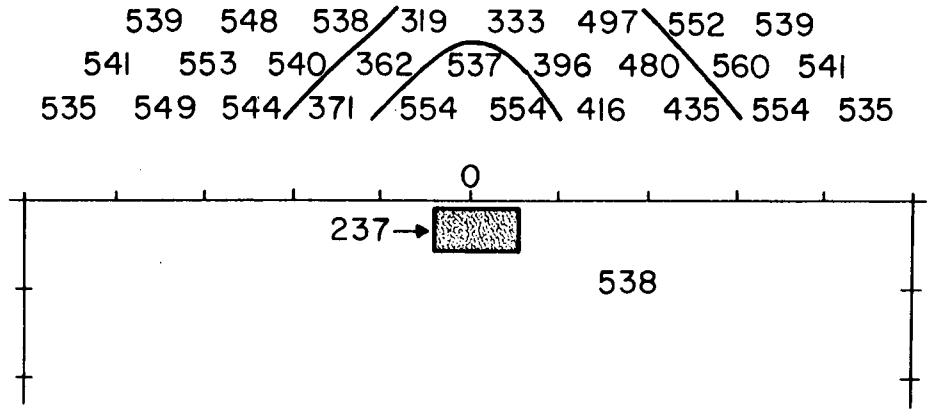

IP MODEL

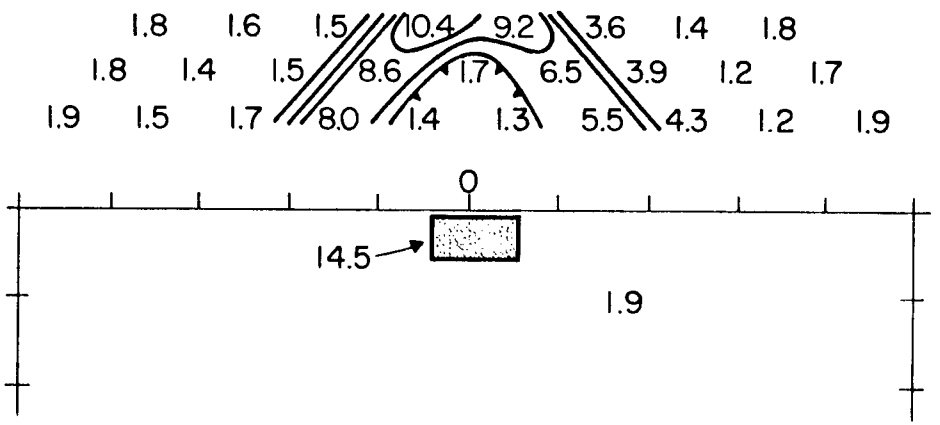

FIG. 31

FIG. 32

COMPUTER INTERPRETATION

OF GEOPHYSICAL DATA

INDUCED POLARIZATION AND RESISTIVITY

CANADIAN SHIELD MASSIVE SULPHIDE DEPOSIT, OVERLAIN BY CONDUCTIVE OVERBURDEN
ISO - COPPERFIELDS LINE 0+00

DETERMINE: HORIZONTAL POSITION
DEPTH TO TOP
WIDTH
RES OF SOURCE
RES OF OVERBURDEN
IP OF SOURCE

DIPOLE-DIPOLE ARRAY X = 100 FEET 100FT

RESISTIVITY DATA - OBSERVED (OHM-METERS)

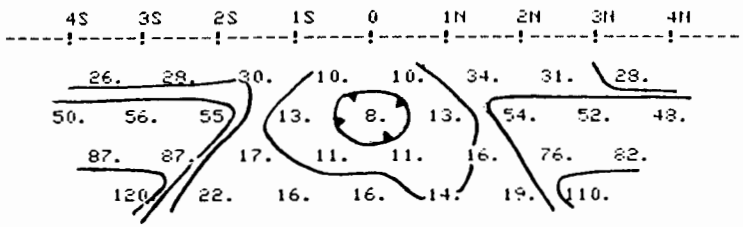

INDUCED POLARIZATION DATA - OBSERVED (PFE)

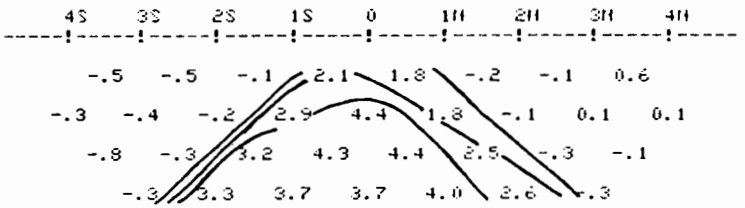

FIG. 33

RESISTIVITY DATA - CALCULATED (OHM-METERS)

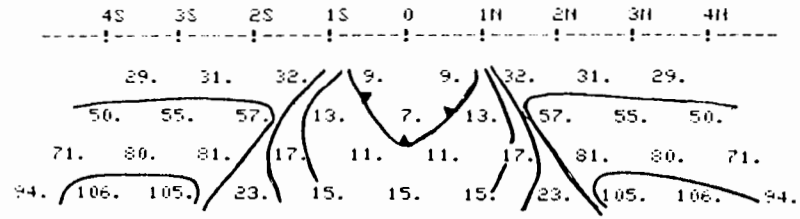

INDUCED POLARIZATION DATA - CALCULATED (PFE)

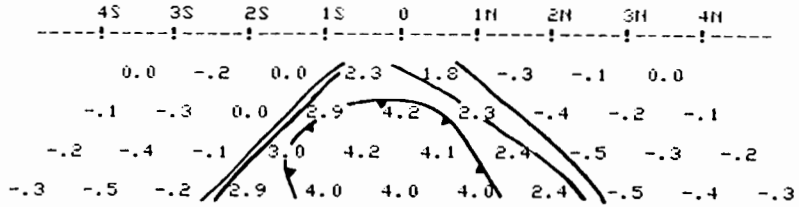

PARAMETERS OF THE CALCULATED SOURCE

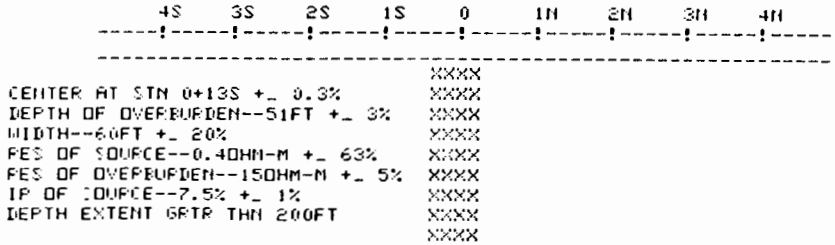

	XXXX
CENTER AT STN 0+13S +_ 0.3%	XXXX
DEPTH OF OVERBURDEN--51FT +_ 3%	XXXX
WIDTH--60FT +_ 20%	XXXX
RES OF SOURCE--0.40HM-M +_ 63%	XXXX
RES OF OVERBURDEN--150HM-M +_ 5%	XXXX
IP OF SOURCE--7.5% +_ 1%	XXXX
DEPTH EXTENT GRTR THN 200FT	XXXX
	XXXX

FIG. 34

LINE - 18E

FINAL MODEL FOR DATA SET 1

OBSERVED DATA

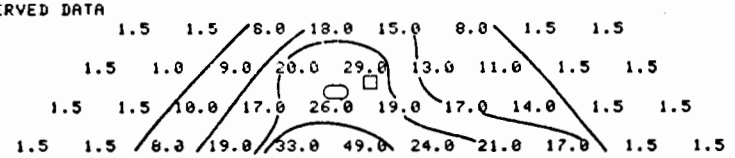

100*DIAGONAL OF INFORMATION DENSITY MATRIX

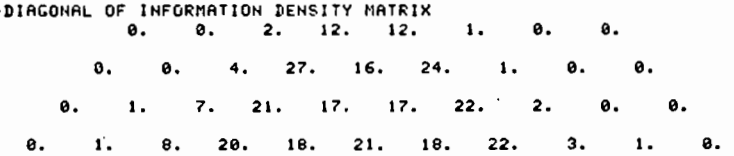

CALCULATED DATA

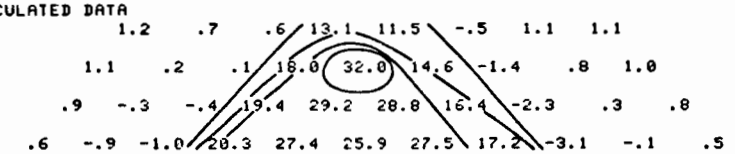

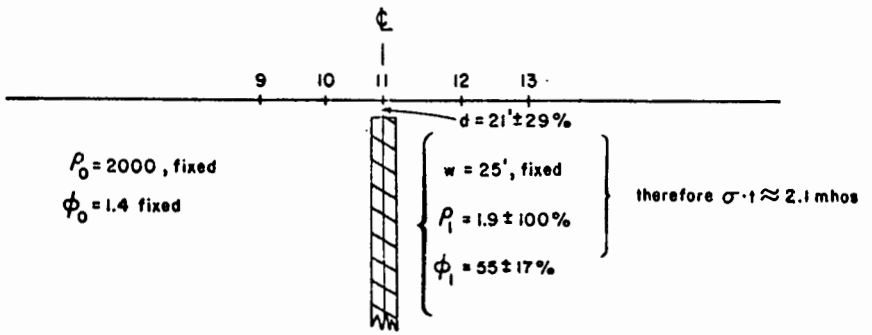

FIG. 35

LINE - 15E

graphite source, with some pyrite

LINE - 15E

phase at 0.3 Hz.

FINAL MODEL FOR DATA SET 1

OBSERVED DATA

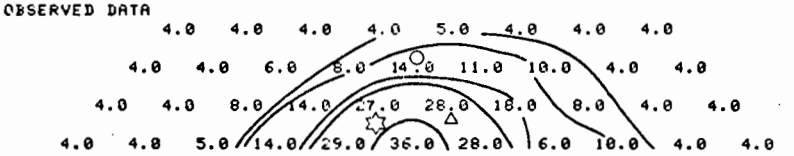

100*DIAGONAL OF INFORMATION DENSITY MATRIX

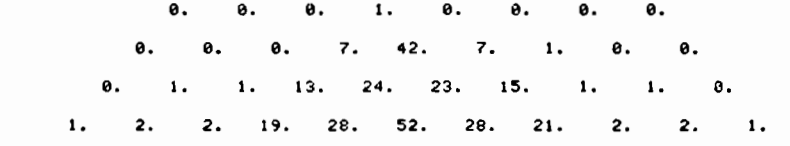

CALCULATED DATA

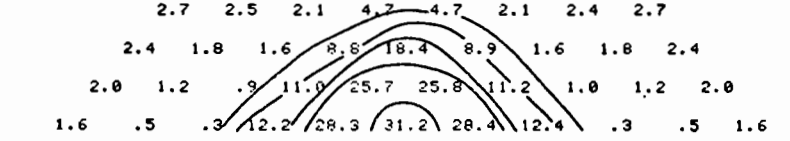

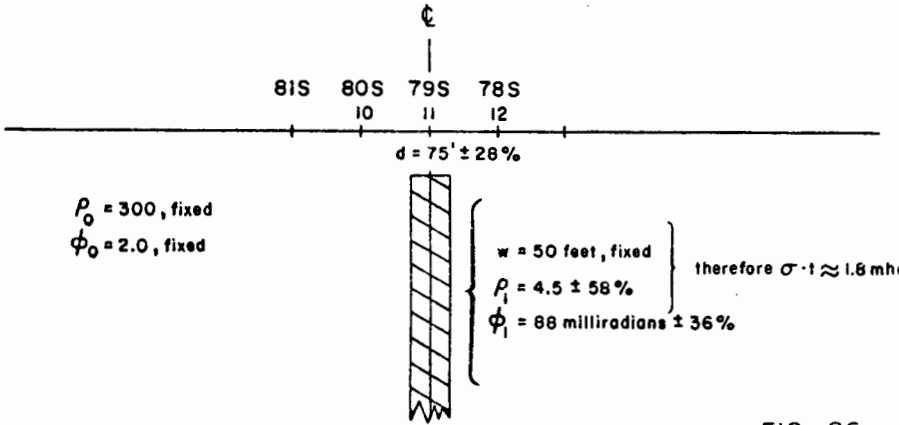

FIG. 36

COMPUTER INTERPRETATION

OF GEOPHYSICAL DATA

INDUCED POLARIZATION AND RESISTIVITY

DEEPLY BURIED SOURCE IN VERY CONDUCTIVE ENVIRONMENT - DETERMINE POSITION, DEPTH, AND PHYSICAL PROPERTIES OF SOURCE

DIPOLE-DIPOLE ARRAY X = 25 METERS 25M

RESISTIVITY DATA - OBSERVED (OHM-METERS)

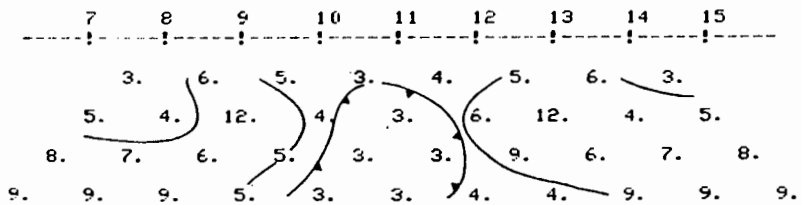

INDUCED POLARIZATION DATA - OBSERVED (PFE)

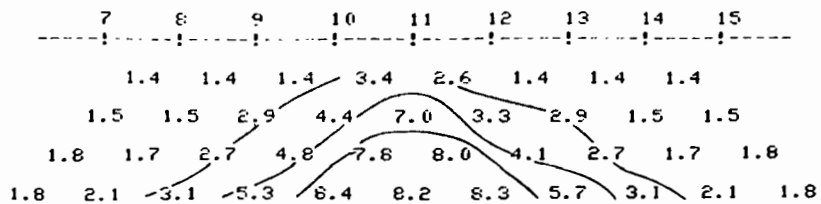

FIG. 37

RESISTIVITY DATA - CALCULATED (OHM-METERS)

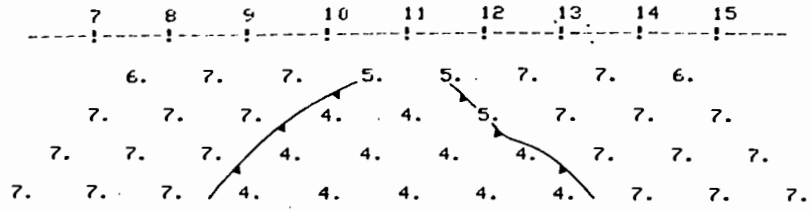

INDUCED POLARIZATION DATA - CALCULATED (PFE)

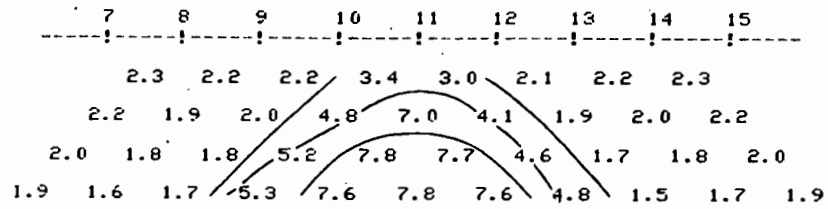

PARAMETERS OF THE CALCULATED SOURCE

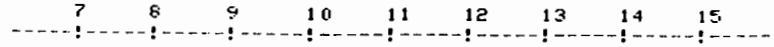

DEPTH TO TOP--23M +_ 11%
RES OF SOURCE--0.30HM-M +_ 45%
RES OF HOST--6.50HM-M +_ 5%
IP OF SOURCE--23 +_ 16%
IP OF HOST--2.3 +_ 11%
CENTER AT STN 10+90 +_ 1%

+++++
+++++
+++++
+++++
+++++
+++++
+++++

DEPTH EXTENT FIXED AT >50M
WIDTH FIXED AT 25M

FIG. 38

sources and massive graphite sources in Canada. More recent determinations have not been added to the plot, although additional field work in North America and Australia has shown the same grouping.

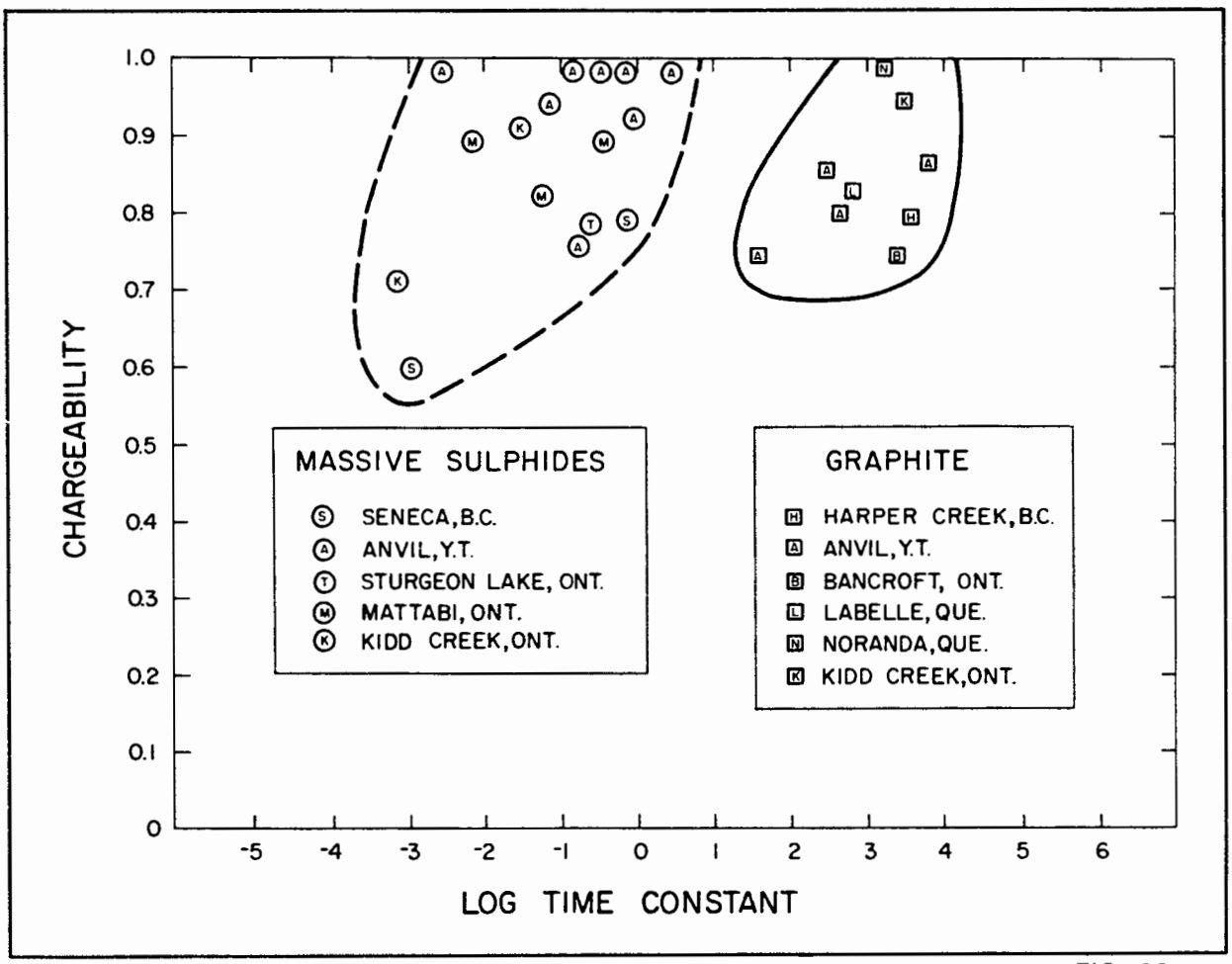

FIG. 39

b) The frequency range of spectral IP measurements with the IPV-3 System extends well up into the range that is normally used for electromagnetic prospecting. Indeed, as we have shown previously, the inductive coupling (EM) effects must be removed from the spectral IP plot before the electrical parameters of the source can be determined. In the near future, it should be possible to use this electromagnetic coupling information to gain further insight about the source.

The induced polarization and resistivity results in Figure 40 are from an area in South Australia. There is a known

pyrrhotite zone at Station 4 to Station 3, and a narrow Pb-Zn-Ag zone at about Station 0. The resistivity data shows a low over the conductive pyrrhotite zone. The raw phase data at 9.0 Hz and 0.11 Hz shows that IP effects are present, but the measurements (particularly at 9.0 Hz) are distorted by inductive coupling (EM) effects. When the inductive effects are removed, there is a definite IP anomaly from the pyrrhotite zone and a weak IP anomaly from the Pb-Zn-Ag zone. (see Figure 41).

The pseudo-sections shown in Figure 42 are a first attempt to use the inductive effects that have been removed from the dipole-dipole IP data. The M3 parameter is the electromagnetic component that has been removed from the measurement with each dipole pair.

The source centered at Station 4 to Station 3 gives a resistivity low, an IP high, and also a very large electromagnetic component. The source centered at Station 0 gives a weak, but definite IP anomaly. This source is not large enough to give a resistivity low using X = 25 meters. However, the electromagnetic coupling between the IP survey wires and the source is different from the resistive coupling between the electrodes and the source. There definitely is an electromagnetic component due to the Pb-Zn-Ag source.

c) With small desk-top computers, the calculation of a single forward IP problem can require five to ten hours. However, recent advances in small computers and new, interaction interfaces between CRT Displays and light-stylus hardware, will soon give the exploration geophysicist almost instantaneous interpretation capability.

For instance, the geometry shown on Figure 43 could be the first guess at the source of an IP anomaly. The geometry would be drawn upon the CRT Display by the geophysicist using an active light-stylus. At the push of a key, the computer would almost instantly display the pseudo-section shown. The computer would then print a "hard copy" of the field data, the calculated data and the geometry and parameters of the source.

The geophysicist could then use the light-stylus to alter the geometry to that shown in Figure 44. A push of the "operate" key would produce the pseudo-section shown in Figure 44. The pattern is only slightly different, but if it has greater similarity to the field data pattern, the geophysicist knows that he is on the right track.

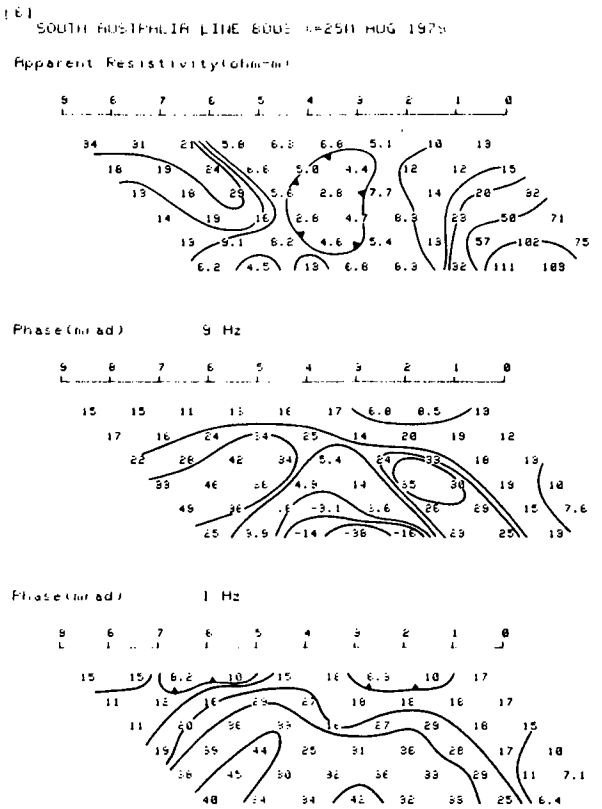

FIG. 40

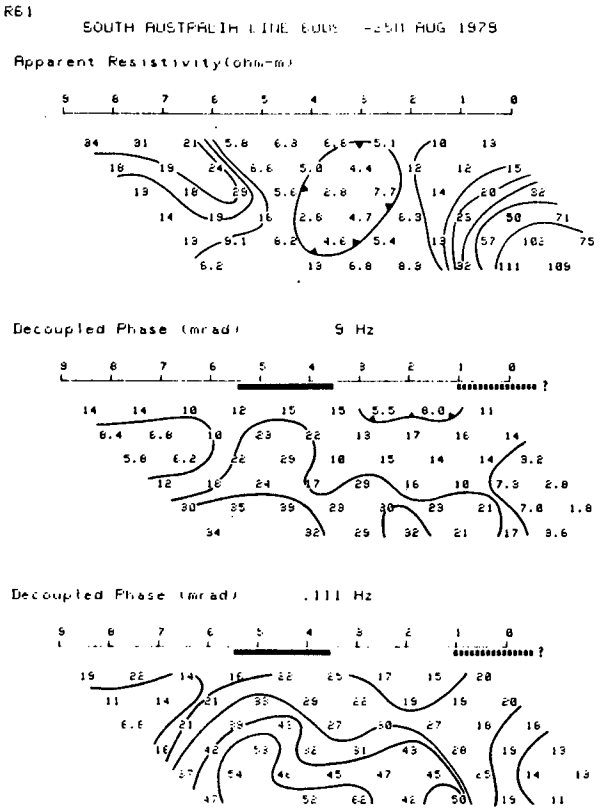

FIG. 41

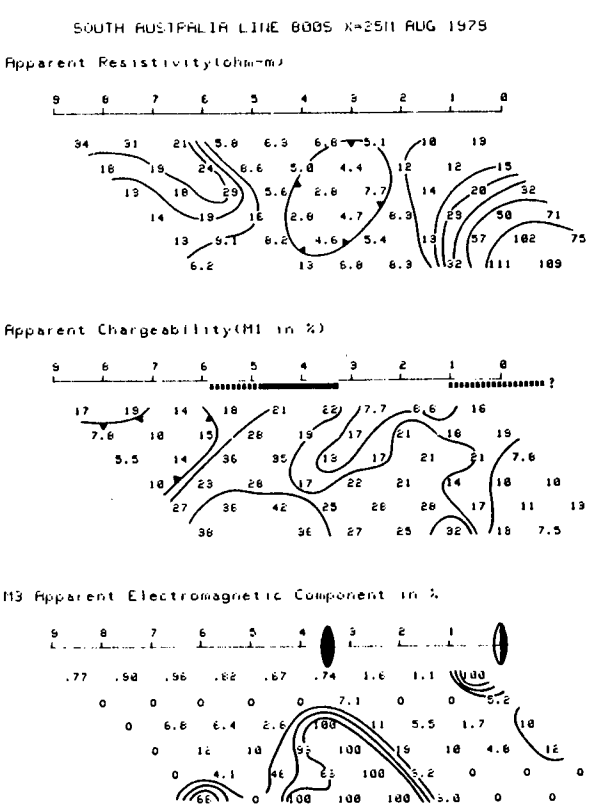

FIG. 42

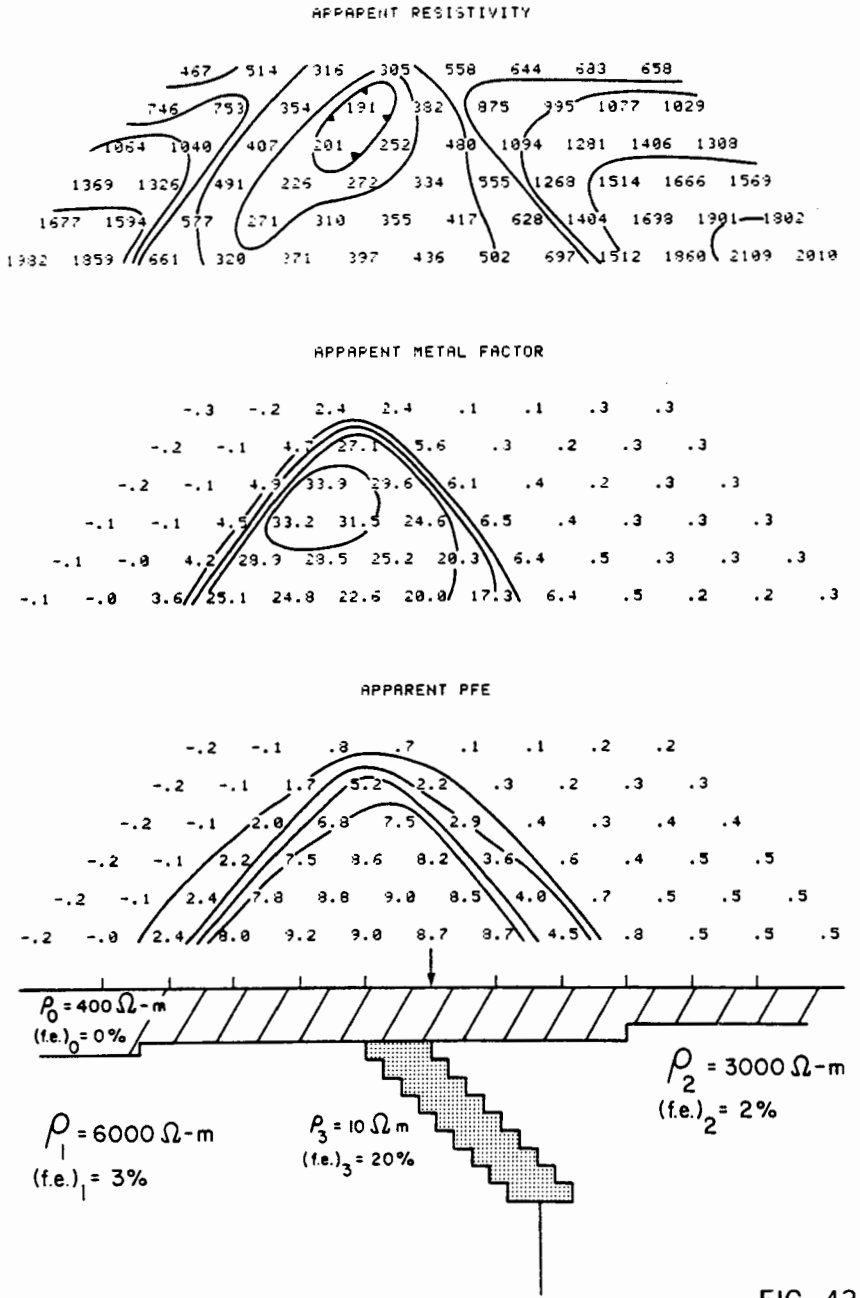
APPARENT RESISTIVITY
APPARENT METAL FACTOR
APPARENT PFE
ρ_0 = 400 Ω-m
(f.e.)$_0$ = 0%
ρ_1 = 6000 Ω-m
(f.e.)$_1$ = 3%
ρ_3 = 10 Ω m
(f.e.)$_3$ = 20%
ρ_2 = 3000 Ω-m
(f.e.)$_2$ = 2%

FIG. 43

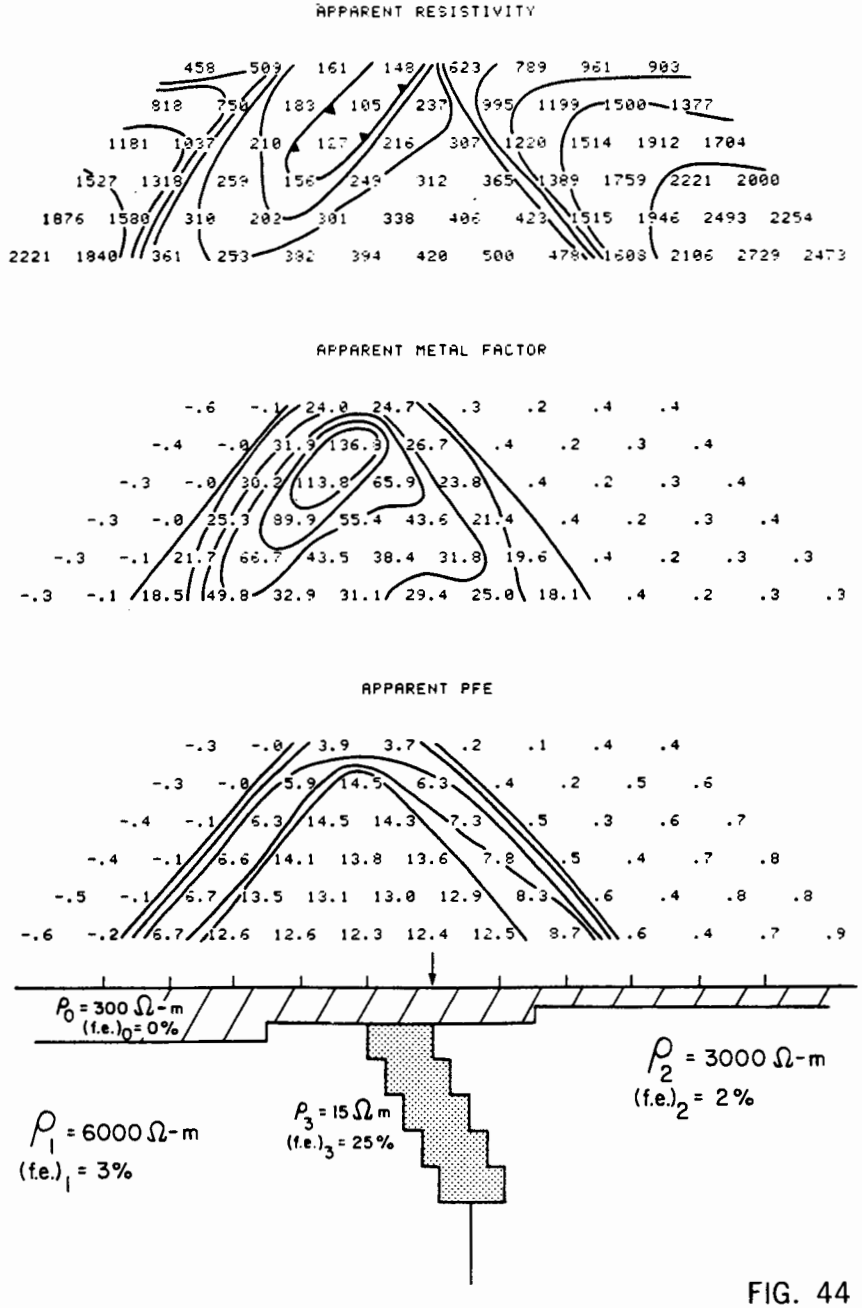
APPARENT RESISTIVITY
APPARENT METAL FACTOR
APPARENT PFE
ρ_0 = 300 Ω-m
(f.e.)$_0$ = 0%
ρ_1 = 6000 Ω-m
(f.e.)$_1$ = 3%
ρ_3 = 15 Ω m
(f.e.)$_3$ = 25%
ρ_2 = 3000 Ω-m
(f.e.)$_2$ = 2%

FIG. 44

Toronto Office: 200 Yorkland Blvd., Willowdale, Ont. M2J 1R5
Vancouver Office: 310 - 885 Dunsmuir St., British Columbia, V6C 1N5
Denver Office: 4690 Ironton St., Colorado, 80239, U.S.A.

DWG. NO. - S.I.P.P. - 3109

PHOENIX GEOPHYSICS LIMITED

RECONNAISSANCE SPECTRAL INDUCED POLARIZATION SURVEY

PLAN MAP

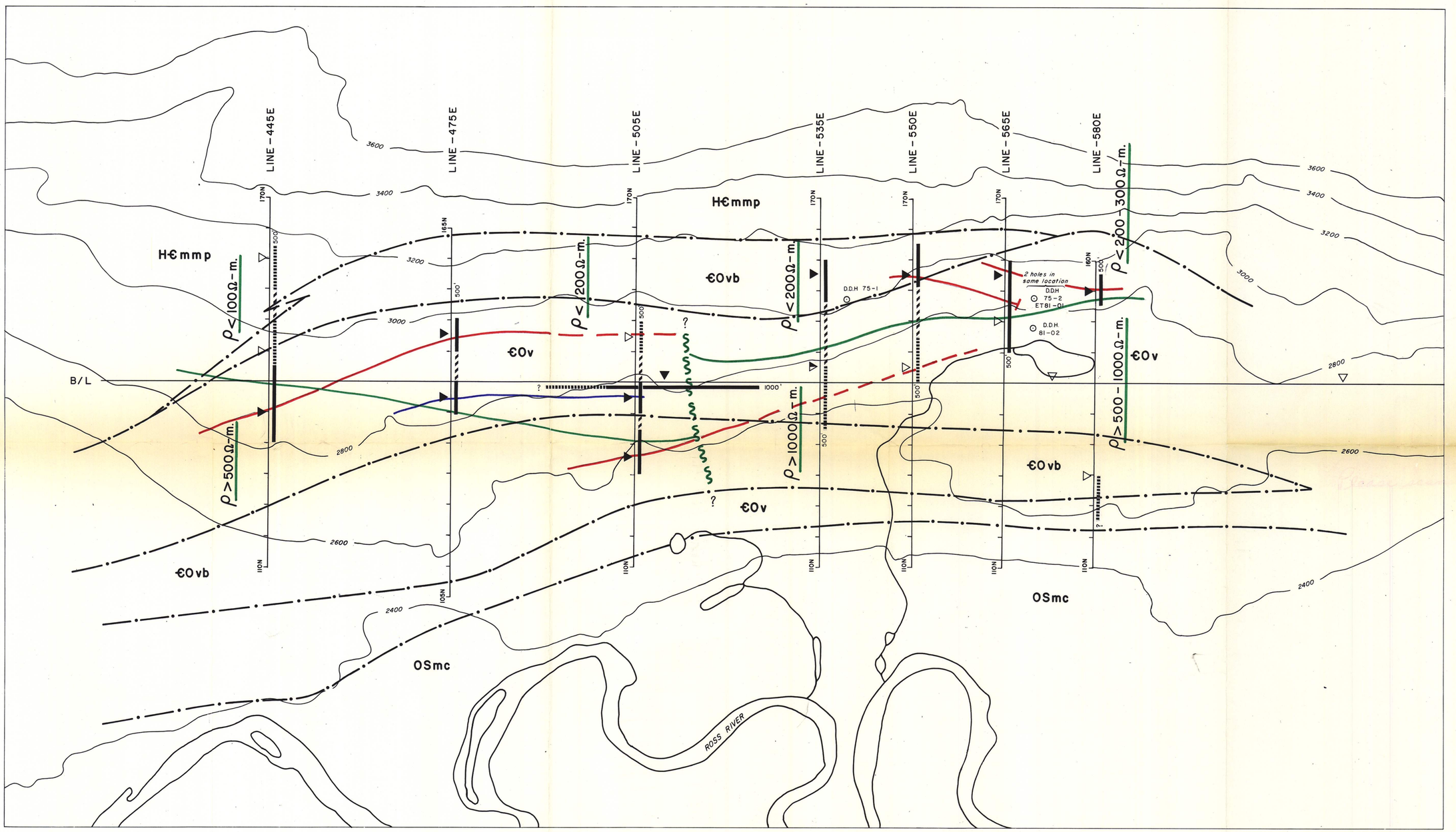

SURFACE PROJECTION OF ANOMALOUS ZONE

DEFINITE ▼
PROBABLE ▼ } NARROW SOURCE
POSSIBLE ▽

NUMBER AT END OF ANOMALIES INDICATES SPREAD USED.

– APPROXIMATE POSITION OF RESISTIVITY CONTACT

– GEOLOGICAL CONTACT

– AXIS OF DEEP IP ANOMALOUS ZONE

– AXIS OF SHALLOW IP ANOMALOUS ZONE

CYPRUS ANVIL MINING CORPORATION

TENAS PROJECT , WHITEHORSE M.D.

YUKON TERRITORY

SCALE

500 0 1000 2000 3000 FEET

100 0 200 400 600 800 METRES

1:10000

inches 0 1 2

centimetres 0 1 2 3 4 5

This reference scale bar has been added to the original image. It will change in size as the image, therefore can be used as a reference for the original size.

YUKON GEOLOGICAL SURVEY

DRAWN: [illegible]

DATE: JAN 1982

APPROVED:

DATE:

PROFESSIONAL ENGINEER OF BRITISH COLUMBIA P. HALLOF

Expiry Date: February 25, 1982

DWG. NO. - S.I.P.P. - 3109